

**Functional-biochemical relationships
in the posterior cingulate cortex, and
their application to the genetic risk
of Alzheimer's disease**

Alison Grace Costigan

A thesis submitted for the degree of Doctor of Philosophy

School of Psychology, Cardiff University

September 2016



Declarations

DECLARATION

This work has not been submitted in substance for any other degree or award at this or any other university or place of learning, nor is being submitted concurrently in candidature for any degree or other award.

Signed (candidate) Date

STATEMENT 1

This thesis is being submitted in partial fulfilment of the requirements for the degree of PhD.

Signed (candidate) Date

STATEMENT 2

This thesis is the result of my own independent work/investigation, except where otherwise stated, and the thesis has not been edited by a third party beyond what is permitted by Cardiff University's Policy on the Use of Third Party Editors by Research Degree Students. Other sources are acknowledged by explicit references. The views expressed are my own.

Signed (candidate) Date

STATEMENT 3

I hereby give consent for my thesis, if accepted, to be available online in the University's Open Access repository and for inter-library loan, and for the title and summary to be made available to outside organisations.

Signed (candidate) Date

STATEMENT 4: PREVIOUSLY APPROVED BAR ON ACCESS

I hereby give consent for my thesis, if accepted, to be available online in the University's Open Access repository and for inter-library loans after expiry of a bar on access previously approved by the Academic Standards & Quality Committee.

Signed (candidate) Date

Thesis Summary

A major challenge in Alzheimer's disease (AD) research is to improve understanding of the earliest brain changes associated with AD, in order to develop treatments to combat this disease. One strategy potentially able to inform this need is the study of brain regions associated with AD in young adults at genetic risk of AD. A key region of increasing interest to AD researchers is the posterior cingulate cortex (PCC). Despite being implicated in AD pathogenesis, its function is not well understood. Neuroimaging studies in young adults who carry the strongest genetic risk factor for AD, the Apolipoprotein (*APOE*) E4 allele, have detected glucose metabolism, activity and functional connectivity alterations in the PCC. A better understanding of PCC function would aid interpretation of these changes, to improve insight into AD pathogenesis.

This thesis applied functional magnetic resonance imaging (fMRI) and magnetic resonance spectroscopy (MRS) to study PCC activity correlates with brain metabolites *in vivo* (Chapters 3 and 4), prior to investigating whether these metabolites might be altered in *APOE*-E4 carriers aged 18-25 years (Chapter 5).

Chapters 3 and 4 detected a category-sensitive fMRI response and fMRI-MRS relationship for the scene condition of a perception task and a working memory task, specifically a positive correlation between PCC activity and the metabolite N-acetyl-aspartate (tNAA), a marker of neuronal integrity associated with neuronal mitochondrial metabolism. The scene conditions of these paradigms previously elicited an altered pattern of PCC activity in young *APOE*-E4 carriers. Chapter 5 therefore compared PCC tNAA and other MRS metabolites between young *APOE*-E4 carriers and non-carriers. No MRS differences, however, were evident between *APOE* groups.

These findings contribute to our understanding of the biochemistry underpinning PCC activity, but suggest that an alteration in such a pathway may not be linked with the activity alterations detected in young *APOE*-E4 carriers.

Acknowledgements

I would like to thank Professor Kim Graham, my primary supervisor, for her invaluable support and guidance throughout my PhD. I am very grateful for her advice that has helped me hone my research ideas and bring my thesis together, as well as gain confidence and develop as a researcher. I am especially grateful for the valuable feedback on my draft Chapters. Thanks go also to my second and third supervisors, Professor Richard Wise and Professor Julie Williams, for the very helpful discussions about fMRI and MRS, and about Alzheimer's disease genetics.

I am also very grateful to Dr John Evans, for all the advice and support he has given me on MRS. Thanks especially for the advice in setting up my MRS acquisitions, and for rating the quality of my spectra. Thank you also to Mark Mikkelsen, for the guidance in spectroscopy theory and analysis, for generously sharing analysis scripts with me, for the numerous helpful discussions we have had about GABA, and for the feedback on my methods Chapter.

I am also very grateful for all the help and advice from everyone in my lab group, particularly to Katja Umla-Runge. Thank you for our regular PhD meetings, and for your guidance on fMRI analysis, help with participant recruitment, and support during my PhD. A big thank you also to Mark Postans for the helpful suggestions on my Chapter drafts, to Carl Hodgetts for the help with fMRI analysis, and to Professor Andrew Lawrence for the very useful discussions about statistics.

In addition, thank you to my fellow PhD students in my lab group, Rebecca, Martina, Beth, Hannah, Matt, Steph and Erika for your encouragement, valuable chats about my results, and for being willing pilot participants on several occasions! Particular thanks to Rebecca, Matt and Martina for being such a great team to be part of for the APOE study, and to Rebecca and Martina for the great company during all the hours we have spent scanning together!

Thank you also to Peter Hobden and Martin Stuart for the training in running the MRI scanner, and for the help with data collection. Thank you also to everyone in CUBRIC who has helped me with scanning. Importantly, thank you also to all of my participants for volunteering for my scans!

I am also grateful for the support of the Alzheimer's genetics team – especially to Rhodri for teaching me how to do DNA extractions, to Jodi and Rachel for performing the *APOE* genotyping, and to Beccy for her genetics advice.

Thanks also go to the Neuroscience and Mental Health Research Institute (NMHRI) for giving me a place on the Integrative Neuroscience scheme, and funding my PhD, which has allowed me to pursue my interest in translational neuroscience.

Outside of work, I am also extremely grateful to my wonderful friends who have helped me cope throughout doing this PhD, and for making sure I do fun things outside of work! Particular thanks go to Amun, Marie and Navit; to my Integrative Neuroscience PhD coursemates Hannah, Lucy, Nick, Tim, Jack, Francesca and Katie; and also to PhD friends in other departments Emma, Stacy, Zoe, Chen and Claudia. In particular thank you to my housemate and PhD pal, Laura, who has never failed to make me laugh during the highs and lows of this PhD. The past three years would definitely not have been as enjoyable without us living together!

Last, but most importantly, thank you so much to my mum, dad, sister Jenny and brother-in-law Paul. Thank you for your support and encouragement, not only throughout this PhD, but during every step that has led me to this point. I certainly could not have done this without you, and am so grateful to you for being my confidence boosters and my rock during this challenge.

Contents page

1	Chapter 1: General Introduction.....	1
1.1	Alzheimer’s disease	1
1.2	Genetic neuroimaging strategy.....	6
1.3	Posterior cingulate cortex.....	8
1.3.1	Anatomy.....	8
1.3.2	Connectivity	9
1.3.3	Metabolism and Function.....	11
1.4	Posterior cingulate cortex in Alzheimer’s disease.....	13
1.4.1	Metabolic alterations.....	13
1.4.2	Activity alterations.....	17
1.5	Posterior cingulate cortex in young <i>APOE</i> -E4 carriers	21
1.6	Key questions to be addressed in this thesis	25
1.6.1	Aims of this thesis and overview of Chapters	27
2	Chapter 2: General Methods.....	29
2.1	Magnetic Resonance Spectroscopy (MRS).....	29
2.1.1	How does MRS work?.....	30
2.1.2	Metabolites assessed via MRS	31
2.1.2.1	N-acetyl-aspartate	33
2.1.2.2	Glutamate	35
2.1.2.3	GABA	36
2.1.2.4	Myo-Inositol.....	37
2.1.2.5	Creatine.....	38
2.1.2.6	Choline.....	39
2.1.3	MRS Scan sequences.....	39
2.1.3.1	PRESS.....	39
2.1.3.2	MEGA-PRESS.....	40
2.1.4	Methodological considerations for MRS	41
2.1.4.1	Reference molecule in metabolite quantification.....	41
2.1.4.2	Effect of menstrual cycle and hormonal contraception on metabolite concentrations	42
2.2	Functional Magnetic Resonance Imaging (fMRI)	44

2.2.1	How does fMRI work?	44
2.2.2	How do we use fMRI to investigate brain function?.....	46
2.2.3	Methodological considerations in fMRI.....	48
2.2.3.1	Correction for multiple comparisons	48
2.3	Combination of MRS with fMRI	48
2.3.1	MRS metabolites correlated with BOLD in this Thesis	49
2.3.2	MRS-fMRI methodological consideration: how to test for a relationship between MRS and fMRI	50
3	Chapter 3: Investigating category-sensitivity in the posterior cingulate cortex using fMRI and MRS	53
3.1	Introduction.....	53
3.1.1	Analysis Strategy and Hypotheses.....	57
3.2	Methods.....	62
3.2.1	Participants	62
3.2.2	Overview of scanning procedure	63
3.2.3	Oddity fMRI Task	63
3.2.4	Stimuli.....	65
3.2.5	fMRI scan parameters	65
3.2.6	Structural scan parameters	66
3.2.7	MRS scan parameters.....	66
3.2.8	Data Analysis	68
3.2.8.1	Behavioural data analysis.....	68
3.2.8.2	fMRI data analysis.....	69
3.2.8.3	MRS data analysis	70
3.2.8.4	fMRI-MRS Relationships	71
3.2.8.4.1	fMRI-MRS – Percent signal change ROI analysis	71
3.2.8.4.2	fMRI-MRS - Voxel-wise GLM with MRS covariate analysis	73
3.2.9	Behaviour-fMRI and behaviour-MRS correlations	74
3.2.10	Statistical analysis	75
3.3	Results.....	75
3.3.1	Data exclusions	75
3.3.2	Behavioural Results	77
3.3.3	fMRI Results – investigating category sensitivity in the PCC ROI.....	78
3.3.4	MRS Results.....	79

3.3.5	fMRI-MRS Relationships	81
3.3.5.1	fMRI-MRS – Percent signal change ROI analysis.....	81
3.3.5.2	fMRI-MRS - Voxel-wise GLM with MRS covariate analysis.....	85
3.3.6	fMRI-Behaviour relationships	87
3.3.7	MRS-Behaviour relationships.....	88
3.4	Discussion.....	89
3.4.1	Chapter Summary.....	93

4 Chapter 4: Investigating working memory load and scene processing in posterior cingulate cortex using fMRI and MRS..... 94

4.1	Introduction.....	94
4.1.1	Analysis strategy and hypotheses.....	101
4.2	Methods.....	103
4.2.1	Participants	103
4.2.2	Scanning procedure	103
4.2.3	fMRI Spatial Working Memory Task.....	104
4.2.4	fMRI Parameters	104
4.2.5	Data Analysis	105
4.2.5.1	Behavioural Data Analysis	105
4.2.5.2	fMRI Data Analysis	106
4.2.5.3	fMRI-MRS Relationships	108
4.2.5.3.1	fMRI-MRS – Percent signal change ROI analysis.....	108
4.2.5.3.2	fMRI-MRS - Voxel-wise general linear model with MRS as a regressor.....	109
4.2.6	Behaviour-fMRI correlations	110
4.2.7	Behaviour-MRS correlations.....	111
4.2.8	Statistical analysis	111
4.3	Results.....	111
4.3.1	Data exclusions	111
4.3.2	Behavioural Results.....	113
4.3.3	fMRI Results.....	115
4.3.4	MRS Results.....	117
4.3.5	fMRI-MRS Relationships	118
4.3.5.1	fMRI-MRS – Percent signal change ROI analysis.....	118

4.3.6	fMRI-MRS Relationships: Voxel-wise GLM with MRS regressor approach.....	120
4.3.7	Behaviour-fMRI relationships	124
4.3.8	Behaviour-MRS relationships.....	125
4.4	Discussion.....	126
4.4.1	fMRI Results: Interaction between spatial complexity and working memory load in PCC.....	128
4.4.2	fMRI-MRS Results: scene-sensitive PCC tNAA-BOLD relationship, but not for GABA+ or Glx	129
4.4.3	fMRI-behaviour results: PCC activity is not related to task performance.....	134
4.4.4	MRS-behaviour results: PCC tNAA is related to rooms 2back performance.....	135
4.4.5	Limitations.....	136
4.4.6	Summary of Chapter.....	137
5	Chapter 5: Investigating metabolite differences between young <i>APOE-E4</i> carriers and non-carriers in posterior cingulate cortex using MRS.....	139
5.1	Introduction.....	139
5.1.1	tNAA: main metabolite of interest.....	141
5.1.2	Additional metabolites of interest.....	146
5.1.2.1	Myo-inositol.....	146
5.1.2.2	Creatine.....	149
5.1.2.3	GABA+ and Glx	150
5.1.3	Analysis strategy and hypotheses.....	151
5.2	Methods.....	153
5.2.1	Participants	153
5.2.2	DNA extraction and genotyping.....	154
5.2.3	Scanning procedure and data analysis	154
5.2.4	Statistics.....	155
5.3	Results.....	156
5.3.1	Participants	156
5.3.2	Data exclusions	157
5.3.3	MRS Results.....	158
5.4	Discussion.....	162

5.4.1	Limitations.....	165
5.4.2	Future directions	166
5.4.3	Summary of Chapter.....	167
6	Chapter 6: General Discussion.....	169
6.1	Summary of the three main findings.....	170
6.1.1	Potential mechanisms behind the positive tNAA-BOLD relationships.....	171
6.1.2	Implications of the category sensitive BOLD response in the PCC ROI.....	173
6.1.3	Potential reasons for no PCC MRS alterations in young <i>APOE-E4</i> carriers.....	174
6.2	Methodological considerations and limitations	176
6.2.1	Choice of strategy to correlate BOLD with metabolites.....	176
6.2.2	Statistics and corrections for multiple comparisons	178
6.2.3	Interpretation of BOLD and BOLD-MRS relationships.....	179
6.2.4	Limitations.....	180
6.2.4.1	Limitations of MRS	180
6.2.4.2	Limitations of fMRI.....	182
6.2.4.3	Sample sizes and participants	182
6.2.4.4	Correlation not causality.....	184
6.3	Future directions	184
6.4	Concluding Remarks	186
	References.....	187

List of Abbreviations

Abbreviation	Description
MRS	Magnetic Resonance Spectroscopy
AD	Alzheimer's disease
ANOVA	Analysis of variance
APOE	Apolipoprotein
APP	Amyloid precursor protein
BF	Bayes Factor
BOLD	Blood oxygen level dependent
Cho	Choline
Cr	Creatine
CRLB	Cramer-Rao-Lower-Bounds
CSF	Cerebro-spinal fluid
DN (or DMN)	Default network (also termed the default mode network)
EPI	Echo planar imaging
FAD	Familial AD
fMRI	Functional magnetic resonance imaging
GABA	γ -amino-butyric acid
GABA+	GABA plus co-edited macromolecules
GLM	General linear model
Glx	Total glutamate (glutamate + glutamine)
GM	Grey matter
GWAS	Genome wide association study
MCI	Mild cognitive impairment
MEGA-PRESS	MEscher-Garwood-Point Resolved Spectroscopy
mI	Myo-inositol
mM	Millimolar
MM	Macromolecules
MRI	Magnetic resonance imaging
MTL	Medial temporal lobe
NAA	N-acetyl-aspartate
NAAG	N-acetyl-aspartly-glutamate

NMR	Nuclear magnetic resonance
OCC	Occipital cortex
PCC	Posterior cingulate cortex
PET	Positron emission tomography
PMC	Posteromedial cortex
ppm	Parts per million
PRESS	Point resolved spectroscopy
PSEN	Presenilin
RF	Radio-frequency
ROI	Region of interest
SNP	Single nucleotide polymorphism
SNR	Signal-to-noise ratio
SVS	Single voxel spectroscopy
T	Tesla
TE	Echo time
TR	Repetition time
tNAA	total NAA (NAA+NAAG)
WM	White matter

1 Chapter 1: General Introduction

1.1 Alzheimer's disease

Alzheimer's disease (AD) is a chronic and progressive neurodegenerative disorder, which was first characterised by the neurologist Alois Alzheimer in the early 1900s (Alzheimer, 1906). AD is the most common neurodegenerative disorder, affecting approximately 11% of the population over the age of 65, which represents 35 million people worldwide and 800,000 people in the UK (Prince et al., 2014; World Health Organization, 2012). The proportion of individuals with AD increases with age, with approximately 45% of the population over the age of 85 years suffering from AD (Alzheimer's Association, 2016). Due to an aging population, the number of people with AD is expected to triple by the year 2050 (World Health Organization, 2012), making this disease an important public health priority (Alzheimer's Association, 2016).

AD constitutes 50-70% of dementia cases, making AD the leading cause of dementia. Dementia is defined as a disorder involving the death of brain cells resulting in progressive cognitive impairment that affects daily life (Alzheimer's Association, 2016). The cognitive impairment experienced by AD patients tends to be evidenced as a deficit in episodic memory (memory for personally experienced events (Tulving, 1972)). Patients typically lose the ability to recall recently learned information and form new memories (McKhann et al., 2011). Additionally, an impairment in spatial navigation is a common early symptom, with many patients reporting getting lost even in familiar environments (Monacelli, Cushman, Kavcic, & Duffy, 2003; Pai & Jacobs, 2004). AD is a progressive degenerating disorder, so the symptoms worsen as the disease progresses. Later symptoms can include additional cognitive deficits such as language impairments, changes in personality (including aggression or apathy), psychiatric symptoms (e.g. hallucinations), with the disease eventually developing into a completely debilitating disorder requiring full-time care (McKhann et al., 2011).

Alzheimer's disease is characterised pathologically by a widespread cortical atrophy (wasting away of brain cells, which is particularly striking around the medial temporal lobe and lateral ventricles, see Figure 1.1A), and a high density of extracellular plaques of amyloid protein and intracellular tangles of hyperphosphorylated tau (Braak

& Braak, 1991, 1995; Reiman & Jagust, 2012; Serrano-Pozo, Frosch, Masliah, & Hyman, 2011). Examples of these pathological hallmarks of AD are shown in Figure 1.1B. The starting point of the disease is controversial, as a number of brain areas are considered to be early affected. Many studies point towards the medial temporal lobe regions of the hippocampus and entorhinal cortex as key regions affected early by AD pathology (Braak & Del Tredici, 2012; Braak, Thal, Ghebremedhin, & Tredici, 2011; Serrano-Pozo et al., 2011). In support of this, immunohistochemical studies of post-mortem brains have detected tau tangles in the hippocampus and entorhinal cortex at early stages of the disease (Braak & Braak, 1995; Braak et al., 2011). Amyloid pathology, on the other hand, may instead originate in association cortex, a proposal supported by immunohistochemical studies and also positron emission tomography of amyloid plaques (Braak & Braak, 1991; Reiman & Jagust, 2012).

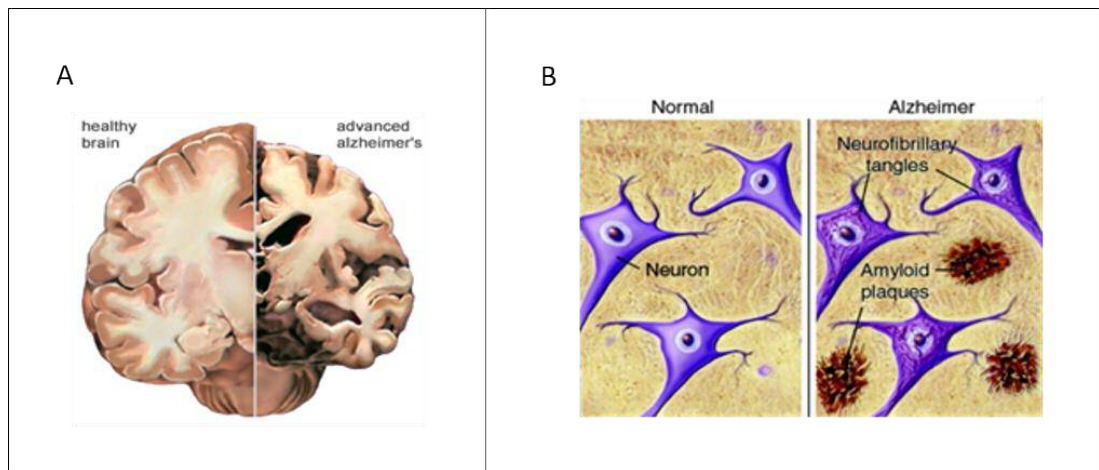


Figure 1.1: Pathology in AD. (A) Gross atrophy in the brain in advanced AD (image taken from http://www.alz.org/braintour/healthy_vs_alzheimers.asp). (B) The pathological hallmarks of AD which are extracellular amyloid plaques and intracellular neurofibrillary tau tangles (image taken from <http://www.brightfocus.org/alzheimers/infographic/amyloid-plaques-and-neurofibrillary-tangles>).

There is no clear cause of AD in the vast majority of cases, which are termed “sporadic AD” cases. The exception to this is that approximately 1% of AD cases are caused by an autosomal dominant mutation, termed “familial AD” cases (FAD) (Tanzi & Bertram, 2001; Van Cauwenberghe, Van Broeckhoven, & Sleegers, 2016). The mutations associated with FAD are in the genes involved in the synthesis and processing of the amyloid protein: *APP*, *PSEN1* and *PSEN2*. These genes respectively encode the amyloid

precursor protein (APP), and presenilins 1 and 2, which are components of the γ -secretase enzyme that cleaves APP (Rocchi, Pellegrini, Siciliano, & Murri, 2003). Carriers of a disease-related mutation in these genes will almost certainly develop AD, as these mutations are almost always fully penetrant (Hollingworth, Harold, Jones, Owen, & Williams, 2011).

In sporadic AD, there is no one genetic cause, however it is still a highly heritable disease (heritability estimate of 79% (Gatz et al., 2006)), suggesting genetic risk factors are an important component. The vast majority of sporadic AD cases arise over the age of 65 years, and are termed "late-onset AD" (LOAD) (Hollingworth et al., 2011). The strongest genetic risk factor associated with LOAD is the Apolipoprotein (*APOE*) E4 allele, which is one of the three common isoforms of the *APOE* gene. The two other *APOE* isoforms are E2 and E3. Compared to the neutral AD risk genotype of *APOE* E3/E3, possession of one copy of E4 increases risk by 3-4 times and possession of two E4 alleles increases risk by 12-14 times (Farrer et al., 1997). By contrast, possession of the E2 allele is suggested to be protective (Farrer et al., 1997). Carrying the *APOE*-E4 allele also decreases the age of possible onset of AD: more specifically, possession of 0, 1 and 2 E4 alleles reduces age of onset from 84 to 76 to 68 years, respectively (Corder et al., 1993). The *APOE* protein has been implicated in a wide range of processes in the brain, including the transport of cholesterol to neurons, synaptogenesis, and in repair following brain injury (Huang & Mahley, 2014; Liu, Kanekiyo, Xu, & Bu, 2013). There is, therefore, a complex picture of how the *APOE*-E4 allele may be associated with increased risk of AD. Hypotheses include that *APOE*-E4 has detrimental effects on synaptogenesis, a lower capacity for amyloid clearance, neuronal mitochondrial dysfunction, neurovascular dysfunction, and reduced protection against excitotoxicity in comparison to *APOE*-E3 or *APOE*-E2 (Huang, 2011; Liu et al., 2013; Mahley & Huang, 2012).

In 2009, a genome wide association study (GWAS) identified further common gene variants that increase risk of sporadic AD (e.g. in the genes *BIN1*, *PICALM*, *CLU*, *CR1* (Harold et al., 2009)). This finding has since been replicated using a larger sample and further gene variants associated with AD have been identified, bringing the total number to 19 (Lambert et al., 2013). These more recently identified gene variants, however, have a much lower odds ratio compared to *APOE*-E4. For example, the common variant of *BIN1*, which is the strongest risk variant identified in these recent studies, had an odds ratio of 1.22 (Lambert et al., 2013), whereas just one copy of the *APOE*-E4 allele has an odds ratio of approximately 3-4 (this value differs slightly depending on ethnicity and

gender) (Farrer et al., 1997). Thus *APOE-E4* remains the strongest genetic risk factor for sporadic AD, and a good candidate for studies aiming to understand how genetic risk of AD may influence brain structure and function. This point will be returned to in Section 2 below.

There is currently no cure for AD nor any effective treatment, and the pathogenic mechanisms behind this disease are still not well understood. Given the large incidence of AD today, and its predicted increase, as well as the vast social and economic burden of AD, developing treatments to combat AD is an important and pressing challenge. Many researchers believe that the AD treatments developed so far have not been effective as they are being given too late in the disease process (e.g. Reiman, Langbaum, & Tariot, 2010; Waite, 2015). Evidence has amassed over the past 20 years that pathological changes underlying AD begin decades before the onset of symptoms, and by the stage patients present with cognitive impairment – which is when treatments are typically given to patients - this is actually a late stage of the disease. By this point treatments have little scope to ameliorate the symptoms experienced by patients (Dubois et al., 2016; Jack et al., 2013; Sperling et al., 2011). Evidence in support of this clinically silent period while pathology is developing comes from studies of FAD mutation carriers, which have detected a higher density of brain amyloid deposition compared to controls, approximately 20 years before their predicted age of onset of AD (Fleisher et al., 2012). In addition, other neuroimaging changes have been detected years before the expected age of onset of AD, including a decrease in glucose metabolism measured via fluoro-deoxyglucose PET (FDG-PET) (Mosconi et al., 2006), an altered profile of brain metabolites assessed via magnetic resonance spectroscopy (MRS) (Godbolt et al., 2006; Londono et al., 2013), and a decrease in volume of key regions implicated in AD (e.g. hippocampal volume) (Fox, Warrington, Stevens, & Rossor, 1996). Further evidence for AD-related brain changes despite no AD symptoms comes from neuroimaging studies of participants who have gone on to develop AD at a follow up study (e.g. Den Heijer et al., 2010; Minoshima et al., 1997; Seo et al., 2012).

These ideas about pre-symptomatic changes in AD were drawn together in a model by Jack et al. in 2010, which was updated in 2013, suggesting the temporal order of brain changes that occur during the “clinically silent” phase of the disease (see Figure 1.2) (Jack et al., 2010, 2013). In these papers, Jack et al. acknowledged three phases of AD development: the pre-symptomatic phase, in which there is an increased density of pathological hallmarks in the brain but no cognitive deficits that affect daily life; the mild

cognitive impairment (MCI) phase in which patients have widespread pathology and some behavioural deficits (e.g. memory impairment), but these are not severe (Petersen, 2004); and the AD phase, in which pathology and atrophy are widespread in the brain and the patient has severe impairment in a range of cognitive domains. These are highlighted in the green band in Figure 1.2 (Jack et al., 2010, 2013).

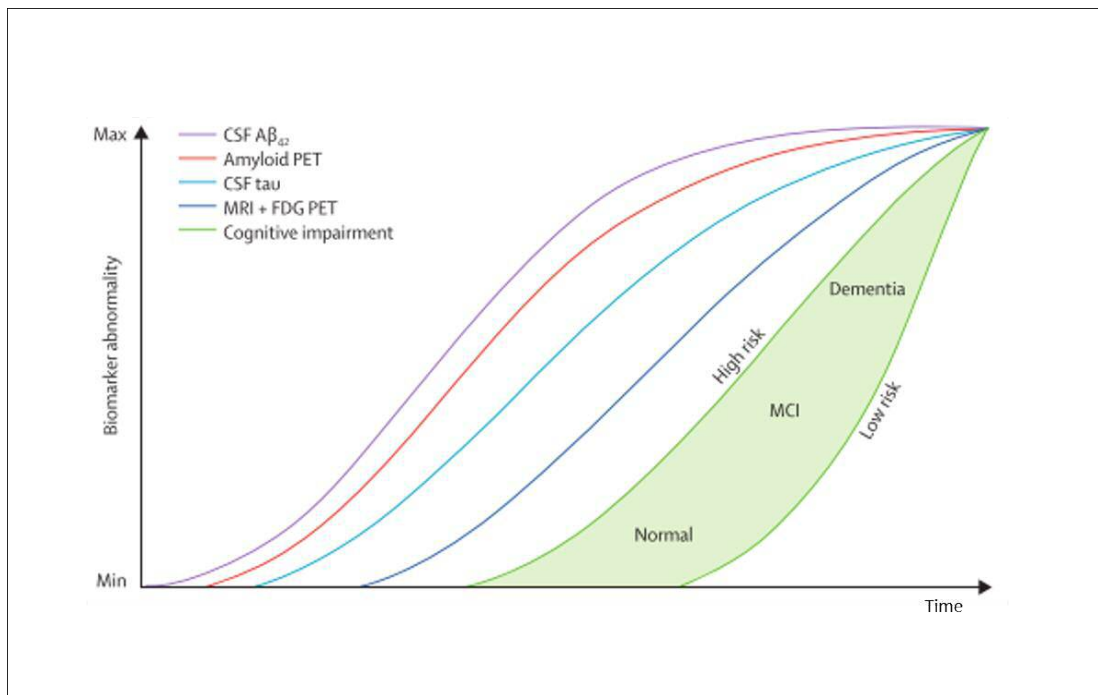


Figure 1.2: Proposed model of the clinically silent phase of AD, where there is development of AD pathology, atrophy and neuroimaging changes before the onset of clinical symptoms (shown in the green band) (Image taken from Jack et al., 2013).

These views, reflected in Jack et al., (2013), suggest that in order to develop successful treatments that target the pathogenic mechanisms of the disease, rather than the consequences or symptoms of the disease, it is important to understand the earliest possible brain changes that may be linked with subsequent AD neuropathology, and in turn cognitive change (i.e. the sequence of events that lead to the brain changes in the pre-symptomatic phase of AD described above).

1.2 Genetic neuroimaging strategy

One potential strategy that might help with this need is to select key brain regions known to show the earliest changes in AD and study these regions using neuroimaging in young people at increased genetic risk of AD in later life. Furthermore, where the neuroimaging technique is able to incorporate a cognitive task (e.g. in fMRI studies), applying paradigms known to be sensitive to the earliest behavioural impairments in AD (e.g. deficits in episodic memory, spatial navigation and scene perception) would be an effective way of increasing sensitivity to detect any early alterations in these genetic risk groups.

In order to obtain the necessary large sample sizes for cognitive studies, while ensuring the study of individuals with a reasonably strong risk of subsequently getting AD (Farrer et al., 1997), researchers have increasingly focused on the *APOE-E4* allele, as this is the strongest single genetic risk factor for sporadic AD. Using this genetic neuroimaging strategy, several studies have designed experiments to assess MTL function in young *APOE-E4* carriers compared to non-carriers (Dennis et al., 2010; Filippini, MacIntosh, et al., 2009; Kunz et al., 2015; Suri, Heise, Trachtenberg, & Mackay, 2013). The rationale behind such studies is that the entorhinal cortex is proposed to be the site of the earliest pathological deposition (Braak & Braak, 1995), the hippocampus is the site that shows the most striking atrophy (e.g. see Figure 1.1), and the MTL is strongly associated with the cognitive domain that is a core impairment in AD, episodic memory (e.g. Scoville & Milner, 1957). Key examples of such studies in young *APOE-E4* carriers are by Filippini et al., (2009), and Kunz et al., (2015). Filippini et al., (2009) applied an fMRI task that was known to elicit activity in the hippocampus, a novelty-encoding task, to compare fMRI activity between young *APOE-E4* carriers and non-carriers (mean age 28 years). Participants were shown images of 4 landscapes and 4 animals outside the scanner, (the familiar items) prior to being shown these same images as well as 48 novel images (24 new landscapes and 24 new animals) inside the scanner. When activity between familiar and novel items was compared, the young *APOE-E4* carriers had higher activity in the hippocampus for the novel vs familiar contrast compared to the non-carriers (Filippini, MacIntosh, et al., 2009). Kunz et al., (2016) applied an object-location memory task in a virtual arena to test activity profiles in the entorhinal cortex (specifically grid-cell like activity) between *APOE-E4* carriers and non-carriers (aged between 18 and 30 years). Participants were asked to navigate around the arena and collect eight objects. Next they were shown each object and asked to place this

item back where it was collected. Comparison of entorhinal cortex fMRI activity between *APOE* groups showed *APOE*-E4 carriers had reduced grid-cell like activity (Kunz et al., 2015). These studies demonstrate that there are activity differences in *APOE*-E4 carriers in AD-vulnerable MTL regions decades before the possible onset of AD.

An additional brain region of increasing interest to AD researchers is the posterior cingulate cortex (PCC). The PCC has received much less attention than the MTL, in both research into how it is affected in AD and into its function in the healthy brain. For example, a quick PubMed search for “posterior cingulate” yields approximately 30 times fewer papers compared to “hippocampus” (roughly 4,000 papers compared to 130,000), and when the term “Alzheimer’s” was added into both searches, this revealed approximately 14 times fewer papers for the PCC than the hippocampus (roughly 700 papers compared to 10,000). Moreover, a recent review articles proposes that the PCC has been neglected in AD research, but is an important region to study: “while the continuing focus on the MTL for memory loss is understandable, it comes at a potential price. There remains the possibility that pathologies in other areas play a key role in disrupting memory, starting from the earliest stages of the disease” (Aggleton, Pralus, Nelson, & Hornberger, 2016). The article goes on to suggest that the PCC (and also the limbic thalamus) should be studied due to accumulating evidence that metabolic, activity and connectivity changes occur in this region at early stages of AD, there is evidence to suggest some of these precede MTL changes, and there is evidence from lesion studies, neuroanatomical tracer studies and fMRI studies that the PCC is involved in memory processes (Aggleton et al., 2016). In addition to better understanding changes in the PCC in AD, there is also the need better understand PCC function more generally in order to interpret alterations evident in young individuals at increased genetic risk of AD, and to design sensitive cognitive paradigms better able to detect early and subtle changes in this critical brain region.

Before expanding on the critical importance of the PCC in AD and in young *APOE*-E4 carriers, the following section provides a framework for the interpretation of these studies by giving an overview of the anatomy, connectivity and function of the PCC in the healthy brain. Section 1.4 will then return to why the PCC is an important brain region to study in AD, followed by studies on the PCC in young *APOE*-E4 carriers in Section 1.5. Section 1.6 will then outline of some gaps in our knowledge about the impact of the *APOE*-E4 allele on the PCC, and about the functional contribution to PCC to perception and memory, which could inform studies on AD and young *APOE*-E4 carriers.

1.3 Posterior cingulate cortex

1.3.1 Anatomy

The PCC is located at the posterior end of the cingulate gyrus, which is the belt of cortex lying superior to the corpus callosum, shown in yellow in Figure 1.3A. The PCC is classed as Brodmann areas 23, 31, and in some studies the PCC also incorporates the retrosplenial cortex, which is Brodmann areas 29 and 30, shown in green and blue respectively in Figure 1.3B. The PCC forms part of the posteromedial cortex (PMC), which comprises the PCC, precuneus (area 7) and retrosplenial cortex (Vann, Aggleton, & Maguire, 2009).

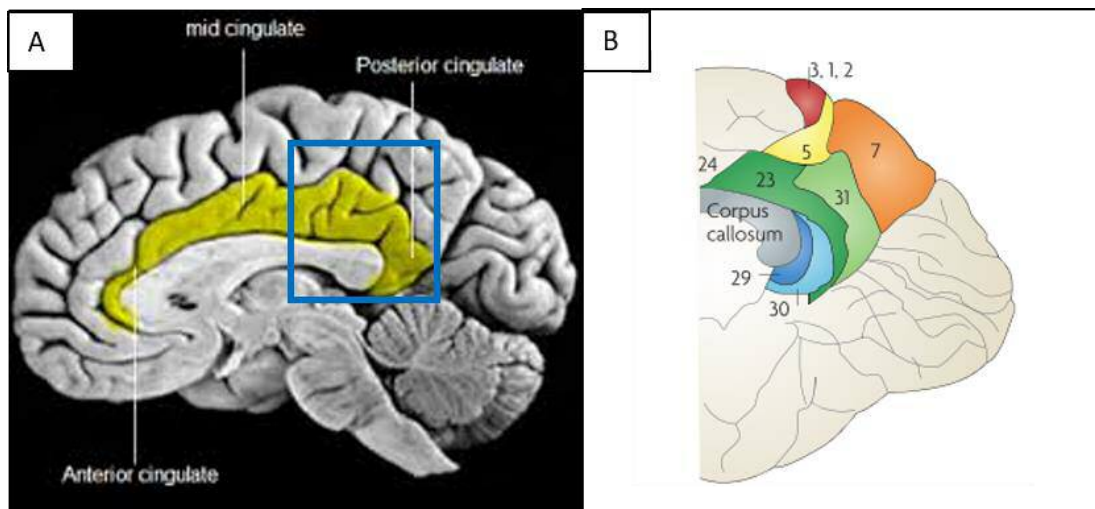


Figure 1.3: PCC neuroanatomy. (A) Location of the PCC at the posterior end of the cingulate gyrus. The cingulate gyrus is shown in yellow, and the PCC is shown within the blue square (image adapted from <http://www.cis.jhu.edu/data.sets/>) (B) Posteromedial cortex regions. PCC regions are shown in green, retrosplenial cortex regions are shown in blue, and precuneus is shown in orange. Numbers correspond to the Brodmann areas (image taken from Vann et al., 2009).

Little is known about the function of the PCC from traditional neuropsychology studies, lesion studies and animal studies. Lesion studies of the PCC in humans are not very common (Leech & Sharp, 2013), and in the few that exist, the damage in this region that resulted from stroke was extensive and affected neighbouring cortical regions (such as retrosplenial cortex and precuneus) and white matter connections (such as the fornix). These studies suggested that such damage was associated with deficits in spatial

navigation, termed topographical disorientation. For example, patients described losing the ability to navigate from point A to point B (Suzuki, Yamadori, Hayakawa, & Fujii, 1998; Takahashi, Kawamura, Shiota, Kasahata, & Hirayama, 1997; Takahashi & Kawamura, 2002). However, it is difficult to understand the specific role of the PCC from these studies, since the retrosplenial cortex, precuneus and fornix have also been implicated in spatial navigation.

A strategy to address this is to perform lesion studies in animals, where the region of damage can be more carefully controlled experimentally. A limitation of this however is that rodents do not have a homologous PCC region to humans, and instead have a larger retrosplenial cortex (Vann et al., 2009). Macaques do have a homologous PCC region (von Bonin & Bailey, 1947), however lesion studies in macaques are rare, due to there being much smaller numbers of macaque studies than rodent studies in general, and due to the medial and deep location of the PCC which makes it practically difficult to lesion (Pflugshaupt et al., 2014). In addition, although the lesion sites are more controlled in macaques than in humans, they are still not highly informative as to the specific function of the PCC, as again the lesions covered a larger region than the PCC. For example, the area encompassed by the lesion included the midcingulate cortex as well as the PCC (Mansouri, Buckley, Mahboubi, & Tanaka, 2015) or the whole of the cingulate cortex (Parker & Gaffan, 1997). The lack of availability and specificity of PCC lesion models has likely had an impact on why the role of the PCC is not well understood.

1.3.2 Connectivity

The PCC is a densely connected brain region. This has been demonstrated in humans using diffusion tensor imaging (DTI) to map the white matter connections associated with the PCC. These studies show that PCC is structurally connected to the MTL via the parahippocampal cingulum, and to the prefrontal cortex via the cingulum bundle (see Figure 1.4B) (Greicius, Supekar, Menon, & Dougherty, 2009; Jones, Christiansen, Chapman, & Aggleton, 2013). Retrograde and anterograde tract tracing studies in macaques, who have a homologous PCC region to humans, support this gross structural connectivity pattern, as well as detecting further smaller connections not easily detectable via DTI in humans. For example, the PCC has dense reciprocal connections with other regions within the PMC (retrosplenial cortex and precuneus, as

shown in the green box in Figure 1.4B), and also with more distal regions, including the thalamus, anterior cingulate cortex, entorhinal cortex and subiculum (Parvizi, Hoesen, Buckwalter, & Damasio, 2006) (see Figure 1.4B).

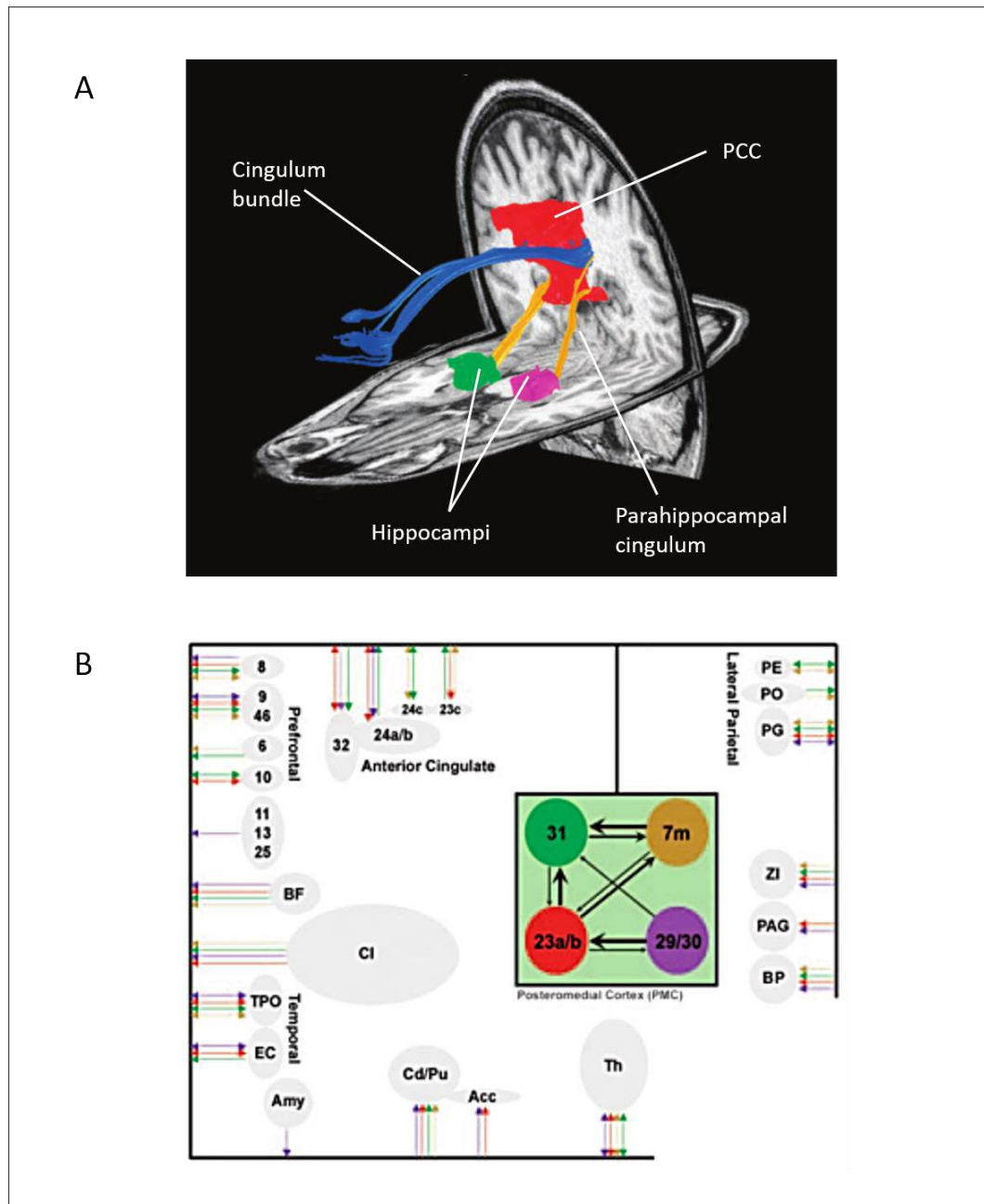


Figure 1.4: The connectivity of the PCC and the PMC. (A) White matter tracts in humans, using DTI. The red region represents the PCC, the blue tract shows the cingulum that connects the PCC to the prefrontal cortex, and the orange tracts show the parahippocampal cingulum that connects the PCC to the hippocampi, shown in green and purple (image taken from Greicius et al., 2009). (B) The connectivity of the PMC in the macaque. The PMC regions are highlighted in the green box where the PCC is represented as areas 31 and 23a/b, the retrosplenial cortex as area 29/30 and precuneus as area 7m (image taken from Parvizi et al., 2006).

1.3.3 Metabolism and Function

In addition to being a highly structurally connected brain region, the PCC is one of the most metabolically active brain regions at rest. This was identified using PET to measure oxygen consumption (oxygen extraction fraction, OEF) in the brains of participants who were at rest in the scanner (i.e. not performing any cognitive task). Rather than a random pattern of brain activity at rest, all participants showed a consistent network of brain regions that were highly metabolically active at rest, with the PCC showing one of the highest levels of metabolism (Raichle et al., 2001) (see Figure 1.5).

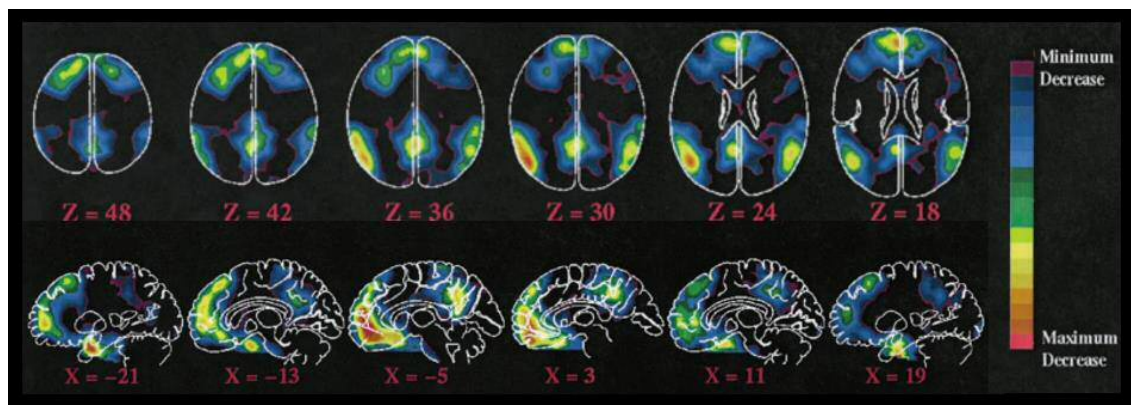


Figure 1.5: Regions of high metabolic activity at rest, which constitute the default network. These are regions that show a higher level of activity during the resting state (i.e. absence of a task) than during a task (image adapted from Raichle et al., 2001).

The observation that the PCC shows high metabolic activity at rest, and that it is a highly connected brain region have led to the proposal that the PCC is a key hub region in the brain's default mode network (DMN), more recently termed the default network (DN). The DN is a network of brain regions that are active at rest (i.e. in the absence of an externally applied task), and that deactivate during a task (Raichle et al., 2001). Other regions in the DN include the medial prefrontal cortex, inferior parietal lobe, and lateral temporal cortex (see Figure 1.5) (Buckner, Andrews-Hanna, & Schacter, 2008; Raichle et al., 2001). The term "hub" refers to a part of the brain that is central within a network, and makes strong contributions to the global network function (van den Heuvel & Sporns, 2013). Evidence in support of the PCC, and neighbouring precuneus, being a key

DN hub comes from their dense connectivity with many other regions in the network (as discussed in Section 1.3.2, e.g. Greicius et al., 2009; Parvizi et al., 2006), and the finding that their level of activity modulates activity in interconnected brain areas (Fransson & Marrelec, 2008; Hagmann et al., 2008; Utevsky, Smith, & Huettel, 2014).

Early studies into the DN suggested that this network of regions were “task-negative” regions, meaning that they were active in the absence of a task. This activity then decreased during application of a goal-directed task. For example, an early study into the DN and task-induced deactivation in this network (defined as areas that show higher levels of blood flow during rest than during the task of interest) identified lower activity in the PCC (and other DN regions) during an auditory control task compared to rest (i.e. there was a deactivation in these areas during the task compared to during rest) (Mckiernan, Kaufman, Kucera-Thompson, & Binder, 2003). Moreover, the task had three levels of difficulty, and it was found that the magnitude of the deactivation was greatest for the most difficult level of the task. Authors suggested the decrease in activity during the task conditions represented a “reallocation of mental resources” from the areas in which task induced deactivation occurs to areas involved in task performance, which increased as the task requirements increased, which they described as a “suspension of internal processing” that occurs in the resting state in order for the brain to perform a task (Mckiernan et al., 2003).

This traditional view that the PCC deactivates during any cognitive task has been challenged, however, and is now considered too simplistic. Instead, other studies have shown that PCC is actually active during certain cognitive tasks, including autobiographical memory, prospection, scene construction, spatial navigation, imagining the self in a different spatial location, and theory of mind tasks (Hassabis & Maguire, 2007; Spreng, Mar, & Kim, 2008; Guterstam, Björnsdotter, Gentile, & Ehrsson, 2015). These findings have led some authors to propose an alternative account of PCC function, according to which the PCC is actively engaged during internally-directed cognition, with autobiographical memory, scene construction, prospection and navigation being examples of such internal thought processes (Andrews-Hanna, 2012).

An additional level of complexity is introduced, however, when one considers that both activation and deactivation of the PCC appears to be important for successful episodic memory. Studies have shown that the PCC is *deactivated* during encoding and *activated* during retrieval; furthermore the magnitude of deactivation during encoding

predicts the magnitude of activation during retrieval, and also behavioural performance in the memory task (Daselaar et al., 2009; Huijbers et al., 2012; Vannini et al., 2011).

There is still, therefore, not a clear consensus, for the circumstances under which the PCC is activated or deactivated, and what role such alterations in brain activity play in cognition (Leech, Braga, & Sharp, 2012; Leech & Sharp, 2013). It is intriguing that several of the cognitive tasks associated with higher PCC activity are cognitive functions that AD patients are impaired on, such as autobiographical memory, episodic memory, spatial navigation and scene construction (Cushman, Stein, & Duffy, 2008; Irish et al., 2015; Lithfous, Dufour, & Després, 2013). Thus, improving our understanding of the function and activity profile of the PCC in tasks that are sensitive to cognitive impairments in AD would contribute to knowledge on the PCC in the healthy brain and also enhance understanding of the changes seen in this region in AD (as discussed in the next section).

1.4 Posterior cingulate cortex in Alzheimer's disease

This section returns to how the PCC is affected in AD and its prodromal stages (pre-symptomatic FAD mutation carriers and MCI), and thus why the PCC is a good candidate region to study using neuroimaging in young *APOE-E4* carriers. By discussing what measures are altered in AD, we can identify what measures might be sensitive to detect alterations in PCC function in individuals who possess the *APOE-E4* allele.

1.4.1 Metabolic alterations

As introduced in Section 1.2, the PCC is an area of increasing interest to AD researchers given evidence that it is the site of the earliest metabolic change in the disease (Minoshima et al., 1997). For example, using FDG-PET, Minoshima et al., (1997) compared glucose metabolism in the brains of patients who had a diagnosis of probable AD, patients with memory impairment without a current diagnosis of AD, but who went

on to develop AD at follow up (so called very early AD patients), and age matched healthy controls. As discussed in Section 1.3.3, the study revealed that the PCC was highly metabolically active in the healthy controls. The study also found that the PCC was the first region to show a decrease in glucose metabolism in the very early AD patients, with metabolism decreasing steadily in AD patients as cognitive decline worsened (as assessed using the Mini Mental State Examination) (see Figure 1.6).

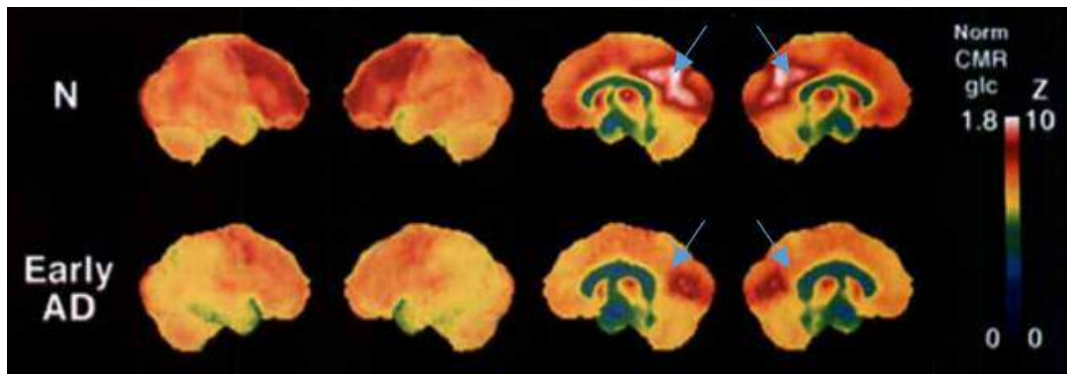


Figure 1.6: Comparison of glucose metabolism during the resting state in healthy controls (top row) and very early AD patients (bottom row). The hotter the colour, the higher the level of glucose metabolism. The PCC region (blue arrows) is highly metabolically active in controls, which is much lower in early AD (image adapted from Minoshima et al., 1997).

Further evidence in support of the PCC being the site of the earliest metabolic change in AD comes from an FDG-PET study of FAD mutation carriers, aged 35-49 years, studied prior to the onset of cognitive symptoms. FAD mutation carriers, compared to age-matched healthy controls, had 20% lower glucose metabolism in the PCC compared to the controls. Moreover, this study suggested that PCC metabolic change is one of the very earliest precursors to disease as there were no MTL volume difference between carriers and non-carriers at this time point (Mosconi et al., 2006).

Metabolic changes in the PCC are also evident in AD and MCI using proton magnetic resonance spectroscopy (^1H -MRS). MRS is a non-invasive *in vivo* neuroimaging technique able to detect and quantify certain metabolites and neurotransmitters in a specified brain region (termed the MRS voxel) (Stagg & Rothman, 2014). MRS has the advantage over FDG-PET that it is non-invasive as it does not require an injection of a

radioactive isotope. The most commonly studied metabolites that can be measured using MRS and what they represent are listed in Table 1.1. The most consistent finding in MRS studies of the PCC in AD patients is that there is a decrease in the neuronal marker N-acetyl-aspartate (NAA) and an increase in the glial marker myo-inositol (mI). For example, an early study of MRS in AD by Kantarci et al., (2000) assessed MRS metabolites in voxels placed in the PCC, superior temporal lobe and occipital lobe of AD patients, MCI patients and age-matched controls (see Figure 1.7A) (Kantarci et al., 2000). The authors chose these voxels because neurofibrillary pathology affects these regions at different stages, with the PCC and superior temporal lobe suggested to be affected relatively early and the occipital lobe affected late (Braak & Braak, 1991, 1995). The study found that the PCC of AD patients had a lower concentration of NAA and a higher concentration of mI than controls and MCI patients, and that MCI patients had a higher concentration of PCC mI than controls. Similarly, there was a lower concentration of NAA in the superior temporal lobe in AD than MCI. There were no metabolite differences in the occipital lobe.

MRS Metabolite	Abbreviation	Metabolite is a marker for:
N-acetyl aspartate	NAA	Neuronal density and integrity
Myo-Inositol	mI	Glial marker, suggests inflammation or gliosis
Creatine	Cr	Energy metabolism
Choline	Cho	Cell membrane turnover/integrity
Glutamate	Glx	Excitatory neurotransmitter
γ -amino-butyric acid	GABA	Inhibitory neurotransmitter

Table 1.1: The most commonly studied metabolites measured using ^1H -MRS, and what they represent.

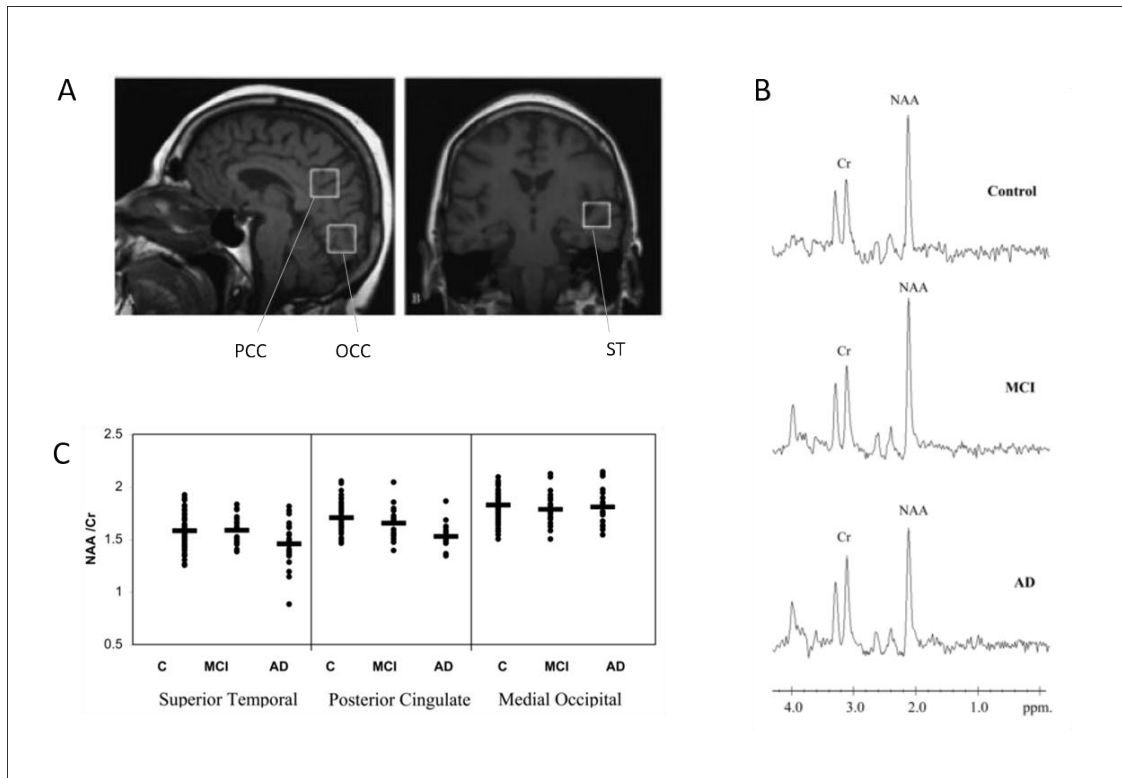


Figure 1.7: MRS study of AD and MCI patients and healthy controls by Kantarci et al., 2000. (A) MRS voxel placements (PCC = posterior cingulate cortex, OCC = occipital cortex, ST = superior temporal lobe). (B) Examples of spectra from the PCC of a control, an MCI patient and an AD patient. (C) The ratio of NAA to the chosen reference metabolite, creatine (Cr), in the three voxels in the three groups of participants. (Images taken from Kantarci et al., 2000).

The PCC MRS finding of lower NAA and higher mI in AD patients has since been replicated several times (Kantarci et al., 2007, 2013; Murray et al., 2014; T. Wang et al., 2012). Although NAA and mI are the most commonly studied metabolites in AD, other reported metabolite changes include a decrease in PCC glutamate (Glx, the primary excitatory neurotransmitter) (Fayed, Modrego, Rojas-Salinas, & Aguilar, 2011), a decrease in PCC GABA (the primary inhibitory neurotransmitter) (Bai et al., 2014), and an increase in choline (Cho) (Kantarci et al., 2000; Walecki, Barcikowska, Ćwikła, & Gabryelewicz, 2011), thought to be a marker of cell membrane integrity, as choline is an important substrate for the phospholipid bilayer constituting the cell membrane (Rae, 2014).

Similar to the FDG-PET findings in prodromal AD, MRS changes are also evident in the PCC in pre-symptomatic FAD mutation carriers, further highlighting that metabolic changes in this brain region are a very early change in AD development. Godbolt et al., (2006), for example, tested PCC MRS in 7 FAD mutation carriers aged between 26 and 49 years compared to age matched controls. The carriers had a decrease in PCC NAA and an increase in PCC mI compared to the controls, and the magnitude of these metabolite changes were correlated with the proximity of age of predicted onset of AD (i.e. larger difference in metabolite concentrations the closer to predicted AD age of onset) (Godbolt et al., 2006).

1.4.2 Activity alterations

Alterations in PCC activity and the network of which it is the key hub (the DN, as introduced in Section 1.3.3) are another consistent finding in AD and MCI patients. This is of interest to AD researchers, as it has been proposed that elevated neuronal activity could be linked to early amyloid deposition (this will be expanded on towards the end of this section). An early study that provided evidence for altered activity in the PCC in AD assessed activity in the DN by using a resting state fMRI scan, comparing this between 13 AD patients and 14 healthy age-matched controls. A decrease in PCC resting-state activity was evident in the AD patients (see Figure 1.8A, which shows areas that are more active in the healthy controls than in the AD group) (Greicius, Srivastava, Reiss, & Menon, 2004). This decrease in PCC activity mirrored the pattern of decreased glucose metabolism in the PCC in the FDG-PET study by Minoshima et al. (1997) described above. A further finding of Greicius et al., (2004) was a lower level of resting-state activity in the hippocampus in the AD group compared to the healthy controls, which was suggested to indicate that altered PCC activity is associated with disrupted connectivity between the PCC and the hippocampus (shown in Figure 1.8B).

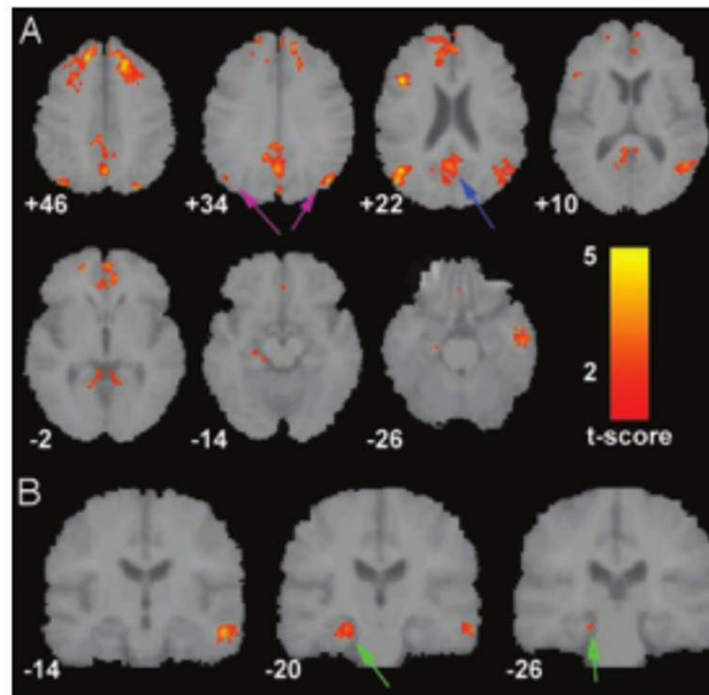


Figure 1.8: Resting state activity alterations in AD compared to healthy aged matched controls. Red areas show regions that are more active in the healthy controls than in the patients. The blue arrow highlights the PCC and the green arrow shows the hippocampus (image taken from Greicius et al., 2004).

Evidence of altered PCC and DN activity during the resting state in AD has been replicated several times (Hafkemeijer, van der Grond, & Rombouts, 2012; Petrella, Prince, Wang, Hellegers, & Doraiswamy, 2007). It has also been detected in MCI: Binnewijzend et al., (2012) studied resting state activity in 43 healthy elderly controls, 39 AD patients, and 23 MCI patients, 7 of which went on to develop AD at follow up and 14 of which remained clinically stable in the MCI phase. They found steadily lower DN functional connectivity in the PCC and precuneus across the four groups in the order of healthy controls, stable MCI patients, MCI patients who converted to AD, and finally AD patients (Binnewijzend et al., 2012).

Not only has PCC activity been found to be altered during the resting state in AD and MCI patients, it is also altered in task-related fMRI studies. For example, Lustig et al., (2003) investigated PCC activity during a word classification task in AD patients and healthy age matched controls, with the aim of comparing the task-induced deactivation in the PCC between groups. The task involved showing participants words in the scanner and asking them to make a semantic classification judgement on whether the item was

living or non-living. This task was intermixed with rest blocks. Compared to activity in the rest blocks, the researchers found that AD patients had less PCC deactivation during the classification task than non-patients (Lustig et al., 2003).

A similar pattern of a “failure to deactivate from the DN” has also been found in MCI patients; for example, this was reported in an fMRI study comparing brain activity in healthy older controls, MCI patients and AD patients during a face-name encoding task (Pihlajamäki & Sperling, 2009). fMRI activity between the task and a fixation baseline was contrasted, and revealed that healthy older controls had significant fMRI task-induced deactivation in the PCC, whereas MCI patients showed a smaller area of deactivation in a similar location (see Figure 1.9). By contrast, AD patients did not show a significant deactivation during the task compared to the baseline. Furthermore, PCC activity was correlated with measures of cognitive function (e.g., the mini-mental state examination (MMSE) and Clinical Dementia Rating Scale), with greater deactivation linked to a better score on these tests.

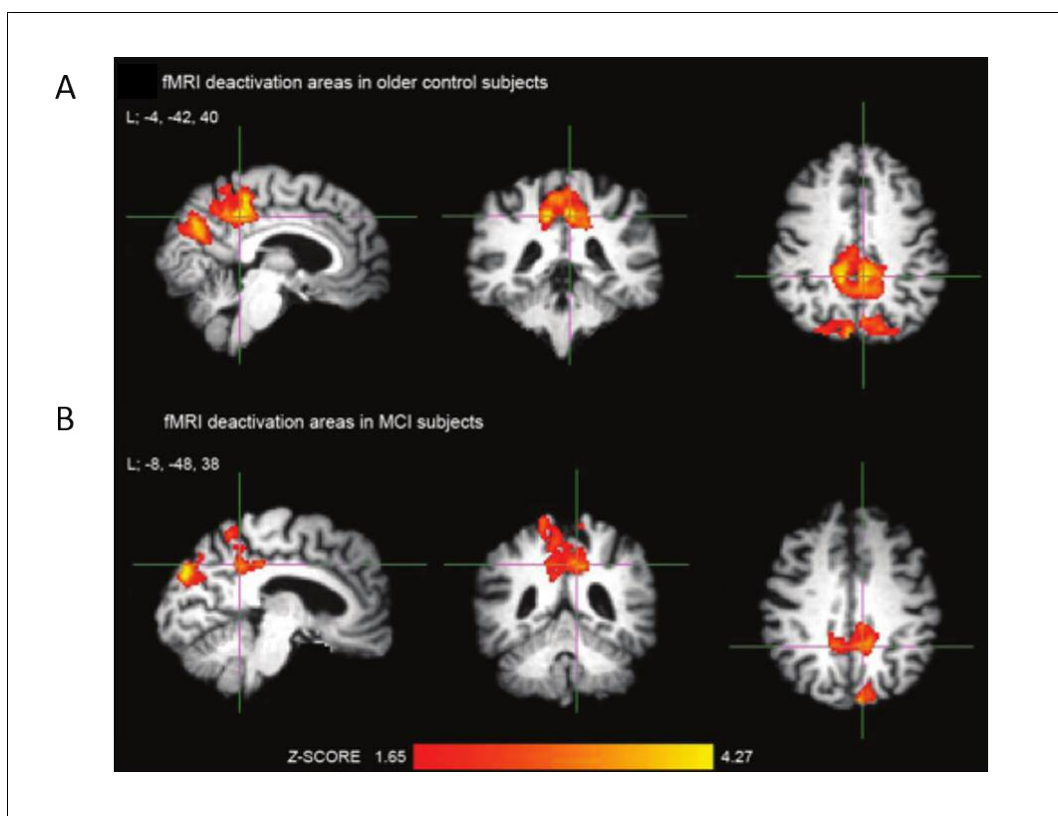


Figure 1.9: fMRI deactivation areas during a face-name association task. There was reduced task-induced deactivation in the PCC in MCI patients (B) compared to healthy older subjects (A) (image taken from Pihlajamäki and Sperling, 2009).

The high level of activity in the PCC/DN in the healthy brain and the altered activation in the PCC in AD and MCI makes the PCC important for understanding risk of AD for three key reasons. First, it has been proposed that the highly active regions within the DN could predispose these regions to amyloid pathology, as there is a strong overlap of DN areas with areas of amyloid deposition (Buckner et al., 2005; Klunk et al., 2004). Evidence in support of this hypothesis comes from the study of DN areas in young healthy participants and comparison with areas of high amyloid deposition in AD patients, the latter measured via PET imaging using [C^{11}] Pittsburgh Compound-B (PIB-PET). Strong convergence between DN regions and amyloid deposition regions was evident (Buckner et al., 2005), a finding that has subsequently been replicated (Seeley, Crawford, Zhou, Miller, & Greicius, 2009). This link is thought to reflect the possibility that high neuronal activity is associated with amyloid synthesis and deposition: for example, in rodents the level of amyloid in the interstitial fluid (ISF) increases following neuronal activity (via electrical stimulation), and decreases when neuronal activity is blocked via application of a sodium channel blocker (tetrodotoxin, TTX) which prevents action potentials (Cirrito et al., 2005). Furthermore, a similar study in an APP transgenic mouse model of AD identified that neuronal activity in regions associated with AD was closely associated with the level of ISF amyloid, which was in turn associated with amyloid plaque deposition, whereas deprivation of neuronal activity decreased amyloid plaque development (Bero et al., 2011). More recently, it has been proposed that amyloid increases when neurons are active because depolarisation of neurons allows intra-neuronal vesicles that contain amyloid precursor protein (APP) and the enzyme that cleaves APP (BACE-1) to merge (Das et al., 2013). Thus, high resting state PCC activity over the lifespan could predispose the PCC to AD pathology, and in turn impact on brain regions highly connected with this hub area (e.g., MTL).

Secondly, as discussed in Section 1.3.3, PCC deactivation during certain tasks impacts on behavioural performance, which is of clinical relevance for the emergence of cognitive deficits in AD. For example, participants who show greater task-induced PCC deactivation during encoding also show greater task-induced PCC activation during retrieval (Daselaar et al., 2009; Vannini et al., 2011). Moreover, a greater deactivation and subsequent activation predicted better memory performance (Daselaar et al., 2009; Vannini et al., 2011). PCC deactivation could be of clinical relevance given the memory impairment in AD, and given the findings of a failure to deactivate from the PCC/DN in MCI and AD patients (Lustig et al., 2003; Pihlajamäki & Sperling, 2009).

Thirdly, activity in the PCC/DN has been linked to MTL activity, which, as previously discussed in Section 1.2, is a brain region clearly implicated in AD. As shown in Figure 1.8B, Greicius et al., (2004) identified that healthy controls show co-activation of the PCC/DN and the hippocampus, and that AD patients show a decrease in activity in both regions. They suggested that the functional connectivity between the PCC and hippocampus is affected in AD. Consistent with this, Zhou et al., (2008) demonstrated that the functional connectivity between the PCC and hippocampus is altered in MCI and AD, using fMRI and DTI (Zhou et al., 2008).

Thus, taken together, the PCC is an important brain region in AD research, as it is the site of the earliest metabolic changes in AD, it shows alterations in activity in both AD and MCI, and its activity seems directly linked to success in episodic memory (a core cognitive domain affected in AD). Furthermore, level of activity in the DN (of which the PCC is the core hub region) seems to predispose this region to AD pathology, with higher levels of activity early on in the lifespan potentially resulting in early deposition of amyloid, and in turn cognitive impairment.

1.5 Posterior cingulate cortex in young *APOE-E4* carriers

The studies discussed above provide strong support that the PCC is a key brain area to study in order to better understand the sequence of brain changes associated with AD. As proposed in Section 1.2, one strategy which could enhance understanding of this sequence, is to study this brain region in young *APOE-E4* carriers. Notably, several of the neuroimaging methods applied in AD have already been used to study PCC metabolism and function in young *APOE-E4* carriers.

Similar to the findings from the FDG-PET studies of glucose metabolism in AD patients, the PCC of young *APOE-E4* carriers also shows glucose hypometabolism. In an FDG-PET study of 12 *APOE-E4* heterozygote carriers compared to 15 non-carriers, where the mean age of the participants was 31 years (range 20-39 years), glucose metabolism during rest was found to be lower in the PCC of the young E4 carriers compared with the

non-carriers (Reiman et al., 2004). This PCC area of the glucose hypometabolism in the young *APOE-E4* carriers had close correspondence with that found in AD patients, although it covered a smaller area (see Figure 1.10).

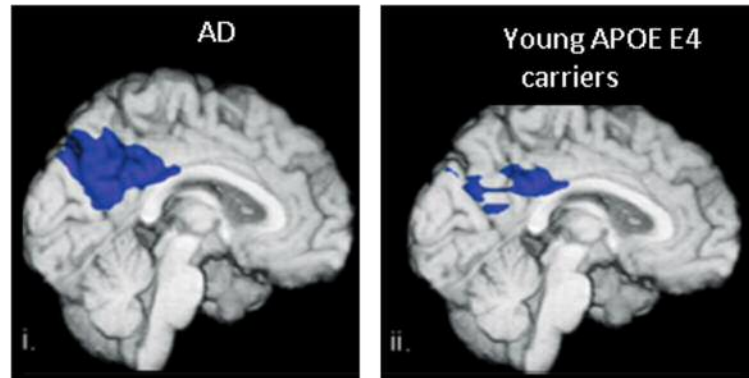


Figure 1.10: Both AD patients (on the left) and young *APOE-E4* carriers (on the right) have decreased glucose metabolism in the PCC area (shown in blue) (image adapted from Reiman et al., 2012).

In addition, and similar to the altered PCC and DN activity seen during rest in AD and MCI patients, resting state PCC activity in young healthy *APOE-E4* carriers is also altered. Filippini et al., (2009) investigated the activity of the DN during the resting state in young *APOE-E4* carriers compared to non-carriers (mean age 29 years, range 18-39 years), and detected a higher level of activity in the PCC/retrosplenial cortex, hippocampus and anterior cingulate areas in the young *APOE-E4* carriers (see Figure 1.11) (Filippini, MacIntosh, et al., 2009).

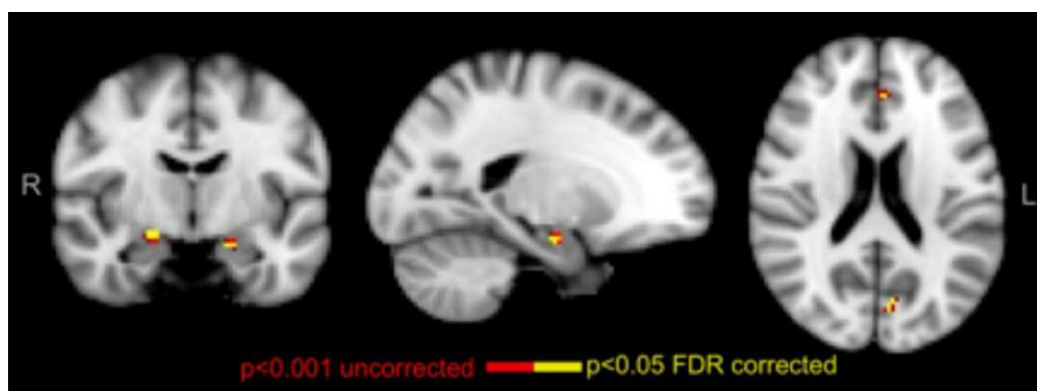


Figure 1.11: Brain regions that show a higher level of activity during the resting state in *APOE-E4* carriers compared to non-carriers. The red/yellow area towards the back of the brain in the image on the right shows the higher level of activity in the PCC/RSC in the young E4 carriers (image taken from Filippini et al., 2009).

As well as alterations in task-free (resting state) PCC activity in young *APOE-E4* carriers, task-induced PCC activity also shows critical differences. To maximise the sensitivity to detect any early alterations in brain activity in young *APOE-E4* carriers, a recent study in our lab applied cognitive paradigms sensitive to behavioural changes in AD to test task-induced fMRI activity in the PCC of young *APOE-E4* carriers compared to non-carriers (mean age 19 years) (Shine, Hodgetts, Postans, Lawrence, & Graham, 2015). The paradigms included were a working memory task and an oddity perception task, both of which contrasted different stimuli conditions, with the prediction that *APOE-E4* carriers would be particularly affected when undertaking perception and short-term memory for scenes, compared to non-scene stimuli. This hypothesis was based on evidence that AD patients show a category-sensitive impairment on scene oddity (A. C. H. Lee et al., 2006; A. C. H. Lee, Levi, Davies, Hodges, & Graham, 2007) and on scene short-term memory conditions (Bird et al., 2010; Pengas, Patterson, et al., 2010). Furthermore the focus on the scene categories of the two paradigms here also stems from the recent account in the memory literature that different cognitive domains (e.g. memory, perception and working memory) rely on the same underlying category-specific representations in the brain. Importantly, the representations for complex scenes are proposed to form a scaffold for memory (Graham, Barense, & Lee, 2010). Since memory, scene perception and scene working memory impairments are evident in AD, it was hypothesised that the scene category may be particularly sensitive to detect any alterations in activity in the young *APOE-E4* carriers.

To test this, Shine et al., (2015) first compared activity elicited in young *APOE-E4* carriers and non-carriers during a 1-back working memory task for the experimental conditions of scenes, faces, objects and scrambled objects versus the baseline condition of rest. This revealed that young *APOE-E4* carriers showed a reduced level of deactivation in PCC for the contrast scenes>rest compared to non-carriers, and this was specific to the scene condition as there was no difference between carriers and non-carriers for the other conditions vs rest (see Figure 1.12 A and B). Using this same PCC area as a region-of-interest (ROI), activity elicited during odd-one-out judgements for scenes, faces and objects (against a baseline size discrimination condition, see Figure 1.12C) was compared across *APOE-E4* carriers and non-carriers. Young *APOE-E4* carriers again showed a smaller degree of deactivation compared to baseline for the scene condition (see Figure 1.12D). Consistent with evidence of a failure to deactivate the PCC/DN in AD and MCI (as discussed in Section 1.4.2) the authors proposed that these findings could provide evidence of a similar difficulty deactivating the PCC during scene

perception and memory tasks, especially those sensitive to the very earliest behavioural impairments in AD (A. C. H. Lee et al., 2006, 2007).

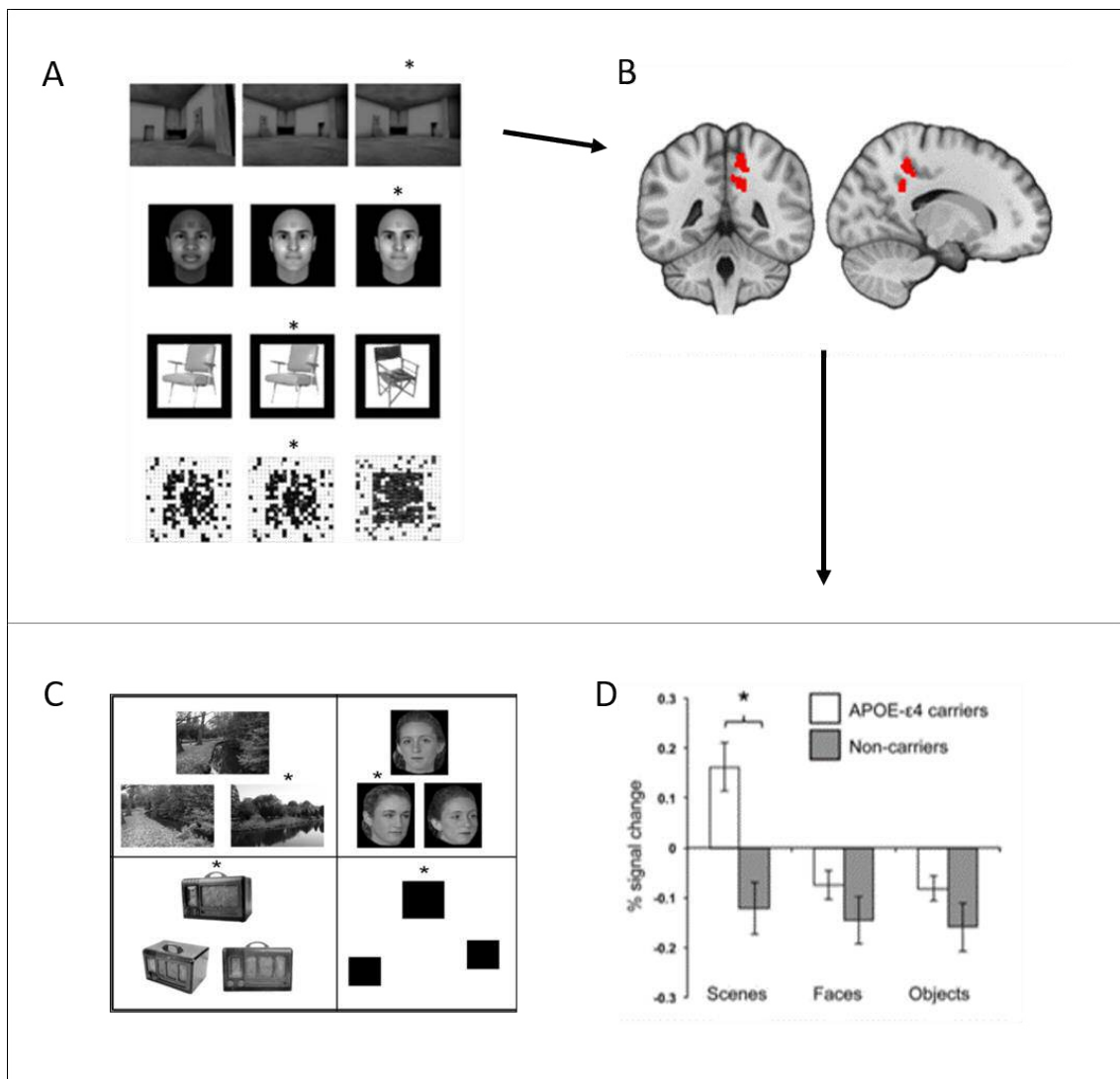


Figure 1.12: Investigation of PCC activity in young *APOE-E4* carriers vs non-carriers during a working memory task and a perception task. (A) The design of the working memory paradigm. Participants were shown a series of scenes, faces, objects and scrambled objects, and were asked to press a response button when the item was identical to that one trial previously (i.e. 1-back working memory task). When activity during each category was contrasted with rest, and compared between the *APOE-E4* carriers and non-carriers, this revealed the brain region shown in (B) to have higher activity in the carriers during the scene condition only. There were no activity differences between groups for the three other stimuli conditions. (C) The design of the oddity perception task. Participants were shown either three scenes, faces, objects, or squares. Two of the images were the same but from a different viewpoint, and the third image was the odd-one-out. Participants were asked to select the odd one out. (D) The BOLD percent signal change in the same ROI as identified in the scene working memory task when each stimuli category in the odd-one-out task was compared to the baseline condition of size. This revealed a more positive level of activity that was specific to scenes in the young E4 carriers, whereas there was no significant differences in activity for the other conditions of faces or objects between *APOE-E4* carriers and non-carriers. (Images adapted from Shine et al., 2015).

1.6 Key questions to be addressed in this thesis

Higher activity in PCC in young *APOE-E4* carriers in response to the visual category, and the same paradigms, that AD patients show impairments is intriguing, and raises the questions about the mechanisms or biological influences that lead to this brain activity alteration. One avenue of research that has not yet been explored in *APOE-E4* carriers at this age is whether this brain activity alteration in PCC is linked to differences in metabolites, as assessed using MRS.

The rationale behind this hypothesis is as follows. Firstly, two recent studies have demonstrated that PCC activation and deactivation are associated with the concentration of PCC GABA and Glx, as measured by MRS (Hu, Chen, Gu, & Yang, 2013; Kapogiannis, Reiter, Willette, & Mattson, 2013). The study by Kapogiannis et al., (2013) tested how the functional connectivity of the DN (measured from a resting state fMRI scan) was associated with concentrations of PCC GABA and Glx, and identified a positive relationship between DN functional connectivity and Glx, and a negative relationship between DN functional connectivity and GABA (Kapogiannis et al., 2013). The second study by Hu et al. (2013) investigated the relationship between PCC GABA and Glx and PCC BOLD during an n-back working memory task. A similar n-back task had been used previously to investigate PCC BOLD activity and showed that when working memory demand increased, the level of PCC deactivation also increased (i.e. more negative BOLD response with increasing task demands) (Esposito et al., 2009). The study by Hu et al. (2013) identified this same pattern of BOLD results in the PCC, where there was a larger deactivation when participants performed a more difficult working memory condition compared to the baseline condition (e.g., the contrast 3back > 0back), but also demonstrated that a larger PCC deactivation (i.e. a more negative PCC BOLD response) was associated with a higher concentration of PCC GABA, and that a smaller PCC deactivation (i.e. a more positive PCC BOLD response) was associated with a higher concentration of PCC Glx (Hu et al., 2013). Overall, these two studies suggest that individual differences in the concentrations of PCC GABA and PCC Glx are related to individual differences in the PCC BOLD response.

A second reason that PCC MRS could be altered in young *APOE-E4* carriers is that MRS alterations are evident in the PCC in AD, MCI, and also older *APOE-E4* carriers. As discussed in Section 1.4.1, both PCC GABA and Glx are affected in AD, where patients show a lower concentration of both metabolites compared to healthy age matched

controls (Bai et al., 2014; Fayed et al., 2011). Alterations are also present in other metabolites, including a decrease in PCC NAA, and an increase in PCC ml (Kantarci et al., 2000, 2007; Walecki et al., 2011). Furthermore, MRS metabolite alterations have been detected in the PCC of older healthy carriers of the *APOE-E4* allele (aged > 50yrs). Although there have only been a few studies, and the results are not very consistent, the PCC metabolite alterations observed in *APOE-E4* carriers aged over age 50 (compared to non-carriers) include a decrease in NAA and creatine (Cr) and an increase in ml and Cho (Gomar et al., 2014; Laakso et al., 2003; Riese et al., 2015).

In further support of my hypothesis that altered PCC BOLD in the young *E4* carriers could be associated with altered PCC biochemistry, an FDG-PET study detected glucose hypometabolism in a similar brain region to the PCC ROI identified in Shine et al., (2015) (see Figure 1.10) (Reiman et al., 2004). In addition, post mortem studies of the PCC of young *APOE-E4* carriers have detected alterations in enzymes involved in energy metabolism (e.g., a decrease in the enzyme cytochrome oxidase C in the PCC of young *E4* carriers (Valla et al., 2010)). This enzyme is part of the mitochondrial electron transport chain required for oxidative respiration. A further study by the same group identified alterations in additional energy metabolism pathways, including alterations in glucose transporter levels, enzymes involved in a glucose metabolism and ketone metabolism, and additional complexes of the mitochondrial electron transport chain identified in their 2010 study (Perkins et al., 2016). The authors proposed that there is a dysregulation of energy metabolism in the PCC of young *APOE-E4* carriers, suggesting that alterations in brain metabolism could contribute to these individuals' risk for developing AD. Together, FDG-PET and post mortem studies offer compelling evidence that there are biochemical alterations in the PCC in young *E4* carriers at a similar age to those individuals who showed brain activity differences in PCC during scene processing in Shine et al., (2015).

Thus there are several factors in support of the rationale that altered PCC BOLD could be linked to altered PCC metabolites in the young *APOE-E4* carriers. Chapter 5 of this Thesis addresses this by comparing PCC MRS metabolites between young *APOE-E4* carriers and non-carriers. The PCC BOLD alterations in the young *APOE-E4* carriers in Shine et al. (2015), however, were only evident on the scene conditions of the perception and working memory tasks. Therefore, prior to testing whether there are differences in PCC metabolites between young *APOE-E4* carriers and non-carriers, in Chapters 3 and 4 I will assess whether individual differences in PCC BOLD, elicited during *scene* perception

and *scene* working memory paradigms, are related to individual differences in PCC metabolites (i.e. there is a relationship between PCC BOLD for scenes with PCC MRS measures, but not for other categories of stimuli such as faces or objects). To be consistent with my hypothesis that altered PCC BOLD for scenes in the *APOE-E4* carriers is related to altered PCC MRS, I predict that there will be a category-sensitive relationship between PCC BOLD and PCC MRS metabolites for the scene conditions of the two tasks used in Shine et al., (2015).

1.6.1 Aims of this thesis and overview of Chapters

This thesis contains three experimental Chapters to address the research questions raised above. The first two experimental Chapters (Chapters 3 and 4) have been designed to address whether PCC BOLD-MRS relationships exist for scene, but not non-scene, conditions applied in the two paradigms used in Shine et al, (2015). These studies also allow me to understand which MRS metabolites might be most sensibly studied in Chapter 5, which asks whether there are differences in PCC metabolites between young *APOE-E4* carriers and non-carriers. In addition to assessing whether there are scene-sensitive BOLD-MRS relationships in the PCC, the first two experimental Chapters also aim to expand understanding of the role and activity profile of the PCC ROI in the healthy brain. As previously stated, this is still not well understood, despite this region being recognised as an important brain region in AD. By assessing the relationship between PCC BOLD and behavioural performance on the two tasks, I can better understand how the PCC is contributing to successful perception and working memory.

In summary, the structure of this thesis is as follows:

Chapter 2 provides an overview of MRS and fMRI methods applied in this thesis, specifically how these methods work and how we can combine measures obtained from these neuroimaging techniques to investigate functional-biochemical relationships in the brain.

Chapter 3 uses the oddity fMRI task reported in Shine et al., (2015) to investigate in more detail the PCC BOLD response during the perception of scenes, faces and objects,

in particular whether the PCC ROI shows a category sensitive response, whether there is a relative activation or deactivation between the different stimuli conditions, and the potential relationship between PCC BOLD and behavioural performance on this task. Collection of PCC MRS data alongside fMRI facilitates assessment of whether individual differences in PCC MRS metabolites are associated with individual differences in PCC BOLD for scene perception, but not face or object perception.

Chapter 4 applies an fMRI paradigm similar to the working memory paradigm used in Shine et al., (2015), but focused on scenes (rather than comparison with other visual categories). Based on the spatial working memory task used in Lee et al., (2010), the experiment involves a 2x2 design modulating working memory load alongside spatial complexity (scenes and shapes). Increasing working memory load has been found to elicit a greater level of deactivation in the PCC in several previous studies (Ceko et al., 2015; Esposito et al., 2009; Hu et al., 2013). This 2x2 design, therefore, allows me to investigate how increasing working memory demands for different categories of spatial complexity influences PCC activity, and how in turn that relates to behavioural performance on the task. As for Chapter 3, MRS will also be correlated with PCC BOLD to investigate BOLD-MRS relationships for the scene compared to non-scene category, to identify whether individual differences in PCC MRS metabolites are associated with individual differences in PCC BOLD for scene, but not shape working memory.

Chapter 5 moves on to ask whether there is any evidence of MRS metabolite differences in the PCC of young *APOE-E4* carriers and non-carriers, applying MRS methods used in Chapters 3 and 4.

Chapter 6 concludes this thesis by bringing together the results from all experimental Chapters, discussing the implications of these findings, some methodological limitations, and how future studies could be developed to extend the findings of the experiments outlined in the three experimental chapters.

2 Chapter 2: General Methods

To address the questions outlined at the end of Chapter 1, this thesis will use magnetic resonance spectroscopy (MRS) and functional magnetic resonance imaging (fMRI). Augmenting the brief summary of these methods in Chapter 1, here I provide a more detailed description of each approach, and how fMRI and MRS can be combined to study functional-biochemical relationships. I also highlight some relevant methodological considerations and how these are addressed in this thesis, for example the use of a reference for metabolite quantification in MRS, and different approaches to quantify the BOLD signal for correlation with MRS metabolites. This Chapter additionally outlines literature informing my decision around the best metabolites for these MRS-BOLD correlations.

2.1 Magnetic Resonance Spectroscopy (MRS)

MRS is a non-invasive neuroimaging technique used to detect and quantify metabolites in a specified region of the brain *in vivo*. Each metabolite produces a unique MRS-signal, which arises from the different spin frequencies (known as resonance frequencies) that the protons within that molecule experience. This signal is plotted on a spectrum, with the x-axis indicating the frequency and the y-axis indicating the amplitude of the signal. Each metabolite's signal is proportional to its abundance within a measured brain region, so can be quantified by calculating the area under its peak (Stagg & Rothman, 2014).

There are three main types of MRS, which use different protons: ^1H -MRS, ^{13}C -MRS and ^{31}P -MRS (hydrogen, carbon and phosphorous respectively). This thesis uses ^1H -MRS, and the following explanations will refer to this MRS approach only. In addition, where the abbreviation MRS has been used throughout this thesis, this refers to ^1H -MRS.

2.1.1 How does MRS work?

MRS uses the phenomenon of nuclear magnetic resonance (NMR) (Bloch, Hansen & Packard, 1946; Purcell & Torrey, 1946), in which a hydrogen proton spins (or precesses) on its axis, which produces a small current, and in turn, a small magnetic field perpendicular to the direction of the current. Under normal circumstances the direction of the magnetic fields of these protons are random and so cancel each other out, however, when placed in a strong magnetic field, such as the 3-Tesla magnet of an MRI scanner (which is 60,000 times stronger than the Earth's magnetic field), these protons align with the magnetic field. The frequency of the proton spins under this magnetic field is governed by the Larmor equation, where frequency = gyromagnetic ratio x external magnetic field, (or $f = \gamma B_0$) (Huettel, Song, & McCarthy, 2009).

A hydrogen proton on its own has a resonance frequency (the frequency of its spin) known as the Larmor frequency (42.58MHz/T). The principle behind MRS is that there is a slight variation in the resonance frequency of hydrogen protons within different molecules depending on their chemical environment (i.e. the bonds the protons form within a molecule). This effect comes about from the concepts of chemical shift and J-coupling. In chemical shift, protons experience different extents of shielding by electrons within a molecule. More specifically, when an electron cloud is drawn more towards a hydrogen proton (i.e. increased shielding), the frequency of the spin decreases; when it is drawn away from a proton (i.e. decreased shielding) the spin frequency increases. J-coupling arises from there often being more than one type of chemical environment for hydrogen protons within a molecule (i.e. hydrogen protons could be part of a CH₃ group, an NH₂ group, a COOH group, etc.). Each of these types of hydrogen environments will result in a different resonance frequency of the hydrogen protons at that site. These signals produce a "spectroscopic fingerprint" for each molecule. As each molecule has a different chemical structure, different molecules can be discriminated from each other based on these different fingerprints (Stagg & Rothman, 2014).

Although MRS can be applied to measure many different molecules, in practice we use it to measure between 15 and 20 molecules within the human brain. This is because there needs to be a large enough concentration of a metabolite present for MRS to successfully detect and quantify a metabolite, and only a small number of metabolites are

present in sufficient quantity to be detected. Water is by far the most abundant source of hydrogen protons within the human brain, producing a very large signal in an MRS spectrum which vastly overshadows the signals from the other metabolites (shown in Figure 2.1B). The metabolites that are detectable in human brain are all at the millimolar level, which is approximately $10^3 - 10^4$ times lower than the concentration of water (Stagg & Rothman, 2014). As MRS studies are interested in the concentration of metabolites rather than water, water suppression is required to visualise the spectra from these other metabolites. An example of a common water suppression method is the CHEMical Shift-Selective method (CHESS) (Haase, 1986). CHESS involves applying a radio-frequency (RF) pulse that has the same frequency as water, to selectively excite the protons that make up the water peak. This causes the water signal to be minimized, while the metabolite signals are unaffected so these can be visualised (depicted in Figure 2.1 B and C).

MRS is able to measure the concentration of metabolites within a specified volume (or voxel) of interest within the brain, which is an approach termed single voxel spectroscopy (SVS). The selection of this MRS voxel is achieved through the application of three radiofrequency (RF) pulses that are at frequencies that match a certain position of the gradients applied to the magnetic field in the x, y and z directions. These RF pulses are able to select a single slice in each plane, and the intersection of these slices is the region where the signal from the spin frequencies of the protons are measured (Stagg & Rothman, 2014) (see Figure 2.1A).

2.1.2 Metabolites assessed via MRS

The metabolites that can be most accurately measured using MRS are N-acetyl-aspartate (NAA), creatine (Cr), choline (Cho), myo-inositol (mI), and the neurotransmitters glutamate (Glx) and γ -amino-butyric acid (GABA). The signals from each of these metabolites in a MRS spectrum are displayed in Figure 2.2. Chapter 1 provided a brief overview of these metabolites, and the next section expands on what each metabolite represents.

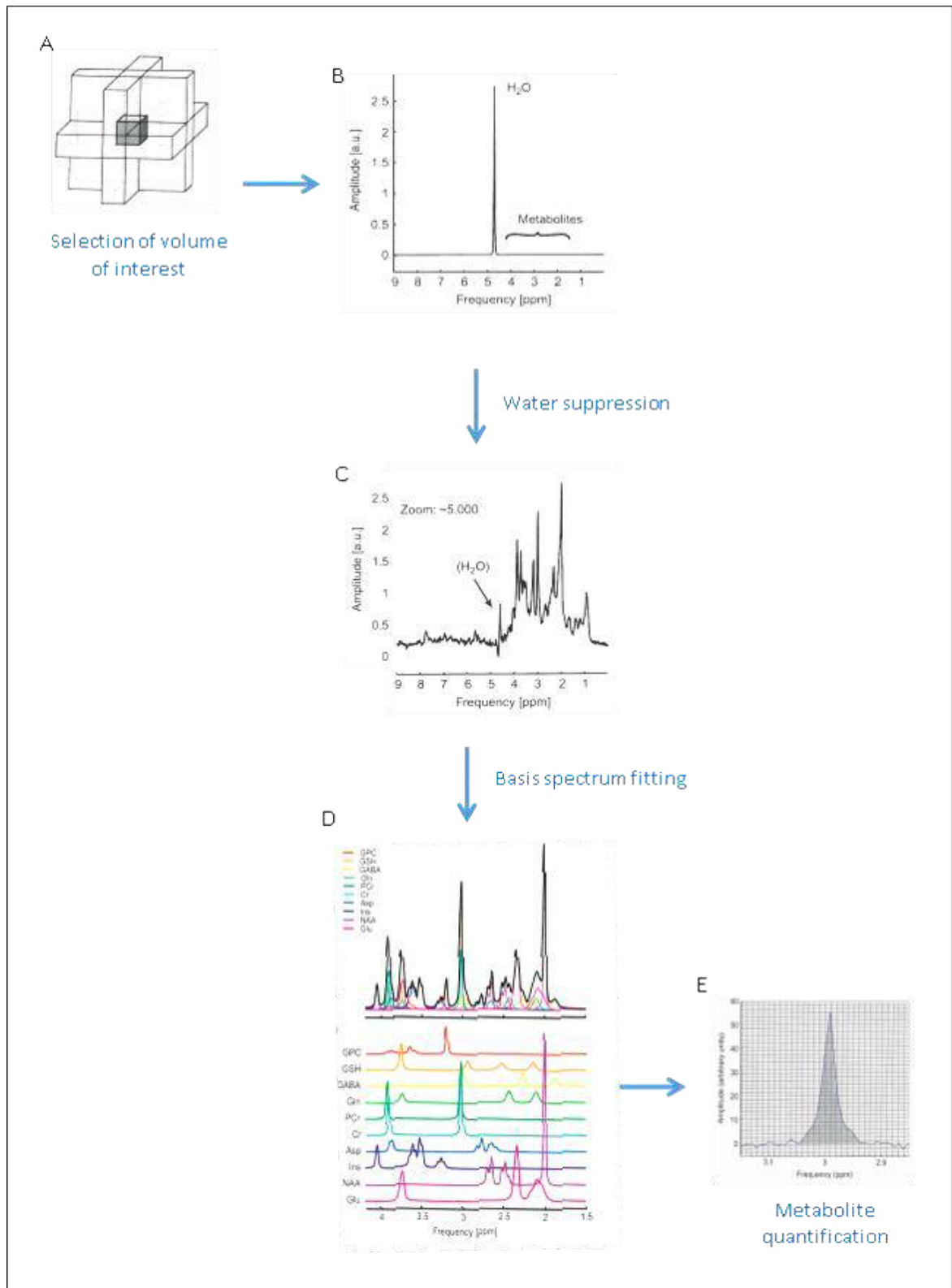


Figure 2.1: MRS scanning and analysis pipeline (images adapted from Stagg and Rothman, 2014).

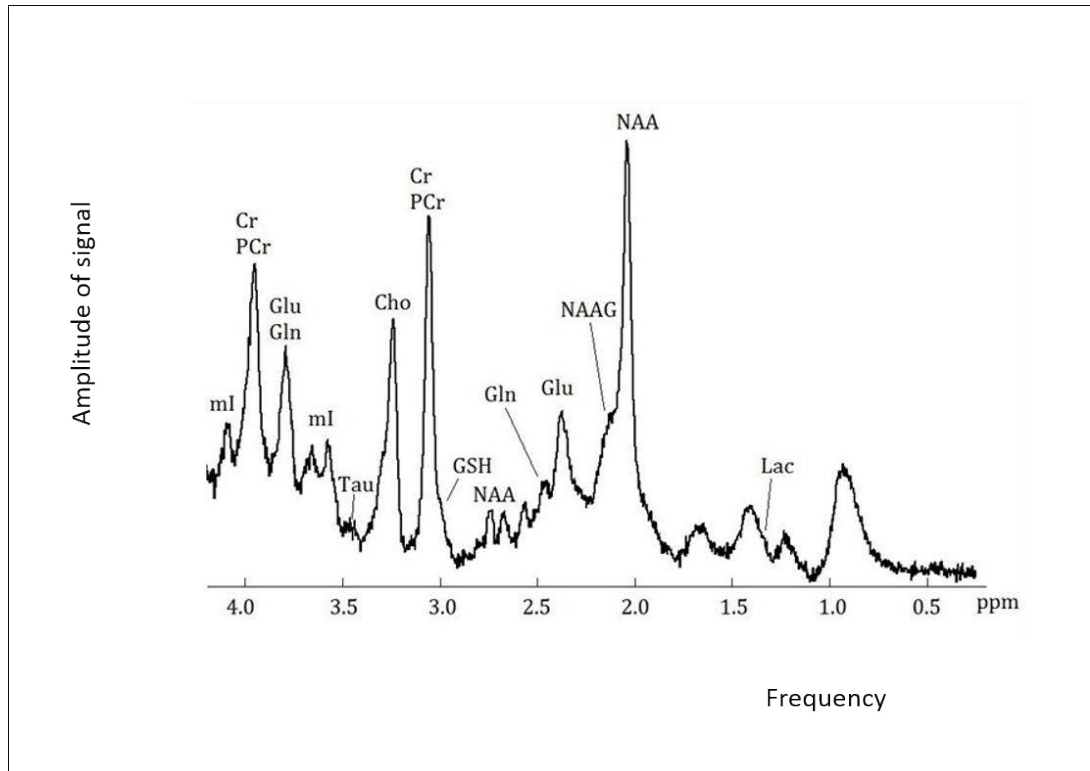


Figure 2.2: Example of a ^1H -MRS spectrum, annotated with the metabolite that each peak represents (image adapted from <https://www.nottingham.ac.uk/magres/research/magnetic-resonance-spectroscopy.aspx>).

2.1.2.1 *N*-acetyl-aspartate

The largest peak in an MRS spectrum is produced by the metabolite *N*-acetyl-aspartate (NAA), as can be seen in Figure 2.2. NAA is the acetylated form of the amino acid aspartate. It is one of the most abundant metabolites in the healthy human brain, with studies reporting concentrations between 10 and 20mM (Rae, 2014). The MRS signal from NAA appears as a single peak, which is due to the presence of the methyl group (CH_3), producing one resonance frequency of hydrogen protons within this molecule. This resonance occurs at 2.01ppm in the MRS spectrum (see Figure 2.1D and 2.2). This peak is difficult to distinguish from the peak created by the neuroactive peptide *N*-acetyl-aspartyl-glutamate (NAAG), for which NAA is the precursor molecule, and which has a similar chemical structure to NAA (Edden et al 2007). NAAG is present at much lower concentrations than NAA, and appears as a small peak on the shoulder of

the large NAA singlet peak. As it is so difficult to accurately separate these peaks, these signals are combined and reported as total NAA, or “tNAA”, which has been done in all experiments in this thesis.

The function of NAA and NAAG is under debate. A leading hypothesis is that the level of NAA is coupled to energy metabolism by neuronal mitochondria (Bates et al., 1996; Maddock & Buonocore, 2012; Moffett, 2007). Supporting this view, in an animal model of brain trauma, the level of NAA was correlated with both the acute decrease in the level of ATP and mitochondrial energy metabolism following the brain trauma, and also with the subsequent increase in ATP and mitochondrial energy metabolism during recovery (Gasparovic, Arfai, Smid, & Feeney, 2001). This study suggested that NAA concentration is associated with the functional capacity of neuronal mitochondria. A second hypothesis for the role of NAA is that it is a substrate for the neuroactive peptide, N-acetyl-aspartyl-glutamate (NAAG) (Rae, 2014; Stagg & Rothman, 2014). NAAG is indirectly involved in neurotransmission by regulating release of neurotransmitters (Rae, 2014). A third hypothesis is that NAA is a source of acetate for myelin synthesis in oligodendrocytes, the glial cells that produce the myelin sheath around axons (Rae, 2014). Evidence supporting this hypothesis is that the aspartoacylase (ASPA) enzyme which catabolises NAA to aspartate and acetate is located in oligodendrocytes, therefore the oligodendrocytes appear to be a target region for NAA (Moffett, 2007). Additional possible hypotheses for NAA’s function are that NAA is a neuronal osmolyte to counteract the anion deficit in neurons, or that it is involved in neuronal-glia signalling given the sites of NAA synthesis and catabolism (Moffett, 2007).

In MRS, tNAA is interpreted as a marker of neuronal density and health (Rae, 2014). Support for this association is that NAA is synthesised in neurons, which occurs predominantly in mitochondria (T. B. Patel & Clark, 1979; Rae, 2014; Urenjak, Williams, Gadian, & Noble, 1992), where NAA is synthesised from aspartate and acetyl co-enzyme A by the enzyme aspartate N-acetyltransferase (Wiame et al., 2010). Further support comes from negative correlations between tNAA and atrophy in neurodegenerative disorders, implying that a lower concentration of tNAA represents lower neuronal density and integrity (Oz et al., 2010, 2014).

2.1.2.2 Glutamate

The second most abundant metabolite in the brain is glutamate. Glutamate is an amino acid, and is the primary excitatory neurotransmitter of the brain. It is present in all brain cell types, but is most concentrated in neurons (Stagg & Rothman, 2014). Unlike NAA, which produces a clear single peak in the MRS spectrum, glutamate produces three broad complex peaks, with each peak representing the spins of the protons from one of the three proton groups within the glutamate molecule. These are at 2.34, 2.08 and 3.74ppm (Govindaraju, Young, & Maudsley, 2000; Maddock & Buonocore, 2012). These peaks are difficult to separate from the peaks created by glutamine, which occur at 2.44, 2.12 and 3.75ppm (Govindaraju et al., 2000; Maddock & Buonocore, 2012). As it is difficult to distinguish the glutamate and glutamine signals to accurately quantify these, the signals from both molecules are commonly combined and reported as Glx (Stagg & Rothman, 2014), an approach I will also use in this thesis.

There are two main roles of glutamate in the brain. One is as an excitatory neurotransmitter, and the other is as a metabolite. In its neurotransmitter role, when a neuron is depolarised, glutamate-containing synaptic vesicles fuse with the pre-synaptic membrane and release glutamate into the synaptic cleft. This glutamate can then bind to one of four types of glutamate receptor on the postsynaptic membrane: NMDA, AMPA, kainite and mGluRs. NMDA, AMPA and kainite receptors are ionotropic receptors (ligand-gated ion channels). Upon glutamate binding, these undergo conformational changes opening cation-permeable ion channels for the influx of positively charged calcium and sodium ions into the postsynaptic cell. The mGluRs are metabotropic glutamate receptors, which activate a G-protein and second messenger signalling cascade, which induce metabolic changes. Glutamate receptors have an excitatory effect as they increase the resting membrane potential of the cell, due to the influx of the positively charged ions, which brings the membrane potential closer to the threshold for generating action potentials.

In glutamate's metabolite role, it is involved in a large number of reactions, for example it is a substrate to several other metabolites and cellular components, such as in the Krebs cycle, and it is a precursor molecular to the neurotransmitter GABA and neuroactive peptide NAAG (Rae, 2014; Stagg & Rothman, 2014). Glutamate measured using MRS, therefore, is likely to be from a combination of neurotransmitter and metabolite pools (Rae, 2014).

2.1.2.3 GABA

GABA is the major inhibitory neurotransmitter of the brain. GABA is present in interneurons, which make up approximately 20-30% of neurons in the cortex (Markram et al., 2004). GABA is synthesised from the amino acid L-glutamate by the enzyme glutamic acid decarboxylase (GAD), which is present only in these GABAergic interneurons (Stagg & Rothman, 2014). GAD exists in two isoforms, GAD₆₅ and GAD₆₇, so named due to their corresponding molecular weights of 65kDa and 67kDa, and these are encoded by separate genes (Erlander, Tillakaratne, Feldblum, Patel, & Tobin, 1991). These two isoforms have different cellular locations, which have been linked to two separate metabolically active pools of GABA (Martin & Barke, 1998). GAD₆₅ is membrane bound, and produces GABA for synaptic vesicles, and GAD₆₇ is present in the cytoplasm of interneurons, and produces cytoplasmic GABA (Soghomonian & Martin, 1998). These two pools of GABA (synaptic and cytoplasmic GABA) have separate roles for GABA in the brain: the GABA in synaptic vesicles is involved in neurotransmission, while cytoplasmic GABA is involved in metabolism (Soghomonian & Martin, 1998; Stagg & Rothman, 2014).

In neurotransmission, when the GABAergic interneuron is depolarised by an action potential, the GABA present in synaptic vesicles is released into the synaptic cleft. Here GABA can bind to two types of GABA receptor on the postsynaptic membrane, GABA_A and GABA_B receptors, with GABA_A receptors being present both intra- and extra-synaptically. These three varieties of GABA receptor have different structures and properties that impact on the speed and type of neurotransmission. (1) Intrasynaptic GABA_A receptors induce fast inhibitory neurotransmission. These receptors are ligand-gated chloride channels (ionotropic receptors), which undergo conformational changes upon the binding of GABA to open the channel for chloride ions, which are negatively charged, to influx into the postsynaptic cell. This has an inhibitory effect as it causes the postsynaptic cell to become hyperpolarised, as it decreases the resting membrane potential of the cell. This makes it less excitable as it takes the membrane potential of the cell further away from the threshold for generating action potentials. (2) Extrasynaptic (or non-synaptic) GABA_A receptors have a role in slow inhibition, and are associated with GABAergic tone. These extrasynaptic receptors have the same ligand-gated chloride ion channel mechanism as the intrasynaptic GABA_A receptors, but have a different conformation to intrasynaptic GABA_A receptors, which causes the different speed of neurotransmission between these receptors. (3) GABA_B receptors are associated with slower and longer lasting inhibition. GABA_B receptors are metabotropic receptors which are linked to

potassium channels (Stagg, Bachtiar, & Johansen-Berg, 2011). When GABA binds to the GABA_B receptors, this causes the activation of a G-protein subunit, which results in the opening of potassium channels. This, in turn, causes efflux of potassium ions, which are positively charged, which has an inhibitory effect by causing the cell to become hyperpolarised and so less excitable.

The concentration of GABA obtained using MRS represents the concentration in the whole MRS voxel. It is difficult, therefore, to determine what the GABA signal measured using MRS represents, since it cannot distinguish between the vesicular pool of GABA used in metabolism and the synaptic pool of GABA used for neurotransmission (Stagg et al., 2011). It has been suggested that MRS-measured-GABA should be interpreted as a measure of inhibitory tone, rather than a measure of neuronal inhibitory activity at the time of scanning (Harris et al., 2015; Rae, 2014). Evidence supporting this suggestion is that in MRS the GABA measurement is obtained over several minutes, rather than in the time window of GABAergic synaptic neurotransmission, which is less than a millisecond (Farrant & Nusser, 2005). Additionally, the large size of an MRS voxel would indicate that we are detecting the GABA signal originating from a very large population of interneurons, which likely better reflect tonic inhibition (Farrant & Nusser, 2005; Rae, 2014). This interpretation of the GABA signal measured using MRS as GABAergic tone is what will be applied in this thesis.

An additional factor in GABA quantification in MRS is that the GABA signal also includes the signal from co-edited macromolecules (Stagg & Rothman, 2014). This is referred to as GABA+, which will be the term used throughout this thesis.

2.1.2.4 Myo-Inositol

Myo-inositol (mI) is a sugar-like molecule, whose structure consists of a 6-carbon ring and six hydroxyl groups, one arising from each carbon atom (Stagg & Rothman, 2014). MI creates a signal on the MRS spectrum at two frequencies (3.52ppm and 3.61ppm) due to the presence of these two types of proton environment within the molecule. mI is synthesised in the brain by dephosphorylation of inositol-1-phosphate (which is produced in the kidney) (Rae, 2014). MI functions as an osmolyte to maintain the osmotic pressure inside cells. It is taken up by cells in the brain across sodium-myoinositol cotransporters, SMIT1 and SMIT2, and hydrogen-myoinositol transporter,

HMIT, and efflux from the cell is via a volume-sensitive osmolyte channel, which occurs in response to cell swelling (Stagg & Rothman, 2014).

In MRS, mI is considered to be a glial cell marker, and also a marker of glial cell proliferation, gliosis and inflammation. Evidence supporting this comes from an MRS study of rat glial and neuronal cell cultures, in which the presence of mI was detected in the glial cell cultures but not in the neuronal cell cultures (Brand et al. 1993). Further support comes from situations where inflammation is known to occur in the brain, as there is an increase in the concentration of mI, for example in multiple sclerosis and glioma (Oz et al., 2014).

The idea that mI is an exclusively glial cell marker, however, has been challenged in more recent studies, as the SMIT and HMIT transporters are present on both neurons and glia, and some situations where there is gliosis are not accompanied by an increase in mI (Stagg & Rothman, 2014). Nevertheless, the interpretation of mI in MRS studies is still that it is a glial cell marker, given that mI concentrations are higher in glia than in neurons. More recent studies, however, do recommend treating this assumption with caution (Rae, 2014).

2.1.2.5 Creatine

Creatine (Cr) creates two peaks on the MRS spectrum, at 3.01ppm and 3.96ppm, which represent the spin frequencies of protons in its N-CH₃ group and its acetate group (Stagg & Rothman, 2014; Pischel and Gastner, 2007). The Cr peaks on the MRS spectrum actually represent the sum of Cr and phosphocreatine (PCr), which is the product of the phosphorylation of Cr by the enzyme creatine kinase (Rae, 2014). This reaction is termed the creatine kinase/phosphocreatine (CK/PCr) energy shuttle, and is an important way that the cell replenishes its supply of ATP, as this reaction converts PCr + ADP to Cr + ATP by the PCr molecule donating a phosphate group to convert ADP to ATP, and vice versa. The direction of this reaction depends on the cellular location: Cr and ADP are used to produce ATP in the mitochondria, while Cr is synthesised from PCr and ATP in the cytosol (Stagg & Rothman, 2014). ATP is vital in the cell for energy, thus Cr and PCr are required to provide a source for ATP synthesis. Since Cr and PCr are important in energy homeostasis, in MRS the Cr peak is used as a marker of energy metabolism (Rae, 2014).

2.1.2.6 Choline

In the MRS spectrum, the choline (Cho) peak occurs at 3.2ppm. This represents the frequency of proton spins in the trimethylammonium group of several choline containing compounds, which include free choline (Cho), phosphocholine (PC) and glycerophosphocholine (GPC) (Barker et al., 1994; Miller et al., 1996). Membrane-bound choline in phospholipids is MRS-invisible (Miller et al., 1991), thus the signal obtained in MRS represents cytosolic choline compounds (Stagg & Rothman, 2014). In MRS, the Cho peak is considered a marker of cell membrane integrity or turnover (Rae, 2014).

2.1.3 MRS Scan sequences

Two forms of MRS scanning are applied in this thesis. The metabolites tNAA, mI, Cr, Cho and Glx have been quantified from a Point Resolved Spectroscopy (PRESS) scan, while GABA+ has been quantified from a MEscher-Garwood-Point Resolved Spectroscopy (MEGA-PRESS) sequence. This next section provides details about each form of MRS scan, and the reason for using a different scan sequence to measure GABA+.

2.1.3.1 PRESS

The PRESS method, developed by Bottomley et al., (1986), enables the detection of metabolites from a voxel of interest by using a double spin-echo sequence, consisting of a 90° excitation RF pulse followed by two 180° refocusing RF pulses. By applying these in conjunction with magnetic field gradients that restrict the effect of the pulses to particular orthogonal planes in space, signals can be detected from a localised volume (the voxel of interest, as shown in Figure 2.1A, which depicts the cube (voxel) created by the intersection of the three slices).

2.1.3.2 MEGA-PRESS

The PRESS method is not able to optimally detect GABA, as GABA produces three peaks in the MRS spectrum at 1.9, 2.3 and 3.0ppm. This is due to the presence of three methylene groups within the GABA molecule. As shown by the coloured bars in Figure 2.3, these peaks are overlapped by peaks from other metabolites which are present in higher concentrations than GABA (e.g. Cr at 3.0ppm), making it difficult to quantify GABA using standard MRS sequences. Instead, a specialised MRS sequence must be used, the most popular of which is MEGA-PRESS (Mescher, Merkle, Kirsch, Garwood, & Gruetter, 1998).

MEGA-PRESS is able to separate the GABA signal from the overlapping signals of other metabolites by taking advantage of scalar coupling (Mullins et al., 2014). Scalar coupling is the interaction between hydrogen nuclei within the same molecule that arises through chemical bonds. By applying a pulse that affects the spins of one group of hydrogen nuclei within a molecule, another group of hydrogen nuclei within the same molecule will be affected. MEGA-PRESS uses the spin coupling between two of the proton groups in the GABA molecule at 1.9 and 3.0ppm.

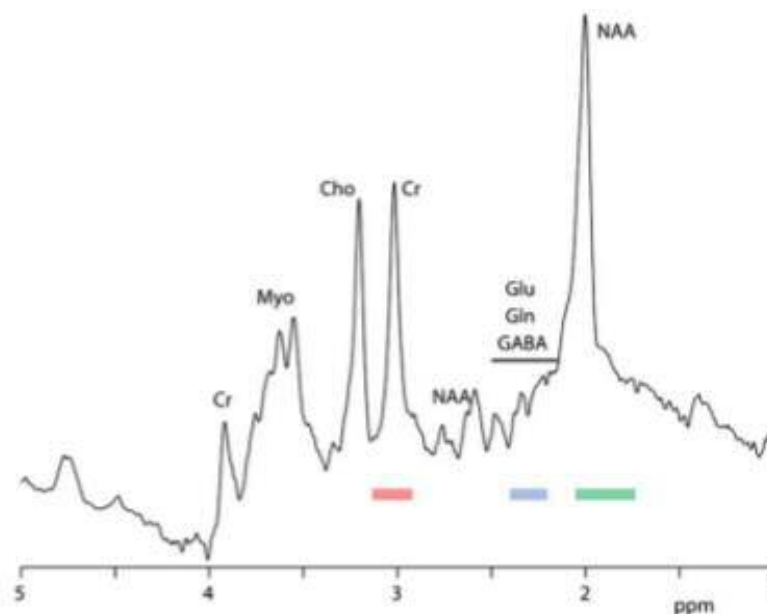


Figure 2.3: ¹H-MRS spectrum, showing the location of GABA peaks by the red, blue and green bars (Image from Puts and Edden, 2012).

There are two scans that comprise a MEGA-PRESS acquisition, which are interleaved. The first scan, which is termed the “ON” scan, applies a frequency-selective RF pulse to GABA proton spins at 1.9ppm, which affects the spins of GABA protons at 3.0ppm. The second scan, termed the “OFF” scan, applies an RF pulse elsewhere so as not to affect any of the GABA signal (Mullins et al., 2014). The resulting ON spectrum is then subtracted from the OFF spectrum, in order to leave only the signal that was affected by the RF pulse applied at 1.9ppm applied in the ON sequence (this difference-editing method is shown in Figure 2.4). This edited spectrum consists of the GABA signal at 3.0ppm, any signals close to 1.9ppm, and the Glx signal at 3.75ppm, as this is coupled to the signal around 2.1ppm. Thus the GABA signal at 3.0ppm can be isolated from overlapping metabolite signals, and detected and quantified more effectively (Mullins et al., 2014).

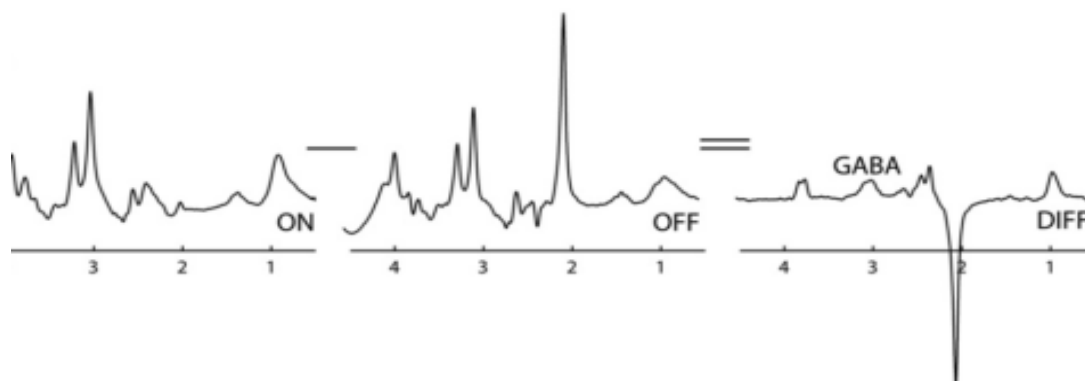


Figure 2.4: MEGA-PRESS difference editing method to isolate signal from GABA at 3.0ppm (image taken from Mullins et al., 2014).

2.1.4 Methodological considerations for MRS

2.1.4.1 Reference molecule in metabolite quantification

To quantify a metabolite, the signal from this metabolite is compared to the signal of a reference compound. Cr is often used as the internal reference compound in MRS studies, where it is used as the denominator in a ratio with the metabolite of interest as

the numerator. By calculating such a ratio using Cr that is measured in the same spectrum as other metabolites, this has the advantage of preventing or correcting for any error from regional magnetic field susceptibility variations and partial volume effects within the voxel area (Li, Wang, & Gonen, 2003).

Water is an alternative internal reference molecule that can be used instead of Cr. To enable this, an extra scan is added to the PRESS or MEGA-PRESS sequence to measure the water concentration. This is done by quantifying the peak produced from protons in water (shown in Figure 2.1B), whereas normally this peak is suppressed via water suppression to detect the much smaller metabolite peaks (e.g. via CHESS (Haase, 1986)). An advantage of using water as the reference molecule is that if the concentration of water is known, this allows the absolute quantification of metabolites in millimolar (mM), rather than relative quantification to Cr (Stagg & Rothman, 2014).

Since there are MRS studies that have detected alterations in the concentration of PCC Cr in AD patients compared to age-matched healthy controls (Jessen et al., 2009; Pilatus et al., 2009; Watanabe, Shiino, & Akiguchi, 2010), and in old *APOE*-E4 carriers compared to non-carriers (Laakso et al., 2003), this thesis has used water as the reference molecule. This is because, if there were PCC Cr changes in the young *APOE*-E4 carriers tested in Chapter 5, then by using Cr as the denominator in the ratio with other metabolites, it would appear that the concentration of numerator was changing. This would mask any true changes in Cr or the other metabolite. This concern has also been raised in other studies, for example in autism MRS research (Ford & Crewther, 2016), and, therefore, using water as the internal reference is considered a more reliable method when it is unknown whether Cr is stable or not (Li et al., 2003; Rae, 2014).

2.1.4.2 Effect of menstrual cycle and hormonal contraception on metabolite concentrations

A potential confound for MRS in female participants is that the concentrations of GABA+, Glx, NAA, Cho and mI may fluctuate between the follicular and luteal phases of the menstrual cycle, due to the influence of the differing levels of hormones oestrogen and progesterone across the cycle (Batra et al., 2008; Epperson et al., 2005; Epperson, Haga, Mason, Sellers, & Gueorguieva, 2002; Harada, Kubo, Nose, Nishitani, & Matsuda,

2011; Rasgon et al., 2001). The metabolite that has been most studied over the course of the menstrual cycle is GABA+, and such studies have detected a decrease in GABA+ concentration from the follicular to luteal phase in the occipital cortex (Epperson et al., 2005, 2002) and in the left frontal lobe and lentiform nucleus, with a trend towards a decrease in left anterior cingulate cortex (Harada et al., 2011). For example, in Epperson et al. (2002), the mean occipital GABA+ concentration changed from 1.65mmol/kg in the follicular phase (days 3-8) to 1.12mmol/kg in the late luteal phase (days 23-28).

Counter to this, however, a recent study added an extra time point during the ovulation phase when there is a peak in luteinising hormone, and found no significant difference in the GABA+/Cr ratio in the dorsolateral prefrontal cortex between follicular and luteal phases, but an increase in GABA+/Cr during this additional ovulation phase (De Bondt, De Belder, Vanhevel, Jacquemyn, & Parizel, 2014). This change was from a GABA+/Cr ratio of 0.089 in the follicular phase (days 2-7), to 0.122 in the ovulation phase (the paper did not specify days, but confirmed this was the ovulation phase using a luteinising hormone urine test), with this ratio returning to 0.089 in the luteal phase (approximately 7 days after the ovulation phase scan) (De Bondt et al., 2014). A possible explanation for the discrepancy in findings across studies is that a potential increase in GABA+ in the ovulation phase may have been included in the follicular phase in previous studies, implying a GABA decrease from follicular to luteal phase. Alternatively, perhaps GABA+ fluctuates between follicular and luteal phase in the occipital cortex, but not in the prefrontal cortex. Taken together, however, studies indicate that phase of menstrual cycle does have an influence on the concentration of GABA in the brain, and that the possible implications of this factor should be controlled for in my studies.

Less research has been done on the menstrual influences on other MRS metabolites, but alterations in Glx, tNAA, Cho and mI have been identified. Batra et al. (2008) found a decrease in the Glx/Cr ratio in the medial prefrontal cortex from the follicular to luteal phase, where the mean Glx/Cr ratio decreased from 5.86 in the follicular phase (days 6-12) to 4.85 in the luteal phase (days 23-28). In addition, between the follicular phase (approx. day 8) and luteal phase (approx. day 26), Rasgon et al. (2001) found a decrease in the mean NAA/Cr ratio in the prefrontal cortex from 1.58 to 1.32, but an increase in the mean NAA/Cr ratio in parietal cortex white matter from 1.62 to 1.78. They also found an increase in the Cho/Cr ratio in the parietal cortex from 0.97 to 1.10, but no difference in the Cho/Cr ratio in the prefrontal cortex, and no difference in

mI/Cr in either voxel, although there was a trend towards an increase in the parietal white matter (Rasgon et al., 2001).

The work above, however, has been undertaken in quite small sample sizes (e.g. n=13 in Batra et al. 2008, and n=6 in Rasgon et al., 2001), which limits generalisation of these findings. Nevertheless, it seems plausible that metabolite levels may fluctuate across the menstrual cycle. In all studies of this thesis, therefore, female participants were asked to take part in the MRS scan session during the luteal phase of their menstrual cycle (days 16-28, where day 1 was classed as the first day of menstruation).

The study by de Bondt et al. (2015) also tested the concentration of GABA in dorsolateral prefrontal cortex in participants who were taking hormonal contraceptives, comparing concentration between a pill-taking day and a pill free day. They found no significant difference in concentration between these time points, with GABA concentration similar to that found in the follicular and luteal phase of participants not taking hormonal contraceptives (De Bondt et al., 2014). This study suggests that female participants taking hormonal contraceptives can be scanned at any time of their menstrual cycle. Given this, no restrictions were placed on when female participants taking such contraception could take part in the MRS studies in this thesis.

2.2 Functional Magnetic Resonance Imaging (fMRI)

2.2.1 How does fMRI work?

fMRI is a non-invasive neuroimaging technique that enables us to investigate brain activity. fMRI is a type of MRI scan which uses the same physics phenomenon of NMR applied in MRS (e.g. when an external magnetic field is applied to protons, the nuclei align to the magnetic field and the frequency of the spin is determined by the strength of the magnetic field, governed by the Larmor equation (Logothetis, 2002)). Whereas MRS uses the information about the frequency of the hydrogen nuclei spins to differentiate different metabolites, however, fMRI uses this frequency information as one method to determine the spatial location of a signal within the volume scanned. This is

known as frequency encoding, and is used in conjunction with slice selection and phase encoding to measure the fMRI signal from each voxel within a 3D space (Huettel et al., 2009).

fMRI is an indirect measure of neuronal activity, as fMRI works by measuring the amount of oxygen in a brain region, with those regions with more active neurons having greater oxygen needs (Logothetis, 2002). fMRI measures the blood oxygenation level dependent (BOLD) contrast which represents the ratio of the amount of deoxyhaemoglobin to oxyhaemoglobin in the blood (Logothetis, Pauls, Augath, Trinath, & Oeltermann, 2001; Logothetis, 2002). This can be estimated because deoxyhaemoglobin and oxyhaemoglobin have different magnetic properties, where oxyhaemoglobin is diamagnetic and deoxyhaemoglobin is paramagnetic (Pauling & Coryell, 1936). The paramagnetic deoxyhaemoglobin creates distortions in the surrounding magnetic field, causing a more rapid decay in the $T2^*$ signal (Brooks et al., 1975). The ratio of oxygenated and deoxygenated blood is altered when neurons are active, thus by measuring this BOLD contrast we can make an inferences as to the underlying neuronal activity. When neurons are depolarised, their metabolic demand for oxygen increases in order to replenish energy stores used during depolarisation, and enable reuptake of neurotransmitters from the synaptic cleft following depolarisation (Logothetis et al., 2001; Logothetis, 2002). Oxygen is extracted from the local capillaries, which changes oxyhaemoglobin to deoxyhaemoglobin, and so causes a decrease in the detected signal. This is only a small signal decrease, lasting for 1-2 seconds, and following this “initial dip” in the signal there is an over-compensation in oxygenated blood flow to the site of neural activity. This latter effect is caused by the vasodilation of capillaries adjacent to this site, which vastly increases the proportion of oxyhaemoglobin to deoxyhaemoglobin, and results, therefore, in a large increase in signal. The peak of this signal occurs approximately 6 seconds after the underlying neural activity, then decreases to below the baseline level after approximately 12 seconds. This latter effect is termed the “post-stimulus undershoot”, which then returns to baseline. This profile of blood flow in response to neuronal activity is termed the haemodynamic response function (HRF, see Figure 2.5) (Huettel et al., 2009), and is the basis of how fMRI is able to (indirectly) measure brain activity.

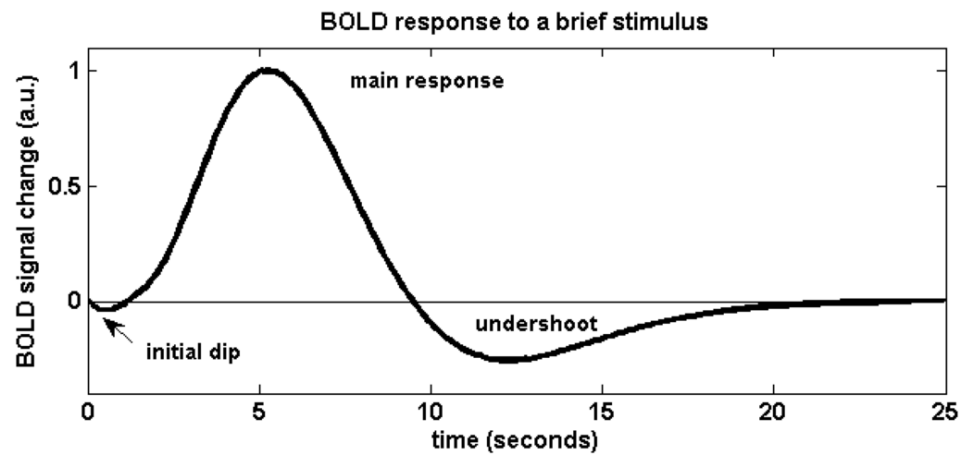


Figure 2.5: The haemodynamic response function (HRF), which shows the change in BOLD signal detected post stimulus due to an increase in blood flow followed by reduction in this blood flow back to the baseline (image from <http://www.mdpi.com/1996-1944/4/11/1941/htm>)

2.2.2 How do we use fMRI to investigate brain function?

The BOLD contrast is measured from many thousands of voxels (3D pixels) in the brain, which are typically 3mm^3 in volume, giving fMRI good spatial resolution (Huettel et al., 2009). In fMRI, participants are asked to view or perform different conditions of a task. By comparing the BOLD contrast across *different* voxels in the brain in different task conditions, we can make inferences as to which regions have higher neuronal activity than others for different conditions. By comparing the BOLD contrast in the *same* voxels between conditions, we can also make inferences as to which task demands elicit greater neuronal activity than others in that region (Amaro & Barker, 2006).

Different fMRI study designs can be applied to investigate brain activity during different task conditions. The two types of design that have been used in this thesis are a cognitive subtraction design (applied in Chapter 3), and a factorial design (applied in Chapter 4) (Henson, 2006; Price, Moore, & Friston, 1997). In a cognitive subtraction design, participants are asked to perform a minimum of two different task conditions. For example, an experiment could consist of conditions A and B, where A is the condition of interest and B is the baseline condition. The BOLD response in task condition B is subtracted from that elicited in task condition A, in order to isolate the activity from the

task condition of interest, A, above the baseline condition, B, (Amaro & Barker, 2006; Henson, 2006). Chapter 3 of this thesis has used this cognitive subtraction design. As will be expanded on in the introduction and methods sections of Chapter 3, this design has been used to compare PCC activity during different task conditions of scene, face and object oddity discrimination compared to a baseline condition of size. In a subtraction design there is one factor that is manipulated, i.e. in Chapter 3, the factor is the category of the stimuli presented.

In a factorial design, more than one factor is manipulated within the same experiment. Such a design enables the investigation of whether the effect of manipulating one factor on the BOLD response of a brain region is modulated by another (Henson, 2006; Price et al., 1997). For example, the two factors in an experiment could be stimulus category and working memory load, and there could be two levels of each factor, where the stimulus categories were scenes and shapes, and the working memory load was low or high. To investigate whether the BOLD contrast was modulated by the first factor of stimulus category, we could perform a cognitive subtraction design, as described above (i.e. BOLD response for scenes minus shapes). A factorial design however, would extend this to test whether the BOLD response for scenes minus shapes was the same or different at the two levels of working memory load, thus telling us whether the second factor had an impact on the outcome of the first factor. If there was no difference in the BOLD response to scenes-shapes between the low and high working memory loads, this would suggest that there is a main effect of the factor of stimulus category, whereas if the BOLD response to scenes-shapes was different at each level of working memory load, this would suggest that there is an interaction effect between the two factors (Henson, 2006; Price et al., 1997). Chapter 4 of this thesis applied exactly this type of factorial design to investigate whether there is an interaction between working memory load and the spatial complexity of stimuli on brain activity in the PCC.

In addition to these different experimental approaches, there are different strategies for fMRI experimental design. These are event related and blocked designs (Henson, 2006; Huettel et al., 2009). An event-related design has been applied in Chapter 3 of this thesis while a blocked design has been applied in Chapter 4. Further details of each design and analysis strategy are provided in the methods section in the appropriate Chapter.

The difference in the BOLD contrast between task conditions can be quantified, by calculating the BOLD percentage signal change between conditions (Huettel et al., 2009). This is the method adopted in Chapters 3 and 4, where I obtain a measure of the difference in PCC BOLD between task conditions in order to correlate this with MRS metabolites. Further details will be given in Section 3.2 of this Chapter, and in the methods Sections of Chapters 3 and 4.

2.2.3 Methodological considerations in fMRI

2.2.3.1 Correction for multiple comparisons

Given that the voxel size in fMRI is typically 3mm^3 , this means that there are many thousands of voxels in one brain volume. In an fMRI analysis, therefore, this results in many thousands of statistical comparisons in order to make inferences about differences in activity within and between voxels. Performing this large number of statistical tests means that there is an increased risk of detecting false positives (Huettel et al., 2009). To correct for this problem, two methods have been adopted in this thesis: (1) lower voxelwise level of significance and (2) a clusterwise correction. These strategies are consistent with the fMRI analyses performed in previous studies that have applied the fMRI paradigms adopted in this thesis (A. C. H. Lee & Rudebeck, 2010; Shine et al., 2015). A more detailed explanation of these corrections is given in the methods section of Chapters 3 and 4.

2.3 Combination of MRS with fMRI

Studies combining fMRI with MRS are quite a recent development in neuroimaging, with the earliest studies appearing in the early 2000s (e.g. Urrila et al., 2003). Although there are not a large number of fMRI-MRS studies, this number is steadily increasing (Duncan, Wiebking, Munoz-Torres, & Northoff, 2013), and the number of metabolites being correlated with BOLD is also expanding, partly due to improvements in MRS methodology (e.g., the development of MEGA-PRESS sequences for more accurate GABA quantification (Mullins et al., 2014)).

The appeal of combining fMRI with MRS is that it enables us to gain insight into the biochemical mechanisms underpinning the BOLD response in the healthy brain (Duncan et al., 2013; Hu et al., 2013), as well as understand the pathophysiology of altered brain activity in neurological or psychiatric disease (Duncan et al., 2013; Duncan, Wiebking, & Northoff, 2014; Enzi et al., 2012).

A further advantage of using MRS alongside fMRI is that MRS is a non-invasive technique enabling measurement of biochemistry *in vivo* (Rae, 2014; Stagg & Rothman, 2014). This is in contrast to the other main method allowing study of human brain biochemistry *in vivo*, Positron Emission Tomography (PET). PET is an invasive technique that requires an injection of a radioactive isotope. This makes PET a less appealing and less feasible technique for studying healthy individuals, and is also more expensive than MRS. PET requires a specialised PET scanner whereas MRS can be performed on a standard MRI scanner, alongside fMRI. Thus MRS-fMRI studies offer the best combination of techniques currently available to gain insight into how the biochemistry of the brain is related to its function non-invasively.

A combined fMRI-MRS approach has been applied in Chapters 3 and 4 of this thesis. As outlined in Chapter 1, this approach allows me to investigate whether individual differences in the PCC BOLD response to scenes, during which young *APOE-E4* carriers showed an altered pattern of activity (see Shine et al., (2015)), are related to individual differences in PCC metabolites measured using MRS. The purpose of this is to assess whether an alteration in PCC metabolites could underlie the altered BOLD response in the PCC of young *APOE-E4* carriers that existed only for the scene conditions of a perception and working memory task.

2.3.1 MRS metabolites correlated with BOLD in this Thesis

Although, as described in Section 2.1.2 of this Chapter, there are six metabolites commonly quantified in MRS studies, only three of these metabolites have been tested in the fMRI-MRS correlations in Chapters 3 and 4. These are Glx, GABA+ and tNAA. The rationale for correlating PCC BOLD with only these three metabolites is that these are the metabolites for which there is both evidence of a relationship with BOLD activity, and evidence of altered levels of these metabolites in the PCC of AD patients compared to

healthy controls. The rationale for selecting these three metabolites, and the previous studies that have detected relationships between BOLD and GABA+, Glx and tNAA, will be discussed fully in the Introduction section in Chapter 3 (see Section 3.1.1).

2.3.2 MRS-fMRI methodological consideration: how to test for a relationship between MRS and fMRI

There are not a large number of papers that have correlated MRS with fMRI, and within this quite small literature there does not appear to be a standard method, as many papers use different approaches to quantify the BOLD response in order to correlate this with the specified MRS measure. The various approaches reported in this literature are summarised in Figure 2.6, and include:

- a) Correlating MRS with the BOLD percentage signal change obtained from the peak fMRI voxel which lies within the MRS voxel (for example, in studies correlating visual cortex BOLD elicited in response to a visual stimulus (e.g. a grating) with GABA+ in an occipital cortex voxel (Harris et al., 2015; Muthukumaraswamy, Edden, Jones, Swettenham, & Singh, 2009; Muthukumaraswamy, Evans, Edden, Wise, & Singh, 2012; Violante et al., 2013)).
- b) Correlating MRS with the mean BOLD percentage signal change obtained in an fMRI ROI identical to the MRS voxel placement (for example, in a study correlating anterior cingulate cortex (ACC) GABA with ACC BOLD, the ROI for quantifying BOLD was identical in size and dimensions to the MRS voxel (Northoff et al., 2007)).
- c) Correlating MRS with the mean BOLD percentage signal change across subject-specific activation within an anatomical ROI (for example, in an additional analysis in Harris et al. (2015) which correlated visual cortex BOLD in response to viewing a grating with occipital GABA+ (Harris et al., 2015)).
- d) Correlating MRS with the peak BOLD activation within the anatomical ROI (an additional comparison analysis in Harris et al (2015)).

- e) Correlating MRS with the mean BOLD activation in an anatomical ROI (for example, in a study which correlated ACC GABA and Glx with the BOLD response extracted from an ACC fMRI ROI defined using atlas tools available in the fMRI software (e.g. cortical and subcortical atlas tools in FSL) (Enzi et al., 2012)).
- f) Using MRS as a regressor in the fMRI general linear model (GLM) to detect which fMRI voxels show activity correlated with MRS. The mask region for such analyses is typically the MRS voxel (for example, this voxelwise approach was used to identify fMRI voxels that showed a BOLD response to a particular contrast in a fear-inducing paradigm that was associated with the concentration of GABA in that region (Lipp et al., 2015)).

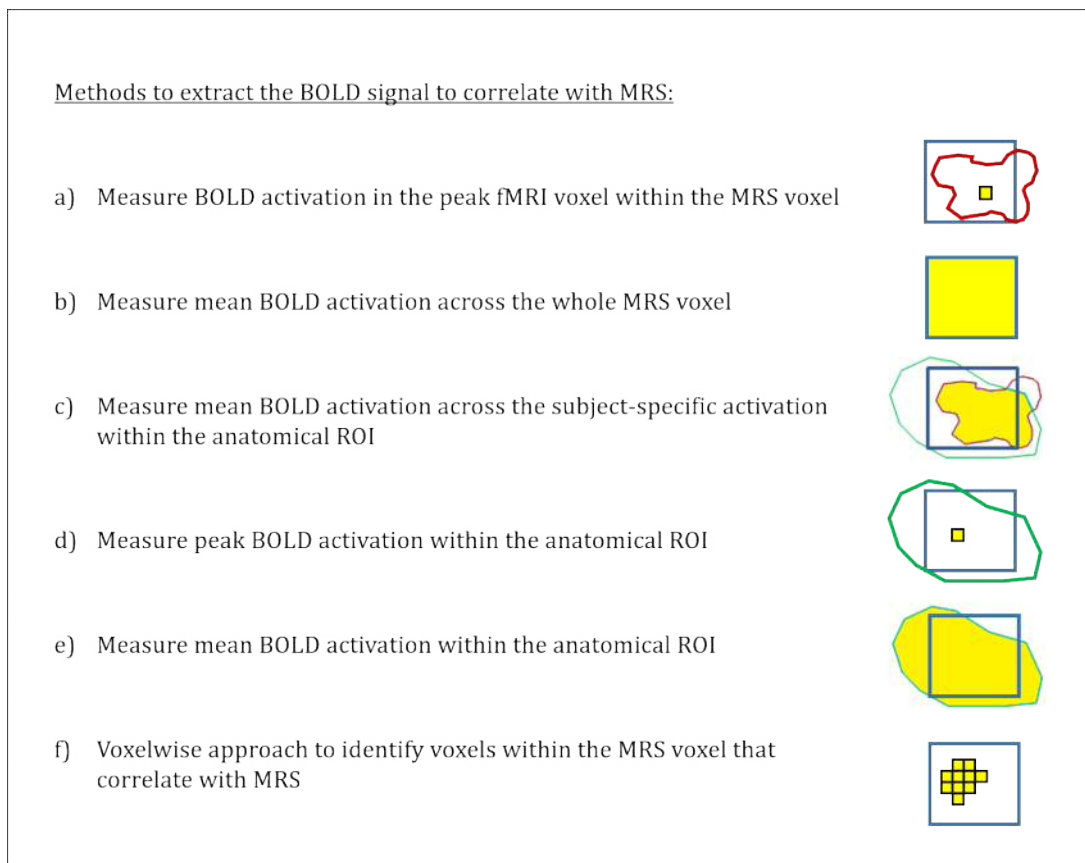


Figure 2.6: Different strategies used in MRS-fMRI literature to extract the BOLD percent signal change to correlate with MRS. The shaded yellow area represents the region within which BOLD is quantified, the blue box represents the MRS voxel, red area represents the subject-specific activation, green area represents the anatomical ROI, small yellow square represents the peak fMRI voxel, and group of small yellow boxes represents a cluster of fMRI voxels within the MRS voxel.

An effective strategy used in some MRS-fMRI studies has been to apply the ROI method in b, c or e alongside the voxelwise method in f (e.g. Enzi et al., 2012; Lipp et al., 2015; Northoff et al., 2007). This enables complementary analysis of functional-biochemical relationships as follows: the first correlation tests whether fMRI activity in a particular brain area of interest (which will contain several fMRI voxels) correlates with MRS metabolites assessed within the MRS voxel, while the second voxelwise approach tests which of the fMRI voxels within the MRS voxel shows activity that is correlated with MRS metabolites. For example, Enzi et al., (2012) first performed a Pearson correlation between ACC Glx and the ACC BOLD percentage signal change quantified from an anatomical ROI (and elicited during the contrast of resting state compared to anticipation of reward). This identified a positive relationship of Glx and BOLD. This was followed by an analysis where Glx was used in the GLM for fMRI activity within the ACC MRS voxel area. This second analysis was able to localise the activity that was positively correlated with Glx to a region in the left ACC, which overlapped with part of the anatomical ROI used in the Pearson correlation (Enzi et al., 2012). By using this dual-method approach, complimentary support can be provided beyond that obtained from the use of each method alone. Furthermore, the voxelwise method has the advantage that it is an unbiased approach, and it can enhance spatial specificity of an MRS-fMRI correlation within the MRS voxel. By contrast, averaging BOLD across the whole MRS voxel may dilute any BOLD effect. This dual-method approach is the approach taken in the fMRI-MRS experiments in Chapters 3 and 4 of this thesis.

3 Chapter 3: Investigating category-sensitivity in the posterior cingulate cortex using fMRI and MRS

3.1 Introduction

As outlined in Chapter 1, it is important to study the brain regions where the earliest changes in AD have been detected, if we are to better understand the pathogenesis of the disorder. The PCC has become a region of key interest to AD researchers, as a decrease in PCC glucose metabolism is one of the earliest alterations identified in AD patients (Minoshima et al., 1997) and in pre-symptomatic FAD mutation carriers (Mosconi et al., 2006). Changes in the structure, (Pengas, Hodges, Watson, & Nestor, 2010), function (Ries et al., 2006) and functional connectivity (Zhou et al., 2008) of the PCC also occur in individuals with AD and MCI compared to healthy age-matched controls. The importance of the PCC in later-life cognitive health is further highlighted by a decrease in glucose metabolism in the PCC of carriers of the *APOE-E4* allele – the strongest genetic risk factor for sporadic AD (Farrer et al., 1997; Lambert et al., 2013) – decades before the onset of any cognitive decline or clinical symptomology associated with AD (Reiman et al., 2004). Furthermore, the magnitude of the reduction in PCC glucose metabolism is related to the number of *APOE-E4* alleles carried, where carriers of two *APOE-E4* alleles have the lowest level of PCC glucose metabolism (Protas et al., 2013). As noted in Chapter 1, it has also been shown that brain activity (Shine et al., 2015), functional connectivity (Dennis et al., 2010) and resting state activity (Filippini, MacIntosh, et al., 2009) of the PCC are altered in young *APOE-E4* carriers. Thus, the PCC appears to be a key region affected in individuals at increased genetic risk of AD, as well as in pre-symptomatic and clinically-affected individuals. Despite the importance of the PCC in the pathogenesis of AD, however, PCC function is not well understood (Andrews-Hanna, 2012; Leech et al., 2012). Improved understanding of its function is an important prerequisite for reliable interpretation of alterations in PCC activity and biochemistry in *APOE-E4* carriers and early AD patients, and also for the development of cognitive paradigms that may be sensitive to the earliest changes in this region.

A leading proposal for PCC function is that it is a key hub in the default network (DN), which is a network of brain regions that are highly active at rest, but that show deactivation during a cognitive task (Raichle et al., 2001), e.g. whilst performing a working memory task (Esposito et al., 2009; Mckiernan et al., 2003). The PCC and neighbouring precuneus have been proposed to be the critical hub region in this network; this conclusion is supported by the direct connectivity of these brain areas with all other regions in this network, and findings that their level of activity modulates activity in interconnected brain areas (Fransson & Marrelec, 2008; Hagmann et al., 2008; Utevsky et al., 2014).

The idea that the PCC is simply activated/deactivated during the absence/presence of a task has been challenged, however, by studies that have shown that the PCC is active during certain cognitive tasks, including autobiographical memory, prospection, scene construction, spatial navigation, imagining the self in a different spatial location, and theory of mind tasks (Hassabis & Maguire, 2007; Spreng, Mar, & Kim, 2008; Guterstam, Björnsdotter, Gentile, & Ehrsson, 2015) (see Figure 3.1 for the results of a conjunction analysis of such tasks, taken from Spreng et al., 2008). These findings have led some authors to propose an alternative account of PCC function, according to which the PCC is actively engaged during internally-directed cognition, with autobiographical memory, scene construction, prospection and navigation being examples of such internal thought processes (Andrews-Hanna, 2012). An additional account, however, proposes that the extent of the activation or deactivation is important for memory encoding and retrieval (Daselaar et al., 2009; Vannini et al., 2011). These studies have identified that the magnitude of PCC deactivation during memory encoding is related to the magnitude of PCC activity at retrieval, and this is also related to behavioural performance on the memory task (Daselaar et al., 2009; Huijbers et al., 2012; Vannini et al., 2011).

Overall then, the circumstances under which the PCC activates and deactivates are unclear, as is how this contributes to cognition. This merits further investigation in order to better understand the function of this key region implicated in AD.

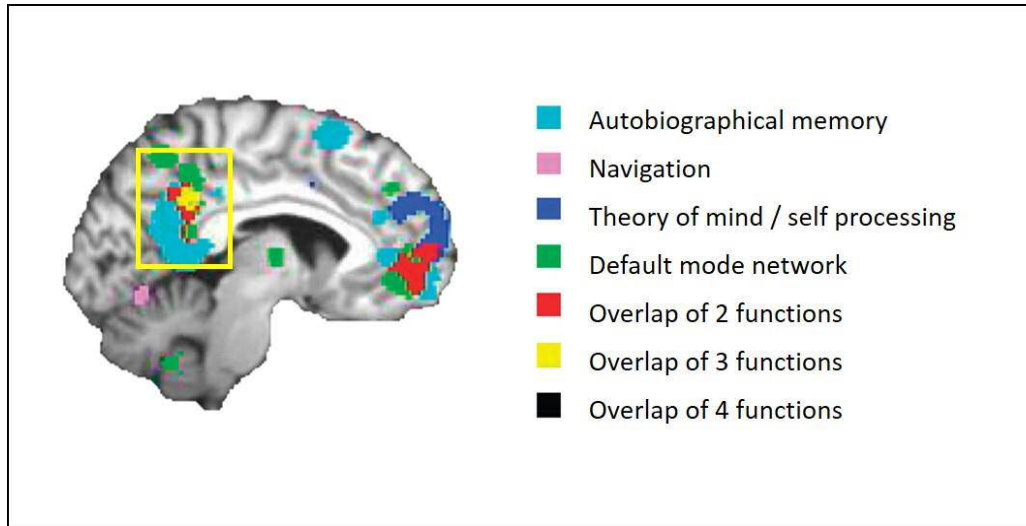


Figure 3.1: A conjunction analysis of studies showing activation of the PCC during cognitive tasks. Note that the overlapping area of PCC activation across these tasks, highlighted by the yellow box, challenges the idea that the PCC necessarily deactivates during cognitive task performance (image adapted from Spreng et al., 2008).

The activity profile of the PCC in response to different categories of visual stimuli is one particular area where enhanced understanding would be beneficial, as this could provide insight into PCC activity alterations in young *APOE-E4* carriers identified in a recent study in our lab, that was briefly described in Section 1.5 of Chapter 1 (Shine et al., 2015). This study used an odd-one-out visual discrimination task, previously shown to be sensitive to scene perception impairments in AD (A. C. H. Lee et al., 2006, 2007). Shine et al., (2015) used this task in conjunction with fMRI to compare the BOLD response to different categories of visual stimuli between *APOE-E4* carriers and non-carriers within a PCC ROI (details of how this ROI was defined is described in Section 4.1 of Chapter 4) (Shine et al., 2015). In the odd-one-out task, participants were shown triplets of images of scenes, faces and objects and asked to choose which image was the odd-one-out. Activity elicited during these stimuli conditions was contrasted with a baseline condition of a size odd-one-out discrimination. Comparison of *APOE-E4* carriers and non-carriers revealed a more positive level of activity in *APOE-E4* carriers during the scene, but not face or object, visual discrimination. Activity for these other conditions in the E4 carriers, and for all three conditions in the non-carriers, showed a negative BOLD response relative to the baseline condition (see Figure 3.2; Shine et al., 2015). The more positive

level of activity for scenes (reduction in deactivation) in the *APOE-E4* carriers was interpreted as a failure to deactivate during scene processing. This failure to deactivate the PCC in these young *APOE-E4* carriers would be consistent with the failure to deactivate the PCC seen in MCI and AD patients, as described in Section 1.4 (Pihlajamäki & Sperling, 2009). A possible alternative explanation could be that the *APOE-E4* carriers are performing the scene condition with less cognitive effort than the other conditions than the non-carriers, as per the *APOE-E4* allele being an example of antagonistic pleiotropy (an advantage early in life, which is detrimental later in life, e.g. in line with Rusted et al., 2013). A better understanding of how the PCC responds to different categories of visual stimuli, and whether greater or reduced deactivation is beneficial for task performance, would aid interpretation of these findings in the young *APOE-E4* carriers.

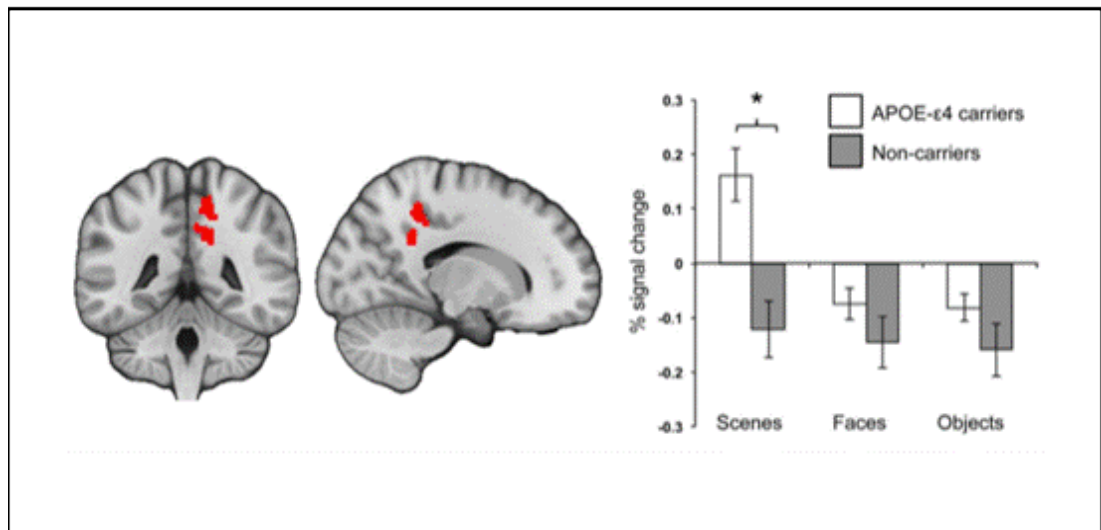


Figure 3.2: Category sensitive activity in PCC in *APOE-E4* carriers and non-carriers. The BOLD percentage signal change was calculated relative to the size baseline and extracted from the PCC ROI shown in the figure on the left hand side of the image (image taken from Shine et al., 2015).

To gain a better understanding of how the PCC ROI responds to different categories of visual stimuli, this Chapter applies the same oddity task used first by Lee et al. (2006) in AD patients then subsequently by Shine et al. (2015) in the young *APOE-E4* carriers, to investigate the activity profiles for different visual stimuli categories. The

oddity task is a well-established cognitive paradigm that has been used to identify stimulus-sensitive patterns of activity in different brain regions, thereby improving our understanding of how the brain supports visual perception for different categories of visual stimuli. For example, this paradigm has been used to assess the stimulus-selectivity of different regions within the MTL to scene, object and face discrimination (Barens, Henson, Lee, & Graham, 2010; A. C. H. Lee, Scahill, & Graham, 2008).

3.1.1 Analysis Strategy and Hypotheses

A number of questions will be addressed in this Chapter. Focusing initially on brain function, I ask whether the PCC ROI shows a category-selective BOLD response during oddity judgements for scenes, object and faces. Secondly, how does functional activity in this region relate to behavioural performance on the oddity task? These questions will help us understand whether the PCC ROI shows a generic or a category-sensitive response during higher-level perception, whether the BOLD response to each category is a relative activation or deactivation compared to the other stimuli categories, and whether successful performance on the task is correlated with the activity of this region.

The topographical and functional overlap between findings of PCC involvement in AD and young *APOE-E4* carriers, as well as the potential sensitivity of scene processing tasks, is intriguing, but importantly, these studies do not tell us anything about the underlying brain changes that might lead to altered behaviour and/or BOLD activity. One way to gain insight into mechanisms behind alterations in BOLD activity is to combine fMRI with MRS, as was introduced in Chapters 1 and 2, because MRS enables the measurement of metabolites and neurotransmitters *in vivo*. The collection of MRS data alongside the fMRI oddity task allows us to ask further critical questions, in particular whether there will be associations between BOLD activity in the PCC ROI (potentially in a stimulus-sensitive manner, depending on the outcome of the first question) and MRS metabolites measured in the same region. More specifically, will individual differences in PCC MRS metabolite levels be associated with the magnitude of PCC BOLD response during scene discrimination, and how, in turn, will this relate to behaviour on the oddity task? The novel combination of MRS with the fMRI oddity task allows us to assess whether a category-sensitive MRS-BOLD relationship could exist in the PCC ROI. If this

was the case, this would support my hypothesis that an alteration in PCC MRS metabolites in the young *APOE-E4* carriers could be associated with the PCC BOLD alteration seen in these individuals for the scene oddity condition only.

As outlined in more detail in Chapter 2, in the MRS literature six MRS metabolites are commonly studied, which are GABA+, Glx, tNAA, mI, Cr and Cho (Rae, 2014; Ross & Sachdev, 2004; Stagg & Rothman, 2014). The majority of MRS-fMRI studies have assessed the relationship between BOLD signal and GABA+ or Glx (Donahue, Near, Blicher, & Jezard, 2010; Duncan, Enzi, Wiebking, & Northoff, 2011; Enzi et al., 2012; Falkenberg, Westerhausen, Specht, & Hugdahl, 2012; Harris et al., 2015; Hu, Chen, Gu, & Yang, 2013; Lipp et al., 2015; Muthukumaraswamy, Edden, Jones, Swettenham, & Singh, 2009; Northoff et al., 2007; Reid et al., 2010; Stan et al., 2014), and a small number of studies have assessed BOLD-tNAA relationships (Hao et al., 2013; Hutcheson et al., 2012; Vigren et al., 2013). Studies correlating Cr, Cho and mI with BOLD are not very common. In this Chapter, correlating BOLD with all six MRS metabolites would mean a low significance threshold after correcting for multiple comparisons, which might increase the risk of reporting a false negative result (type II error). Therefore, to reduce the number of statistical comparisons, this Chapter selected the three metabolites where the literature suggests there may be relationship with BOLD: GABA+, Glx and tNAA.

Previous MRS-fMRI studies testing the relationship between GABA+, Glx and tNAA with BOLD have suggested that a more positive BOLD response is typically associated with a lower concentration of GABA+, a higher concentration of Glx, and a higher concentration of tNAA (Ende, 2015; Falkenberg et al., 2012; Hao et al., 2013; Hu et al., 2013; Lipp et al., 2015; Muthukumaraswamy et al., 2009). The most relevant example of this for the present Chapter is the MRS-fMRI study by Hu et al. (2013), as their region of interest was also the PCC. In this study, they assessed the relationship between PCC GABA and Glx with PCC BOLD during an n-back working memory task using letters as stimuli (see Figure 3.3A for task design). They found that the PCC showed a larger deactivation when participants performed a more difficult working memory condition compared to the baseline condition (the contrast 3back>0back), and that a larger PCC deactivation (i.e. a more negative PCC BOLD response) was associated with a higher concentration of PCC GABA, and a smaller PCC deactivation (i.e. a more positive PCC BOLD response) was associated with a higher concentration of PCC Glx (see Figure 3.3 for n-back task design and MRS-fMRI correlations) (Hu et al., 2013).

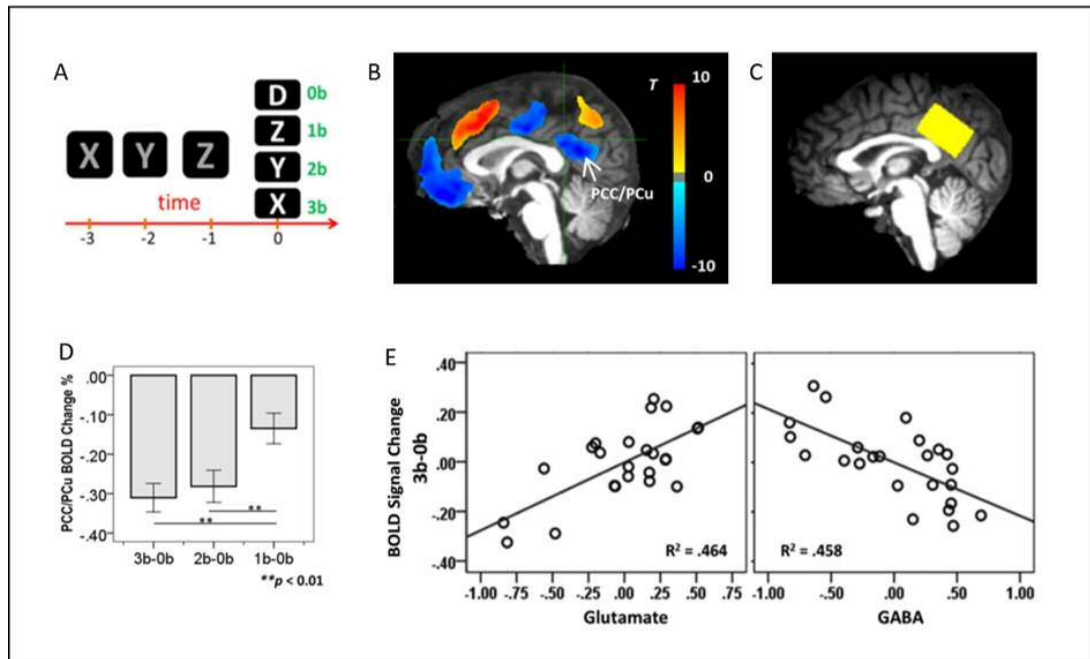


Figure 3.3: Experimental design and results of the PCC MRS-fMRI study by Hu et al. (2013) investigating the relationship between PCC deactivation and PCC biochemistry. (A) Design of the n-back fMRI working memory task, in which participants viewed letters on the screen inside the scanner, and were asked to press a button when the letter on the screen was a D (i.e. target letter) for the 0back (0b) condition, when the letter was the same as that seen in either 1-, 2-, or 3- trials previously (1back, 2back, 3back conditions respectively). (B) fMRI results from the 3b>0b condition. Blue regions show areas that had a lower BOLD response for the 3b condition compared to the 0b condition (i.e. a deactivation), and red regions show areas that had a higher BOLD response for this contrast (i.e. an activation). The area highlighted with the arrow represents the PCC/precuneus (PCu). (C) The location of the PCC MRS voxel (voxel size 2.4 x 3.2 x 3.6cm, which is similar to the PCC voxel size of 2x2x2cm used in this Thesis). (D) Mean BOLD percentage signal change in the PCC for the contrasts 3b>0b, 2b>0b and 1>0b. (E) Relationships between PCC BOLD percentage signal change for the contrast 3b>0b with PCC glutamate and GABA. Scatter plots show that a more negative PCC BOLD response (i.e. greater deactivation) is associated with a lower concentration of PCC Glx and a lower concentration of PCC GABA (Figures taken from Hu et al., 2013).

Similar to Hu et al., in this Chapter I applied an fMRI-MRS strategy to assess how PCC biochemistry was related to its BOLD activity during visual discrimination, in a novel approach to assess whether such associations would be differentially affected by the category of the stimuli presented in the visual discrimination task.

My hypotheses for the first two aims of this Chapter were that the PCC ROI would show a preferential response to scenes compared to the other categories of stimuli. This is based on the accumulating evidence from the AD and *APOE* literature that alterations in PCC structure, function or biochemistry are linked to activity or behavioural performance during scene-related tasks, thus implicating the PCC as having a role in such scene processing. More specifically, I predicted that the PCC ROI will show less deactivation (i.e. a more positive BOLD response) to scenes compared to faces or objects. Furthermore, I predicted that there would be a positive correlation between PCC BOLD for scene oddity and accuracy on this task (i.e. higher the accuracy on the scene oddity task, would be associated with less PCC deactivation), whereas there will be no such relationship for faces or objects.

Following the same directions of BOLD-MRS relationships in the PCC from Hu et al., (2013), I hypothesised that a greater concentration of PCC GABA+ would be associated with greater PCC deactivation, and a greater concentration of PCC Glx would be associated with less PCC deactivation. In addition, based on the small number of studies of tNAA-BOLD relationships, and based on the finding that tNAA is associated with neuronal integrity and density and has been localised to neuronal mitochondria (Hao et al., 2013; Moffett, 2007; Rae, 2014), I predicted that a greater concentration of PCC tNAA would be associated with less PCC deactivation. This is because, if the PCC is involved in scene perception, then the neurons in this area should respond more to scenes, thus requiring a greater supply of oxygen to be used by the mitochondria, which would mean this region would show a greater BOLD response.

By contrast, to establish category and regional sensitivity of these relationships (Duncan et al., 2013), I predicted no association between BOLD activity for non-scene categories and any MRS metabolites, as well as no evidence of associations between BOLD and MRS metabolites in our control voxel, which was placed in the occipital lobe. The occipital lobe (OCC) was chosen as the region to place the control MRS voxel for three reasons: firstly, linking to the later *APOE* MRS study in Chapter 5, primary sensory cortex is one of the latest cortical areas to develop amyloid and tau pathology in Alzheimer's disease (Braak & Braak, 1991, 1995). To ensure consistency in the MRS protocol across this thesis, both this Chapter and Chapter 4 employ the same OCC control voxel as Chapter 5. Secondly, the occipital cortex contains visual processing regions that are engaged by relatively low-level visual stimulus properties; area V1 for instance is specialised for processing stimulus orientation (Hubel & Wiesel, 1959), whereas area V5

is specialised to process stimulus motion (Born & Bradley, 2005). Area V8 is specialised to process stimulus colour (Hadjikhani, Liu, Dale, Cavanagh, & Tootell, 1998). Use of an OCC ROI would enable us to compare between PCC BOLD for scenes with PCC metabolites (which, according to our hypotheses, may have a relationship with PCC BOLD) and PCC BOLD for scenes with OCC metabolites (which we hypothesise would not show any preference for particular stimulus categories). A similar approach was taken in Hu et al., (2013) when comparing PCC BOLD with PCC MRS and OCC MRS, to investigate MRS-BOLD correlations of the PCC in DN deactivation (Hu et al., 2013). Thirdly, OCC MRS is a well-established MRS protocol in CUBRIC and has been able to successfully quantify GABA in this region with good test-retest reliability (Mikkelsen, Singh, Sumner, & Evans, 2015; Muthukumaraswamy et al., 2009).

To investigate the relationship between MRS and success on visual discrimination we compared behavioural performance (accuracy) on scene, face and object oddity with metabolite assessments from the PCC, versus OCC, voxels. Previous literature has shown a positive correlation between regional NAA and performance on the function that that region is proposed to support. For example, a positive correlation was identified between hippocampal tNAA and memory (Gimenez et al., 2004), and between prefrontal cortex tNAA and IQ (T. Patel, Blyth, Griffiths, Kelly, & Talcott, 2014). Based on this literature, and based on our predictions that the PCC will show a selective response to scene stimuli, I predicted that a higher concentration of PCC tNAA would be associated with better performance on the scene oddity condition of the task. Furthermore, I predicted there would no relationship between PCC tNAA and performance on the face or object oddity conditions.

The literature is not as clear for GABA+ or Glx relationships with behaviour, as previous studies assessing the relationship between these metabolites and behaviour have tended to investigate patients, or have focused on emotions and impulsivity, rather than measurements of perception accuracy. These findings suggest, however, that correlations between behaviour and GABA+ or Glx do exist. For example, a lower concentration of GABA+ in the dorsomedial prefrontal cortex is associated with impulsivity (Boy, Evans, Edden, Lawrence, & Singh, 2011), a higher concentration of GABA+ in the ventromedial prefrontal cortex with anxiety (Pizzi et al., 2016), and a higher concentration of Glx in the anterior cingulate cortex with trait anxiety (Modi, Rana, Kaur, Rani, & Khushu, 2014), and with impulsivity (Hoerst et al., 2010). This implies that if these metabolites are measured in a brain region that has been associated with a particular task, then a relationship may exist between performance on this task

and the MRS metabolites. In this study, if the PCC is involved in scene perception, then there may therefore be a relationship between performance and the concentrations of GABA or Glx. It is difficult to make directional predictions for these relationships based on the previous GABA or Glx and behaviour literature on impulsivity and anxiety, therefore the correlations between oddity performance and the concentrations of PCC Glx and GABA will be more of an exploratory investigation.

3.2 Methods

3.2.1 Participants

Forty students from Cardiff University were included in this study (12 male; age range 18-25 years, mean age 22.1 years, standard deviation 2.1). This sample size is comparable to those reported in previous MRS-fMRI cognitive studies (e.g., Enzi et al., 2012 (n=19); Falkenberg, Westerhausen, Specht, & Hugdahl, 2012 (n=40); Hu et al., 2013 (n=28)). An a-priori power calculation was also conducted using G-power software (Faul, Erdfelder, Buchner, & Lang, 2009), to calculate the sample size required to detect a BOLD-MRS correlation using two-tailed Pearson correlation statistics. This power calculation used the software's default values of an alpha of ≤ 0.05 and power of 0.8, and estimated the approximate effect size to be 0.43 (based on the average of the estimated effect sizes of the results of the three papers referenced above). This resulted in a required sample size of 32 participants, which was increased to 40 participants to allow for sample attrition during scanning and analysis.

All participants had normal or corrected-to-normal vision, no history of neurological or psychiatric disorders and were right-handed. The study was approved by the Cardiff University School of Psychology ethics committee, and all participants were provided with detailed information sheets, and gave written informed consent. Participants received £40 for taking part in the study.

3.2.2 Overview of scanning procedure

Participants attended the Cardiff University Brain Research Imaging Centre (CUBRIC) for two imaging sessions, arranged on separate days. The mean interval between imaging sessions was 22 days (standard deviation 21 days, range 1-76 days). Session 1 included an fMRI spatial working memory task (to be described in Chapter 4), two field maps, and a 30-direction DTI scan (not analysed as part of the PhD thesis), with a total scan duration of 80min. Session 2 consisted of a structural MRI scan, four MRS scans, the fMRI oddity task reported here, and two field maps, with a total scan duration of 110min. Scan parameters are described in detail in sections 1.2.5-1.2.7. All scans were performed on a 3T General Electric (GE) HDx scanner using an 8 channel phased array head coil. Tasks were viewed in a mirror mounted on top of the head coil, which allowed participants to view a projector screen located behind the scanner.

3.2.3 Oddity fMRI Task

The oddity task was identical to that used in Shine et al., (2015). Participants were shown three images simultaneously, all from the same stimulus category, arranged in the top middle, bottom left, and bottom right of the screen. Four different stimulus categories were presented: scenes, faces, objects and squares. For the scene, face and object categories, two of the images represented the same item but were shown from a different viewpoint, and the third image was obtained from a visually similar, but unique, scene, person or object. The squares acted as a baseline condition, with two of the squares being of equal size, while the third square differed in size. Examples of a trial from each condition are shown in Figure 3.4. In the scanner, participants were asked to view the three images presented in each trial and indicate which image was the odd-one-out by pressing the corresponding button on a three button MRI-compatible response box, held in their right hand. The position of the correct item was randomised throughout the experiment so that the correct item appeared in each location an equal number of times within each condition. All images were trial-unique, so that the brain activity measured was related to the perception of the images rather than reflecting any additional activity linked to stimulus memory (as in Lee et al., 2005).

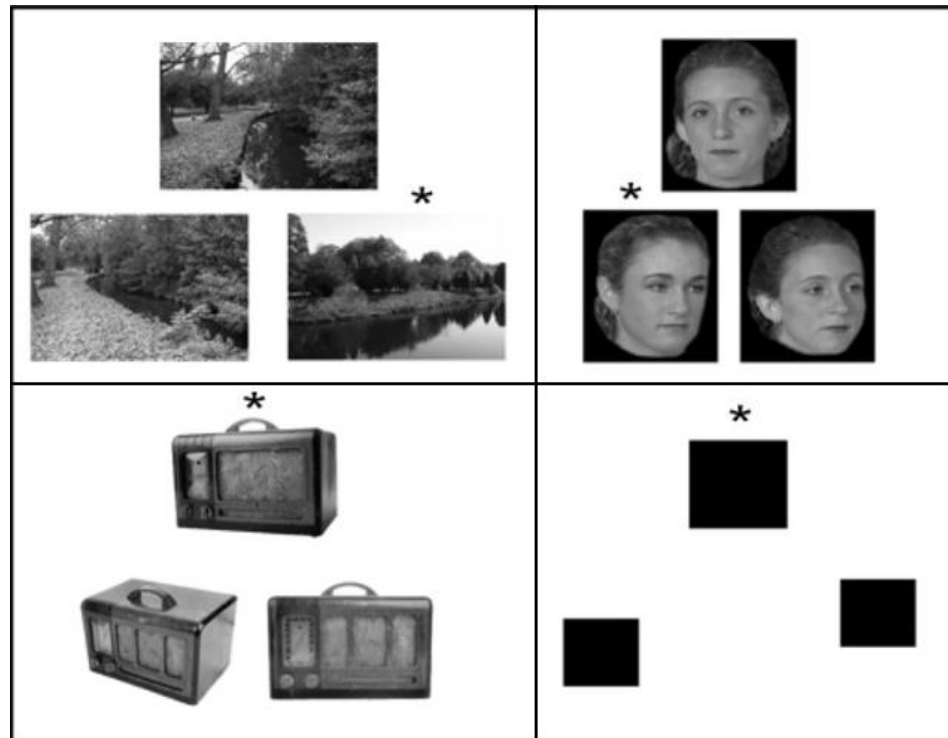


Figure 3.4: Examples of a trial for each stimulus category in the oddity task. An asterisk has been added to indicate the correct response (the item that is the odd-one-out). (Image taken from Shine et al., 2015).

The experiment used an event-related design. Each trial was presented for six seconds, and participants were required to make their response before the images disappeared from the screen. There was a jittered inter-trial interval of 500-4000ms, during which participants were presented with a blank white screen. Trials were arranged into mini-blocks of three trials per stimuli category, to reduce task-switching demands. The order of mini-block categories was counterbalanced between participants. In total, there were 54 trials per condition, creating a total of 216 trials across the whole experiment. The experiment was divided into three fMRI runs, each consisting of 72 trials, and each run lasted 11 minutes. The use of three fMRI runs enabled correction for scanner drift, and provided the participant with a short break between runs to prevent fatigue during the task. The experiment was implemented using E-prime version 2.0 (Psychology Software Tools, Inc., Sharpsburg, PA).

3.2.4 Stimuli

Real-world scenes, objects and faces were presented in black and white format. Stimuli were identical to those used in Shine et al., (2015). The scene stimuli were obtained from a collection held by our research lab and were photographs of outdoor scenes. The face stimuli were also taken from a collection held by our research lab and were photographs of male and female human faces, overlaid on a black background which had the dimensions 170 x 216 pixels. An equal number of male and female faces were used (27 face trials for each gender). For the object condition, photographs of common objects (e.g. chair, television, kitchen implements) taken from the Hemera object data base, Vol 1-3, were used. The squares were filled in black, with the size difference between the odd-one-out image and the two non-target squares varying between 9 and 15 pixels.

3.2.5 fMRI scan parameters

A gradient-echo, echo-planar imaging (EPI) sequence was used to acquire T2*-weighted images with a TE of 35ms, TR of 3000ms, flip angle of 90°, field of view of 220mm and a matrix of 64x64. Each of the three fMRI runs consisted of 240 volumes, with each volume comprising 42 axial slices collected in a bottom-up sequential order. Each slice had a thickness of 2.8mm and an interslice gap of 1.0mm, which created a voxel size of 3.4x3.4x2.8mm. Slices were aligned along the anterior commissure-posterior commissure (AC-PC) line, then tilted 30° backwards as in Shine et al., (2015), with the aim of attenuating signal dropout in the medial temporal lobe (MTL) caused by distortion of the fMRI signal due to nearby air-tissue and bone-tissue interfaces (Olman, Davachi, & Inati, 2009). Two field maps were also obtained, one at a TE of 7ms and the other at a TE of 9ms, in order to correct for distortions in EPI images due to inhomogeneities in the magnetic field (as in Shine et al., 2015). Each fMRI run began with four dummy volumes, to allow equilibration of the magnetic field, and these volumes were removed prior to analysis.

3.2.6 Structural scan parameters

A high-resolution 3D T1-weighted structural MRI scan was obtained for each participant. This scan had the parameters of a TE of 3.0ms, TR of 7.9ms, flip angle of 20°, resolution (i.e. voxel size) of 1mm isotropic, matrix of 256x192x176mm, field of view of 256x192x176mm, and an acquisition time of 7 minutes. This structural scan was used to: 1) guide accurate placement of the MRS voxels (see section 2.7 below), 2) perform segmentation of the MRS voxels into cerebro-spinal fluid (CSF), grey matter (GM) and white matter (WM) using FAST in FSL prior to MRS analysis (Zhang, Brady, & Smith, 2001), and 3) co-register the low spatial resolution fMRI data onto a high resolution anatomical image.

3.2.7 MRS scan parameters

Single voxel spectroscopy was used to acquire spectra from two regions: the PCC (our MRS voxel of interest), and the occipital cortex (OCC, our control voxel). The PCC voxel measured 2x2x3cm and the OCC voxel measured 3x3x3cm. Examples of PCC and OCC voxel placement are shown in Figure 3.5.

The difference between OCC and PCC voxel size arose because there was a trade-off between a large enough voxel in the PCC to be able to accurately detect metabolites, and a decrease in this voxel size to ensure spatial specificity of the PCC ROI. An OCC voxel size of 3x3x3cm reliably produces good quality MEGA-PRESS spectra to quantify GABA at CUBRIC (e.g. Muthukumaraswamy et al., 2009; Muthukumaraswamy, Evans, Edden, Wise, & Singh, 2012) and has been recommended for MEGA-PRESS scanning (Mullins et al., 2014). This is because large voxels are necessary to quantify GABA+, as GABA+ is present in low concentrations and smaller voxels have a lower-signal-to-noise ratio. A PCC voxel of this size, however, would have reduced the spatial specificity, and in this case would have led to a large overlap of the two voxels. As the spatial specificity of the PCC voxel was of key interest here, the size of this voxel was reduced from the standard 3x3x3cm voxel commonly used in MEGA-PRESS scans to 2x2x3cm. To counteract the reduction in SNR from this reduction in volume, the length of the MEGA-PRESS scan was increased to improve PCC MEGA-PRESS data quality and to match the signal-to-noise

ratio (SNR) of the two voxels. This approach was determined via a pilot study investigating test-retest reliability of the PRESS and MEGA-PRESS scans.

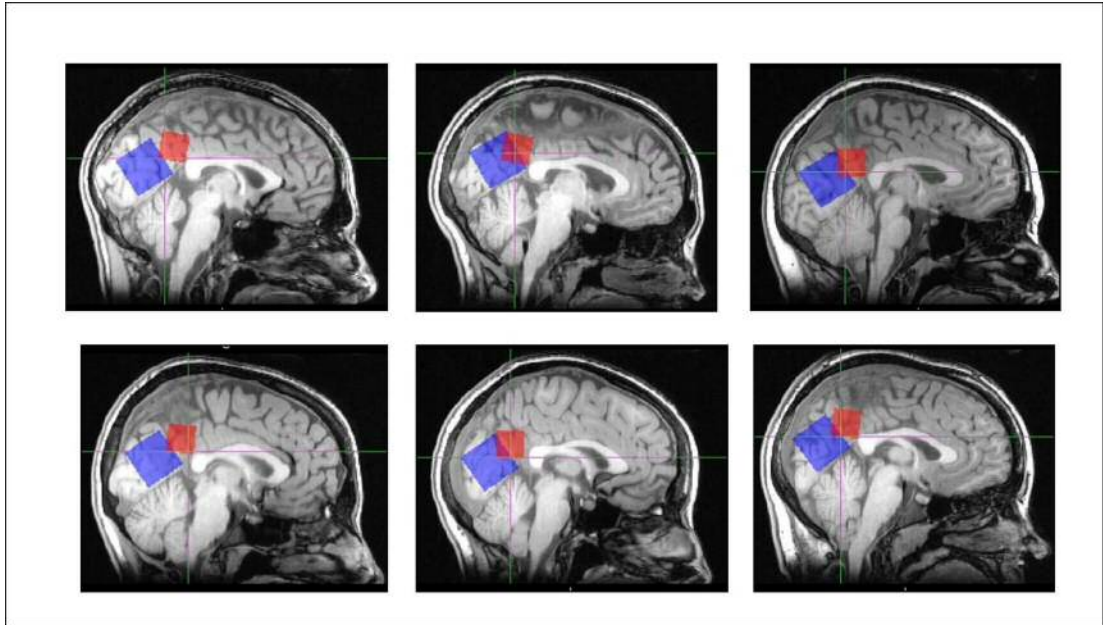


Figure 3.5: Examples of placement of PCC MRS voxel (red) and OCC MRS voxel (blue). Voxel placement is shown in six representative participants to display inter-individual variability in brain structure and consequently inter-individual variability in voxel placement.

Voxels were placed using a systematic approach developed from the pilot study, consisting of six individuals, which was designed to assess data quality from the PCC and OCC regions, and the test-retest reliability of metabolite concentrations in these two voxel. This pilot study revealed voxel placement was quite variable between individuals, due to inter-individual differences in brain anatomy and lack of use of a landmark for voxel placement by the experimenter. The following steps were, therefore, designed to improve consistency of voxel placement: first, to place the OCC voxel, a rotate-localiser aligned to the tentorium cerebelli was obtained, and the OCC voxel was placed on top of this. The voxel was adjusted so that it did not overlap with the scalp, which would cause lipid-contamination in the MRS spectra. For PCC voxel placement, a sagittal localiser scan of the centre of the brain was obtained to provide a higher resolution scan of the corpus callosum. The resulting image from this scan was then used to align a second rotate-localiser line along the base of the corpus callosum. This rotate-localiser line was widened to consist of an odd number of slices, measured from the bottom to the top of

the corpus callosum (typically 5 or 7 slices, depending on each individual's brain anatomy). The central slice of this rotate-localiser was then employed as the lowest edge for PCC voxel placement. The PCC voxel sat on top of this central line of the rotate-localiser, and the voxel was adjusted to lie posterior to the ventricles to avoid placing the voxel in an area of CSF, which would distort the MRS signal.

In each voxel, one PRESS scan was obtained to quantify the metabolites tNAA and Glx, and one MEGA-PRESS scan was obtained to quantify GABA+ (see Chapter 2 for reasons for using different scan types for different metabolites). Scan parameters for the PCC and OCC PRESS scans were TE 35ms, TR 1500ms, number of averages (i.e. the number of times the spectrum was sampled over the scan acquisition) was 128, and the acquisition time was 4 minutes. Scanning parameters for the PCC and OCC MEGA-PRESS scans were a TE of 68ms, TR of 1800ms, and spectral width of 5kHz. For the OCC MEGA-PRESS scan, the number of averages was 332 and acquisition time was 10minutes. For the PCC MEGA-PRESS scan, the number of averages was 512 and acquisition time was 15minutes. Shimming was performed before all MRS scans to ensure water-linewidth of 10kHz or lower, in order to obtain sharp peaks in the resulting MRS spectrum.

3.2.8 Data Analysis

3.2.8.1 Behavioural data analysis

Behavioural performance on the oddity task was assessed by calculating the accuracy (ACC, proportion of correct odd-one-out responses), reaction time (RT, difference between stimulus presentation and button press, in milliseconds, for correct trials only), and inverse efficiency (IE, a speed/accuracy trade off measure, in milliseconds, calculated using the formula: reaction time/proportion of correct responses) for each participant on each of the four stimulus conditions. This was calculated for each experimental run separately, and values were then averaged over the three runs to obtain a mean ACC, RT and IE measure for each condition and participant. The resulting mean ACC, RT and IE values were then averaged again across all participants to obtain an overall group mean behavioural performance for each condition.

3.2.8.2 fMRI data analysis

The fMRI data was preprocessed and analysed using FSL version 4.1, via the FMRI Expert Analysis Tool (FEAT) (<http://www.fmrib.ox.ac.uk/fsl/>). Preprocessing included removal of the brain from the skull via the FSL brain extraction tool (BET) (Smith, 2002), motion correction using MCFLIRT (Jenkinson, Bannister, Brady, & Smith, 2002), spatial smoothing using a full-width-at-half-maximum (FWHM) Gaussian kernel of 5mm, mean-based intensity normalisation, high pass temporal filtering set to a cut-off value of 100seconds, and unwarping the EPI data using the two field maps to correct for distortion due to inhomogeneities in the magnetic field (Jenkinson, 2003).

The fMRI analysis used an event-related design. The first stage of the analysis was to carry out a single-subject level analysis for each of the three experimental runs. This was performed using a general linear model (GLM) for the haemodynamic response function consisting of four explanatory variables (the four task conditions: scenes, faces, objects and size). Consistent with Shine et al., (2015), trials were modelled for each condition beginning at the start of the trial presentation and lasting for the full 6 second trial duration. Trial start times were obtained from each participant's E-prime output file. Only trials with accurate responses were included in this analysis. A parameter estimate was created for the contrasts of scene, face and object conditions relative to the baseline condition of size (i.e. scenes>size, faces>size and objects>size). To ensure good quality fMRI data, each run was examined for participant movement. A run was excluded if movement exceed one fMRI voxel (>3.4mm) (see section 3.3.1 for details of data exclusions). The second stage of the fMRI analysis was to combine the three experimental runs for each participant using a fixed-effects group analysis. The third stage of analysis was to quantify the percent signal change in the PCC ROI for each contrast of scenes, faces and objects relative to size, using the Featquery tool in FSL. The PCC ROI chosen for the Featquery analysis was the region identified in Task A of Shine et al.'s (2015) study, where *APOE*-E4 carriers showed a different profile of BOLD activity compared to non-carriers for scenes>rest during a one-back visual working memory task for scenes, faces objects and scrambled objects (ROI shown in Figure 3.6). Using this ROI here ensures linkage with Chapter 5 where I aim to compare PCC metabolites between young *APOE*-E4 carriers and non-carriers.

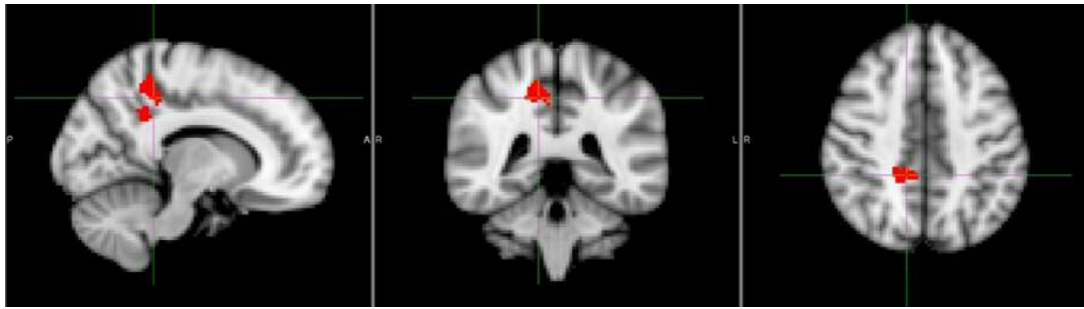


Figure 3.6: PCC region of interest, taken from Shine et al., (2015).

3.2.8.3 MRS data analysis

To quantify tNAA and Glx, the PRESS data were analysed using TARQUIN (Totally Automatic Robust Quantification In NMR) (version 4.3.3) (Wilson, Reynolds, Kauppinen, Arvanitis, & Peet, 2011). To ensure good quality data, metabolites were excluded if the Cramer Rao Lower Bound (CRLB) was above 20%, which is consistent with the exclusion criteria commonly found in the MRS literature (Cavassila, Deval, Huegen, Van Ormondt, & Graveron-Demilly, 2001; Hu et al., 2013; Stagg & Rothman, 2014). As is common in the MRS literature, since it can be difficult to accurately separate the large peak of NAA at 2.01ppm from the small NAAG peak at 2.04ppm, these were combined to create a “total NAA” or tNAA measure. Similarly, it is difficult to accurately separate the peak of glutamate from glutamine which lie between 2.2 and 2.4ppm, therefore these measures were combined to create a composite glutamine + glutamate measure, or “Glx” (Rae, 2014; Stagg & Rothman, 2014) (see Chapter 2 for more details).

MEGA-PRESS data were analysed using GANNET (version 2.0) (Edden, Puts, Harris, Barker, & Evans, 2014). Data quality was assessed using a 3-point rating scale (as in Lipp et al., 2015): spectra were rated by two assessors on a 3-point rating scale (very good, satisfactory, reject). Assessors included myself and the CUBRIC MRI lab manager, who is highly experienced in GABA spectroscopy. Where one assessor rated a spectrum as reject and there was a difference of opinion, ratings were discussed and spectra were excluded if one assessor’s rating was still reject after the discussion (i.e. the average rating was less than satisfactory). The GABA+ measured in this MEGA-PRESS scan actually represents GABA plus macromolecules, as the peak contains resonances from co-edited

macromolecules, and is referred to in the literature as “GABA+” (see Chapter 2 for more details).

All metabolite concentrations were corrected for the partial volume effect of CSF, by multiplying the metabolite concentrations by the fraction of CSF, GM and WM within the voxels (as in Harris et al., 2015; Lipp et al., 2015). This fraction was obtained by segmenting the voxels using the FAST tool to obtain three values, one for each of the proportion of GM, WM and CSF within the MRS voxel (Zhang et al., 2001).

All metabolites were quantified relative to H₂O. H₂O was chosen as the reference signal as opposed to Creatine (Cr), which is also frequently used in the literature, for two reasons. First, H₂O is present in the brain at much higher concentrations than Cr and is, therefore, is a more accurate measure, since the estimate of variance on the water concentration will be a much smaller proportion of this large concentration of water than of the relatively miniscule concentration of Cr. Second, it remains possible that Cr is altered in young *APOE-E4* carriers, as seen in MRS studies of older *APOE-E4* carriers (Laakso et al., 2003). If this was true, the use of Cr as the reference signal could confound analysis of the influence of *APOE-E4* on other MRS metabolites planned as the focus later in this PhD thesis. Consequently, H₂O was used as the reference signal for all experiments.

3.2.8.4 fMRI-MRS Relationships

3.2.8.4.1 fMRI-MRS – Percent signal change ROI analysis

To assess whether individual differences in PCC fMRI activity were related to individual differences in the concentration of tNAA, GABA+ and Glx in the PCC, Pearson correlations were performed between the BOLD percentage signal change in the PCC ROI for the contrasts scenes>size, faces> size and objects>size and measurement of each of the three PCC metabolites.

To establish whether any identified fMRI-MRS relationship between PCC and MRS metabolites were regionally specific to the PCC for our key contrast of interest, Pearson correlations were also performed to identify whether there was a potential association

between PCC BOLD percent signal change for the contrast scenes>size with the metabolite levels for tNAA, GABA+ and Glx in the OCC control voxel.

In total, this created 12 correlations, with three being of particular interest (e.g., based on scenes>size), six considered experimental controls within PCC, and three control analyses applied in a different brain regions (OCC). This created different “families” of comparisons (as in Cao & Zhang, 2014). To correct for multiple comparisons, Bonferroni correction was applied within each family of three tests (i.e. family-wise error correction: $0.05/3 = p\ 0.167$); this avoided an overly stringent Bonferroni correction which would have had the potential for a high risk of false negative results (Nakagawa, 2004).

To test whether any correlations between PCC BOLD and metabolites in the PCC and OCC voxels were statistically different from each other, and in order to confirm any regional and category sensitivity, two-tailed Steiger Z-tests were performed, using the QuantPsy package (I. A. Lee & Preacher, 2013; available from <http://quantpsy.org/corrtest/corrtest2.htm>).

Bayes factor analysis was also carried out, using the JASP software (available from <https://jasp-stats.org/>), providing a complementary statistical approach to assess the evidence in favour or against my predictions (as in Harris et al., 2015). Bayesian statistics has the advantage that it is not necessary to correct for multiple comparisons, as unlike p values which are based on the likelihood of a result occurring by chance, Bayes factors assess whether the evidence for a hypothesis is sufficient and produces a value that represents the strength of this evidence (Rouder, Speckman, Sun, Morey, & Iverson, 2009). A further advantage of Bayes is that it can test the evidence *against* an effect, as well as *for* an effect. This is denoted as a one-tailed Bayes test in favour of the null hypothesis (BF_{01}), or a one-tailed Bayes test in favour of the hypothesis (BF_{10}). A BF_{01} or BF_{10} of greater than 3 suggests there is sufficient evidence either against or in favour of the hypothesis; a BF_{10} above 3 represents that the data are three times more likely to occur under the hypothesis than under the null hypothesis, and vice versa for the BF_{01} value (Jarosz & Wiley, 2014). Where the results of the p value statistics and Bayesian statistics are consistent with each other, this strengthens the confidence in either result alone.

3.2.8.4.2 fMRI-MRS - Voxel-wise GLM with MRS covariate analysis

In addition to the main analysis described above which focused on identifying relationships between the BOLD response quantified from the PCC ROI with metabolites measured in the MRS voxels, a complementary regressor analysis was conducted to identify any fMRI voxels within the PCC MRS voxel area where metabolites correlated with BOLD activity. This complementary analysis is consistent with the dual-approach discussed in Section 2.3.2 of Chapter 2. This complementary regressor analysis facilitated consideration of the relationship between BOLD and metabolite levels within the larger PCC MRS voxel, rather than constraining the analysis to the relatively small PCC fMRI ROI identified in Shine et al. (2015). Additionally, by using a voxel-wise approach within this larger PCC voxel, this analysis may be more sensitive to particular regions where BOLD activity was related to metabolite concentrations, rather than the BOLD values for the main analysis being averaged across the PCC ROI (thus adding noise from non-selective voxels).

Three separate general linear models (GLMs) were created for the contrasts of scenes, faces and objects compared to size, where each model included demeaned values of either PCC tNAA, Glx or GABA+ as a regressor. Contrasts were set up so that results would show any voxels that were positively or negatively correlated with each metabolite for that contrast. The mask region for the MRS voxel used in this group-level analysis was created by adding participant's PCC MRS voxel masks together within standard space. The number of participants used to create the masks differed for the tNAA, Glx and GABA+ analyses, as there were different numbers of participants remaining for these analyses after exclusions following data quality control (tNAA n=33, Glx n=32, GABA+ n=24) (masks shown in Figure 3.7).

The statistical threshold for the fMRI analysis was voxel-wise, uncorrected at $p < 0.01$ (as in Hodgetts et al., 2015). To prevent false positives due to multiple-comparisons (as there were approximately 4000 voxels within each mask), Monte-Carlo simulation was used to determine whether the size of any resulting cluster was statistically significant, using the 3dClustSim command in AFNI (https://afni.nimh.nih.gov/pub/dist/doc/program_help/3dClustSim.html). A cluster-corrected threshold of $p < 0.01$ was selected (as in Hodgetts et al., 2015), which determined that any cluster larger than 42 voxels was statistically significant at $p < 0.01$ for the tNAA mask and Glx mask, and 40 voxels for the GABA+ mask.

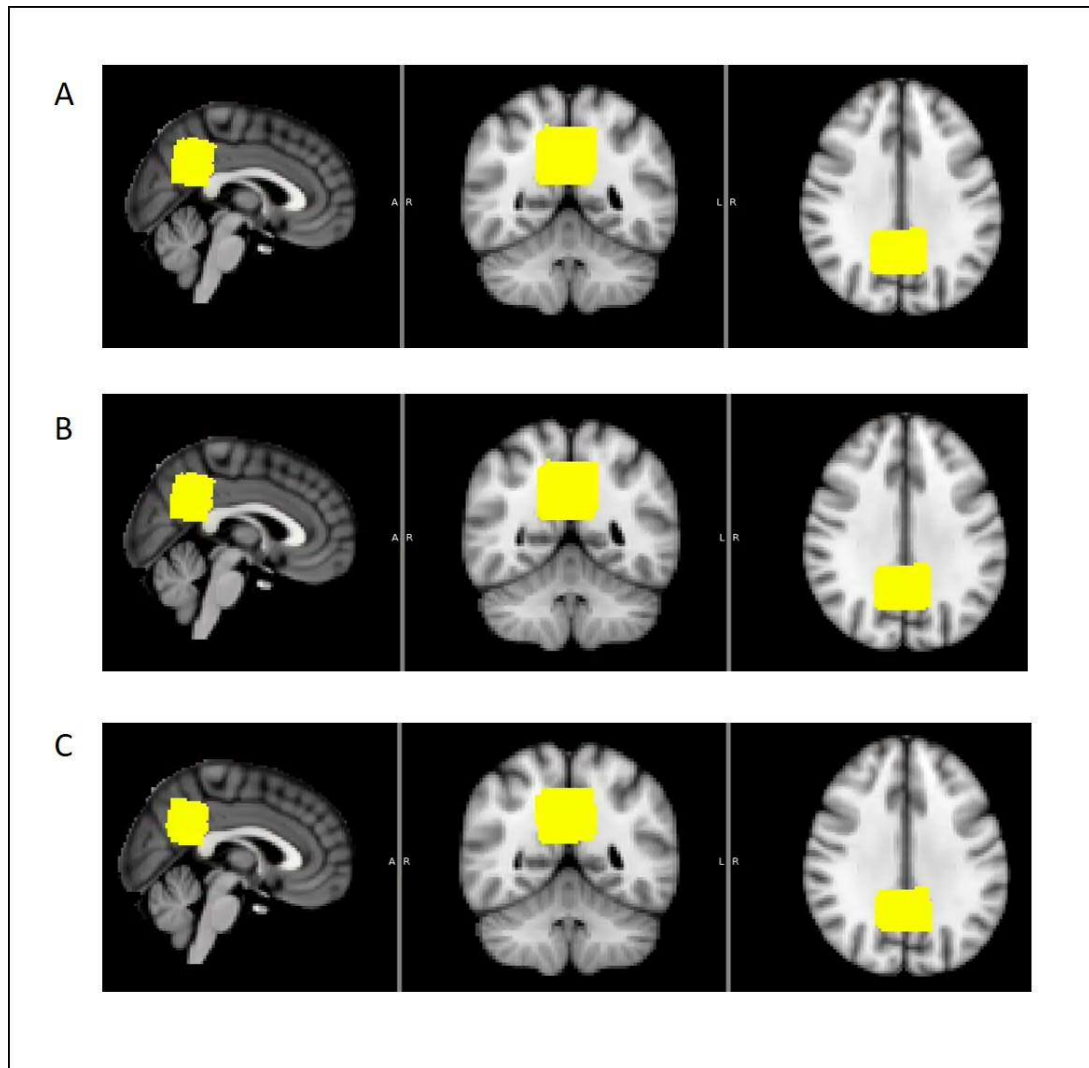


Figure 3.7: Masks used for voxel-wise GLM analysis to investigate MRS-fMRI relationships within the MRS voxel area for each metabolite separately. (A) Mask for tNAA (n=33, mask volume = 4619 voxels. (B) Mask for Glx (n=32, mask volume = 4593 voxels. (C) Mask for GABA+ (n=24, mask volume 3889 voxels).

3.2.9 Behaviour-fMRI and behaviour-MRS correlations

To investigate the relationships between behavioural performance for the scene, face and object conditions of the oddity task and PCC BOLD and PCC MRS, Pearson correlations were performed between the proportion of correct responses for each condition with PCC BOLD for the corresponding contrast, and with PCC tNAA, Glx and GABA+.

3.2.10 Statistical analysis

For the repeated measures ANOVAs, Mauchly's test was used to assess the assumption of sphericity across the three conditions. Where this assumption was violated, the Greenhouse-Geisser correction was applied, and this is stated in the results.

3.3 Results

3.3.1 Data exclusions

Details of the exclusions of behavioural, fMRI and MRS data are summarised in Table 3.1. Of the 40 scanned participants, one participant was excluded because they withdrew from the study after the first scan session, and two participants were excluded due to scanner errors. The fMRI data quality assessment of the remaining 37 participants resulted in the exclusion of a further two participants' fMRI data due to excessive movement (greater than one fMRI voxel (3.4mm)) during more than one fMRI run, leaving a sample size of 35 participants for the fMRI analysis. Of these 35 participants, one of the three fMRI task runs was excluded in five data sets, due to excessive movement during that run (the remaining two runs for these five participants were included in subsequent analyses).

The behavioural analysis was based on the 35 participants whose data was used in the fMRI analysis. For the five participants for whom one of the three fMRI runs was excluded due to movement, the behavioural data from all three runs were used, in order for their behavioural data to be comparable with that of the rest of the participants (rather than only representing two thirds of this).

Following the MRS data quality control measures of the 37 participants, 11 MEGA-PRESS spectra were rejected as these were rated as less than satisfactory on the 3-point rating scale, and 7 PRESS metabolites (two PCC tNAA, three PCC Glx, one OCC tNAA and one OCC Glx) had a CRLB greater than 20%, so were also rejected.

As there were different sample sizes remaining for the behavioural, fMRI and MRS data, different sample sizes were used in the correlations between these measures, which are given in Table 3.1.

Data type		Exclusions due to scanning issue + data quality issue (fMRI + MRS)	N remaining from original sample size of 40
Behaviour (only for participants where there is fMRI data)		3 + 2	35
fMRI		3 + 2	35
PCC MRS	tNAA	3 + 2	35
	Glx	3 + 3	34
	GABA+	3 + 11	26
OCC MRS	tNAA	3 + 1	36
	Glx	3 + 1	36
	GABA+	3 + 1	36
Correlations between measures	fMRI and PCC tNAA	3 + (2 + 2)	33
	fMRI and PCC Glx	3 + (2 + 3)	32
	fMRI and PCC GABA+	3 + (2 + 11)	24
	fMRI and OCC tNAA	3 + (2 + 1)	34
	fMRI and OCC Glx	3 + (2 + 1)	34
	fMRI and OCC GABA+	3 + (2 + 1)	34
	fMRI and behaviour	Same as fMRI sample size	Same as fMRI sample size
	MRS and behaviour	Same as fMRI and MRS correlation sample size	Same as fMRI and MRS correlation sample size

Table 3.1: The number of participants' data remaining in each part of this study after data exclusions due to scanning issues (participant withdrawal and scanner failures) and data quality control assessments. The numbers of participants for each type of exclusion are listed in the third column, and subtracted from the original sample size of n=40 in the fourth column. For the correlations between measures, the values in the third column refer to the scanner issues + (fMRI data quality issues + MRS data quality issues). For the fMRI and MRS correlations, no participant had both poor quality fMRI and MRS data, thus exclusions for fMRI and MRS have been combined.

3.3.2 Behavioural Results

Repeated measures ANOVAs were performed for accuracy, reaction time and inverse efficiency. No significant differences were evident in accuracy between the four conditions: $F(3,102)=1.16$, $p=0.33$ (see Figure 3.8A), but there was a significant effect of condition on reaction time, $F(3,102)=97.25$, $p<0.001$ (see Figure 3.8B). Post-hoc analyses confirmed that reaction time was significantly faster in the size compared to the scene ($t(34)=14.34$, $p<0.001$), face ($t(34)=11.13$, $p<0.001$) and object conditions ($t(34)=11.71$, $p<0.001$). Reaction time to faces ($t(34)=3.02$, $p=0.01$) and objects ($t(34)=2.83$, $p<0.01$) was also faster than scenes. There was also a significant effect of condition evident on inverse efficiency ($F(3, 102)=53.78$, $p<0.001$ (see Figure 3.8C). As in the reaction time analysis, post-hoc tests revealed a significant difference between the size condition and scenes ($t(34)=11.90$, $p<0.001$), faces ($t(34)=7.78$, $p<0.001$), and objects ($t(34)=10.85$, $p<0.001$), where IE was faster for size. Faces was also significantly faster than scenes ($t(34)=2.56$, $p<0.05$).

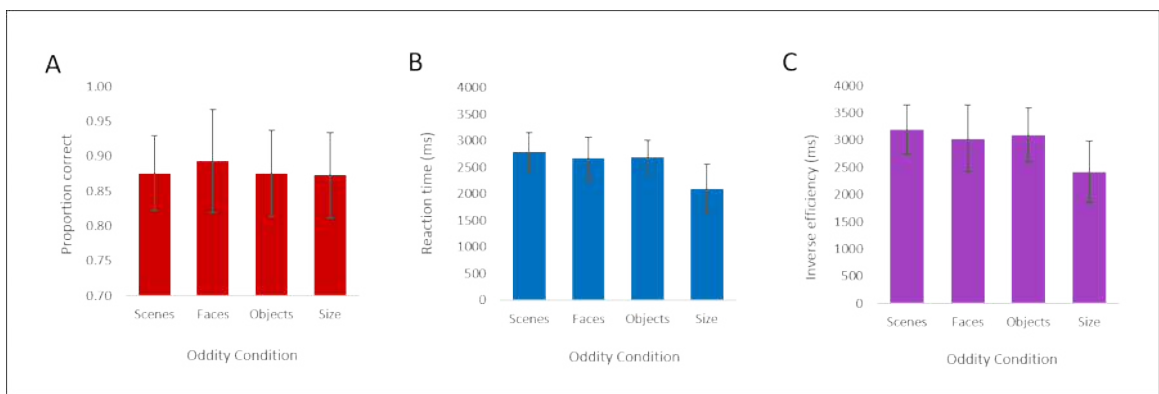


Figure 3.8: Behavioural results for the four stimulus categories (mean and standard error). (A) Proportion correct (calculated as hits – false alarms), (B) Reaction time (ms), (C) Inverse efficiency (ms) (calculated as RT/proportion correct).

3.3.3 fMRI Results – investigating category sensitivity in the PCC ROI

The contrasts scenes>size, faces>size and objects>size were applied in the PCC ROI to investigate whether this region shows a category-sensitive BOLD response. The horizontal bars in Figure 3.9 show the mean BOLD percentage signal change in the PCC ROI for each of these contrasts, and the dots represent individual participants. A repeated-measures ANOVA revealed a significant main effect of oddity condition on the PCC ROI BOLD response: $F(1.42, 48.21)=34.68, p<0.001$ (Greenhouse-Geisser corrected). Planned comparisons between scenes with each of the other two conditions confirmed this main effect reflected a greater PCC deactivation during both the face and object conditions compared to the scene condition: scenes>size versus faces>size ($F(1, 34)=14.92, p<0.001$), and scenes>size versus objects>size ($F(1, 34)=52.65, p<0.001$).

Figure 3.9 shows that there is a data point for scenes>size that has a relatively large positive percentage signal change for scenes>size compared to the other 34 participants' data points (the yellow data point at the top of the Figure). This data point would not be classed as an outlier, however, if an outlier is defined by the distance from the mean, as it lies less than three standard deviations from the mean (which is a commonly used criteria for outlier detection (e.g. Osborne & Overbay, 2004)). In addition, this participant had comparable behavioural performance on the scene condition as the other participants, and there were no differences in the data quality (e.g. movement) for this participant, thus the difference in their response to scenes could not be due to the participant performing the task incorrectly or an issue during scanning. Since I am interested in correlating individual variability in BOLD with MRS, this data point could provide interesting variance, therefore was kept in. To address any concern that this data point might be affecting the mean BOLD percent signal change for scenes>size, and thus impacting on the repeated measures ANOVA, if this data point for scenes>size were to be removed the results of the ANOVA remained significant: $F(1.55, 51.13)=36.25, p<0.001$ (Greenhouse-Geisser corrected), with mean BOLD for scenes>size changing from -0.02% to -0.03%. The BOLD-MRS correlations below have also been checked to test whether this data point was driving any correlations, and, as reported below, it had no impact on these findings.

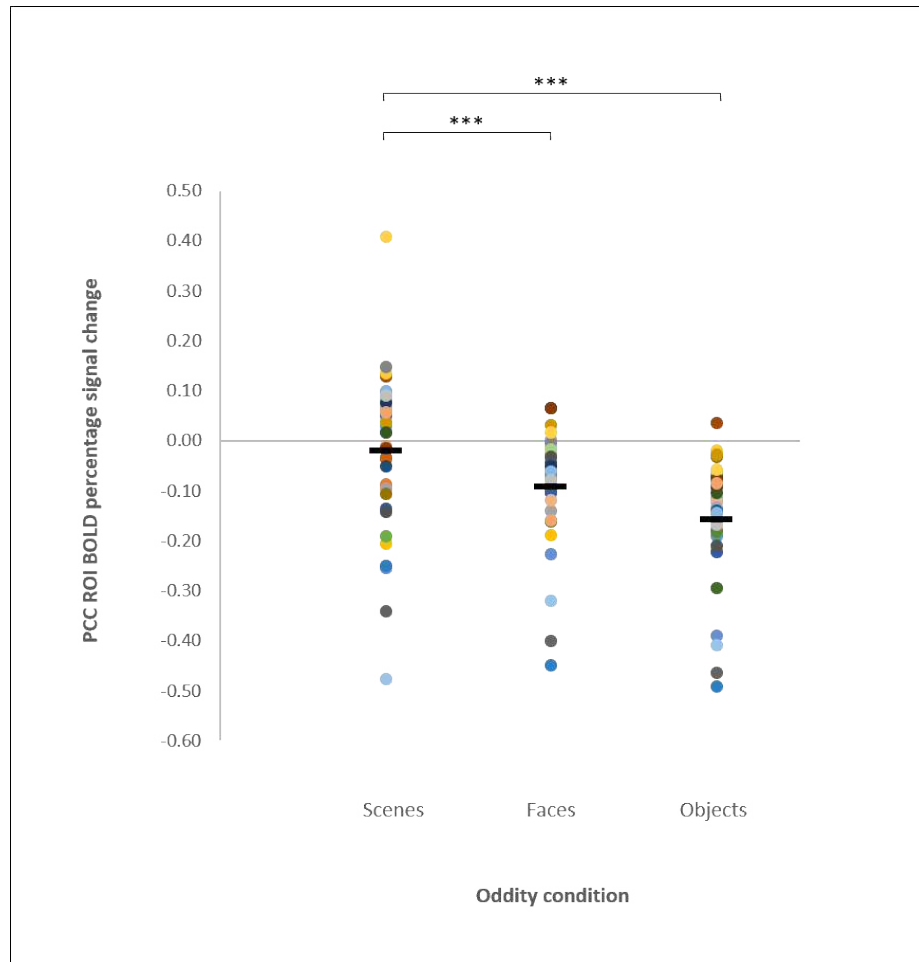


Figure 3.9: BOLD percentage signal change in the PCC ROI for scenes, faces and objects contrasted to the size baseline. Dots represent individual participants and the horizontal black bars show the mean for each condition. The asterisks represent the significance level of the comparisons between scenes and faces and scenes and objects, where * indicates a significant difference at $p < 0.001$.**

3.3.4 MRS Results

Examples of a MEGA-PRESS and PRESS spectra in each voxel are shown in Figure 3.10. Mean and standard deviations for PCC and OCC metabolites are shown in Table 3.2.

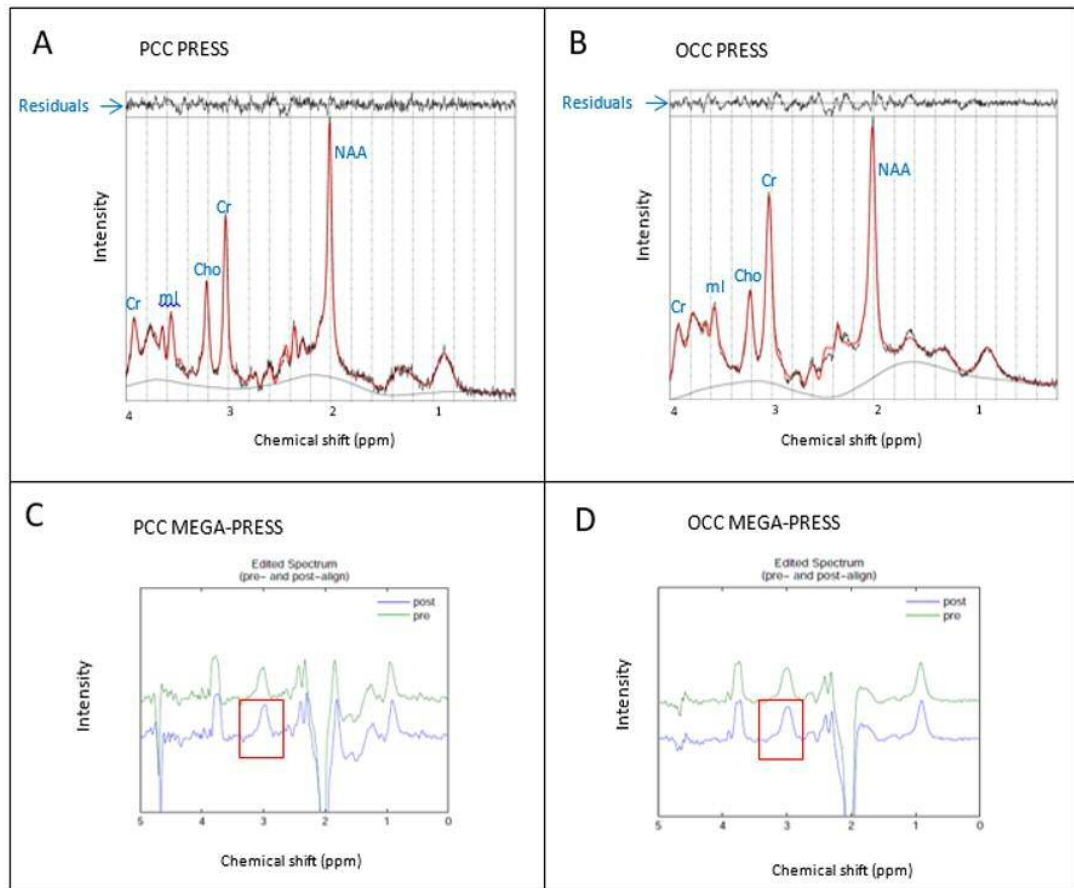


Figure 3.10: Examples of each type of MRS spectrum in each voxel. In C and D, the red squares indicate the GABA peak.

	PCC MRS			OCC MRS		
	tNAA	Glx	GABA+	tNAA	Glx	GABA+
Mean concentration (mM)	16.38	20.71	1.83	13.44	21.50	1.98
Standard deviation	0.91	2.86	0.28	1.37	2.74	0.19

Table 3.2: Mean concentration and standard deviation of each metabolite for the different sample sizes remaining after data exclusions (given in Table 3.1).

3.3.5 fMRI-MRS Relationships

3.3.5.1 fMRI-MRS – Percent signal change ROI analysis

As discussed in Section 3.3.2.8.4.1, Pearson correlations were performed to assess the relationship between BOLD percentage signal change for scenes>size in the PCC ROI with PCC tNAA, Glx and GABA+. To assess category sensitivity, a further six correlations investigated associations between PCC BOLD activity for faces>size and objects>size, and PCC metabolites. To assess regional sensitivity, PCC BOLD for for scenes>size was correlated with OCC metabolites. Results are displayed in Table 3.3 and Figure 3.11.

	Correlation between		N	r	p	Bayes factor
	PCC BOLD contrast (>size)	MRS measure				
A. Correlations of interest	Scenes	PCC tNAA	33	0.42	0.016 *	BF ₁₀ = 7.03 *
		PCC Glx	32	-0.25	0.16	BF ₁₀ = 0.10
		PCC GABA+	24	0.10	0.64	BF ₁₀ = 0.14
B. Test for category sensitivity	Faces	PCC tNAA	33	0.18	0.31	BF ₀₁ = 2.79
		PCC Glx	32	-0.09	0.63	BF ₀₁ = 4.07 *
		PCC GABA+	24	-0.09	0.67	BF ₀₁ = 3.62 *
	Objects	PCC tNAA	33	0.25	0.16	BF ₀₁ = 1.81
		PCC Glx	32	-0.10	0.59	BF ₀₁ = 3.96 *
		PCC GABA+	24	-0.04	0.86	BF ₀₁ = 3.88 *
C. Test for regional sensitivity	Scenes	OCC tNAA	34	0.09	0.63	BF ₀₁ = 4.18 *
		OCC Glx	34	-0.07	0.71	BF ₀₁ = 4.38 *
		OCC GABA+	34	-0.001	0.99	BF ₀₁ = 4.69 *

Table 3.3: PCC BOLD correlations for each oddity condition (relative to the size baseline) with PCC and OCC metabolites. Part A shows the correlations of interest, and Parts B and C the control correlations to assess stimuli specificity and regional specificity. N is the sample size remaining after combining MRS and fMRI data sets following exclusions of each data type due to quality control measures, r is the Pearson correlation coefficient, and the p value is 2-tailed (Bonferroni corrected, $p = 0.0167$). The double lines between each three correlations represent the family of comparisons within which Bonferroni correction has been applied. For the Bayes factors, BF₁₀ represents a one-tailed Bayes test in favour of the hypothesis (i.e. that there is a relationship between MRS and BOLD), while BF₀₁ represents a one-tailed Bayes test in favour of the null hypothesis (i.e. that there is no relationship between MRS and BOLD). A Bayes factor of three and above suggests there is sufficient evidence to support the specified hypothesis.

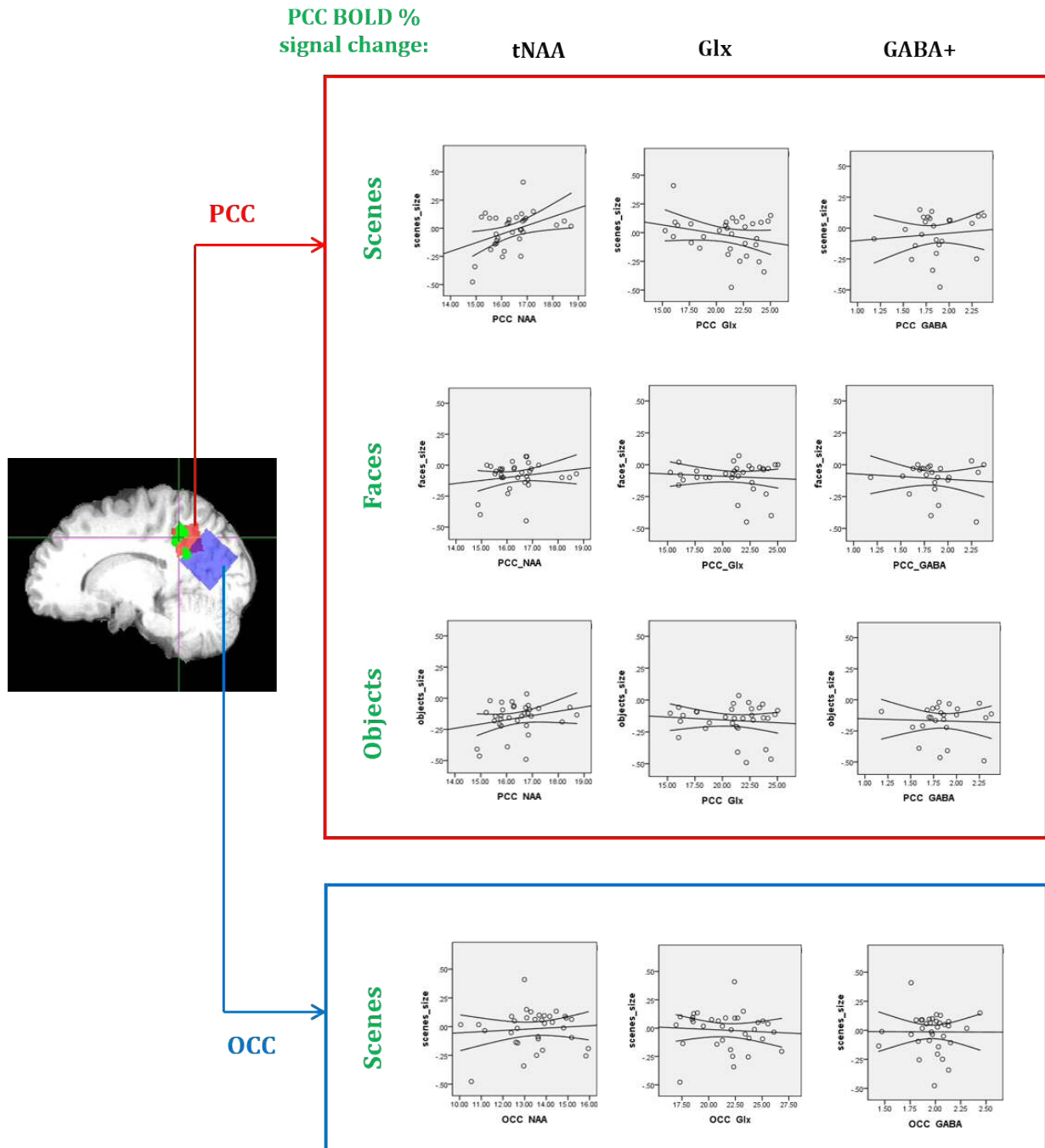


Figure 3.11: Plots of correlations between the BOLD percentage signal change in the PCC ROI for each oddity condition relative to the size baseline with PCC or OCC metabolites. The PCC voxel is shown in red and OCC in blue. The green area is the PCC fMRI ROI obtained from Shine et al 2015. 95% confidence intervals have been plotted onto these graphs. The correlation between PCC tNAA and scenes>size is significant at $p = 0.0167$, and all other correlations are non-significant ($p > 0.05$).

There was a significant positive correlation between PCC BOLD for scenes and PCC tNAA, where the level of significance was just below the threshold set by the family-wise Bonferroni correction (i.e. $p=0.0167$). In support of this correlation, the Bayes Factor was 7.03, indicating there was sufficient evidence in favour of a positive association between PCC BOLD activity elicited for scenes and PCC tNAA. Returning to the concern that a potential outlier for scenes may be driving a correlation, the top left plot in Figure 3.11 shows that the participant with the most positive BOLD percent signal change for scenes has a concentration of PCC tNAA that is close to the mean of the group; thus, this individual point cannot be driving the correlation. Indeed, if this data point were to be removed, the correlation becomes slightly stronger and more significant: $r=0.43$, $p=0.015$, and the Bayes factor in favour of relationship (BF_{10}) would increase slightly to 7.29.

The relationship between PCC BOLD for scenes and tNAA appeared to be regionally specific to the PCC, as there was no significant correlation between PCC BOLD for scenes and OCC tNAA, additionally confirmed by a Bayes factor against a correlation (BF_{01}) of 4.18. Despite this, the difference between the correlations of PCC BOLD for scenes with PCC tNAA and with OCC tNAA did not reach statistical significance in the Steiger Z-test ($Z=1.31$, $p=0.19$). For GABA+ and Glx, there were no significant relationships between scene PCC BOLD and these metabolites in the OCC voxel.

Regarding category-sensitivity, there were no significant correlations between PCC BOLD for faces or objects with PCC tNAA, which would suggest that PCC BOLD-tNAA relationships were sensitive to scene stimuli. However, the BF_{01} values for the relationships of PCC BOLD for faces and objects with PCC tNAA were less than 3, which would suggest that there is insufficient evidence to have strong confidence in these null effects. Furthermore, when the correlations between PCC tNAA and PCC BOLD for scenes, faces and objects were compared using Steiger Z-tests, the correlation for scenes was not significantly different from that with faces ($Z=1.85$, $p=0.065$) nor objects ($Z=1.35$, $p=0.18$), although the difference between the correlations for faces and scenes was nearly significant.

For the metabolites GABA+ and Glx, no significant relationships were evident between PCC BOLD for scenes and PCC GABA+ or Glx, which were also supported by the Bayes factors of less than 3. In addition, there were no significant relationships between

PCC BOLD for faces or objects with PCC GABA+ or Glx. Finally, there were no significant relationships between PCC BOLD for scenes and OCC GABA+ or Glx.

The lack of difference between the correlations obtained for PCC tNAA and PCC BOLD activity for scenes, faces and objects (all contrasted with size) could be attributed to the high correlations between the BOLD responses to these three conditions (scenes vs faces, $r = 0.73$, $p < 0.001$; scenes vs objects, $r = 0.73$, $p < 0.001$; faces vs objects, $r = 0.88$, $p < 0.001$). In order to further explore whether there was a scene-sensitive relationship between PCC BOLD and PCC tNAA, the variance in PCC BOLD that could be explained by faces>size and objects>size was regressed out of each participant's PCC BOLD for scenes>size. The resulting value after removing this shared variance was each participant's PCC BOLD percent signal change that could solely be attributed to the scene condition. These BOLD values for all participants were then correlated with the concentration of PCC and OCC metabolites in order to assess the relationship between metabolites and the variance in BOLD percent signal change attributed solely for scenes. This resulted in a significant positive correlation between the remaining BOLD percent signal change for scenes>size and PCC tNAA ($r = 0.38$, $p = 0.032$), providing support for the category specificity of this tNAA-BOLD relationship. In addition, there was no correlation of this remaining BOLD percent signal change for scenes>size with OCC tNAA ($r = 0.03$, $p = 0.87$), confirming the regional specificity of this tNAA-BOLD relationship (see Figure 3.12). There were no significant correlations between this remaining BOLD percent signal change for scenes with GABA+ or Glx in either voxel.

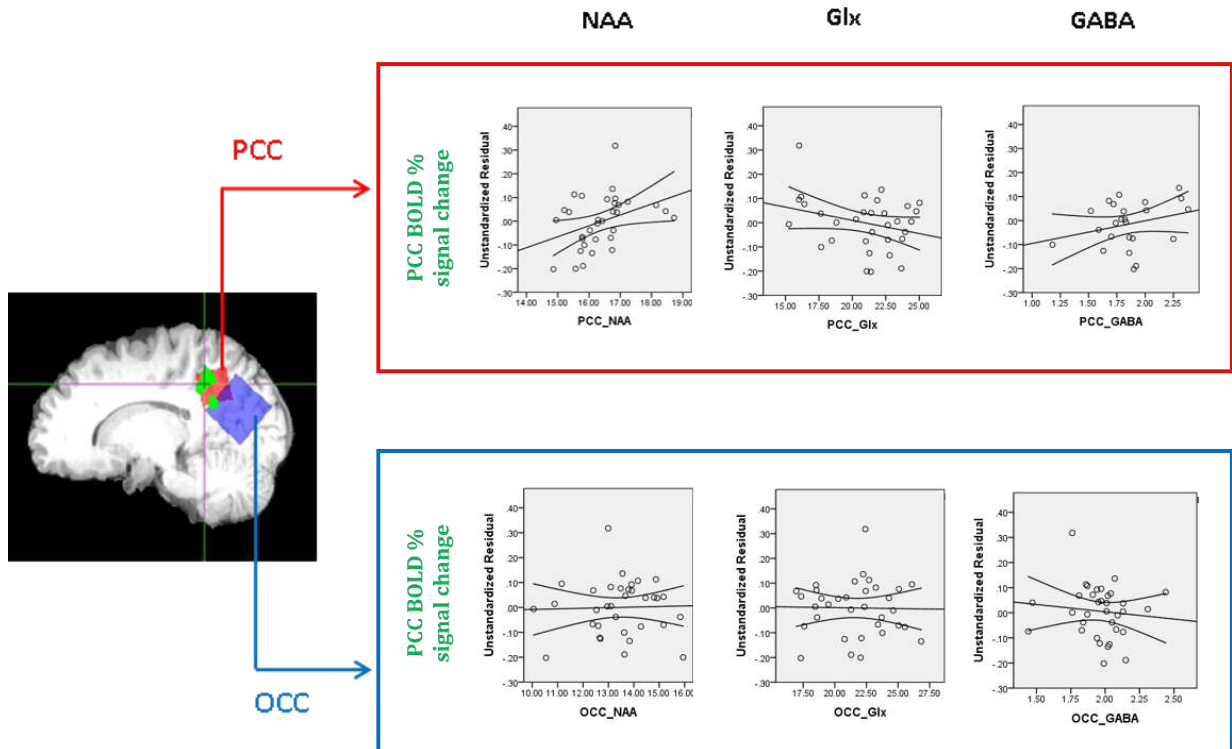


Figure 3.12: Correlations between metabolites and PCC BOLD for the scenes>size condition when the shared variance for the other two conditions of faces>size and objects>size was regressed out. The PCC voxel is shown in red and OCC in blue. The green area is the PCC fMRI ROI obtained from Shine et al 2015. 95% confidence intervals have been plotted.

3.3.5.2 fMRI-MRS - Voxel-wise GLM with MRS covariate analysis

Following the MRS analysis, the overlap of the PCC MRS voxel with the PCC fMRI ROI was assessed. Although there was good overlap of the PCC MRS voxel with the PCC fMRI ROI in some of the participants, it was discovered that in other cases there was not a high overlap between the PCC MRS voxel and the PCC fMRI ROI. More specifically, the mean percentage of the fMRI ROI that lay within the PCC MRS voxel was 20% (standard deviation = 24%; range = 0-82%; median = 9%). In the cases of low or no overlap, visual inspection revealed that the MRS PCC voxel had been placed more posteriorly than the fMRI PCC ROI described by Shine et al., (2015), due to inter-individual variability in brain anatomy (e.g. large ventricles, or small brain volume). This could be a limitation in the MRS-fMRI analyses above since if the overlap of the fMRI ROI and MRS voxel were small,

then the ROI based PCC MRS-fMRI correlations may reflect correlations between activity and metabolites quantified across slightly different regions.

To address this potential limitation post hoc, a complementary fMRI-MRS analysis was performed. This involved undertaking a group-level fMRI analysis using PCC tNAA as a regressor in the general linear model, to identify any fMRI voxels within the PCC MRS voxel where the BOLD response to scenes>size was significantly associated with tNAA (similar to Enzi et al., 2012; Lipp et al., 2015; Northoff et al., 2007). This analysis was also run for the control contrasts of faces>size and objects>size to assess category sensitivity. If the positive relationship identified above between PCC BOLD for scenes and PCC tNAA is robust, then this secondary analysis should identify a cluster of voxels in the PCC MRS voxel in which tNAA is again associated with the BOLD response to scenes, but not faces or objects (vs size).

Consistent with this, a cluster of 63 voxels was evident within the PCC MRS voxel mask, suggesting that PCC tNAA is positively correlated with individual differences in BOLD response to scenes>size (see Figure 3.13). This cluster passed the clusterwise significance threshold of $p < 0.01$ determined using the Monte-Carlo simulation (which was 42 voxels for the tNAA mask). This cluster did not show a correlation between PCC BOLD for faces and PCC tNAA, but there was a small cluster that showed a correlation between PCC BOLD for objects and PCC tNAA, although this was below the clusterwise threshold to be significant (35 voxels).

This analysis was repeated replacing tNAA for Glx and GABA separately, but yielded very small clusters of a few voxels that were correlated with BOLD for scenes>size, faces>size and objects>size, therefore these were not significant at the cluster-wise corrected threshold.

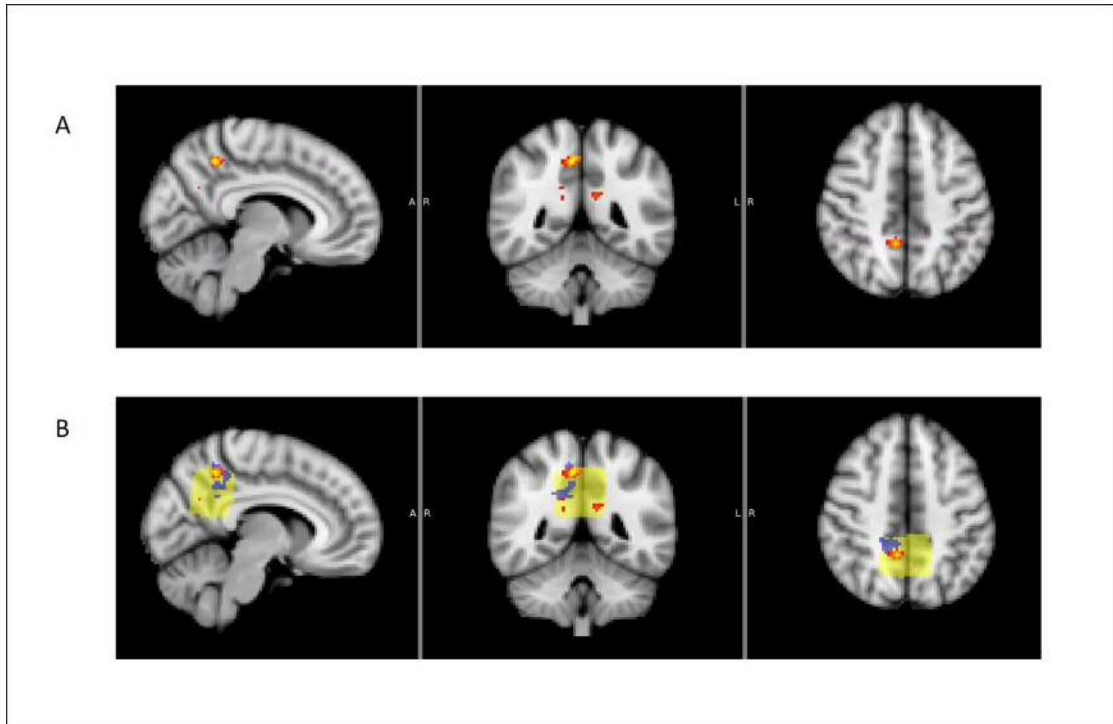


Figure 3.13: (A) The red/yellow shows the cluster of 63 voxels that has a significant correlation between PCC NAA and PCC BOLD for scenes>size within the PCC MRS voxel, when the threshold was set to a voxel-wise threshold of 0.01 and a clusterwise threshold of $p < 0.01$ (equivalent to a threshold of 42 voxels). (B) Figure depicts this same cluster in comparison to the fMRI ROI used in the previous section from Shine et al., (2015) in blue, and the position of the NAA voxel mask used for this secondary analysis in pale yellow.

3.3.6 FMRI-Behaviour relationships

In the next analyses, I asked whether PCC BOLD for scenes was correlated with accuracy (proportion correct) on the scene, face and object conditions of the oddity task (see Figure 3.14). No significant relationship was found between PCC BOLD for scenes and scene oddity accuracy ($r=0.15$, $p=0.40$); nor was there a significant relationship between PCC BOLD elicited during face oddity with face oddity accuracy ($r= -0.09$, $p=0.60$) nor PCC BOLD for objects with object oddity accuracy ($r= -0.07$, $p=0.70$).

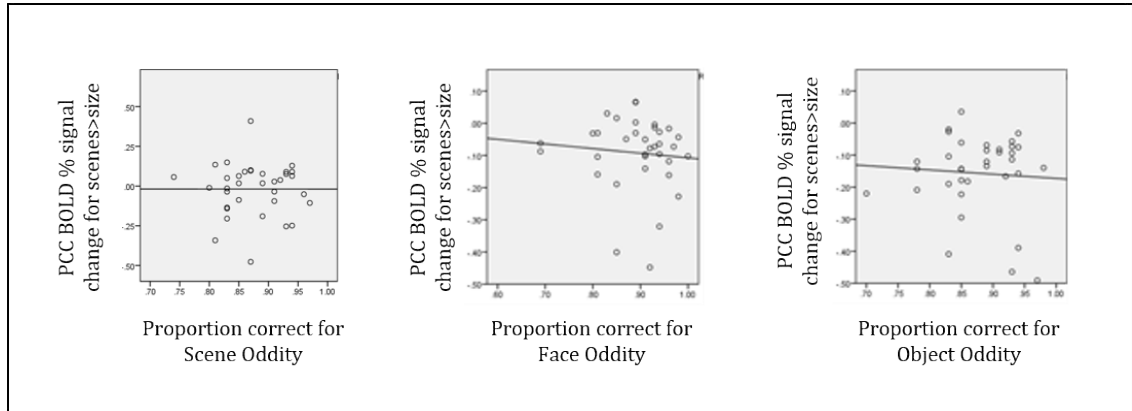


Figure 3.14: Relationships between PCC BOLD percentage signal change for the contrasts scenes>size, faces>size and objects>size with accuracy on each oddity task condition respectively (n = 35).

3.3.7 MRS-Behaviour relationships

A similar set of Pearson correlations were performed to study MRS and behavioural associations. Contrary to my predictions, there were no relationships between PCC tNAA, Glx or GABA+ with accuracy for the scene condition (see Table 3.4). This was also the case for the control conditions of faces and objects.

Correlation between		n	r	p	BF ₁₀
Proportion correct for each task condition	PCC metabolite				
Scenes	tNAA	33	0.24	0.19	0.50
	Glx	32	0.13	0.47	0.28
	GABA+	24	0.28	0.19	0.57
Faces	tNAA	33	0.07	0.70	0.23
	Glx	32	-0.10	0.60	0.25
	GABA+	24	-0.12	0.58	0.29
Objects	tNAA	33	-0.05	0.81	0.22
	Glx	32	0.06	0.75	0.23
	GABA+	24	0.15	0.48	0.32

Table 3.4: Correlations of PCC metabolites with proportion correct. The p value significance threshold was 0.0167. The p values and Bayes factors (BF₁₀) are two-tailed.

3.4 Discussion

This study aimed to investigate whether the PCC, focusing on a specific ROI identified in a previous study of *APOE*-E4 carriers (Shine et al., 2015), showed a profile of BOLD activity sensitive to the visual category of stimuli presented in a visual discrimination task. Analyses revealed a category-sensitive response of our PCC ROI to scene discriminations, where there was, overall, less deactivation from the size baseline compared to that seen during object and face oddity discrimination. This is an interesting finding because it is inconsistent with proposals that PCC, as a critical component of the DN, simply shows a generic deactivation response during any cognitive task (Esposito et al., 2009; Hu et al., 2013; Raichle et al., 2001). Since it was established that the three conditions of scenes, faces and objects were matched on accuracy, this finding suggests that the difference in BOLD between these conditions is due to the nature of the visual stimuli rather than task difficulty.

This study, however, was not able to answer the question of whether activation in this region was associated with degree of accuracy on the task, as there was no relationship evident between individual differences in PCC BOLD for scenes and participant variation in accuracy on the scene task. A possible explanation for this null finding could be that the task was not sufficiently difficult to elicit a wide enough range of performance, as the mean proportion correct was 88%, with a range of 74%-97%.

The study also aimed to investigate whether PCC BOLD for scenes was associated with MRS metabolites in this region. The first fMRI-MRS analysis, which correlated the BOLD percent signal change quantified from the PCC fMRI ROI with MRS metabolites, suggested a significant positive correlation between PCC BOLD for scenes (compared to size) with PCC tNAA. More specifically, the higher the concentration of tNAA in the PCC in an individual participant the less PCC deactivation they show to scenes. The category sensitivity of this MRS-fMRI association, however, was not clear, because whilst PCC tNAA was not correlated with PCC BOLD activity for faces or objects in the same ROI, there was no significant difference in the correlations obtained for each of the three different visual categories (as measured by Steiger z-tests). Having said this, when a further analysis was undertaken to remove the variance in PCC BOLD percent signal change that the scenes>size contrast shared faces>size and objects>size (to take into account the high correlations between BOLD for faces, scenes and objects), a positive correlation between PCC NAA and the BOLD response to scenes was indeed evident.

Furthermore, this finding was supported by the second fMRI-MRS analysis, which was the regressor approach, as this detected a cluster that overlapped with the PCC ROI where PCC tNAA correlated with PCC BOLD for scenes. Taken together, these three different analyses provide complimentary support for a scene sensitive BOLD-tNAA relationship in the PCC.

Combining fMRI with MRS allows us to investigate the biochemical underpinnings of the BOLD response. The finding that increased tNAA is associated with increased BOLD just for the scene condition is intriguing, as tNAA is a marker of neuronal density and integrity (Rae, 2014). This result may mean that a higher density of neurons in the PCC are specialised for scene perception than perception of the other visual stimuli. Furthermore, NAA is synthesised in the mitochondria of neurons (T. B. Patel & Clark, 1979), which is the organelle responsible for the conversion of glucose and oxygen to produce ATP in aerobic respiration. Corresponding to this, the level of tNAA has been found to be coupled to the level of ATP (Signoretti et al., 2001). A higher concentration of tNAA would therefore suggest that a greater amount of aerobic respiration could occur, so if there was increased respiration required during the scene condition this could require a greater flow of oxygenated blood to the PCC which would be consistent with this region showing a greater BOLD response. As the two other experimental Chapters in this thesis will build on this tNAA-BOLD correlation for scenes, Chapter 6 (General Discussion) will return to this relationship, relate it to findings in the other experimental Chapters and provide more detailed discussion of possible mechanisms that could link tNAA with the BOLD response.

It was surprising that no relationships between PCC BOLD and PCC GABA+ or Glx were identified, based on previous studies that have shown that the concentration of these metabolites is associated with the BOLD response, for example a higher concentration of GABA+ in the occipital lobe has been shown to be associated with a lower BOLD response to a visual grating in the primary visual cortex (Muthukumaraswamy et al., 2009), and the concentration of Glx in the anterior cingulate cortex has been reported to be associated with a higher BOLD response during an auditory cognitive control task (Falkenberg et al., 2012). Most relevant to the present study, PCC GABA+ and Glx were shown to be associated with the magnitude of deactivation of the PCC during a working memory task, where higher GABA+ was related to greater deactivation, and higher Glx was related to less deactivation (Hu et al., 2013). One potential reason for a lack of relationship between PCC BOLD and PCC GABA+ could

be a lack of power due to the lower sample size of 24 participants used in this part of the analysis, after excluding a third of the PCC GABA+ measures due to the spectra being poor quality. In comparison, in Hu et al, (2013) the sample size was 28 participants. Another reason could be the discrepancy between metabolites in the large PCC voxel and BOLD activity measured in a small fMRI ROI. This could have had the effect of making the GABA+ and Glx measures not specific enough to the fMRI PCC ROI. Having said this, the null findings of the secondary voxel-wise analysis did support the lack of significant results in the Pearson correlation approach for GABA+ and Glx (i.e. for no relationship between PCC BOLD for any stimuli category and PCC GABA+ or Glx). Nevertheless, the MRS metabolite measure is a mean value over the whole voxel, so even in this voxel-wise approach the large voxel size may still be a limitation. This is not a limitation just of this study however, but rather an inherent problem in all MRS-fMRI research. MRS voxels need to be sufficiently large in order to detect sufficient quantities of metabolites due to the low signal to noise ratio in MRS; this is particularly problematic for GABA quantification. An attempt was made at reducing the size of the PCC MRS voxel from the standard 3x3x3cm to 2x2x3cm, to make this more regionally specific. This came, however, at the cost of several PCC MEGA-PRESS spectra being too poor quality to use the GABA+ measurement obtained in this region.

A further possible limitation of this study could be the choice of fMRI ROI. The rationale behind using this ROI was due to the focus of this thesis on investigating the fMRI BOLD response of this *APOE-E4* relevant ROI to scenes and assess whether this was related to the biochemistry of this region as measured using MRS. In considering the role of the PCC more generally, however, this may have been a limitation since activity in this *APOE-E4* relevant ROI might not be generalizable to the role of the whole PCC, or the peak BOLD response in the PCC region may have been missed by quantifying the BOLD percent signal change solely within this ROI. A strategy to address this could be to calculate whole brain maps to demonstrate the location of clusters that show a greater BOLD response to scenes than other stimuli categories, and assess how close such clusters may overlap with the PCC ROI used here. As highlighted in Figure 2.6 (page 51) there are also several alternative approaches to quantifying the BOLD response in this region, which may be more generalizable to the role of the PCC. For example, to measure the BOLD percent signal change in an anatomical PCC ROI. This approach was not chosen here, as a limitation of this is that the PCC anatomical mask region obtained using the Harvard-Oxford cortical structural atlas in FSL is very large (consists of 10,184 voxels) therefore could have diluted any effects. Instead, another approach that may be more

generalizable could be to use a different independent fMRI ROI. For example, Hodgetts et al., (2016) performed an fMRI study on young, healthy participants who were not genotyped for APOE. Participants performed a 1-back functional localiser fMRI task involving viewing images of scenes, faces and objects. They performed a whole brain analysis using the contrast scenes>faces+objects to investigate the category sensitivity of what they described as typical core scene processing ROIs, including hippocampus, retrosplenial cortex and parahippocampal place area, and extracted the BOLD percent signal change from these regions using anatomical ROIs. Interestingly, consistent with the work in this Chapter, their whole brain analysis also elicited a cluster within the PCC region that they did not quantify (Hodgetts, Shine, Lawrence, Downing, & Graham, 2016). An alternative strategy, therefore, could be to use this PCC cluster as an fMRI ROI, and repeat the analysis performed in this Chapter. It would be interesting to compare the results detected in the *APOE-E4* relevant PCC ROI used in this Chapter with this different ROI as this could further this work by assessing spatial selectivity of activity to different categories within the PCC area.

Returning to my interest in *APOE-E4*, the positive correlation between PCC BOLD levels elicited for scenes and PCC tNAA could imply that young *APOE-E4* carriers may have a higher concentration of tNAA in the PCC. This is since the *APOE-E4* carriers showed a pattern of less deactivation to the scene oddity condition compared to the non-carriers in Shine et al. (2015). If so, this effect would be interesting, as tNAA is one of the key metabolites altered in AD and MCI, where patients show a *decrease* in PCC tNAA (Kantarci et al., 2000; Kantarci et al., 2007). Histopathologically, this decrease in PCC tNAA in AD has been associated with a decrease in synapse density (Murray et al., 2014). If young *APOE-E4* carriers had a higher concentration of PCC tNAA, which later decreased in individuals who went on to develop AD, this would be a similar pattern observed in fMRI studies of the hippocampus in young and old *APOE-E4* carriers (Filippini et al., 2011), where we see higher and then lower levels of activation across the lifespan. This pattern in Filippini et al.'s study was suggested to reflect a compensatory overactivity response early in life, leading to a burn out effect, and thus a decrease in activity later in life and in AD. This could be the case in the PCC of *APOE-E4* carriers, where BOLD activity and tNAA could be increased early in life as a compensatory mechanism. To be consistent with lower tNAA being associated with lower synaptic density in the study by Murray et al., (2014), higher NAA would suggest higher synaptic density. An increase in synaptic density in the PCC of young E4 carriers would be in line with a recent study that identified PCC volume is increased in young *APOE-E4* carriers

relative to non-carriers (Foley et al., 2016). These ideas, however, are just speculative. To test these ideas, the concentration of PCC metabolites in *APOE*-E4 carriers and non-carriers and their relationship to PCC BOLD will be assessed in Chapter 5 of this thesis.

3.4.1 Chapter Summary

In summary, this study has addressed its first main aim by demonstrating that the PCC ROI shows a category sensitive response, in that there was a reduced scene deactivation from the baseline condition compared to face or object perception. The second question of how this PCC BOLD response contributes to accuracy on the scene perception task still remains however, since there was no significant relationship between fMRI measures and behavioural performance on any condition, including scenes. Future studies could address this question by using a more difficult scene perception task that would place higher demands on scene processing regions, which could now include this PCC ROI. The third main aim of this study was to assess whether the category sensitive BOLD-MRS relationships existed in the PCC ROI. Analyses showed a positive correlation between PCC BOLD for scenes and PCC tNAA (i.e. individuals who showed less deactivation to scenes had a higher concentration of PCC tNAA). This category-sensitive finding is in support of my hypothesis for Chapter 5 that an alteration in PCC BOLD for scene oddity in young E4 carriers in Shine et al., (2015) could be associated with an alteration in PCC MRS metabolites. In Chapter 4, I apply the same combination of MRS and fMRI, but using an alternative spatial task involving working memory; this allows a replication study to determine the robustness of the significant MRS-fMRI effects identified here.

4 Chapter 4: Investigating working memory load and scene processing in posterior cingulate cortex using fMRI and MRS

4.1 Introduction

The fMRI and fMRI-MRS findings of Chapter 3 suggested that the PCC ROI (determined from the study of young *APOE-E4* carriers in Shine et al., (2015)) shows a different BOLD response for scene compared to face or object perception. More specifically it shows less deactivation for scenes compared with faces and objects (all compared to a size baseline). Additionally, individual differences in the BOLD response for scenes in this ROI were positively correlated with the concentration of the MRS metabolite tNAA (i.e. a higher concentration of tNAA was associated with less PCC deactivation). This category sensitive response in both BOLD and the BOLD-tNAA relationship is intriguing because the scene condition of the oddity task was the condition to which the young *APOE-E4* carriers showed less deactivation in the PCC ROI compared to non-carriers in Shine et al., (2015), and it is also the same condition of the oddity task that is selectively impaired in AD patients (Lee et al 2006). Moreover, this category sensitive MRS-BOLD finding is consistent with my overarching hypothesis that an MRS metabolite alteration in the PCC of young *APOE-E4* carriers could be associated with their altered pattern of PCC activity on the scene oddity task.

The present Chapter applies a similar approach to Chapter 3 to investigate the activity of the PCC ROI using fMRI and its relationship to PCC MRS, but focuses on a spatial working memory instead of a perception task. In Shine et al. (2015), a different pattern of activity was evident in the PCC ROI in young *APOE-E4* carriers compared to the non-carriers for scene working memory, making this a useful paradigm aligned to the aims of this thesis. The task used in Shine et al. (2015) was a one-back working memory task (design shown in Figure 4.1), where participants were shown 3D virtual reality scenes, artificial faces, real-world objects or scrambled objects, and asked to respond

when the image presented matched the image seen one trial previously (i.e. “one-back”). Activity for each condition was contrasted with a rest block, and compared between the *APOE*-E4 carriers and non-carriers. The analysis revealed a cluster in the PCC (the PCC ROI used in Chapter 3) as having higher activity during the scene working memory condition in the *APOE*-E4 carriers compared to the non-carriers, whereas no region showed an activity difference between *APOE* groups for the face, object or scrambled object working memory conditions. Similar to Chapter 3, I will test here whether individual differences in PCC BOLD during a scene working memory task show a category-sensitive relationship with PCC MRS, potentially associated with tNAA given the findings from Chapter 3.

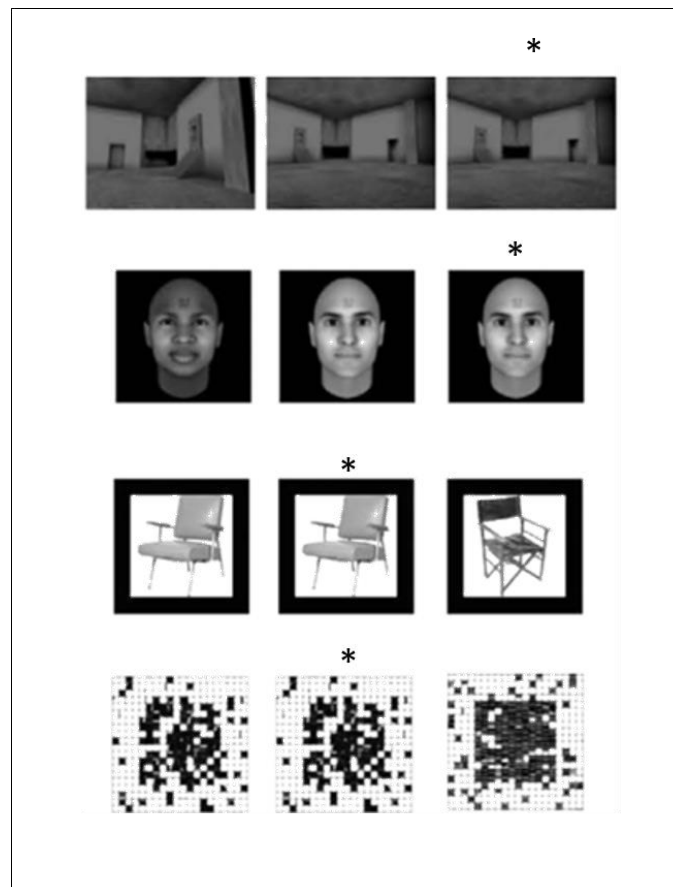


Figure 4.1: The working memory task used in Task A of Shine et al., (2015). The task was a 1-back working memory paradigm with four stimuli categories: scenes, faces, objects and scrambled objects. The asterisks indicate the target images (where the image was identical to that one trial previously). In the fMRI analysis, activity for each category was contrasted with rest, then compared between *APOE* groups within a postero-medial region mask (PCC + retrosplenial cortex + precuneus). This resulted in a cluster in the PCC for the comparison of scenes>rest where there was higher activity for the E4 carriers compared to the non-carriers. This cluster is the PCC ROI used in the previous Chapter and this Chapter (see Figure 3.3). (Figure taken from Shine et al., 2015).

Working memory tasks have been shown to be effective paradigms to investigate PCC activity: such tasks consistently produce a deactivation in the BOLD response in the PCC, and the magnitude of this deactivation increases as the working memory load increases. For example, in Esposito et al., (2009) an n-back working memory task was used to investigate activity in the DN at different levels of working memory demand (Esposito et al., 2009). The task required participants to view a series of numbers, and press a response button whenever a number appeared in consecutive trials (1-back condition), when separated by 1 trial (2-back condition), when separated by 2 trials (3-back condition), and when they saw a target number (0-back condition, designed to be the baseline condition). When activity was contrasted between the 0-back and the three different n-back conditions, the researchers found a decrease in activity which was greatest for the most demanding 3-back condition. This pattern of a greater PCC/DN deactivation with increasing working memory load appears to be robust, replicated by Hu et al., (2013) and Ceko et al., (2015), both of which used a letter n-back task with 0, 1, 2 and 3-back conditions (Ceko et al., 2015; Hu et al., 2013).

In addition, an n-back working memory paradigm has been shown to be an effective approach to investigate BOLD-GABA+ and BOLD-Glx relationships for PCC deactivation. The letter n-back task in Hu et al., (2013) (described in detail in Chapter 3 (see Figure 3.3)) correlated PCC BOLD with GABA+ and Glx from the PCC or from the OCC (control region). They found that greater PCC deactivation was associated with a higher concentration of PCC GABA+ and a lower concentration of PCC Glx, and was not associated with OCC GABA+ or OCC Glx (Hu et al., 2013). This finding suggests that individual differences in PCC deactivation as working memory load increases are related to individual differences in PCC metabolites. The finding that there was no OCC MRS-PCC BOLD associations suggests that this MRS-BOLD relationship may be regionally specific to the PCC.

Instead of using letters or numbers as stimuli in an n-back working memory task, an n-back task which modulated the category of the stimuli to include both scene and non-scene images would allow us to combine an increase in working memory load with a manipulation of the spatial complexity of the images. If the PCC response to increasing working memory load is not different when spatial complexity is manipulated (i.e. if there was a main effect of working memory load but no interaction effect of working memory and spatial complexity), it would suggest that this region is not specifically involved in processing scenes. Whereas if there was a difference (i.e. if there was an

interaction between working memory load and spatial complexity) then that would suggest that this region is involved in scene processing. Furthermore, the collection of MRS alongside the fMRI working memory paradigm, as in Hu et al., (2013), allows the assessment of whether individual differences in the PCC's deactivation to increasing working memory load for scenes, but not non-scenes, is related to inter-individual differences in MRS metabolites. The metabolites of interest are the same as those tested in Chapter 3 (the neuronal marker, tNAA, the excitatory neurotransmitter, Glx, and the inhibitory neurotransmitter, GABA).

Here, therefore, I will use the spatial n-back paradigm designed by Lee and Rudebeck, (2010). In their study, this paradigm was used to investigate fMRI activity in the MTL, as several studies had suggested that the hippocampus shows a category sensitive response to scenes (e.g. Barense, Henson, Lee, & Graham, 2010; Lee, Scahill, & Graham, 2008), as well as a response to working memory (e.g. Hartley et al., 2007; Piekema, Kessels, Mars, Petersson, & Fernández, 2006). To bring these two literatures together, Lee and Rudebeck, (2010) developed a 2x2 factorial n-back paradigm which modulated working memory demand as one factor (1back or 2back) and spatial complexity of the stimuli as the second (3D rooms where features of the rooms (e.g. doorways, arches, stairs) moved around between trials or an array of 2D shapes where three shapes moved between trials). This created 4 conditions: shapes 1back, shapes 2back, rooms 1back and rooms 2back. The spatial n-back paradigm is shown in Figure 4.2.

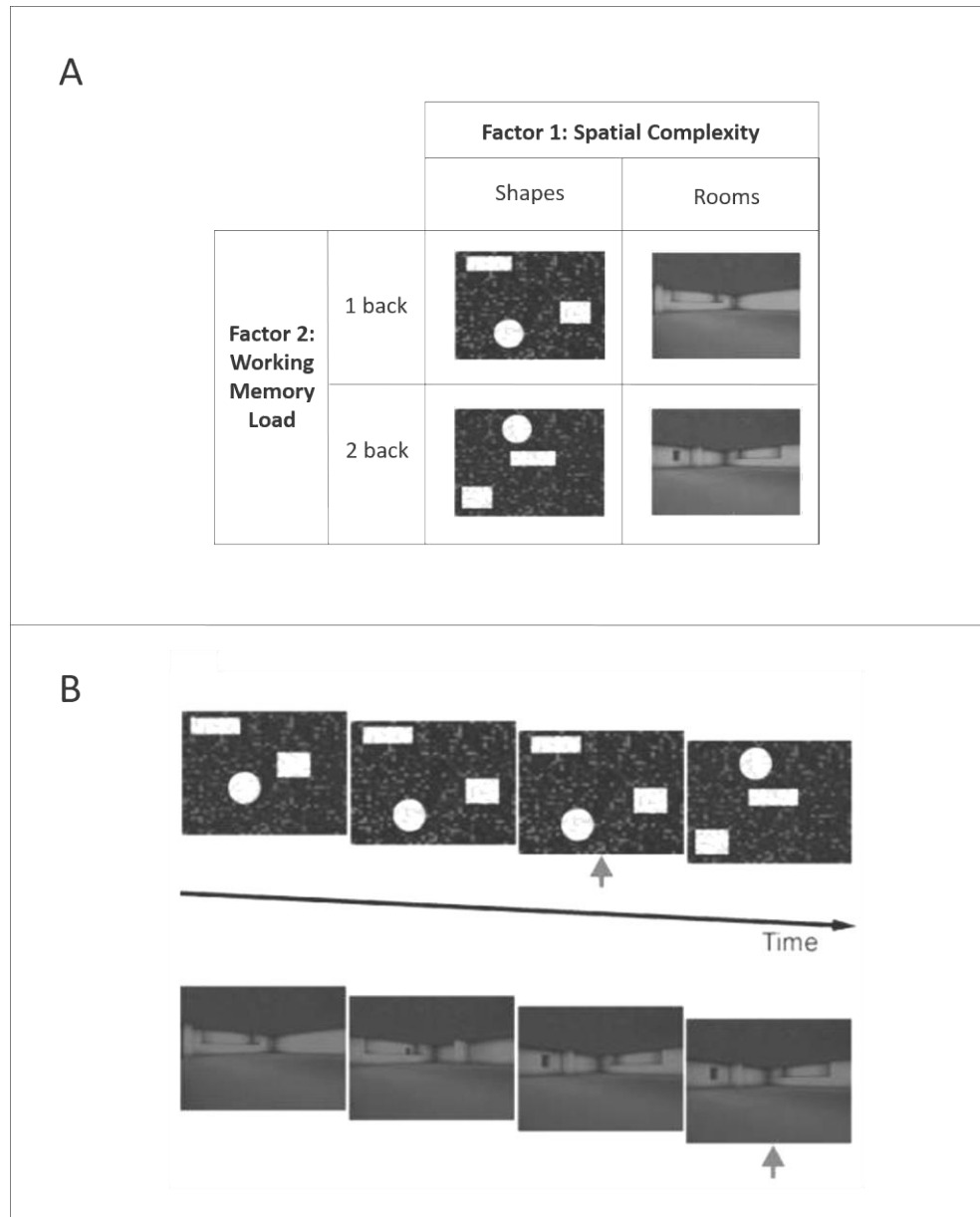


Figure 4.2: Spatial working memory task used in Lee and Rudebeck (2010). (A) The 2x2 factorial design of the task, which creates the 4 task conditions of shapes 1-back, shapes 2-back, rooms 1-back and rooms 2-back. Participants viewed images of arrangements of 2D shapes and virtual reality 3D rooms, and were asked to alternate between a 1-back task and a 2-back task, by pressing a response button when the image the viewed was identical to that either 1 trial previously for the 1-back conditions, or 2 trials previously for the 2-back conditions. (B) Examples of the experimental design for 1back shapes in the top row and 1back rooms in the bottom row. Correct responses are shown by the arrows (image adapted from Lee and Rudebeck, 2010).

A 2x2 factorial design is an effective method to determine whether a region shows an effect of one variable (i.e. a main effect) or whether the effect of one variable depends on the effect of a second variable (i.e. an interaction) (Price et al., 1997). The rationale of the Lee and Rudebeck (2010) study was that if MTL regions have a role in scene processing but not in working memory, then an increase in the spatial complexity of the stimuli from shapes to scenes would result in a significant increase in activity in the MTL regardless of the working memory load (hypothesis 1). Vice versa, if MTL regions have a role in working memory but not in processing scenes, then an increase in the working memory load from 1back to 2back would result in a significant increase in MTL activity, regardless of the spatial complexity of the stimuli (hypothesis 2). If both factors are critical, the BOLD response to increasing working memory load should be modulated by the different spatial processing demands (hypothesis 3). Consistent with these first hypotheses, they found a main effect of spatial complexity in a right hippocampal ROI (see Figure 4.3A), a main effect of working memory load in a left hippocampal ROI (see Figure 4.3B), and a significant interaction effect between working memory load and spatial complexity in a different right hippocampal ROI (see Figure 4.3C).

While Lee and Rudebeck (2010) did not focus on PCC, it is worth noting that an exploratory whole brain analysis (reported in the supplementary material) identified a PCC cluster showing an interaction effect for spatial complexity and working memory load, with the peak voxel located at 4, -50, 16 (corresponding to x, y, z in MNI coordinates). This is in a slightly different location to the central voxel of the PCC ROI from Shine et al., (2015) which was 16, -46, 30, although it is not possible to identify the overlap of this cluster with the PCC cluster from Shine et al., (2015) as the size and spread of the PCC cluster in Lee and Rudebeck (2010) was not given. Use of this task, therefore, seems an effective elicitor of PCC activity, as well as a useful design to test working memory/spatial complexity relationships with MRS metabolites of interest.

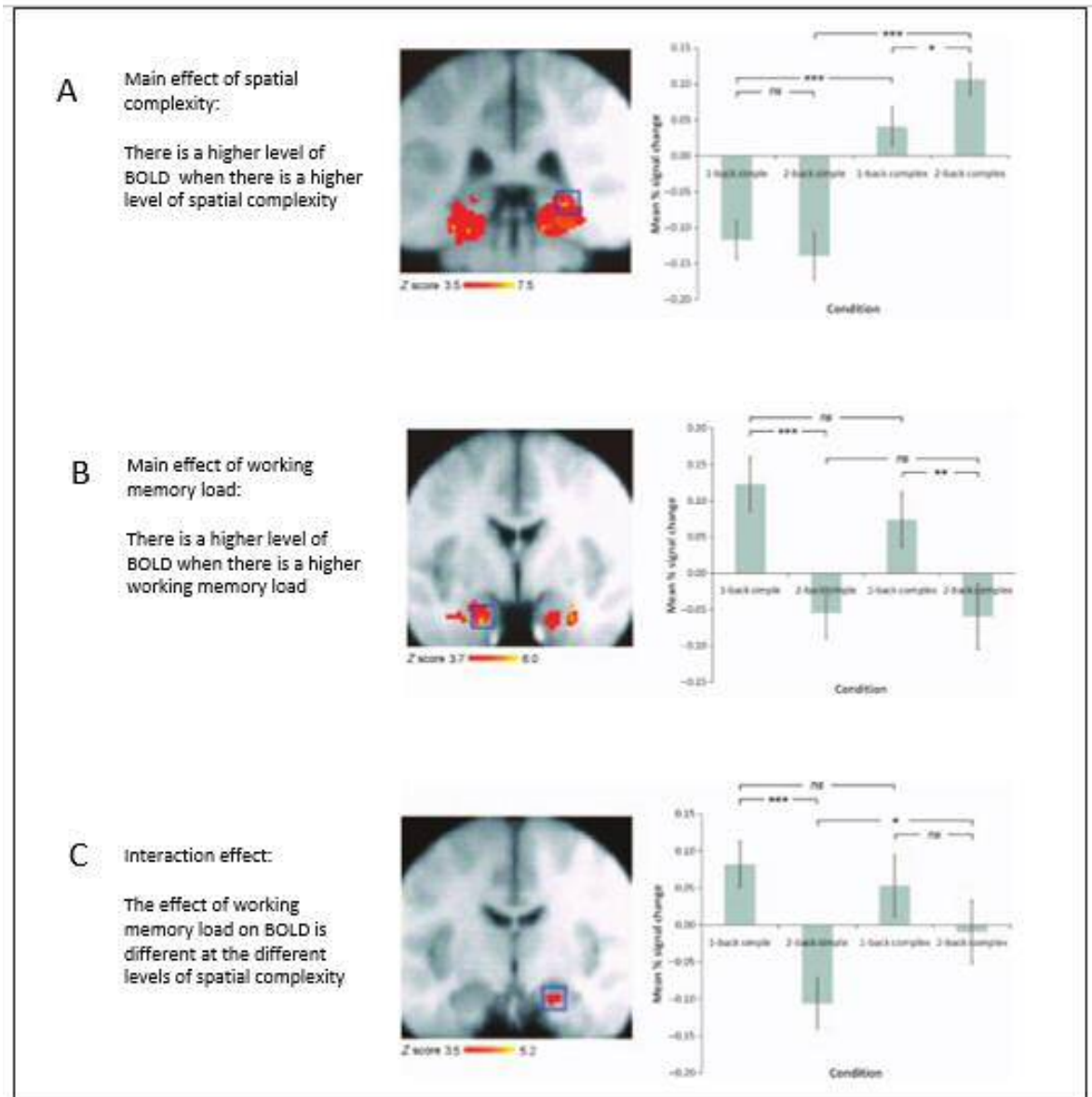


Figure 4.3: Examples of three different outcomes of the BOLD analysis in the spatial working memory task in three different ROIs, taken from Lee and Rudebeck, 2010. The labels of simple and complex on the graphs refer to the shapes and rooms conditions respectively. (A) The ROI in the right hippocampus (centred on MNI x, y and z co-ordinates of 28, -38, -6) shows the pattern of an increase in activity when there is an increase in spatial complexity (i.e. a main effect of spatial complexity). (B) The ROI in the left hippocampus (-20, -4, -28) shows the pattern of a decrease (in contrast to their predictions of an increase) in activity when there is an increase in working memory load (i.e. a main effect of working memory load). (C) A different ROI in the right hippocampus (20, -12, -22) shows the pattern of an interaction effect, where the effect of one variable on BOLD is modified by the other variable (i.e. the difference in BOLD between 1 and 2 back for shapes is greater than that for rooms). (Images adapted from Lee and Rudebeck, 2010)

4.1.1 Analysis strategy and hypotheses

Four main analyses have been performed using this spatial working memory fMRI-MRS experimental design. First, to ask whether the PCC ROI has a role in processing scenes, I tested whether there was an interaction effect of working memory load and spatial complexity within the PCC ROI. This was achieved by quantifying the BOLD percentage signal change for each of the four conditions relative to the unmodelled baseline (e.g. as in the analysis taken from Lee and Rudebeck, (2010), shown in Figure 4.3). Values were entered into a 2x2 repeated measures ANOVA to test for main effects and an interaction, consistent with the methods of Lee and Rudebeck (2010). Based on the exploratory whole brain analysis in Lee and Rudebeck (2010), I hypothesised there would be an interaction effect of working memory and spatial complexity.

Second, to understand whether PCC BOLD elicited during spatial working memory was associated with MRS metabolites, individual differences in PCC BOLD (obtained for the contrast rooms 2back > rooms 1back) were correlated with PCC tNAA, Glx and GABA+. The category sensitivity of any such relationship was additionally tested by correlating PCC metabolites with PCC BOLD for the contrast shapes 2back > shapes 1back. The regional sensitivity of any significant effect was tested by correlating OCC metabolites with both rooms 2back > rooms 1back and shapes 2back > shapes 1back. The scene sensitive tNAA-BOLD relationship identified in Chapter 3 suggests that a higher concentration of tNAA is associated with less PCC deactivation. I hypothesised, therefore, that PCC BOLD for rooms 2back > rooms 1back would be positively correlated with tNAA (i.e. greater deactivation for rooms 2back > rooms 1back would be associated with lower levels of PCC tNAA). I also predicted that shapes 2back > shapes 1back would not be correlated with PCC tNAA, as the correlation in Chapter 3 was sensitive to complex scene stimuli only. Since Chapter 3 did not detect a scene sensitive correlation of GABA+ or Glx with PCC BOLD, I did not expect there to be a category sensitive relationship between these metabolites and PCC BOLD. Instead, I hypothesised that MRS-BOLD relationships for both shapes 2back>shapes 1back and rooms 2back>rooms 1back would replicate the pattern report in Hu et al., (2013), where there was a negative correlation between PCC BOLD and PCC GABA+, and a positive correlation between PCC BOLD and PCC Glx (i.e. greater BOLD deactivation in PCC would be associated with higher GABA+ and lower Glx). In the correlations of PCC BOLD with OCC MRS metabolites, I predicted that there would be no significant correlations between either of

the PCC BOLD contrasts and OCC metabolites. This would establish regional specificity of any PCC BOLD-PCC MRS correlations to the PCC.

Third, to investigate the impact of PCC deactivation for the different stimuli categories on behaviour, BOLD-behaviour relationships were assessed, taking a similar approach to that applied in Chapter 3. It has been proposed that the magnitude of PCC deactivation is related to success on working memory tasks, with greater deactivation associated with higher accuracy (Anticevic, Repovs, Shulman, & Barch, 2010; Hu et al., 2013). In line with this work, I predicted a negative relationship between PCC BOLD and task performance, so that individuals who show the greatest PCC deactivation would have the most accurate task performance. Additionally, if PCC deactivation to rooms and shapes was different (e.g., the expected smaller level of deactivation to rooms than shapes, as hypothesised above), this should impact on accuracy for these different categories. I predicted, therefore, better performance on the shapes 2back condition than the rooms 2back conditions, and on the shapes 1back compared to the rooms 1back condition. Other studies, however, have challenged the idea that the magnitude of PCC deactivation is linked to behavioural success, suggesting instead that PCC deactivation is not required for accurate working memory performance, as chronic pain patients who do not have a responsive DN do not show impaired performance on a working memory task (Ceko et al., 2015). This work would suggest an alternative hypothesis, whereby there would be no relationship between PCC activity and behaviour, for either stimuli condition.

Previous working memory studies assessing BOLD-behaviour relationships have correlated behaviour with the BOLD contrasts of different working memory load conditions relative to a 0back baseline (Ceko et al. (2015), Hu et al. (2013) and Esposito et al. (2009)). The spatial working memory task applied in this Chapter consisted of a 2x2 design, thus does not have a 0back condition. Therefore, the BOLD measures used here were the contrasts of rooms 2back > rooms 1back and shapes 2back > shapes 1back, in order to measure BOLD activity changes from the low to the high working memory load condition. The behavioural measure used to correlate with this was the corresponding change in performance from the 1back to the 2back condition for each stimuli condition.

The fourth and final analysis tested whether behavioural performance on the task was related to PCC metabolites, and whether any MRS-behaviour relationships differed

depending on the spatial complexity of the stimuli. There are inconsistent results in the MRS-behaviour literature as to whether tNAA correlates with task performance. A positive relationship between tNAA in the left occipito-parietal white matter and a general cognitive factor (a composite measure of neuropsychological tests) was reported by Jung et al. (1999), whereas other studies have detected no relationship between occipital cortex NAA and a neuropsychological battery, but there was a weak relationship with frontal NAA (T. Patel et al., 2014). Additionally, a recent study proposed that parietal NAA was associated with spatial/verbal reasoning but not working memory (Paul et al., 2016). To test whether PCC metabolites are associated with working memory and whether any relationship is different depending on the spatial complexity of the stimuli, this Chapter has correlated behavioural performance for each of the four task conditions with each PCC MRS metabolite.

4.2 Methods

4.2.1 Participants

The same 40 participants reported in Chapter 3 took part in this experiment (see Section 3.2.1).

4.2.2 Scanning procedure

The scanning procedure was described in Chapter 3. The relevant scans for this Chapter were the fMRI spatial working memory task and field maps in scan session 1, and the structural MRI and four MRS scans in session 2. The structural MRS and MRS scans and the analysis of these scans was the same as in Chapter 3 (see Chapter 3, sections 3.2.6 and 3.2.7).

4.2.3 fMRI Spatial Working Memory Task

The identical spatial working memory paradigm reported in Lee and Rudebeck (2010) was used in this experiment. The fMRI task had a 2x2 factorial design, with factors of spatial complexity and working memory. The two levels of spatial complexity were simple (arrangements of 2D shapes) and complex (virtual reality 3D rooms). The two levels of working memory load were 1-back and 2-back. This created 4 task conditions: (A) shapes 1-back, (B) shapes 2-back, (C) rooms 1-back, (D) rooms 2-back. Stimuli were presented in a blocked design, which alternated through the four task conditions in the order ABCD. There were 8 trials per block, 8 blocks per condition, 32 blocks per run, and there were 4 fMRI runs. Each block lasted 20s, and each trial was presented for 2.2sec, with a 0.3s inter-stimulus-interval. Blocks began with an instruction of either “1-back” or “2-back” which informed the participant which level of working memory task to perform. In the 1-back conditions participants were asked to press a response button when the image they viewed was identical to that shown one trial previously (see Figure 4.1A). In the 2-back condition, participants were asked to press the response button when the image they viewed was identical to that shown two trials previously (see Figure 4.1B). Participants were instructed that each block contained either one or two images where participants should respond (targets), in order to maintain the working memory demand throughout the whole block. Half of the blocks contained one target, and the other half contained two targets. The order of targets and non-targets was randomised throughout each block.

4.2.4 fMRI Parameters

Gradient echo, echo-planar imaging (EPI) T2* images covering the whole brain were acquired. The sequence used a TE of 35ms, TR of 3000ms, flip angle of 90°, field of view of 220mm, and the matrix dimensions were 64x64. Each of the four fMRI runs consisted of 240 volumes, with a scan duration of 12 minutes. Each volume consisted of 42 axial slices, collected in a bottom-up sequential order. The slice thickness was 2.4mm, and there was an inter-slice gap of 1.0mm. This created a voxel size of 3.4x3.4x2.8mm. Slices were aligned along the AC-PC line then tilted backwards by 30° to address medial temporal lobe signal dropout, as in Chapter 3. Each run began with 4 dummy volumes, to

allow for equilibration of the magnetic field, and these volumes were removed during analysis. Two field maps were acquired, one at a TE of 7ms, and the other at a TE of 9ms, to correct for inhomogeneities in the magnetic field.

The fMRI parameters were matched as closely as possible to those used in Lee and Rudebeck (2010). Slight adjustments had to be made, however, to be consistent with optimal fMRI parameters for the MRI scanner in CUBRIC. Differences were that Lee and Rudebeck (2010) used a four channel head coil (rather than an 8 channel head coil as used in this study – as described in Chapter 3), a TE of 30ms, and their voxel size was 3x3x3cm.

4.2.5 Data Analysis

4.2.5.1 Behavioural Data Analysis

Using the same behavioural analysis method as Lee and Rudebeck (2010), four measures of behavioural performance were calculated using signal detection theory. These were each participant's proportion of hits (proportion of correct button presses on target trials relative to the total number of target trials); proportion of false alarms (the proportion of button presses during non-target trials relative to the total number of non-target trials); sensitivity (to assess their ability to discriminate between targets or non-targets); and bias (to assess their tendency to say a trial was a target rather than a non-target (i.e. how conservative or liberal they were with their button presses) (Lynn & Barrett, 2014)). For each participant, these four measures were calculated for each condition and for each fMRI run separately, then averaged across the four runs.

The purpose of using these four measures was to enable a more thorough representation of performance on the task rather than solely relying upon the proportion of hits which does not capture performance across all trials. An extreme example of this would be if a participant pressed the response button on every trial (i.e. all targets and non-targets). If only the proportion of hits was calculated, it would appear that the participant was very good at the task, as they would have pressed the response button for every target, whereas they would actually be performing the task at chance (when false alarms were taken into account). Additional consideration of false alarms,

sensitivity and bias helps tell us whether the participants were pressing the response button for a high number of non-target trials alongside the target trials, or whether they were being very conservative and pressing the response button just for the target trials.

These four measures were calculated using the formulae as described in Lee and Rudebeck (2010): proportion of hits (hits/number of targets), the proportion of false alarms (false alarms/number of non-targets), sensitivity ($\text{natural log } x \left[\frac{\text{hits}(1-\text{false alarms})}{[\text{false alarms}(1-\text{hits})]} \right]$), and bias ($0.5 \times \left[\text{natural log } x \left[\frac{(1-\text{false alarms})(1-\text{hits})}{[\text{hits}(\text{false alarms})]} \right] \right]$). Where hits or false alarms were equal to 1 or 0, this was adjusted by 0.01 (if value was 1, 0.01 was subtracted; if value was 0, 0.01 was added), to enable the formulae above to be performed, consistent with Lee and Rudebeck (2010).

The formulae for sensitivity and bias described in Lee and Rudebeck (2010) were the versions of these formulae to use when there is a logistic distribution, meaning a high kurtosis of the distribution (very tall peak, very flat tails), taken from Snodgrass and Corwin, (1988). The sensitivity term here was denoted as d_L . When there is a normal distribution, rather than a logistic distribution, the sensitivity term is denoted d' or d' . This d' measure was the behavioural measure that was correlated with BOLD in Hu et al. (2013).

For the BOLD-behaviour correlations and MRS-behaviour correlations, this d_L version of d' was considered more appropriate for the behavioural data obtained in this study. Using one rather than all four behavioural measures to correlate with BOLD and MRS would prevent a very large number of correlations, which would require a strict correction for multiple comparisons. Choosing this one sensitivity measure was designed to replicate the approach used in Hu et al. (2013), where the most sensitive measure of behavioural performance (d') was also selected.

4.2.5.2 fMRI Data Analysis

Preprocessing of the fMRI data used the same methods as Chapter 3, with the only difference being an increase in the size of spatial smoothing kernel to a full-width-at-half-maximum (FWHM) Gaussian kernel of 8mm, to be consistent with Lee & Rudebeck (2010) (increase from the smoothing kernel with a FWHM of 5mm used in the previous Chapter). (NB. The amount of smoothing is determined by the width of the Gaussian

peak, which can be measured either by the peak's standard deviation (SD), or by the width of the peak at its maximum height (FWHM). Using FWHM and SD would result in different size smoothing kernels, since the SD is measured at a different place on the Gaussian peak to the FWHM. These can be converted to each other using the formula $FWHM \sim 2.55 \times SD$ (Poldrack, Mumford, & Nichols, 2011). It is important to note here that both the FEAT tool in FSL used here and the Lee and Rudebeck (2010) paper used the FWHM measure of the Gaussian peak for spatial smoothing). The fMRI analysis also replicated that of Lee and Rudebeck (2010), and consisted of three stages. The first stage involved an individual level analysis for each of the four runs for each participant. This was performed using a GLM consisting of four explanatory variables (the four task conditions). Block start times for each condition were obtained from each participant's output file. Consistent with Lee and Rudebeck (2010), blocks were included if they contained no false alarms, and at least one hit, to ensure the analysis contained the blocks where the participant was completing the task correctly. For each individual, this resulted in the exclusion of an average of one block in the shapes 1back condition, three blocks in the shapes 2back condition, one block in the rooms 1back condition and four blocks in the rooms 2back condition. This was a similar pattern of exclusion to that reported in Lee and Rudebeck (2010), where an average of one block was removed in each of the two 1back conditions, and an average of three blocks in each of the two 2back conditions. Parameter estimates were created for each of the four conditions separately (shapes 1back, shapes 2back, rooms 1back, rooms 2back) by contrasting each condition to the unmodelled baseline. This allowed generation of the main effect contrasts of rooms>shapes (main effect of spatial complexity), and 2back>1back (main effect of working memory), and the interaction effect ((rooms 2back - rooms 1back) > (shapes 2back - shapes 1back)). Two additional contrasts were added for this study that were not used in Lee and Rudebeck (2010), which were for the effect of working memory load in each of the spatial conditions separately ((rooms 2back > rooms 1back) and (shapes 2back > shapes 1back)). The purpose of including these contrasts was to use them in the fMRI-MRS analysis (see Section 2.5.3).

The second stage of the fMRI analysis involved combining the four runs for each participant, using a fixed-effects group analysis. The third stage of analysis quantified the BOLD percentage signal change in the PCC ROI for the four conditions and five key contrasts outlined above using the Featquery tool in FSL. The same PCC ROI as that used in Chapter 3 was adopted for this analysis (see Figure 3.6).

4.2.5.3 fMRI-MRS Relationships

As discussed in Chapter 2 (see Section 2.3.2) and as implemented in Chapter 3 (see Section 3.2.8.4), two complementary methods for assessing the relationship between fMRI and MRS were implemented: the first testing the relationship between fMRI in the PCC ROI and MRS using Pearson correlations, and the second using MRS metabolites as regressors in the fMRI GLM analyses within the PCC MRS voxel.

4.2.5.3.1 fMRI-MRS – Percent signal change ROI analysis

To assess whether individual differences in the concentrations of PCC tNAA, Glx and GABA+ were related to individual differences for increasing working memory load for scenes, Pearson correlations were performed between each metabolite and the BOLD percentage signal change in the PCC ROI (ROI shown in Chapter 3, see Figure 3.6) for the contrast rooms 2back > rooms 1back. To test category sensitivity of these relationships, each metabolite was also correlated with the PCC ROI BOLD percentage signal change for the contrast shapes 2back > shapes 1back. Two-tailed Steiger Z-tests were performed to assess whether any correlations between PCC metabolites and PCC BOLD for 2back > 1back for rooms or shapes were statistically different from each other.

The regional sensitivity of any MRS-BOLD relationships was also assessed using Pearson correlations between the two PCC BOLD contrasts described above and OCC metabolites. Again, application of Steiger Z-tests enabled assessment of whether MRS-PCC BOLD and MRS-OCC BOLD relationships were statistically different from each other.

This approach created 12 correlations in total. As in Chapter 3, to correct for multiple comparisons, a trade-off between the overly conservative Bonferroni correction (which would run the risk of type II error) and no correction (which would run the risk of type I error) was applied. This approach was to create different “families” of comparisons consisting of three tests, and correct for family-wise error across these tests by applying Bonferroni correction within each family (i.e. $0.5/3 = p 0.0167$). The different families of three tests were (1) PCC metabolites and PCC BOLD for rooms 2back>1back, (2) PCC metabolites and PCC BOLD for shapes 2back>1back, (3) OCC metabolites and PCC BOLD for rooms 2back>1back, and (4) OCC metabolites and PCC BOLD for shapes 2back>1back.

Also consistent with the fMRI-MRS analysis in Chapter 3 (section 3.2.8.4.1), Bayes factor analysis was carried out, providing a complementary statistical approach to assess the evidence in favour (denoted BF_{10}) or against (denoted BF_{01}) my hypotheses (as in Harris et al., 2015).

4.2.5.3.2 fMRI-MRS - Voxel-wise general linear model with MRS as a regressor

As in Chapter 3, a complementary regressor analysis was performed to identify any fMRI voxels within the PCC MRS voxel area where the BOLD response to rooms 2back > rooms 1back was significantly associated with tNAA, Glx or GABA+. This was achieved by creating three separate GLMs for the fMRI contrast rooms 2back > rooms 1back, with each model including demeaned values of either PCC tNAA, Glx or GABA+ as a regressor. Contrasts were set up to reveal any fMRI voxels within the MRS voxel mask that were either positively or negatively correlated with each of our key metabolites. This analysis was also run for the contrast of shapes 2back > shapes 1back as a control, in order to test the category sensitivity of any clusters where there was a relationship between BOLD for rooms 2back > rooms 1back and PCC metabolites.

The number of participants for each PCC BOLD-MRS metabolite GLM differed depending on MRS data exclusions related to quality control measures. Thus the PCC MRS voxel mask for each metabolite was created using different numbers of participants (tNAA $n=31$, Glx $n=30$, GABA+ $n=23$) (masks shown in Figure 4.4). The statistical threshold and correction for multiple comparisons was consistent with that described in Chapter 3, which was a voxelwise threshold set at $p<0.01$ ($Z>2.3$), and was corrected for multiple comparisons using a clusterwise threshold of $p<0.01$ determined by Monte-Carlo simulation using the 3dClustSim command in AFNI. Any cluster larger than 92 voxels was statistically significant for the tNAA and Glx masks and larger than 90 voxels for the GABA+ mask. These cluster sizes are larger than in Chapter 3 due to the smoothing on the data being larger in this Chapter, as it was 8mm compared to 5mm in Chapter 3.

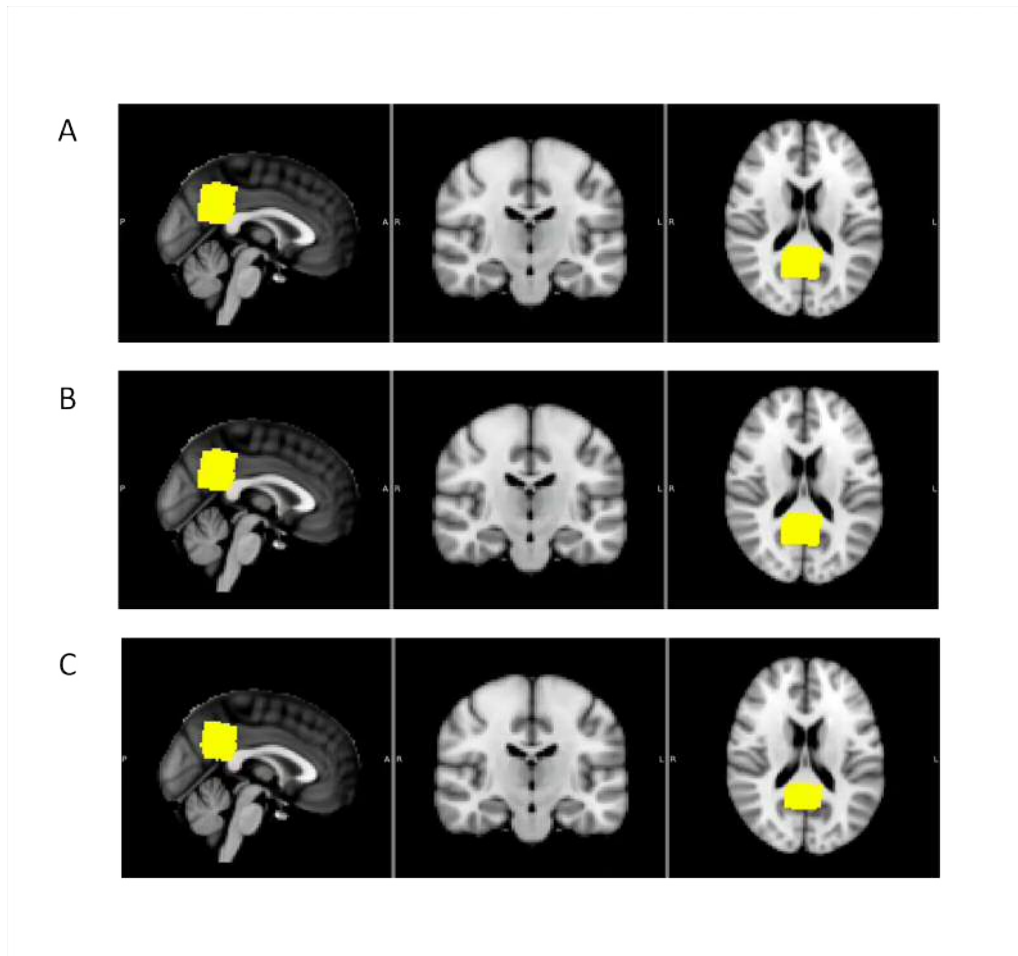


Figure 4.4: Masks used for voxel-wise GLM analysis to investigate MRS-fMRI relationships within the MRS voxel area for each metabolite separately. (A) Mask for tNAA (n=31, mask volume = 4576 voxels). (B) Mask for Glx (n=30, mask volume = 4549 voxels). (C) Mask for GABA+ (n=23, mask volume 3882 voxels).

4.2.6 Behaviour-fMRI correlations

For each level of spatial complexity separately, Pearson correlations were applied to investigate associations between the magnitude of the PCC BOLD deactivation in response to increasing working memory load and behavioural performance. The BOLD measures used were the contrasts of shapes 2back > shapes 1back and rooms 2back > rooms 1back, and the behavioural measure was the difference in the d_L measure (outlined in Section 4.2.5.1) obtained from low to high working memory load. This difference measure was used in order to emulate the BOLD measure, which was also a

difference in activity from 1back to 2back. BOLD-behaviour correlations for rooms and shapes were compared using the Steiger Z-test.

4.2.7 Behaviour-MRS correlations

Pearson correlations were performed to investigate the relationship between the d_L measure for each of the four task conditions (shapes 1back, shapes 2back, rooms 1back, rooms 2back) with PCC tNAA, Glx and GABA+.

4.2.8 Statistical analysis

Where multiple correlations were performed, correction for multiple comparisons was applied. The corrected p value is stated in the analysis for each section, as this differed between analyses depending on how many comparisons were performed.

4.3 Results

4.3.1 Data exclusions

Table 4.1 summarises the exclusions of behavioural, fMRI and MRS data, and the remaining sample sizes for correlations between these measures. Of the total 40 scanned participants, one participant was excluded because they withdrew from the study after the first scanning session, and two participants were excluded due to scanner errors. The fMRI data quality assessment of the remaining 37 participants resulted in the exclusion of four participants' fMRI data due to movement greater than one voxel ($>3.4\text{mm}$) during two or more fMRI runs. Two participants moved more than 3.4mm during only one of the four fMRI runs, so this run was removed from their analysis. The behavioural data analysis was based on the same participants where there was usable fMRI data, thus the sample size for behavioural analysis matches that of the fMRI analysis.

Following the MRS data quality control assessment of the remaining 37 participants, 11 MEGA-PRESS spectra were rejected as these were rated as less than satisfactory on the 3-point rating scale (described in Chapter 3). Seven PRESS metabolites (two PCC tNAA, three PCC Glx, one OCC tNAA and one OCC Glx) had a CRLB greater than 20%, so were also rejected. For the correlations between fMRI and MRS data, there was no overlap between the data excluded for fMRI or MRS, except for the PCC GABA+ and BOLD correlation, where one participant excluded for movement in fMRI also had poor quality MEGA-PRESS spectra.

Data type		Exclusions due to scanning issue + data quality issue	N remaining from original sample size of 40
Behaviour (only for participants where there is fMRI data)		3 + 4	33
fMRI		3 + 4	33
PCC MRS	tNAA	3 + 2	35
	Glx	3 + 3	34
	GABA+	3 + 11	26
OCC MRS	tNAA	3 + 1	36
	Glx	3 + 1	36
	GABA+	3 + 1	36
Correlations between measures	fMRI and PCC tNAA	3 + 4 + 2	31
	fMRI and PCC Glx	3 + 4 + 3	30
	fMRI and PCC GABA+	3 + 4 + (11-1)	23
	fMRI and OCC tNAA	3 + 4 + 1	32
	fMRI and OCC Glx	3 + 4 + 1	32
	fMRI and OCC GABA+	3 + 4 + 1	32
	fMRI and behaviour	Same as fMRI sample size	Same as fMRI sample size
	MRS and behaviour	Same as fMRI and MRS correlation sample size	Same as fMRI and MRS correlation sample size

Table 4.1: The number of participants' data remaining in each part of this study after data exclusions due to scanning issues (participant withdrawal and scanner failures) and data quality control assessments. The numbers of participants for each type of exclusion are listed in the third column, and subtracted from the original sample size of n=40 in the fourth column. For the correlations between measures, the values in the third column refer to the scanner issues + fMRI data quality issues + MRS data quality issues. The only situation where there was an overlap of data quality issues for these correlations was for fMRI and PCC GABA+, where one participant had poor fMRI and MRS data, and this has been listed as (11-1).

4.3.2 Behavioural Results

The behavioural results for the proportion of hits, false alarms, sensitivity and bias are displayed in Figure 4.5. A 2x2 repeated measures ANOVA was performed for each of these behavioural measures, as in Lee and Rudebeck (2010).

For hits, there was a significant main effect of working memory load, $F(1,32)=103.74$, $p<0.001$, a significant main effect of spatial complexity, $F(1,32)=13.29$, $p<0.01$, and no significant interaction between these factors, $F(1,32)=0.56$, $p=0.49$.

For false alarms, there was a significant main effect of working memory load, $F(1,32)=101.44$, $p<0.001$, a significant main effect of spatial complexity, $F(1,32)=120.36$, $p<0.001$, and a significant interaction between these factors, $F(1,32)=37.67$, $p<0.001$. To characterise the interaction, a follow up paired samples t-test revealed this reflected a greater increase in false alarms from the 1back to 2 back conditions when the stimuli were rooms compared to when they were shapes, $t(32)=6.66$, $p<0.001$.

For the sensitivity measure, there was a significant main effect of working memory load, $F(1,32)=396.74$, $p<0.001$, a significant main effect of spatial complexity, $F(1,32)=62.73$, $p<0.001$, and no significant interaction, $F(1,32)=1.94$, $p=0.17$.

For the bias measure, there was a significant main effect of working memory load, $F(1,32)=11.67$, $p<0.01$, a significant main effect of spatial complexity, $F(1,32)=5.89$, $p<0.05$, and a significant interaction, $F(1,32)=4.20$, $p<0.05$. A follow up paired samples t-test revealed the significant interaction reflected a significantly larger effect of bias between the 1back and 2back conditions when the stimuli were shapes compared to rooms, $t(32)=2.05$, $p<0.05$.

This pattern of results suggests that the two 2back conditions were more difficult than the 1back conditions, the two 1back conditions were of a similar level of difficulty, and that the rooms 2back was more difficult and more prone to false alarms than the shapes 2back condition. This pattern was similar to that found in Lee and Rudebeck (2010), where main effects of spatial complexity and working memory were reported, as well as significant differences between the two 2back conditions in terms of proportion of false alarms, sensitivity and bias.

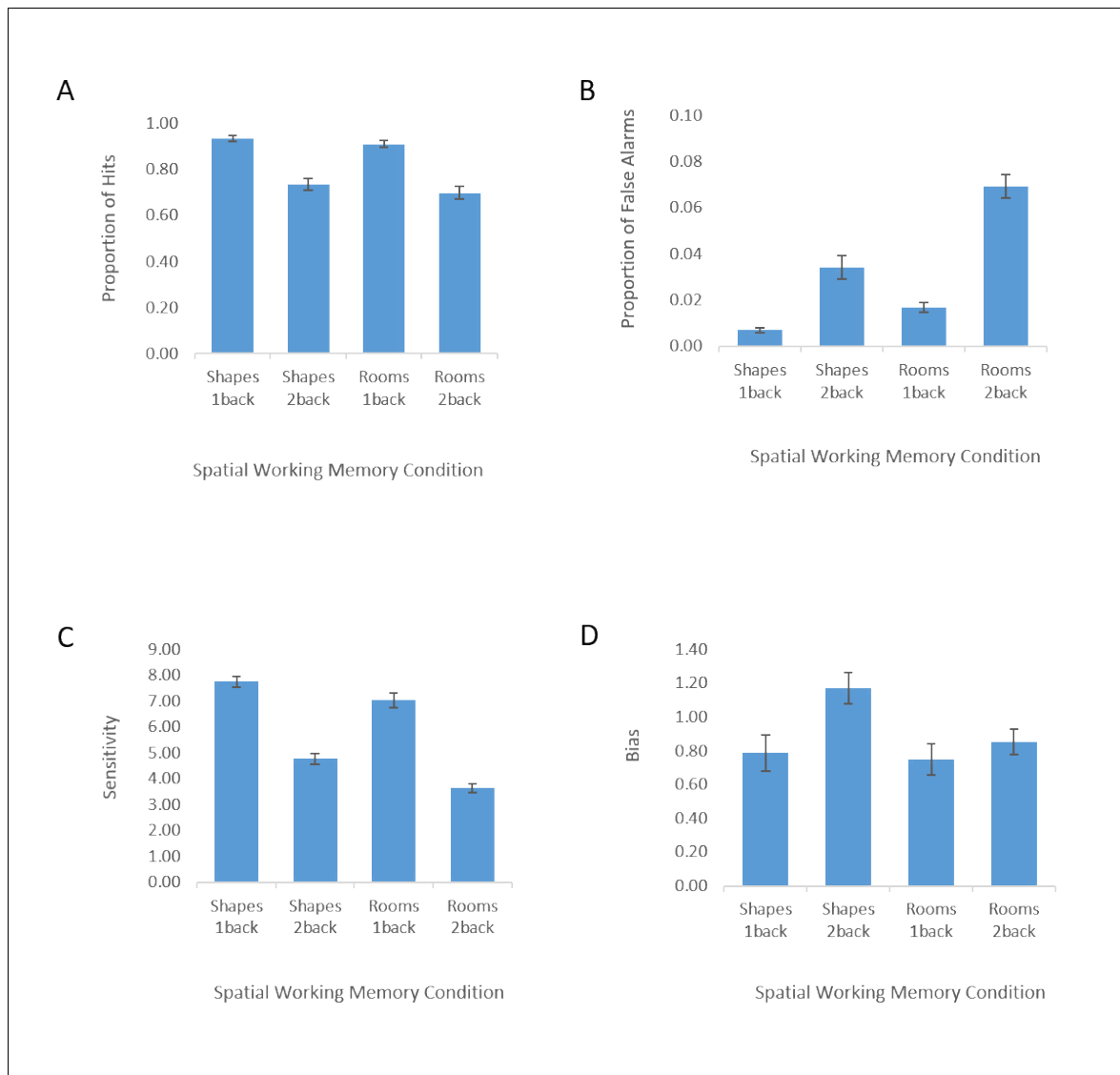


Figure 4.5: Plots of the mean behavioural performance for the 33 participants whose fMRI data were analysed. (A) proportion of hits, (B) proportion of false alarms, (C) sensitivity, and (D) bias. The mean values were obtained by averaging each participant's behavioural data across the 4 runs, then averaging each measure between participants. Error bars represent the standard errors.

4.3.3 fMRI Results

Figure 4.6 shows the BOLD percentage signal change in the PCC ROI for the four conditions relative to the unmodelled baseline. Using a 2x2 factorial ANOVA to compare activity across these four conditions, there was a significant main effect of working memory on PCC BOLD, $F(1,32)=32.92$, $p<0.001$, with less activity (i.e. greater deactivation) for the 2back compared to the 1back conditions. There was a significant main effect of spatial complexity on PCC BOLD, $F(1,32)=65.07$, $p<0.001$, with greater activity (i.e. less deactivation) for the room stimuli compared to shapes. There was also a significant interaction between working memory load and spatial complexity, $F(1,32)=5.91$, $p<0.05$.

To investigate the interaction effect further, pairwise t-tests were performed. These revealed there was a significant deactivation in the PCC ROI for rooms 2back and shapes 2back compared to their relevant 1back conditions (shapes: $t(32)=5.10$, $p<0.001$; rooms: $t(32)=4.49$, $p<0.001$), but also that both rooms conditions showed significantly less deactivation than their shape counterpart at each level of working memory load (e.g., 1back: $t(32)=3.53$, $p<0.01$; 2back: $t(32)=7.06$, $p<0.001$). The significant interaction effect, therefore, arose from the deactivation for shapes 2back compared to shapes 1back being larger than the deactivation for rooms 2back compared to rooms 1back, $t(32)=2.75$, $p<0.05$. This finding suggests greater deactivation in the PCC ROI for increased working memory load for shapes compared to rooms.

The BOLD percentage signal change in the PCC ROI for the contrasts shapes 2back > shapes 1back and rooms 2back > rooms 1back are displayed in Figure 4.6. Individual participant values from these contrasts have also been plotted to show the degree of inter-individual variability for the BOLD-MRS correlations undertaken in Section 3.5.1.

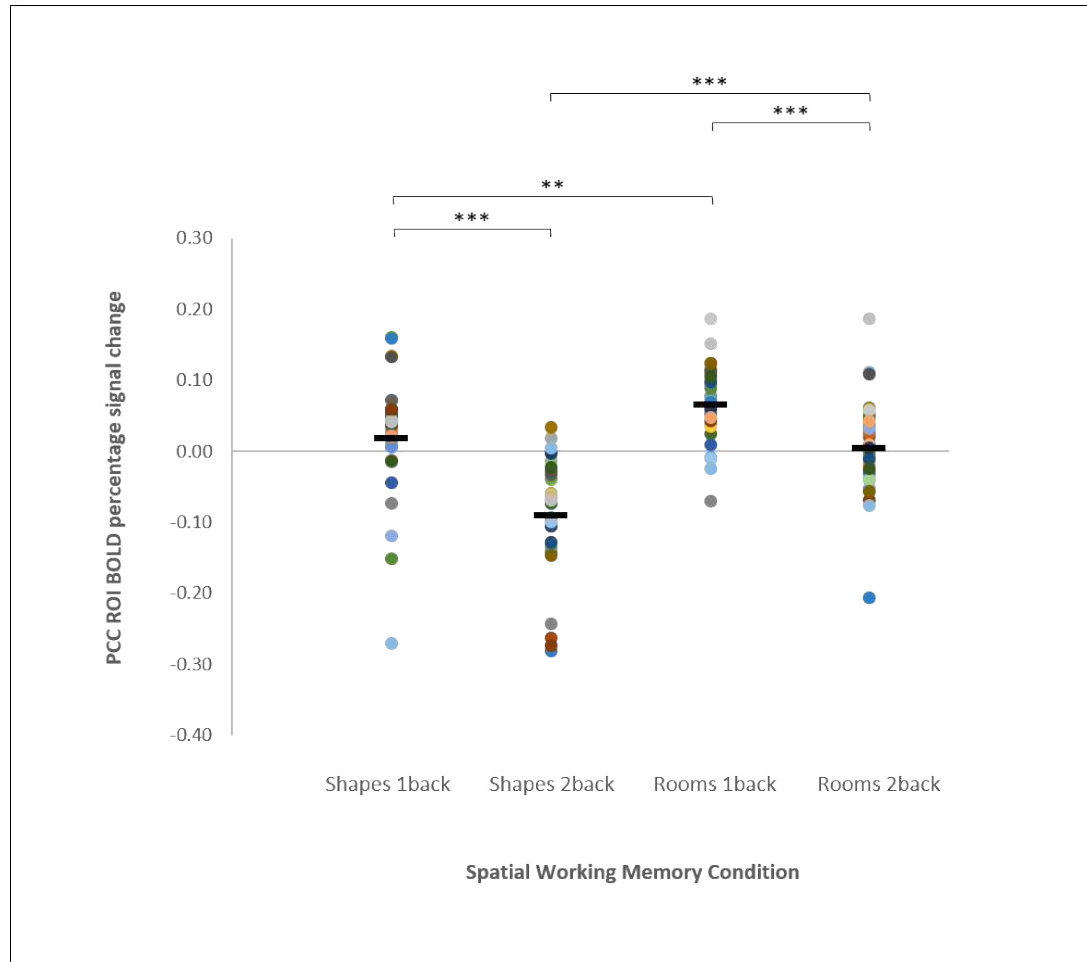


Figure 4.6: BOLD percentage signal change in the PCC ROI relative to the unmodelled baseline. Dots represent individual participants, and the horizontal black bars show the mean for each condition. The asterisks across the top of the graph represent the significance level of the comparison between two conditions, where ** denotes a difference at $p < .01$ and * denotes $p < .001$.**

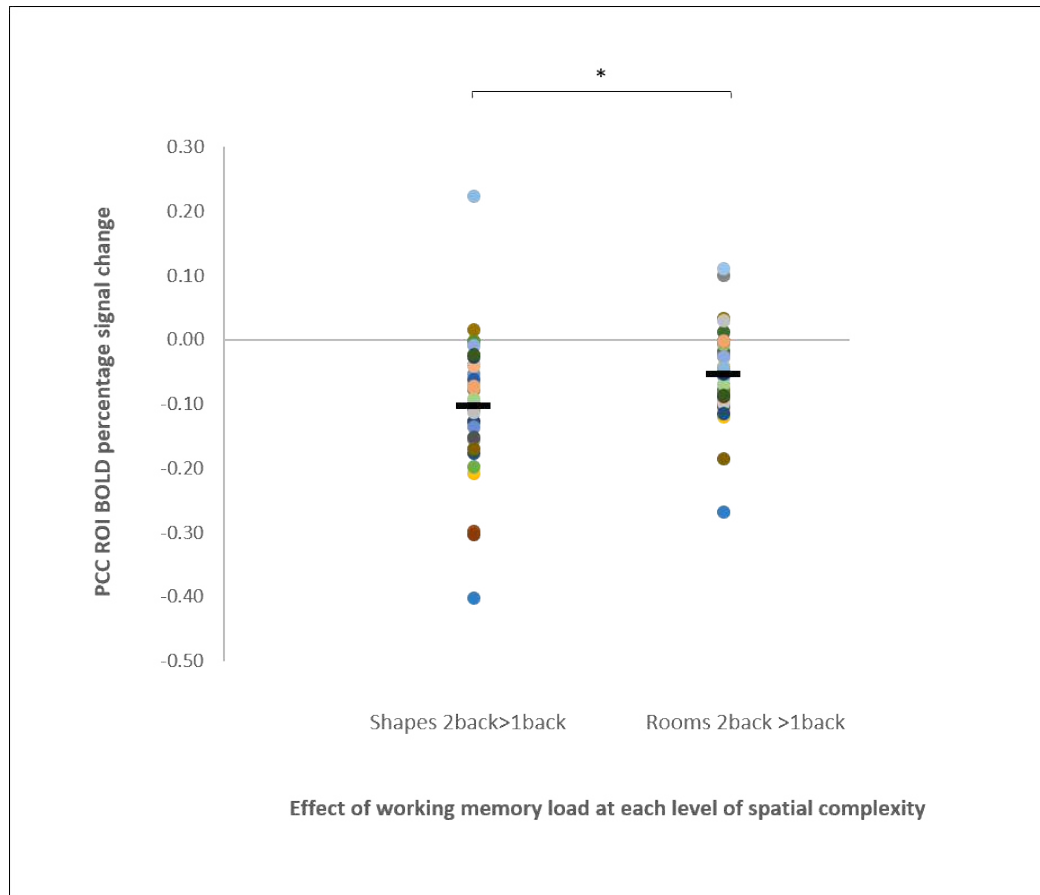


Figure 4.7: BOLD percentage signal change for the effect of increasing working memory load for the different stimuli categories of shapes and rooms. Dots represent individual participants and the horizontal black bars show the mean for each contrast. The asterisk represent the significance level of $p < 0.05$.

4.3.4 MRS Results

The same MRS scans as used in Chapter 3 were used in this Chapter, therefore the MRS results are the same as those shown in Table 3.1 and Figure 3.6 in Chapter 3.

4.3.5 fMRI-MRS Relationships

4.3.5.1 fMRI-MRS – Percent signal change ROI analysis

Table 4.2 and Figure 4.8 display the results of the Pearson correlations between PCC metabolites tNAA, Glx and GABA+ and the PCC ROI BOLD percentage signal change for increasing working memory load when the stimuli were scenes (the contrast rooms 2back > rooms 1back). Also displayed are the control correlations between PCC metabolites and PCC ROI BOLD when the stimuli were shapes (the contrast shapes 2back > shapes 1back) to assess category sensitivity, and between both of these PCC BOLD contrasts and OCC metabolites, to assess regional sensitivity of any relationships.

	Correlation between		N	r	p	Bayes factor
	PCC BOLD contrast	MRS measure				
A. Correlations of interest	Rooms 2back>1back	PCC tNAA	31	-0.13	0.50	BF ₁₀ = 0.14
		PCC Glx	30	0.07	0.97	BF ₁₀ = 0.23
		PCC GABA+	23	-0.15	0.48	BF ₁₀ = 0.50
B. Test for category sensitivity	Shapes 2back>1back	PCC tNAA	31	-0.02	0.99	BF ₀₁ = 4.48 *
		PCC Glx	30	-0.14	0.47	BF ₁₀ = 0.14
		PCC GABA+	23	0.18	0.41	BF ₁₀ = 0.15
C. Test for regional sensitivity	Rooms 2back>1back	OCC tNAA	32	-0.20	0.28	BF ₀₁ = 2.62
		OCC Glx	32	-0.21	0.26	BF ₀₁ = 2.46
		OCC GABA+	32	0.18	0.32	BF ₀₁ = 2.84
	Shapes 2back>1back	OCC tNAA	32	-0.02	0.93	BF ₀₁ = 4.53 *
		OCC Glx	32	-0.27	0.14	BF ₀₁ = 1.61
		OCC GABA+	32	-0.13	0.49	BF ₀₁ = 3.64

Table 4.2: Correlations of PCC ROI BOLD for the effect of increasing working memory load for each level of spatial complexity (rooms or shapes) with PCC and OCC metabolites. Part A shows the correlations of interest, and Parts B and C the control correlations. N is the sample size remaining after exclusions of each data type due to quality control measures, r is the Pearson correlation coefficient, and the p value is 2-tailed (Bonferroni corrected, p = 0.0167). For the Bayes factors, BF₁₀ represents a one-tailed Bayes test in favour of my directional hypotheses (i.e. that there is a positive relationship for PCC tNAA and PCC Glx with both rooms 2back>back and shapes 2back>1back, and a negative relationship for PCC GABA+ with both contrasts), while BF₀₁ represents a Bayes test in favour of the null hypothesis (i.e. that there is no relationship between MRS and BOLD). A Bayes factor of three and above suggests there is sufficient evidence to support the specified hypothesis.

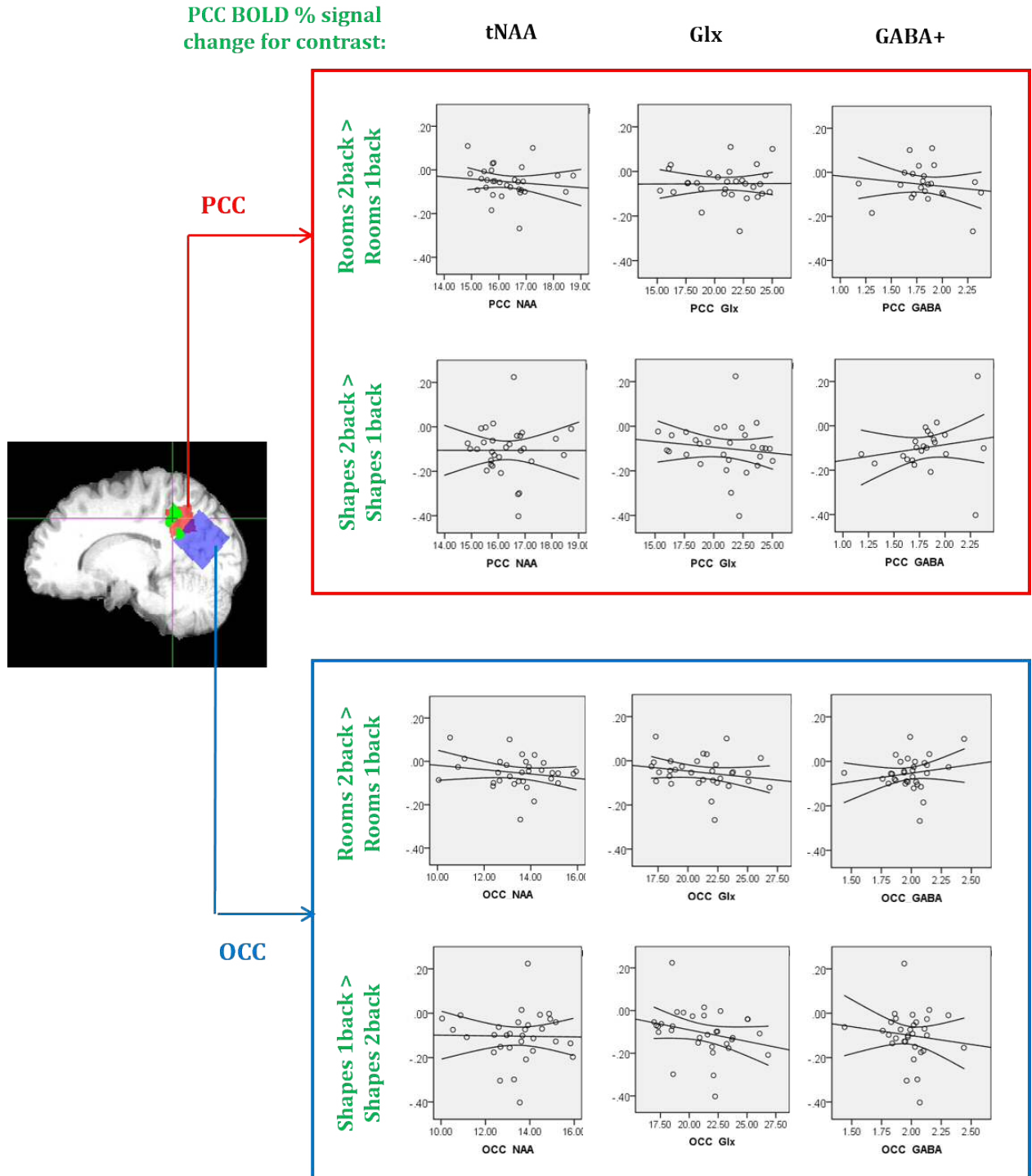


Figure 4.8: Plots of correlations between PCC BOLD for increasing working memory load for rooms and shapes with PCC and OCC metabolites. The PCC voxel is shown in red and OCC in blue. The green area is the PCC fMRI ROI obtained from Shine et al 2015. 95% confidence intervals have been plotted onto these graphs.

There were no significant correlations between PCC BOLD for rooms 2back > rooms 1back and PCC tNAA, Glx or GABA+. This was in contrast to my predictions of a positive correlation for PCC tNAA and Glx and a negative correlation for PCC GABA+. The very small Bayes factors in favour of a relationship (BF_{10}) of 0.14, 0.23 and 0.50 for these three correlations support the lack of significant correlations assessed using p values. Indeed, when Bayes factors were calculated to assess the strength of the evidence *against* my hypotheses (BF_{01}), these were 3.59, 4.40 and 3.04 for the relationship of PCC BOLD for rooms 2back > rooms 1back with tNAA, Glx and GABA+ respectively.

Similarly, there were no significant correlations between any PCC metabolite and PCC BOLD for shapes 2back > shapes 1back. This was consistent with my prediction of no tNAA-BOLD relationship for shapes, but in contrast to my predictions of a positive correlation with Glx and a negative correlation with GABA+. These findings were supported by the Bayes factor against a relationship with tNAA of 4.48, and very small Bayes factors in favour of a relationship with Glx or GABA+ of 0.14 and 0.15.

In contrast to another of my hypotheses, there was no significant difference between the correlations obtained for PCC tNAA with shapes 2back>shapes 1back compared to PCC tNAA associated with rooms 2back>rooms 1back ($Z = -0.62$, $p = 0.53$). Also, there were no significant differences between the correlations for shapes 2back>shapes 1back and rooms 2back>rooms 1back with PCC Glx ($Z = 1.02$, $p = 0.31$) or with PCC GABA+ ($Z = -1.43$, $p = 0.15$).

There were also no significant correlations between either BOLD for rooms 2back>1back or shapes 2back>1back with any of the three metabolites measured in the control OCC region.

4.3.6 fMRI-MRS Relationships: Voxel-wise GLM with MRS regressor approach

This analysis was performed to identify any fMRI voxels within the PCC MRS voxel area where the BOLD response to either rooms 2back>rooms 1back or shapes 2back>1back was significantly associated with tNAA, Glx or GABA+. All clusters reported

here were significant at a voxelwise threshold of $p < 0.01$ ($Z > 2.3$) and a clusterwise significance threshold of $p < 0.01$ determined using the Monte-Carlo simulation (this was 92 voxels for tNAA and Glx and 90 for GABA+). The co-ordinates are the peak voxel in MNI space (in the order x,y,z).

A cluster of 103 fMRI voxels was identified within the PCC MRS voxel mask in the analysis of rooms 2back>rooms 1back when tNAA was used as a regressor to test for a positive correlation between these factors (see Figure 4.9, MNI co-ordinates 4, -50, 48). There was no cluster where tNAA was negatively correlated with BOLD for rooms 2back>rooms 1back. There were no significant clusters present when tNAA was used for the analysis of shapes 2back>shapes 1back, in either the positive or negative direction. These findings are consistent with my prediction that there would be a positive correlation of PCC tNAA with PCC BOLD for rooms but not for shapes.

When Glx was used as the regressor, this revealed no clusters where Glx was positively correlated with BOLD for either rooms 2back>rooms 1back or shapes 2back>shapes 1back, in contrast to my predictions. There was also no cluster where Glx was negatively correlated with BOLD for rooms 2back>1back. There was a cluster of 179 fMRI voxels, however, that showed a significant *negative* relationship between Glx and PCC BOLD for shapes 2back>1back (see Figure 4.9, MNI co-ordinates -2, -34, 44). This is intriguing as this relationship is in a different direction from my prediction of a positive correlation between Glx and BOLD, as found in Hu et al (2013).

With respect to GABA+, the regressor analysis revealed a cluster of 291 fMRI voxels where PCC GABA+ had a *positive* relationship with PCC BOLD for rooms 2back>rooms 1back (see Figure 4.9Ci, MNI co-ordinates 4, -54, 42), and two clusters where PCC GABA+ had a positive relationship with BOLD for shapes 2back>shapes 1back (see Figure 4.9Cii, cluster 1 = 127 voxels, MNI co-ordinates -14, -50, 42; clusters 2 = 121 voxels, MNI co-ordinates 12, -58, 44). There were no clusters where PCC GABA+ had a negative relationship with either BOLD for rooms 2back>1back or shapes 2back>1back.

To show where these clusters are in relation to the PCC fMRI ROI used in the correlation analysis approach in the previous section, how they lie within the metabolite-specific MRS mask area, and the relationship between the two GABA+ clusters, these areas have been overlain in Figure 4.10.

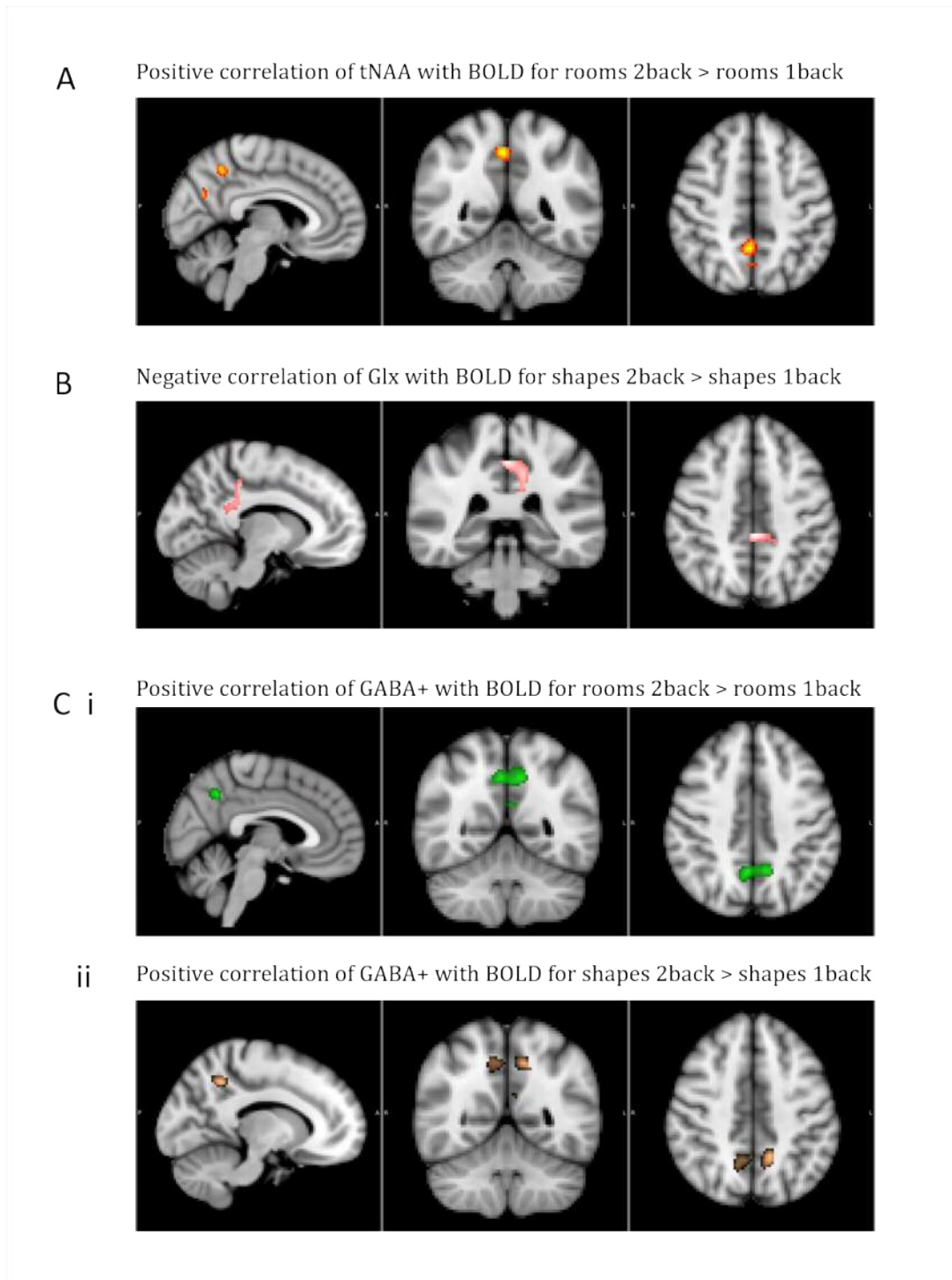


Figure 4.9: Clusters within the metabolite-specific MRS voxel masks where activity correlates with MRS. Images show clusters that are significant at a voxel-wise threshold of $p < 0.01$ ($Z = 2.3$) and a cluster wise threshold of $p < 0.01$. (A) The red/yellow cluster of 103 voxels shows where PCC tNAA is positively correlated with activity for rooms 2back>1back (MNI co-ordinates are $x = 6, y = -50, z = -72$). (B) The pink cluster of 179 voxels shows where PCC Glx is negatively correlated with activity for shapes 2back>1back (MNI $x = -10, y = -36, z = 44$). (C i) The green cluster of 291 voxels shows where PCC GABA+ is positively correlated with BOLD for rooms 2back>1back (MNI $x = 4, y = -54, z = 42$). (C ii) The two copper clusters of 127 and 121 voxels show where PCC GABA+ is positively correlated with BOLD for shapes 2back>1back (MNI $x = -12, y = -54, z = 44$).

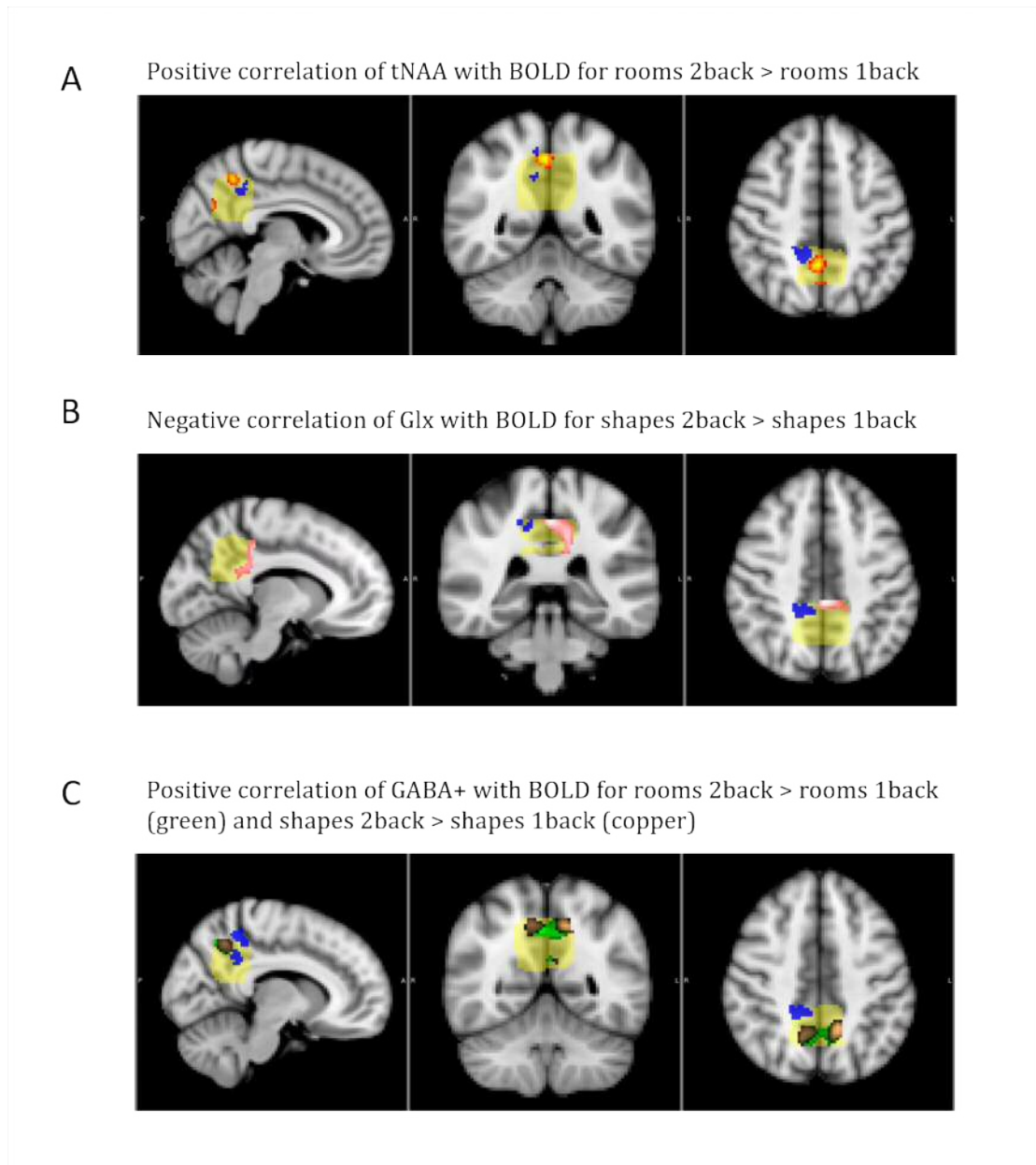


Figure 4.10: Clusters from Figure 4.9 overlaid with the PCC mask regions (pale yellow) and the PCC ROI mask (blue). (A) tNAA+ cluster that positively correlates with BOLD for rooms 2back>1back (red) (MNI $x=6, y=-50, z=48$). (B) Glx cluster that negatively correlates with BOLD for shapes 2back>1back (pink) (MNI $x=-10, y=-36, z=44$). (C) GABA+ clusters that positively correlate with BOLD for rooms 2back>1back (green) and shapes 2back>1back (copper) (MNI $x=10, y=-54, z=44$).

4.3.7 Behaviour-fMRI relationships

Pearson correlations were performed to assess whether individual differences in the degree of PCC deactivation from the 1back to the 2back conditions was related to individual differences in behavioural performance on these conditions. A more negative BOLD value for the contrast 2back>1back indicates greater deactivation from the 1back to 2back condition. A more positive d_I difference score from 1back to 2back conditions indicates there was less of a change (drop) in behavioural performance from the 1back to 2 back conditions.

Figure 4.11 shows the results of the behaviour-fMRI correlations. No significant relationship was found between PCC deactivation (for either rooms 2back > rooms 1back or shapes 2back > shapes 1back) with the performance change measure (rooms: $n=33$, $r=0.27$, $p=0.14$; shapes: $n=33$, $r=0.15$, $p=0.40$).

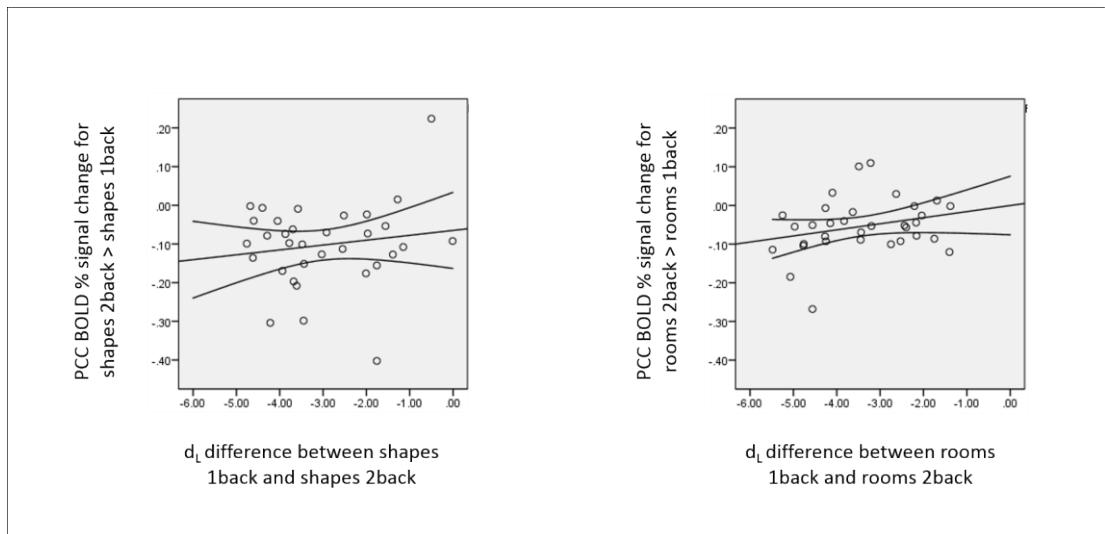


Figure 4.11: Behaviour-fMRI relationships for shapes (left hand side plot) and rooms (right hand side plot). 95% confidence intervals are shown.

4.3.8 Behaviour-MRS relationships

Pearson correlations tested the relationship between the concentration of the three PCC metabolites and the behavioural performance (d_L) on each of the four task conditions. To correct for multiple comparisons, a familywise error correction was applied, where each metabolite was considered as a family. Each metabolite was used in a correlation four times (once per behavioural measure), thus the significance threshold was reduced to $p = 0.05/4 = 0.0125$. Results are shown in Table 4.3.

Correlation between		n	r	p	BF ₁₀
d_L for each task condition	PCC metabolite				
Shapes 1back	tNAA	31	0.09	0.60	0.25
	Glx	30	0.22	0.24	0.44
	GABA+	23	-0.15	0.51	0.32
Shapes 2back	tNAA	31	0.33	0.07	1.10
	Glx	30	0.09	0.60	0.26
	GABA+	23	-0.02	0.93	0.26
Rooms 1back	tNAA	31	0.26	0.16	0.57
	Glx	30	0.22	0.24	0.43
	GABA+	23	-0.23	0.29	0.44
Rooms 2back	tNAA	31	0.45	0.01 *	4.76 *
	Glx	30	0.04	0.84	0.23
	GABA+	23	0.01	0.98	0.26

Table 4.3: Correlations between PCC metabolites and behavioural performance (sensitivity, d_L) on the four task conditions. N denotes the sample size, r the Pearson correlation coefficient, p the p value, and BF₁₀ the Bayes factor in favour of a correlation. The asterisks denote a significant correlation.

There was a significant positive correlation between PCC tNAA and d_L for rooms 2back (see Table 4.3). This was supported by the Bayes factor in favour of a relationship of greater than 3. The significant correlation indicates that a higher concentration of PCC

tNAA is associated with better performance on the rooms 2back condition. There were no other significant MRS-behaviour correlations. When the correlation between tNAA and d_L for rooms 2back was compared with the correlation between tNAA and d_L for rooms 1back, however, these were not found to be significantly different: $Z(1.31, p=0.19)$. Similarly, when compared with the correlation between tNAA and d_L for shapes 2back, there was also no significant difference ($Z=0.99, p=0.32$). These three correlations have been plotted in Figure 4.12.

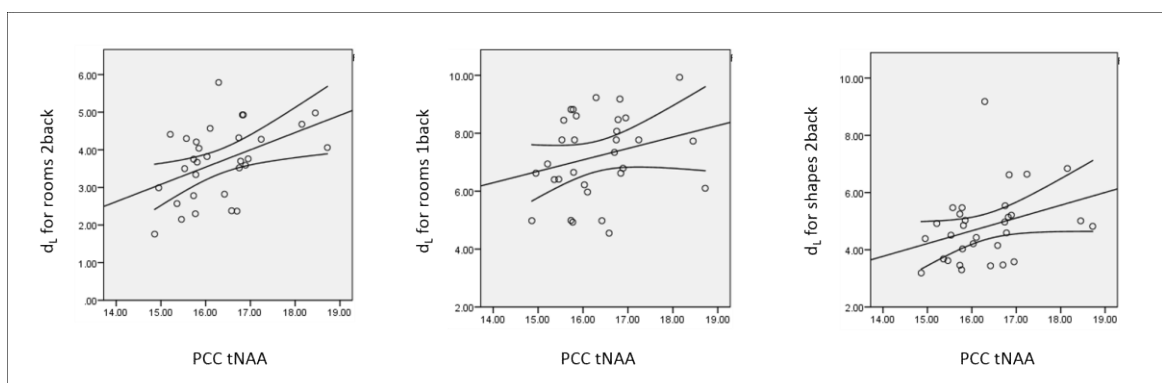


Figure 4.12: Significant positive correlation between PCC tNAA and behavioural performance (assessed using sensitivity (d_L)) for the rooms 2back condition, $r=0.45$, $p=0.011$, $BF_{10} = 4.76$, and the two non-significant correlations between PCC tNAA and d_L for rooms 1back and between PCC tNAA and d_L for shapes 2back.

4.4 Discussion

To investigate the relationship between PCC biochemistry and activity during a working memory task in the PCC ROI identified in Shine et al. (2015), and ask how PCC fMRI and PCC MRS impact on task performance, this Chapter reports findings from the spatial working memory fMRI paradigm used by Lee and Rudebeck (2010). The aims of the study were to (1) determine whether the expected alteration in activity associated with working memory in our key PCC ROI is modulated by the spatial complexity of the stimuli (rooms vs shapes), (2) assess whether individual differences in the pattern of

PCC deactivation for room working memory, but not shape working memory, are associated with inter-individual variation in PCC MRS, (3) assess potential associations between changes in PCC ROI activity across working memory load and behavioural performance on the task, and whether these differ between stimuli categories, and (4) test whether behavioural performance on the task is related to PCC MRS, and compare this between the stimuli categories.

As a summary of the main findings, before a more detailed discussion of the results, the fMRI analysis established that, as expected and as seen in previous PCC working memory studies (e.g. Esposito et al., 2009; Hu et al., 2013; Mckiernan, Kaufman, Kucera-Thompson, & Binder, 2003), there was a significant deactivation in the PCC when working memory load increased, which occurred for both stimuli categories of rooms and shapes. When the effect of stimuli category on this deactivation response was assessed, this revealed a main effect of spatial complexity, but also that spatial complexity impacts on the activity of PCC as there was an interaction with working memory load. More specifically, there was less of difference between 1back and 2back conditions for the rooms compared to the shapes stimuli. The fMRI-MRS Pearson correlation analysis found no relationship between PCC MRS metabolites and PCC deactivation for increasing working memory load for either the room or shape conditions. The fMRI-MRS regressor analysis, however, identified metabolite-specific clusters within the MRS voxel mask area where activity for rooms 2back>1back was positively associated with tNAA and GABA+ (i.e. less deactivation = higher tNAA and higher GABA+), and where activity for shapes 2back>1back was positively associated with GABA+ and negatively associated with Glx (i.e. less deactivation = higher GABA+ and lower Glx). The fMRI-behaviour correlations suggested that poorer performance in the 2back condition (compared to the 1back condition) was unrelated to the degree of changes in the PCC ROI activity as working memory load was increased. This lack of relationship applied to both the rooms and shapes conditions. The MRS-behaviour correlations suggested that performance on the rooms 2back conditions is related to PCC tNAA, with better performance linked to higher concentration of PCC tNAA. This correlation, however, was not significantly different from the correlations obtained between PCC tNAA and the rooms 1back or shapes 2back conditions.

4.4.1 fMRI Results: Interaction between spatial complexity and working memory load in PCC

The fMRI interaction effect detected between working memory load and spatial complexity is consistent with the PCC finding from the whole brain exploratory analysis in Lee and Rudebeck, (2010). In their interaction effect, there was a greater difference between shapes 2back > shapes 1back compared to rooms 2back > rooms 1back, which is the same pattern as shown in Figure 4.6. Linking this with previous accounts of PCC function, this finding that increasing working memory for scenes, but not shapes, elicits a different amount of deactivation in the PCC ROI confirms that this brain region does not deactivate in a generic manner for increasing working memory load for different stimuli categories, and concurs with the findings in Chapter 3 whereby the PCC ROI also showed a category-sensitive profile of brain activity. These findings challenge the early studies on DN/PCC function, which suggested that it was simply a task-negative area, which means it is active when there is no task and deactivates when performing a task (Raichle et al., 2001). Additionally, this interaction finding adds to the previous studies investigating PCC activity in response to increasing working memory load, as these have used only one type of stimuli: for example, McKiernan et al. (2003) used auditory stimuli, Esposito et al. (2009) used numbers and Hu et al. (2013) used letters.

Chapter 3 found a distinct BOLD response in the PCC ROI for the perception of different categories of stimuli (scenes, faces, objects). Although faces and objects were not assessed here, the finding of a different pattern of BOLD activity in PCC to rooms than shapes here further confirms that the PCC shows category sensitivity patterns, and that these are evident for both perception and working memory. Furthermore, the work reported in this Chapter extends Chapter 3 by demonstrating differences within the spatial domain, rather than between different stimuli categories. This Chapter suggests that a spatial arrangement that forms a scene (high spatial complexity) engages the PCC differently to spatial arrangements comprising of shapes that do not form a scenes (low spatial complexity).

In the original spatial working memory study by Lee and Rudebeck (2010), they detected a different pattern of activity in eight different MTL ROIs. There was no region that showed the same interaction pattern as identified in this Chapter. The two regions that showed the closest similarity to my PCC findings were the right entorhinal cortex

and right hippocampus. In these regions, there was a smaller decrease in activity for rooms compared to shapes during high compared to low working memory, and the activity for the rooms condition at low working memory load was more negative than at high working memory load (see Figure 4.3C for the BOLD findings in the right hippocampal ROI. The interaction finding in the right entorhinal cortex was highly similar to this pattern of results). Structural connectivity studies using DTI in humans and using retrograde and anterograde tracers in macaques indicate that the PCC is strongly connected to both the hippocampus and the entorhinal cortex (Greicius et al., 2009; Parvizi et al., 2006) (see Figure 1.4). To better understand whether activity in the PCC is related to activity in these two MTL regions, a further research step could be to correlate BOLD from the PCC ROI with BOLD in each of these regions, thereby assessing if there is functional connectivity between these regions during scene and shape working memory conditions.

4.4.2 fMRI-MRS Results: scene-sensitive PCC tNAA-BOLD relationship, but not for GABA+ or Glx

Turning now to the BOLD-tNAA results, the regressor analysis showed that there was a cluster within the PCC MRS voxel where BOLD for rooms 2back>1back, but not BOLD for shapes 2back>1back, correlated with PCC tNAA. This would suggest that the PCC deactivation seen when working memory load increases is related to PCC tNAA when the stimuli have high spatial complexity (rooms), but not when they have low spatial complexity (shapes). This finding is similar to that found in Chapter 3, where there was a category-sensitive tNAA-BOLD relationship for scenes, but not for the other categories of faces or objects. Thus across both perceptual and working memory tasks, individuals who show a less prominent deactivation to scenes seem to have higher concentrations of tNAA in the PCC.

The tNAA-BOLD relationship in this present Chapter, however, does not seem as clear cut as that found in Chapter 3, however, as the two approaches to correlate PCC tNAA with PCC BOLD did not produce the same pattern of results, as was the case in Chapter 3. More specifically, the Pearson correlation analysis suggested no significant relationship between PCC ROI BOLD for rooms 2back > rooms 1back with PCC tNAA, yet

the regressor analysis identified a cluster within the PCC MRS voxel where PCC tNAA does positively correlate with BOLD for rooms 2back > rooms 1back. This differing pattern of results was also identified in a previous study by Lipp et al. (2015), when a similar dual approach was applied to investigate BOLD-GABA+ relationships. In their study, the percentage signal change obtained from an insula fMRI ROI did not correlate with GABA+ from the MRS voxel placed in the insula, yet there was a region within the insula MRS voxel where GABA+ did correlate with BOLD in their regressor analysis. Conversely to both this Chapter and Lipp et al. (2015), however, when this dual approach was applied in Enzi et al. (2012), there was a significant relationship between BOLD and Glx in both the Pearson correlation and in the regressor analysis.

One possible explanation for these discrepancies is there is a lack of overlap between the fMRI ROIs and the fMRI clusters identified via the regressor analyses in this Chapter and in Lipp et al. (2015). This is confirmed in Figures 4.11A and 4.14A where the ROIs and clusters appear to be positioned adjacent to each other. Thus in this Chapter the region where BOLD for rooms 2back > rooms 1back correlates with the metabolite in the regressor analysis is different from the region used in the Pearson correlation analysis (there was only one fMRI voxel that was common to both the ROI and cluster). In contrast, the ROI and cluster do overlap in Enzi et al. (2012) (see Figure 4.14B) and there is evidence of a greater overlap of the fMRI ROI and cluster in the analyses reported in Chapter 3 (25% of the fMRI voxels in the cluster identified in the regressor analysis were within the PCC fMRI ROI from Shine et al. (2015); see Figure 3.13B). One implication of these findings could be that a regressor approach may be more sensitive than an fMRI ROI approach in testing MRS-fMRI relationships. This will be further discussed in the general discussion of this thesis (see Chapter 6).

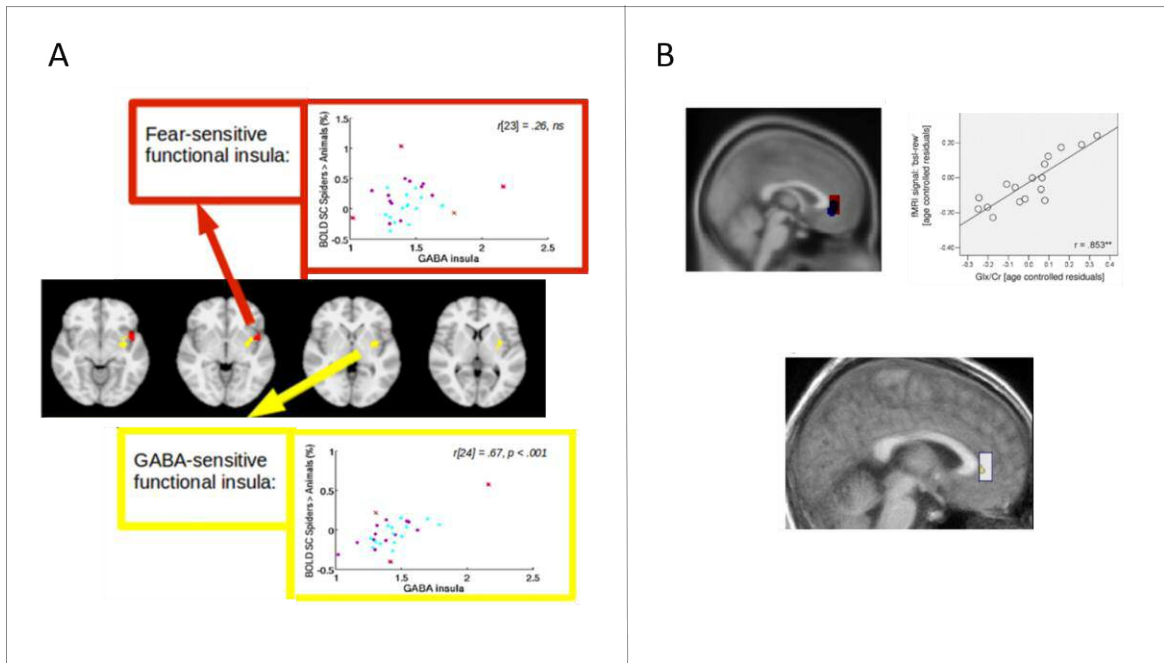


Figure 4.13: Examples of two fMRI-MRS studies that used both a Pearson correlation approach, where the MRS metabolite was correlated with the BOLD percentage signal change obtained from a specified fMRI ROI, and a regressor approach, where MRS was entered as a regressor in the BOLD analysis, to reveal voxels where the metabolite was correlated with BOLD. (A) GABA-BOLD study by Lipp et al., (2014). The red cluster is the fMRI ROI, and there was no-significant correlation between insula GABA and the BOLD percentage signal change in this ROI ($r(23)=0.26$, ns). The yellow cluster is the region identified in the regressor analysis where BOLD does show a correlation with the metabolite ($r(24)=0.67$, $p<0.001$). (Image adapted from Lipp et al., 2014). (B) Glx-BOLD study by Enzi et al. (2012). The dark red region in the brain image represents the MRS voxel, and the dark blue region represents the fMRI ROI. The scatterplot shows there is a positive correlation between ACC Glx and ACC BOLD ($r=0.85$, $p<0.001$). The bottom figure shows the cluster within the MRS voxel where Glx was correlated with BOLD in the regressor analysis. (Images adapted from Enzi et al., 2012).

Turning to the BOLD-GABA+ and BOLD-Glx results, again the Pearson correlations and regressor analyses did not produce consistent results. There were no significant relationships when the Pearson correlation approach was used, but again the regressor analyses revealed similar clusters where BOLD for rooms 2back > rooms 1back and BOLD for shapes 2back > shapes 1back were positively associated with PCC GABA+, and a cluster where BOLD for shapes 2back>shapes 1back was negatively associated with PCC Glx. As for tNAA, the clusters identified for GABA+ and Glx did not overlap with the PCC fMRI ROI, a most likely reason for the non-significant Pearson correlations (see Figure 4.10 B and C).

The motivation behind assessing PCC BOLD and PCC MRS relationships was to investigate whether individual differences in PCC BOLD for scene working memory were associated with individual differences in PCC MRS, and whether any such relationship was category sensitive for scenes (e.g., restricted to rooms but not shapes). The PCC clusters identified in the analysis that showed a positive relationship between PCC GABA+ and PCC BOLD for rooms 2back > rooms 1back and for shapes 2back > shapes 1back, were in a highly similar location, as depicted in Figure 4.10C. This suggests that the PCC BOLD-GABA+ relationship is not category sensitive to scenes, but instead appears generic to both stimuli categories. Linking to the *APOE* study by Shine et al. (2015), the alteration in PCC BOLD in the young *APOE*-E4 carriers was sensitive only to the scene condition of the working memory task. Therefore, the category unspecific GABA+ finding in this Chapter would suggest that an alteration in PCC GABA+ is unlikely to be associated with the specific brain activity changes evident in the young *APOE*-E4 carriers. In addition, there was no relationship between PCC Glx and PCC BOLD for rooms 2back > rooms 1back; instead there was a cluster that showed a negative correlation between PCC Glx and PCC BOLD for *shapes* 2back > shapes 1back. Similar to the situation for GABA+, since there was no scene sensitive PCC Glx-PCC BOLD relationship, this finding implies that any alteration in PCC BOLD for scene working memory in the young *APOE*-E4 carriers is unlikely to be linked to PCC Glx.

It is puzzling that correlations where Glx or GABA+ was associated with BOLD were in the opposite direction than predicted based on Hu et al. (2013). Hu identified a positive relationship between Glx and BOLD where reduced deactivation to increasing working memory load was associated with higher Glx. They also identified a negative relationship between GABA and BOLD where greater deactivation was associated with higher GABA. In contrast, the results of this Chapter suggest that the BOLD response elicited to increasing working memory load for shapes is *negatively* related to Glx and *positively* related to GABA (i.e. reduced deactivation = less Glx, but more GABA), and for rooms is positively related to GABA.

Examining the differences between this study and that of Hu et al. (2013), in order to identify potential reasons for the discrepant patterns of BOLD-GABA+ and BOLD-Glx results, one obvious difference reflects the contrasts used to obtain the BOLD measurement. Hu et al. (2013) used a 0back condition as the condition of low working memory load, and contrasted that with conditions of higher working memory load (1back>0back, 2back>0back and 3back>0back). I did not apply a 0back condition here,

using instead a 1back condition to contrast with the 2back condition, to create a contrast of high>low working memory load (e.g. rooms 2back>rooms 1back), as in Lee and Rudebeck (2010). This difference in the low working memory load condition in the BOLD contrasts could have meant that there may not have been as large a difference between the PCC BOLD response to the 1back and 2back conditions in this Chapter as there was between the 0back and 2back conditions of Hu et al. (2013). The larger range in Hu et al. (2013) may have meant their study had greater power to detect a correlation between BOLD and MRS metabolites. A proposal for how this could be tested is outlined below.

An additional difference between Hu et al. (2013) and the approach taken in this Chapter is the nature of the stimuli used. Hu et al. (2013) used single letters, whereas this study used images of scenes or shapes. Thus perhaps there is something about the nature of the stimuli that could result in the different pattern of BOLD-GABA+ and BOLD-Glx correlations, or the strategy used to complete the working memory task when the stimuli category is different. For example, if presented with a series of letters and asked to hold these in working memory, then the strategy might be to mentally rehearse these and repeat the name of the letters to oneself. Whereas if shown a series of scene images, it is not possible to rehearse this by repeating the name of the image. Instead it would require holding features of the scene and their spatial relationships in working memory. Thus perhaps participants' strategies, and thus the neural correlates required to effectively perform the working memory tasks, differs for distinct forms of visual information.

A further difference is that the fMRI ROI used to correlate with the MRS metabolites in Hu et al. (2013) was selected as the region that was deactivated during the working memory task. This could be considered as a biased approach, since the same data was used to identify the region where there was the activity change and also to correlate this activity change with the MRS metabolites. Whereas in the present Chapter the fMRI ROI was independently created in a separate study by Shine et al. (2015), and the clusters that were correlated with PCC GABA+ and Glx in the regressor analysis were identified in an unbiased approach.

To better understand why there may be a BOLD-GABA+ and BOLD-Glx relationship in different directions for letter stimuli compared to shape and scene stimuli, and test some of the ideas raised here, these factors could be combined in a further study. The experimental design could include scene stimuli and letter stimuli (leaving out the shape

condition to limit the number of conditions, thereby increasing power for scenes and letters). The task could be a blocked design and include 0back, 1back and 2back conditions, making this a 2x3 repeated measures design, where factors are stimuli type (scenes vs letters) and n-back condition (3 levels). The 0back condition for the letters would be the same as in Hu et al. (2013) where there is a target letter which when presented requires the participant to press the response button. In the case of the scene condition, there could be a target scene, and as for the target letter, the participant should press the response button when this was viewed. This design would address the issue that the baseline condition between Hu et al. (2013) and the present study are different. When correlating BOLD and MRS the unbiased regressor approach could be used. This would test whether the BOLD-MRS correlations for letter working memory identified in Hu et al. (2013) can be replicated using this alternative approach. Moreover, using the regressor approach would allow replication of the BOLD-MRS correlations reported in this Chapter. Finally, the participants could be asked about their strategy for completing the n-back task, to investigate whether participants rehearse the letters to themselves in the letter n-back conditions, or whether they hold it as an image in their minds eye as predicted for the scene conditions. This de-briefing of participants would enable greater insight into whether a different task strategies are adopted for different stimuli conditions.

4.4.3 fMRI-behaviour results: PCC activity is not related to task performance

The BOLD-behaviour correlation results suggest that the magnitude of PCC deactivation is not significantly correlated with behavioural performance. This was consistent with a recent study by Ceko et al. (2015) that showed that a group of chronic pain patients, who have a less responsive DMN than healthy controls, did not show have any difference in working memory task performance. The interpretation of this finding was that PCC deactivation was not required for successful working memory performance. This could have implications for the *APOE* study, and also AD studies. If young *APOE*-E4 carriers show less PCC deactivation, and if PCC deactivation is not related to task performance, then correspondingly a failure to deactivate the PCC in the young *APOE*-E4 carriers should have no impact on behavioural performance for working

memory. This is indeed what has been found in the study of PCC activity in Shine et al. (2015), as there was no behavioural differences between the *APOE*-E4 carriers and non-carriers despite a difference in PCC activity for working memory.

4.4.4 MRS-behaviour results: PCC tNAA is related to rooms 2back performance

Finally, the MRS-behaviour correlations revealed that PCC tNAA is positively correlated with performance on the rooms 2back condition, suggesting that a higher concentration of PCC tNAA is associated with better performance on this task condition. The behavioural results displayed in Figure 4.5 indicate that the rooms 2back condition may be the most difficult condition, as it has the lowest mean proportion of hits and the highest mean proportion of false alarms. Since hypotheses for the biological function of tNAA include neuronal or synapse density and energy metabolism via mitochondria (Maddock & Buonocore, 2012; Murray et al., 2014; T. B. Patel & Clark, 1979; Rae, 2014), this significant correlation could suggest that for more difficult tasks, a higher density of PCC neurons, or a higher functional capacity of the mitochondria in PCC neurons, is beneficial. Whereas this is not beneficial when the task difficulty is lower. This is a tentative suggestion, however, as although there were no significant correlations between PCC tNAA and the other task conditions, the differences in the correlation between tNAA and rooms 2back, rooms 1back and shapes 2back were not significantly different from each other, potentially undermining this assertion. Moreover the tNAA-behaviour literature includes a mixture of significant and non-significant correlations, suggesting there is no clear picture for tNAA-BOLD relationships (Jung et al., 1999, 2005; Nikolaidis et al., 2016; T. Patel et al., 2014; Paul et al., 2016). An implication of the correlation between PCC tNAA and performance on the rooms 2back condition detected in this Chapter could be that future studies assessing NAA-behaviour relationships should include tasks of high difficulty to best capture any relationships that may exist.

4.4.5 Limitations

As in Chapter 3, there are limitations to using MRS, for example the large voxel sizes required to quantify metabolites present at very low concentrations, the overlap of the PCC and OCC voxels in some individuals, and the technical difficulties in quantifying GABA+. Since these issues apply to all three experimental Chapters, these themes will be returned to in the general discussion Chapter (see Chapter 6).

A potential limitation of the fMRI part of this study is that the rooms 2back condition may have been too difficult, as there was a higher proportion of false alarms for this condition compared to the other three conditions. This resulted in the exclusion of a higher number of blocks for the 2back condition (e.g., an average of 4/8 blocks per run for the rooms 2back condition, vs 1/8 blocks per run for the rooms 1back condition), since strict criteria about behavioural performance were used to decide which blocks should be included in the fMRI analysis (as applied in Lee and Rudebeck (2010)). While the benefit of these criteria is that they ensure data fMRI data included in the analysis are of high quality, a possible limitation is that there may be less power to detect BOLD signal change for rooms 2back as there are less blocks included in the analysis. To address this, an improvement to the task design would be to make the room stimuli more different in order to reduce the number of false alarms for the 2back condition, and thus increase the number of usable rooms 2back blocks.

The size of the fMRI smoothing kernel may also have been a limitation in this Chapter. The kernel applied here had a FWHM of 8mm, which is larger than the kernel of FWHM of 5mm more typically used in fMRI studies and applied in Chapter 3. The choice of this larger kernel was to be consistent with the original spatial working memory study of Lee and Rudebeck (2010). Since smoothing involves averaging the signal over adjacent voxels, using a larger kernel may have blurred and diluted any effects over a wider region (Poldrack et al., 2011). The BOLD results may have been different therefore using an 8mm vs 5mm FWHM kernel, as the spatial specificity of any effects and the magnitude of the peak BOLD response may have been greater for a 5mm kernel. It would be interesting to repeat the analysis in this Chapter using a 5mm kernel, to examine whether this causes any change in the magnitude of the BOLD response extracted from the PCC ROI or the spatial extent of the clusters identified in this study.

A further possible limitation, as discussed in Chapter 3, is the choice of fMRI ROI. Again, in the context of this thesis, this fMRI ROI was chosen to examine activity in this *APOE-E4* relevant ROI for scene working memory and relate this to the biochemistry of this region. However, as outlined in the Discussion section of Chapter 3, activity in the ROI may not be generalizable to the function of the PCC (please see page 91). Alternative strategies to quantify the BOLD percent signal change to different stimuli conditions in this region, such as those outlined in the Chapter 3 Discussion and Figure 2.6, could be used, and compared with the findings from the ROI used in this Chapter.

4.4.6 Summary of Chapter

In summary, this Chapter has demonstrated that in a working memory task, there is less deactivation in the PCC ROI to increasing working memory load when the stimuli are scenes (3D rooms) compared to when they are 2D shapes. This is in support of the findings of Chapter 3 that the BOLD response in the PCC ROI shows category sensitivity. Also consistent with Chapter 3, no significant BOLD-behaviour correlations were detected. This finding challenges previous studies that suggest PCC deactivation has a relationship with task difficulty, and instead, could imply that it may be a property of viewing scenes that is associated with the different pattern of deactivation across scenes and shapes. Similar to the tNAA-BOLD relationship identified in Chapter 3, individual differences in the magnitude of this deactivation to scenes, but not to shapes, was related to individual differences in PCC tNAA. This suggests there may be a category sensitive PCC BOLD-PCC tNAA relationship for scene working memory, as well as a category sensitive PCC BOLD-PCC tNAA relationship for scene perception, as indicated in Chapter 3. PCC tNAA was the only metabolite that appeared to show a category-sensitive relationship for scenes, as the region within the PCC that showed a correlation between GABA+ and BOLD for scenes was highly similar to a region that showed a correlation between GABA+ and shapes. This adds new knowledge to the MRS-BOLD literature, as category sensitivity in working memory studies has not previously been assessed. The complementary findings of a PCC tNAA-PCC scene BOLD relationship on the two paradigms that young *APOE-E4* carriers showed an altered pattern of activity in the PCC ROI (less deactivation) (Shine et al., 2015) provide support for the hypothesis that the alteration in PCC BOLD in the *APOE-E4* carriers could be associated with an alteration in

PCC MRS, with a tNAA now being the strongest candidate for a potential metabolite alteration. The next Chapter will investigate this question, asking whether young *APOE*-E4 carriers and non-carriers show different profiles of tNAA concentration in the PCC.

5 Chapter 5: Investigating metabolite differences between young *APOE-E4* carriers and non-carriers in posterior cingulate cortex using MRS

5.1 Introduction

The purpose of this final experimental Chapter was to investigate whether there are differences in MRS metabolites in the PCC of young *APOE-E4* carriers compared to non-carriers. The rationale for testing MRS in these groups was, as introduced in Chapter 1, that such an approach allows us to investigate potential biochemical differences in a key brain region implicated in AD pathogenesis, in order to gain insight into how and why this disease may develop in some at risk individuals. Several neuroimaging studies have adopted this strategy to study the impact of the *APOE-E4* allele in young people in the PCC; these suggest alterations in PCC resting state fMRI activity (Filippini, MacIntosh, et al., 2009), task-related fMRI activity (Shine et al., 2015), functional connectivity (measured using fMRI) (Dennis et al., 2010), and glucose metabolism (measured using FDG-PET) in *APOE-E4* carriers (Reiman et al., 2004). A question that has not yet been addressed in this age group is whether there are also biochemical differences in the PCC region measured using MRS.

MRS is a valuable neuroimaging technique to apply here, as it can provide additional biochemical information to augment the findings from fMRI and FDG-PET studies, as outlined in Chapters 1 and 2. FMRI tells us about spatial specificity of any activity differences between E4 carriers and non-carriers, but it does not tell us very much about the biological mechanisms behind why brain regions are more active. If we can better understand the biological pathways behind the altered brain activity in these individuals, it could provide clues as to what biological pathways, potentially linked to risk genes, may pre-dispose an individual to develop AD later in life. FDG-PET is another technique that provides biochemical information as this tells us about glucose metabolism, however MRS can augment the information gleaned using this research

technique as it provides extra biochemical information on different biological markers, such as markers of inflammation, energy metabolism and neuronal density (Rae, 2014). Furthermore, MRS is more appealing than FDG-PET, since MRS is a non-invasive technique and can be performed in a standard MRI scanner, whereas FDG-PET involves radioactive isotopes and is more expensive (Johnson, Fox, Sperling, & Klunk, 2012). Another method to assess biochemistry is post-mortem histology studies, but such studies are very rare thus are not an optimal method of investigation (despite being incredibly informative, e.g. Perkins et al., 2016, Valla et al., 2010, a point which will be further discussed later in this introduction).

In the general introduction Chapter, I hypothesised that alterations in PCC MRS metabolites in *APOE-E4* carriers (compared to non-carriers) might underlie the differences in PCC fMRI activity evident between these groups in Shine et al. (2015). In support of this hypothesis, biochemical alterations have been detected in young *APOE-E4* carriers compared to non-carriers, using FDG-PET (Reiman et al., 2004) and in post-mortem studies of young *APOE-E4* carriers (Perkins et al., 2016; Valla et al., 2010); MRS metabolite alterations also exist in AD, MCI, older *APOE-E4* carriers, as well as pre-symptomatic FAD mutation carriers (e.g. Bai et al., 2014; Fayed, Modrego, Rojas-Salinas, & Aguilar, 2011; Godbolt et al., 2006; K. Kantarci et al., 2000; Kejal Kantarci et al., 2007; Laakso et al., 2003; Walecki, Barcikowska, Ćwikła, & Gabryelewicz, 2011).

Important for my hypothesis, however, is that it is possible for scene-sensitive BOLD-MRS relationships to exist. Chapters 3 and 4 provided novel information that PCC BOLD for just the scene conditions of a perception task and a working memory task (which were the same or similar to the tasks in Shine et al., (2015)) were indeed related to PCC MRS metabolites, thus addressing this missing link in support of my hypothesis. More specifically, a region towards the superior medial surface of the PCC had a positive relationship with PCC tNAA. As tNAA was positively correlated with PCC BOLD during the scene conditions of these two tasks, and *APOE-E4* carriers showed a more positive BOLD response to both scene conditions of these tasks in Shine et al. (2015), then the next question is whether *APOE-E4* carriers have a higher concentration of tNAA which could underlie their higher PCC BOLD response to scenes.

The rationale and approach applied here to link altered fMRI activity (during a task sensitive to behavioural impairments in a disease) with altered MRS biochemistry is similar to that an approach that has been successfully used in schizophrenia research.

First, it was established that schizophrenia patients show behavioural impairment in cognitive control, which is defined as the ability to flexibly switch between different thoughts and actions (Dreisbach, 2012). An example of this is that patients show poorer performance than healthy controls in the Stroop task, which requires the ability to inhibit reading the colour in which a word is printed (Hepp, Maier, Hermle, & Spitzer, 1996). Next, fMRI was used in healthy controls to investigate which brain regions are important for cognitive control. This revealed that the ACC is involved in cognitive control tasks, as evidenced by increased activity in this brain region during conditions of high compared to low cognitive control demands (Falkenberg, Specht, & Westerhausen, 2011). Third, a metabolite that was most likely to be altered in schizophrenia was selected to be studied (glutamate, given the glutamatergic imbalance hypothesis behind schizophrenia pathogenesis (Moghaddam & Javitt, 2012)). Then MRS was used to measure ACC Glx in healthy controls; this was found to be correlated with fMRI activity during an auditory cognitive control task (Falkenberg et al., 2012). Fourth, the researchers then studied schizophrenia patients to investigate whether ACC Glx was different in patients compared to healthy controls (Falkenberg et al., 2014; Reid et al., 2010). Finally, this study assessed whether the Glx-BOLD relationship evident during cognitive control tasks was the same as that found in healthy controls or whether it was altered (Falkenberg et al., 2014). Aligned to this series of studies in schizophrenia, the MRS study in this Chapter represents the fourth step in this series. It aimed to investigate whether the metabolite that has been associated with the BOLD response during scene processing tasks sensitive to impairment in AD, and which shows altered activity in young *APOE*-E4 carriers, is different in *APOE*-E4 participants compared to non-carriers.

5.1.1 tNAA: main metabolite of interest

Given that Chapters 3 and 4 found that there was a category sensitive relationship between PCC tNAA and PCC BOLD for scenes in both the perception and working memory paradigms, whereas there was no such category-sensitive association of Glx or GABA+ with PCC BOLD, tNAA is the main metabolite of interest in this study. As well as this finding, there are further reasons why tNAA is a good candidate to study differences in the PCC between young *APOE*-E4 carriers and non-carriers, although, intriguingly these other reasons do not always support the direction of the tNAA patterns found in Chapters 3 and 4.

First, PCC tNAA is one of the most robust MRS metabolites to be altered in AD. Several studies have detected that AD patients have a lower concentration of tNAA or tNAA/Cr in the PCC compared to age-matched healthy controls. For example, one of the earliest studies to investigate PCC tNAA in AD was by Kantarci et al. (2000), who detected a PCC tNAA reduction in 21 AD patients compared to 67 healthy aged matched controls (mean age 80 years), but no tNAA difference in a brain region known to be affected late in AD (the occipital cortex, which was their control region) (Kantarci et al., 2000). Since then many studies have replicated this finding, and a meta-analysis of 15 studies on PCC tNAA/Cr changes in AD patients calculated the effect size of the tNAA difference in AD to be -1.05 (Hedge's *g* value) (H. Wang et al., 2015). One of the most interesting replications of this finding was by Murray et al. (2014). This study correlated PCC tNAA from an ante-mortem MRS study in AD patients, and correlated this with post-mortem immunohistochemistry markers of synapse density, amyloid and tau pathology. The researchers found a positive correlation between PCC tNAA/Cr with synapse density, and a negative correlation with amyloid pathology (Murray et al., 2014). These results strengthen potential links between PCC tNAA and genesis of AD, and highlight potential mechanisms underpinning the pathobiology of the disease.

Second, a PCC tNAA alteration has been detected prior to diagnosis of AD, thus implicating a PCC tNAA change early in the temporal sequence of brain changes that lead to AD. For example, this has been found in pre-symptomatic familial AD mutation carriers, compared to age matched controls (Godbolt et al., 2006). In these carriers, the magnitude of the PCC tNAA change was positively correlated with the proximity of age-of-onset of AD (i.e. greater tNAA reduction the closer the age of onset). In addition, a reduction in PCC tNAA has been detected in MCI patients compared to healthy age-matched controls, and the magnitude of the decrease in PCC tNAA has been shown to be predictive of conversion to AD (i.e. the greater the PCC tNAA reduction, the more likely a person is to convert from MCI to AD) (Kantarci et al., 2007). These studies suggest that a tNAA change in PCC is an early preclinical metabolic alteration in AD.

Additionally, it has been suggested that PCC tNAA is altered in old *APOE*-E4 carriers compared to non-carriers, which also supports the idea that PCC tNAA may change before the possible onset of AD. Riese et al., (2015) compared PCC metabolites in 9 *APOE*-E4 carriers and 27 non-carriers, and identified a significant decrease in PCC tNAA in the *APOE*-E4 carriers (mean age across both groups was approximately 72 years). A limitation of this study, however, was the small sample size of *APOE*-E4

carriers. This significant decrease in PCC tNAA has not been replicated in three other studies of PCC MRS in old *APOE-E4* carriers which studied tNAA, two of which used larger sample sizes (Gomar et al., 2014; Kantarci et al., 2002; Laakso et al., 2003), although a slight non-significant trend towards this pattern is evident. Thus there is currently not a clear picture of whether PCC tNAA is altered or not in old *APOE-E4* carriers. Within these studies, the youngest participant was aged 50 years, thus an outstanding question is whether a PCC tNAA change may be evidenced earlier in life.

Third, post mortem studies of the PCC in young *APOE-E4* carriers and non-carriers have detected biochemical alterations in *APOE-E4* carriers; these alterations are seen in pathways linked with a hypothesised role of NAA in neuronal mitochondrial function, as discussed in Chapter 2. Valla et al., (2010) found that *APOE-E4* carriers (who had an age range of 18-40 years, mean 34 years) had a lower level of the cytochrome oxidase C enzyme in the PCC compared to non-carriers. This enzyme is an important for aerobic respiration in mitochondria, as it is complex IV of the mitochondrial electron transport chain. Further evidence that mitochondrial energy metabolism may be altered in young *APOE-E4* carriers comes from a follow-up study by Perkins et al., (2016). This study found alterations in protein expression of several enzymes in the electron transport chain (complexes I-V) (Perkins et al., 2016). NAA is linked with mitochondria, as mitochondria are the proposed site of NAA synthesis (T. B. Patel & Clark, 1979), and mitochondrial energy metabolism (measured via ATP level) is coupled with NAA concentration (Maddock & Buonocore, 2012). Additionally, the levels of mitochondrial respiratory chain enzymes have been associated with the level of in NAA, as pharmacological inhibition of these enzymes was associated with a decrease in NAA (Bates et al., 1996). Thus the two post-mortem studies in young *APOE-E4* carriers provide evidence that mitochondrial function is altered in these individuals. This could have an impact on NAA synthesis in mitochondria, therefore resulting in a decreased NAA concentration measured using MRS in the young *APOE-E4* carriers.

The fourth reason for tNAA being our main metabolite of interest is that the *APOE-E4* protein itself has been found to damage neuronal mitochondria. Again, this could impact on NAA synthesis, if NAA is synthesised in mitochondria (T. B. Patel & Clark, 1979). The research indicating that the *APOE-E4* protein may be harmful to neuronal mitochondria comes from several studies from the Huang lab (Huang & Mahley, 2014; Mahley & Huang, 2012). They have identified that the difference in the protein structure of the *APOE-E4* isoform compared to the E3 or E2 isoform gives *APOE-E4* a different

These four reasons raise the possibility that tNAA could be *reduced* in young E4 carriers relative to non-carriers. Notably, however, this is the opposite direction to that predicted based on the results of Chapters 3 and 4, where I found evidence that *higher* PCC tNAA was associated with less PCC deactivation to the scene categories of the perception and working memory tasks. Since the young *APOE-E4* carriers showed reduced PCC deactivation for the scene categories in Shine et al. (2015), I would have expected higher PCC tNAA in these carriers. One theory that could address this discrepancy in these hypotheses is that the *APOE-E4* allele may be an example of antagonistic pleiotropy, in which possession of this allele is beneficial in early life, but detrimental later in life, given its association with AD. These ideas have been proposed to explain BOLD and behavioural findings in young *APOE-E4* carriers (Han & Bondi, 2008; Rusted et al., 2013; Tuminello & Han, 2011), therefore, it could be the case that the concentration of tNAA may also demonstrate this pattern.

To my knowledge, only one study to date has performed MRS in *APOE-E4* carriers and non-carriers below the age of 50 years. This study investigated individuals who had a mean age of 13.5 years, and were living in a region of high air pollution in Mexico city (Calderon-Garciduenas et al., 2015). These participants were selected as this research group have claimed that air pollution is an environmental factor that could contribute to AD development (Calderon-Garciduenas et al., 2012). Their MRS acquisition did not actually test the PCC, but instead tested nearby parietal white matter, with a voxel placed in each hemisphere, along with five other voxels of interest (right and left hippocampi, right and left prefrontal cortex, and pons). The paper claims that in the left parietal white matter there was a decrease in tNAA/mI (i.e. when tNAA is calculated as a ratio with myo-inositol (mI)) in the young *APOE-E4* carriers. Upon closer inspection of the methods and results of this paper, however, this finding is unconvincing (with their pairwise test between parietal tNAA/mI in the *APOE-E4* carriers and non-carriers significant at a p value of $p=0.057$). Not only is this non-significant based on the standard alpha level of $p=0.05$, the authors did not take account the multiple tests across seven brain regions, requiring correction for multiple comparisons.

A further limitation reducing confidence in their findings, which this Chapter aims to improve on, is a difference in the participants in the two *APOE*-groups. Although participants were well matched for age, they do not appear to be homogeneous on cognitive performance. The *APOE-E4* group show significantly lower performance on several of the tests in the Wechsler Intelligence Scale for Children-Revised (WISC-R)

cognitive battery (Wechsler, 1974), including verbal IQ, full scale IQ, digit span, and arithmetic. Since there is debate in the literature as to whether MRS is correlated with IQ and fluid intelligence (Jung et al., 1999, 2005; Nikolaidis et al., 2016; T. Patel et al., 2014; Paul et al., 2016), the differences in performance on the WISC-R battery could be related to the potential differences in MRS identified. In contrast, the participants tested in the present Chapter are a homogenous population: all undergraduate students on the same university course. By measuring MRS in a homogenous sample, we are better placed to isolate any potential effect of the *APOE*-E4 allele on PCC MRS.

An additional improvement on the methods in Calderon-Garciduenas et al. (2015) is the use of a 3T scanner here (compared to the 1.5T in Calderon-Garciduenas et al.). A higher strength magnetic field enables higher signal-to-noise when performing MRS, and results in more accurate metabolite quantification (Stagg & Rothman, 2014). Therefore, the MRS methods used in this Chapter should enable a more sensitive measure of MRS metabolites.

5.1.2 Additional metabolites of interest

In addition to tNAA, two other metabolites not yet studied in this thesis are of interest. These are mI, a marker of inflammation and gliosis, and Cr, a marker of energy metabolism and commonly used as an internal reference metabolite (Rae, 2014; Stagg & Rothman, 2014). These were not studied in Chapters 3 and 4 because no study had linked mI or Cr to BOLD, thus I focused on tNAA, Glx and GABA associations with BOLD. There is, however, a rationale for why these additional metabolites may be altered in young *APOE*-E4 carriers which is why they will be additionally assessed in this Chapter.

5.1.2.1 Myo-inositol

PCC mI has consistently been found to be altered in AD and MCI patients, with both patient groups showing an increase in mI or mI/Cr relative to controls (Kantarci et al., 2000; Voevodskaya & Sundgren, 2016). The meta-analysis mentioned above calculated the effect size of the increase in mI/Cr in AD to be 0.85 (H. Wang et al., 2015). Moreover, mI has been proposed to be the first metabolite to be altered in the PCC (Kantarci et al.,

2000; Voevodskaya & Sundgren, 2016). In support of this view, a comparison of PCC metabolites between AD patients, MCI patients and healthy controls identified a significant decrease in PCC tNAA/Cr and a significant increase in PCC mI/Cr between AD patients and controls, and a significant increase in PCC mI/Cr between MCI patients and controls, but no difference in PCC tNAA (Kantarci et al., 2000). Thus a PCC mI change may precede a PCC tNAA change.

Further evidence in support of the idea that PCC mI changes before tNAA comes from a large study comparing PCC metabolites in four groups of participants: cognitively healthy participants with normal CSF amyloid, cognitively healthy participants with abnormal CSF amyloid, participants with subjective cognitive decline and abnormal CSF amyloid but no diagnosis of MCI, and MCI patients with abnormal CSF amyloid. Abnormal CSF amyloid was assessed in this study via a decrease in A β 42, as this can be detected 10-20 years before the onset of AD (Bateman et al., 2012; Buchhave et al., 2012). The mean age of participants across the four groups was in the early 70s, and the age range was 60-80 years. Similar to the study by Kantarci et al. (2002), this study found a significant increase in PCC mI/Cr from the cognitively healthy amyloid normal to cognitively healthy amyloid abnormal groups, and a trend towards a decrease in PCC tNAA between these two groups, but this was non-significant (Voevodskaya & Sundgren, 2016) (see Figure 5.2 A and B).

Of particular interest to this Chapter, this study also split each group into *APOE*-E4 carriers and non-carriers, and found that *APOE*-E4 carriers in the cognitively healthy amyloid normal group had a higher concentration of PCC mI/Cr (see Figure 5.2 C) (Voevodskaya & Sundgren, 2016). Similarly, Gomar et al. (2013) detected a significant elevation in PCC mI in older healthy *APOE*-E4 carriers compared to non-carriers aged 50-86 years (Gomar et al., 2014). Applying these findings to the young *APOE*-E4 carriers and non-carriers in this Chapter, we might expect that young *APOE*-E4 carriers may have a higher PCC mI than the non-carriers.

A finding of higher PCC mI in older *APOE*-E4 carriers has not always been detected, however. Kantarci et al. (2002) and Laakso et al. (2003) did not find a significant difference in PCC mI between old cognitively healthy *APOE*-E4 carriers and non-carriers (mean age for the Kantarci et al. (2002) and Laakso et al. (2003) studies were 80 and 77 years respectively). These two studies may not have found an effect of *APOE*-genotype on PCC mI due to the use of older participants than in the studies by Voevodskaya et al.

(2016) and Gomar et al. (2013). Gomar et al. (2013) found, however, a near significant interaction of age and *APOE*-genotype on PCC mI ($p=0.06$), and a significant effect of age on PCC mI. If age is significantly associated with PCC mI, as suggested by Gomar et al. (2013), then the *APOE*-E4 non-carriers control group may also have shown an increase in PCC mI, diluting any difference between *APOE*-E4 carriers and non-carriers. Taken together, as for tNAA, there is not yet a clear picture for whether an mI change may exist in young *APOE*-E4 carriers, a gap in our research understanding that this Chapter will aim to address.

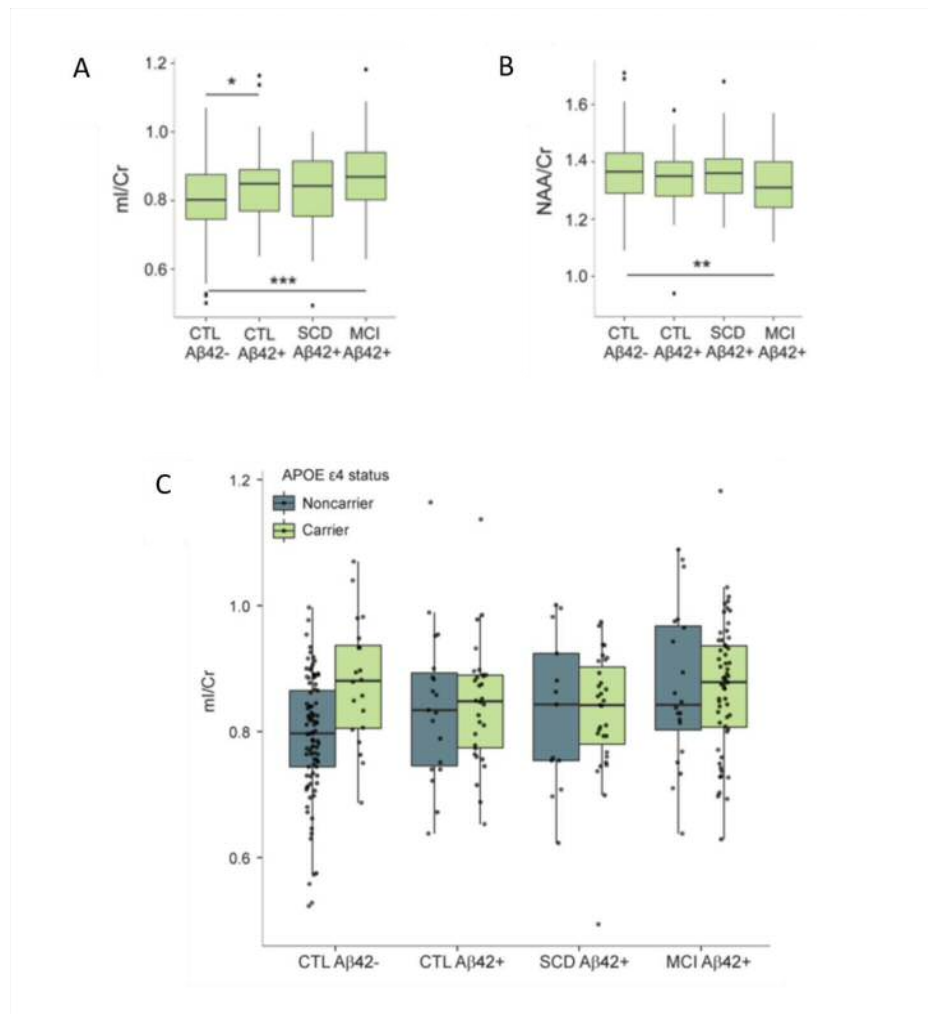


Figure 5.2: Results from the PCC MRS study by Voevodskaya et al. (2016). (A) The ratio of mI to Cr in the PCC of four participant groups: cognitively healthy participants with normal CSF amyloid (CTL Aβ42-), cognitively healthy participants with abnormal CSF amyloid (CTL Aβ42+), participants with subjective cognitive decline and abnormal CSF amyloid but no diagnosis of MCI (SCD Aβ42+), and MCI patients with abnormal CSF amyloid (MCI Aβ42+). (B) The ratio of PCC NAA to Cr in the four groups. (C) The ratio of PCC mI to Cr in the four groups, where each group has been split into *APOE*-E4 carriers and non-carriers. (Images taken from Voevodskaya et al., 2016).

A further rationale for quantifying PCC mI is to enable the ratio of tNAA/mI to be calculated. This ratio may be more sensitive than measuring early alterations in tNAA and mI separately in the MCI and pre-symptomatic phases of AD. For example, Godbolt et al. (2006) compared PCC metabolites between pre-symptomatic FAD mutation carriers and non-carriers, and detected an 18% difference in tNAA/Cr, a 19% (but non-significant at $p=0.07$) difference in mI/Cr, but a 25% difference when the metabolite ratio tNAA/mI was used. Similarly, in an MRS study of healthy controls, MCI and AD patients, the ability to discriminate between controls and patients was much higher for the tNAA/mI ratio (achieved a discriminating potential value of 2.72) compared to tNAA/Cr alone (1.50) or mI/Cr alone (0.58) (T. Wang et al., 2012). Therefore, in this Chapter, quantifying the tNAA/mI ratio may detect an alteration between groups that could not have been detected by measuring each metabolite separately.

5.1.2.2 Creatine

Throughout the discussion above regarding metabolite changes in AD, MCI and older *APOE-E4* carriers, some metabolites have been measured using water as a reference, while others have Cr as a ratio. It is not clear which of the two approaches are best when studying metabolite changes in a disease or disease risk group. This is because the metabolite Cr itself may be altered in the disease. This has been cautioned against (Rae, 2014; Stagg & Rothman, 2014), yet is still common practice in the MRS literature. The problem of using Cr as a ratio denominator is demonstrated in a recent MRS AD paper, which identified a different pattern of metabolite differences when metabolites were used in a ratio to water or to Cr: for example there was a significant difference in PCC tNAA between AD patients and healthy controls (a pattern consistent with several other studies), whereas there was no significant difference in tNAA/Cr difference between groups. This implies that Cr may be altered in the disease, but as Cr on its own was not measured in this study it is not possible to determine this based on the study's results (Fayed et al., 2011).

The approach taken in the previous experimental Chapters of this thesis was to use water rather than Cr as the reference, since there may be a change in Cr in old *APOE-E4* carriers. This pattern was identified in the MRS study by Laakso et al (2003), who found a significant decrease in PCC Cr in old E4 carriers compared to non-carriers. Other

studies of old *APOE*-E4 carriers compared to non-carriers have not replicated this since they have not assessed Cr on its own. Instead they have used Cr as the denominator in metabolite ratios (Gomar et al., 2014; Kejal Kantarci et al., 2002; Voevodskaya & Sundgren, 2016). If Cr is altered between *APOE*-groups, however, this would impact on these metabolite ratio findings. In order to address the issue of whether there may be a difference in PCC Cr in the young *APOE*-E4 carriers, which would impact on whether a ratio to Cr is a good strategy or not in future MRS studies of young *APOE*-E4 carriers, this Chapter has compared Cr as a ratio with water between the young *APOE*-E4 carrier and non-carrier groups.

5.1.2.3 GABA+ and Glx

Although Chapters 3 and 4 did not find any relationships between PCC BOLD for scenes and PCC GABA+ or Glx, this may not necessarily mean that there are no differences in these metabolites in young *APOE*-E4 carriers compared to non-carriers; instead it could be the case that there are differences in GABA+ and Glx, but they are not related to PCC BOLD. As discussed above, PCC tNAA is the main metabolite of interest for this study, but for completeness PCC GABA+ and Glx were also assessed as a further exploration of any other biochemical changes that may not be related to the altered BOLD.

The rationale for still being interested in PCC GABA+ and Glx in young *APOE*-E4 carriers is that both GABA+ and Glx are altered in AD patients. Bai et al (2014) detected significantly lower GABA+/Cr in the PCC of 15 AD patients compared to 15 age-matched controls (mean age 66 years). Fayed et al (2011) detected significantly lower Glx and Glx/Cr in the PCC of 30 AD patients compared with 28 controls (mean age of the two groups was 78 and 70 years).

These changes have been suggested to occur before the onset of AD, thus implicating them in the early brain changes associated with transition to AD, as the same pattern of a decrease in both metabolites has also been detected in MCI patients. Riese et al. (2015) identified a decrease in PCC Glx and GABA+ in 15 MCI patients compared to 21 controls (mean age 72 years), when GABA and Glx were referenced to water. Furthermore, the participants in this study were also divided into groups by *APOE*-genotype, consisting of 9 *APOE*-E4 carriers and 27 non-carriers. The *APOE*-E4 carriers

showed a trend towards a lower concentration of PCC GABA+, although this was non-significant, likely due to the small sample size (Riese et al., 2015). This finding requires replicating in a larger sample size. No other study has yet assessed GABA+ or Glx in the PCC in MCI or in young *APOE-E4* carriers and non-carriers, thus by testing PCC GABA+ and Glx in young *APOE-E4* carriers and non-carriers in this Chapter, this would address the gap in the literature to assess these metabolites below the ages tested in this small number of papers.

5.1.3 Analysis strategy and hypotheses

To investigate whether there are differences in PCC metabolites in young *APOE-E4* carriers and non-carriers, the metabolites tNAA, mI, Cr and Glx were quantified using a PRESS scan, and GABA+ was quantified using a MEGA-PRESS scan. The PCC voxel placement was consistent with that used in Chapters 3 and 4. These metabolites were also obtained in the OCC MRS voxel as in Chapter 3 and 4. In these previous Chapters OCC MRS had been used to assess regional sensitivity of PCC BOLD-PCC MRS relationships. In this present Chapter OCC metabolites have been used to assess the regional sensitivity of any metabolite differences that may exist in the PCC between *APOE*-groups. To be able to conclude that a metabolite difference between *APOE*-group is specific to our PCC voxel of interest, there should be no difference in the concentration of that metabolite in our OCC control region.

The OCC was selected as the control voxel, as this region of sensory cortex is thought to be spared from AD pathology until late in the disease, whereas the PCC is a cortical region affected early in AD pathogenesis (Braak & Braak, 1991, 1995). This is a similar strategy to that implemented in Kantarci et al. (2000), who tested MRS in AD and MCI patients in two brain regions proposed to be affected early in AD, the PCC and superior temporal sulcus, and in a third brain region, the occipital cortex (their control region).

The analyses in this Chapter compare PCC metabolites and OCC metabolites between *APOE*-groups. PCC and OCC metabolites within groups will not be compared, as the question of interest in this Chapter is whether there is a difference between *APOE-E4* carriers and non-carriers in PCC metabolites, rather than asking whether PCC and OCC

metabolites are different to each other. Instead this would inform us about regional differences in MRS, which was not the purpose of this Chapter.

Regarding my hypotheses, the findings from Chapters 3 and 4, where I found an association between higher PCC tNAA and reduced PCC deactivation, implies that young *APOE-E4* carriers may have a higher concentration of PCC tNAA than non-carriers, given that Shine et al. (2015) found they have less PCC deactivation to scene perception and scene working memory. However, based on the tNAA findings in AD, MCI and old *APOE-E4* carriers, and evidence of altered mitochondrial function in the PCC in post-mortem studies of young *APOE-E4* carriers, young *APOE-E4* carriers could have lower PCC tNAA than the non-carriers. In order to address this bi-directional hypothesis, two-tailed independent samples t-tests have been applied.

For the additional metabolites tested, I hypothesised the young *APOE-E4* carriers would have a higher concentration of PCC mI than the non-carriers, based on the findings of increased mI in old *APOE-E4* carriers and in MCI. I also hypothesised that the *APOE-E4* carriers would have a lower tNAA/mI ratio than the non-carriers. Based on the findings of lower Cr in old *APOE-E4* carriers by Laakso et al. (2003), I predicted a lower concentration of PCC Cr in the young *APOE-E4* carriers. Finally based on the findings of a decrease in PCC Glx and GABA+ in AD and MCI, I predicted a decrease in PCC Glx and GABA+ in the young *APOE-E4* carriers. These predictions follow the findings evident in older *APOE-E4* participants, however, it may be the case that metabolite differences in young *APOE-E4* carriers may be in the opposite direction, following the theory of antagonistic pleiotropy, as discussed above for tNAA. Therefore, again, two tailed t-tests have been applied to take account of these possible bidirectional hypotheses.

5.2 Methods

5.2.1 Participants

Participants were undergraduate students from the Psychology department of Cardiff University. Nineteen participants were recruited from the thirty participants who took part in the fMRI study by Shine et al. (2015); this group comprised 10 *APOE*-E4 carriers and 9 non-carriers, with one male in each group (reflecting the predominantly female undergraduate Psychology cohort). These participants were originally recruited from a sample of 125 participants who had provided a saliva sample for DNA extraction and *APOE*-genotyping (details provided in section 5.2.2). To augment this sample of participants, thereby meeting the sample sizes of other MRS studies, a further 229 participants were recruited for studies aiming to look at *APOE*, including this one. Examples of sample sizes in other MRS studies include studies of schizophrenia patients vs controls, in which sample sizes were 17 patients vs 17 healthy controls (Falkenberg et al., 2014) and 28 patients vs 28 controls (Hutcheson et al., 2012); in studies of participants at genetic risk of schizophrenia, sample sizes were 22 risk participants vs 22 controls (Yoo et al., 2009) and 23 risk participants vs 24 controls (Tandon et al., 2013); and in the recent *APOE*-MRS paper the sample size was 22 *APOE*-E4 carriers vs 28 non-carriers (Calderon-Garciduenas et al., 2015). The recruitment of the further 229 participants was based on the estimate that 1 in 5 people carry at least one E4 allele (Farrer et al., 1997), and allowed for dropout of participants (e.g. due to MRI contraindications or not meeting other inclusion criteria). From this cohort of 229 participants, 28 participants took part in MRS scanning, with a genotype split of 10 *APOE*-E4 carriers and 18 non-carriers. In total, therefore, 20 *APOE*-E4 carriers and 27 non-carriers were used in this study.

Participants were matched for age, family history of dementia, and family history of psychiatric illness. Participants were excluded if they had a self-reported history of depression or psychiatric illness, or were taking any psychoactive medication. All participants were right-handed, with normal or corrected-to-normal vision.

A double-blind strategy was adopted for this study, whereby both participants and researchers collecting and analysing data were blind to the participants' *APOE*-genotypes, in order to prevent any bias during analyses. All procedures were approved

by Cardiff University School of Psychology Ethics committee. Participants gave written informed consent before taking part.

5.2.2 DNA extraction and genotyping

Procedures for DNA extraction from saliva and *APOE* genotyping were the same for the first cohort of 125 participants and the second cohort of 229 participants. DNA was obtained from saliva using Oragene OG-500 saliva kits (DNA Genotek, Inc., Ontario, Canada). DNA extraction and *APOE*-genotyping were performed in the Centre for Neuropsychiatric Genetics and Genomics at Cardiff University. Since *APOE* isoforms differ due to a single nucleotide polymorphism (SNP) at two sites in the gene, a single SNP genotyping assay was performed for each site to determine *APOE* genotype. The SNP rs429358 was determined by KASP genotyping and rs7412 by Taqman genotyping (Butchart et al., 2015, Ide et al., 2016). These were detected on Tecan infinite F200 pro and StepOnePlus™ Real-Time PCR System platforms, respectively. Haplotypes corresponding to *APOE* E2, E3 and E4 were then deduced.

Genotyping was successful in 100/125 participants from the first cohort and 224/229 participants from the second cohort. The distribution of genotypes of those successfully genotyped in the first cohort was E2/E2 (1/100, 1%), E2/E3 (10/100, 10%), E2/E4 (1/100, 1%), E3/E3 (69/100, 69%), E3/E4 (19/100, 19%), and E4/E4 (0/100, 0%). The genotype distribution in the second cohort was E2/E2 (0/224, 0%), E2/E3 (38/224, 17%), E2/E4 (7/224, 3%), E3/E3 (125/224, 56%), E3/E4 (52/224, 23%), and E4/E4 (2/224, 1%).

5.2.3 Scanning procedure and data analysis

Participants took part in two scanning sessions. Female participants took part in the MRS scan session during the luteal phase of their menstrual cycle (consistent with Chapters 3 and 4), thereby preventing menstrual cycle phase having any influence on metabolites across the two *APOE* groups. The relevant scans for this Chapter were a

structural scan, PCC PRESS scan, PCC MEGA-PRESS scan, OCC PRESS scan and OCC-MEGA-PRESS scan. The scan parameters, MRS voxel placement, analysis for the structural and MRS scans, and correction of MRS metabolites for the fraction of GM, WM and CSF were identical to that used in Chapters 3 and 4. The only differences were that in this Chapter two additional metabolites were quantified, which were ml and Cr, and the ratio of tNAA/ml was also calculated, by dividing the tNAA concentration by the ml concentration.

5.2.4 Statistics

MRS data from the two *APOE* groups were compared using an independent samples t-test for each metabolite in each brain region. Since a comparison of a total of six metabolites or metabolite ratios were performed, correction for multiple comparisons was required to prevent type I error due to the inflation of the alpha value with the multiple tests. As in previous Chapters, Bonferroni correction here would be too strict and increase the likelihood of type II errors, and is not a recommended correction when performing a large number of tests as it would make the alpha level far too conservative (Streiner, 2015). A similar multiple corrections strategy to Chapters 3 and 4 was applied here, therefore, which was a trade-off between no correction and the overly stringent Bonferroni correction. Several MRS studies have taken the approach of no corrections for multiple comparisons, thus this trade-off was an improvement on these methods (Calderon-Garciduenas et al., 2015; Emir, Tuite, & Öz, 2012; Tandon et al., 2013; Yoo et al., 2009). The approach used in this Chapter was a family-wise correction, where a family was considered as one metabolite. Each metabolite was measured in two regions, the PCC and OCC voxels, therefore the alpha value was divided by 2. Thus a difference in a metabolite in one of the regions of interest would be significant at $p < 0.025$.

Data were examined for a normal distribution and homogeneity of variance. Where data did not meet this assumption of homogeneity of variance (via Levene's test), the corrected values were used (and is indicated in the results). Where any data point looked far from the mean, these were not treated as outliers. This is because possession of the *APOE-E4* allele does not necessarily mean someone will develop AD, and, vice

versa, lack of the *APOE*-E4 allele does not mean that someone will not develop AD. Thus any extreme points could be informative with respect to inter-individual variance enabling investigation of why such individuals might be extreme outliers.

5.3 Results

5.3.1 Participants

Table 5.1 shows the genotype split and mean age of each group. An independent samples t-test confirmed no difference in age between the *APOE*-E4 carriers and non-carriers, $t(44)=1.14$, $p=0.26$.

	<i>APOE</i> -E4 carriers	<i>APOE</i> -E4 non-carriers
Total n who took part in MRS scanning	20	27
Genotypes	18 E3/E4 1 E2/E4 1E4/E4	24 E3/E3 3 E2/E3
Mean age \pm st dev	21.15 (\pm 1.87)	20.54 (\pm 1.75)
Age range	18.81-25.36	18.58-25.02
Females/Males	19/1	26/1

Table 5.1: Demographic information about the groups of *APOE*-E4 carriers and non-carriers.

5.3.2 Data exclusions

Using the same MRS data quality criteria used in Chapters 3 and 4, data were excluded for a total of 7 PCC PRESS and 6 MEGA-PRESS metabolites for the *APOE*-E4 carriers, 15 PCC PRESS and 8 MEGA-PRESS metabolites for the *APOE*-E4 carriers, 8 OCC PRESS and 1 MEGA-PRESS metabolites for the *APOE*-E4 carriers, and no OCC PRESS or MEGA-PRESS metabolites for the *APOE*-E4 non-carriers (see Table 5.2 for sample size of each metabolite remaining after data quality control).

MRS Voxel	Metabolite or metabolite ratio	N remaining from original sample sizes	
		<i>APOE</i> -E4 carriers (original sample size=20)	<i>APOE</i> -E4 non-carriers (original sample size=27)
PCC (voxel of interest)	tNAA	19	25
	Glx	19	25
	GABA+	14	19
	mI	16	17
	tNAA/mI	16	17
	Cr	19	26
OCC (control voxel)	tNAA	19	27
	Glx	18	27
	GABA+	19	27
	mI	16	27
	tNAA/mI	16	27
	Cr	19	27

Table 5.2: The sample size remaining for each metabolite in the two *APOE*-groups following MRS data quality control assessments.

5.3.3 MRS Results

Figure 5.3 shows representative examples of MRS spectra from each *APOE* group. Table 5.3 displays the mean concentrations of metabolites in the PCC and OCC voxels for each *APOE* group. Figure 5.4 shows the individual differences in each metabolite measure for each group in the PCC voxel and Figure 5.5 shows this in the OCC voxel.

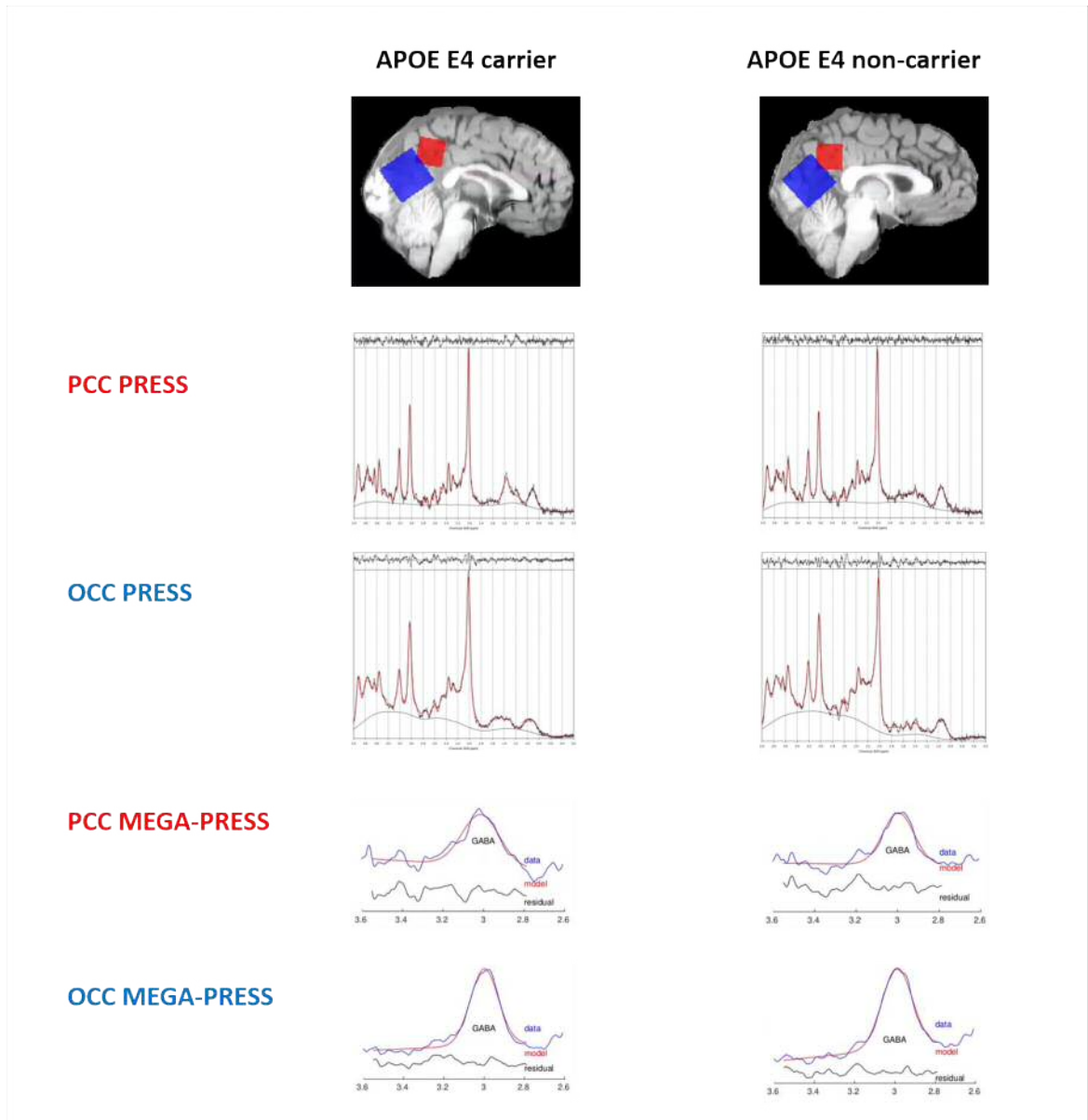


Figure 5.3: Examples of MRS voxel placement, and each type of MRS spectra in each voxel from one participant from each *APOE* group. Red indicates the PCC voxel and blue the OCC voxel.

The main metabolite of interest to compare between E4 carriers and non-carriers was tNAA. Independent samples t-tests revealed that there was no significant difference between tNAA in the PCC voxel (or in the OCC control voxel) between *APOE* groups (see Table 5.3, Figure 5.2A and Figure 5.3A). There were also no significant differences in Glx, GABA+, ml, Cr or the metabolite ratio of tNAA/ml between groups in either MRS voxel (all $p > 0.20$) (see Table 5.3).

To rule out any effect of grey matter fraction and voxel placement on the metabolite concentrations between the two *APOE* groups, these were also compared. There was no difference in PCC voxel grey matter fraction, $t(44) = -1.35$, $p = 0.18$, nor in OCC voxel grey matter fraction, $t(44) = -1.41$, $p = 0.17$ between groups. There was no difference in the percentage of overlap between the PCC voxel and the PCC fMRI ROI from Shine et al. (2015), $t(44) = -1.14$, $p = 0.26$.

MRS voxel	MRS metabolite or ratio	<i>APOE</i> -E4 carriers	<i>APOE</i> -E4 non-carriers
PCC (voxel of interest)	tNAA	15.79 (± 1.41)	16.31 (± 2.38)
	Glx	20.86 (± 3.57)	21.21 (± 3.75)
	GABA+	2.07 (± 0.47)	2.21 (± 0.87)
	ml	6.66 (± 0.93)	7.05 (± 2.03)
	tNAA/ml	2.44 (± 0.43)	2.40 (± 0.40)
	Cr	11.82 (± 1.09)	11.83 (± 1.45)
OCC (control voxel)	tNAA	13.07 (± 2.60)	13.73 (± 1.51)
	Glx	21.01 (± 4.03)	20.59 (± 4.52)
	GABA+	1.91 (± 0.15)	1.96 (± 0.24)
	ml	6.27 (± 0.77)	6.27 (± 0.56)
	tNAA/ml	2.09 (± 0.42)	2.20 (± 0.21)
	Cr	10.80 (± 0.85)	11.09 (± 1.20)

Table 5.3: Mean metabolite concentrations in each MRS voxel for each *APOE* group, in mM. Values in brackets are standard deviations.

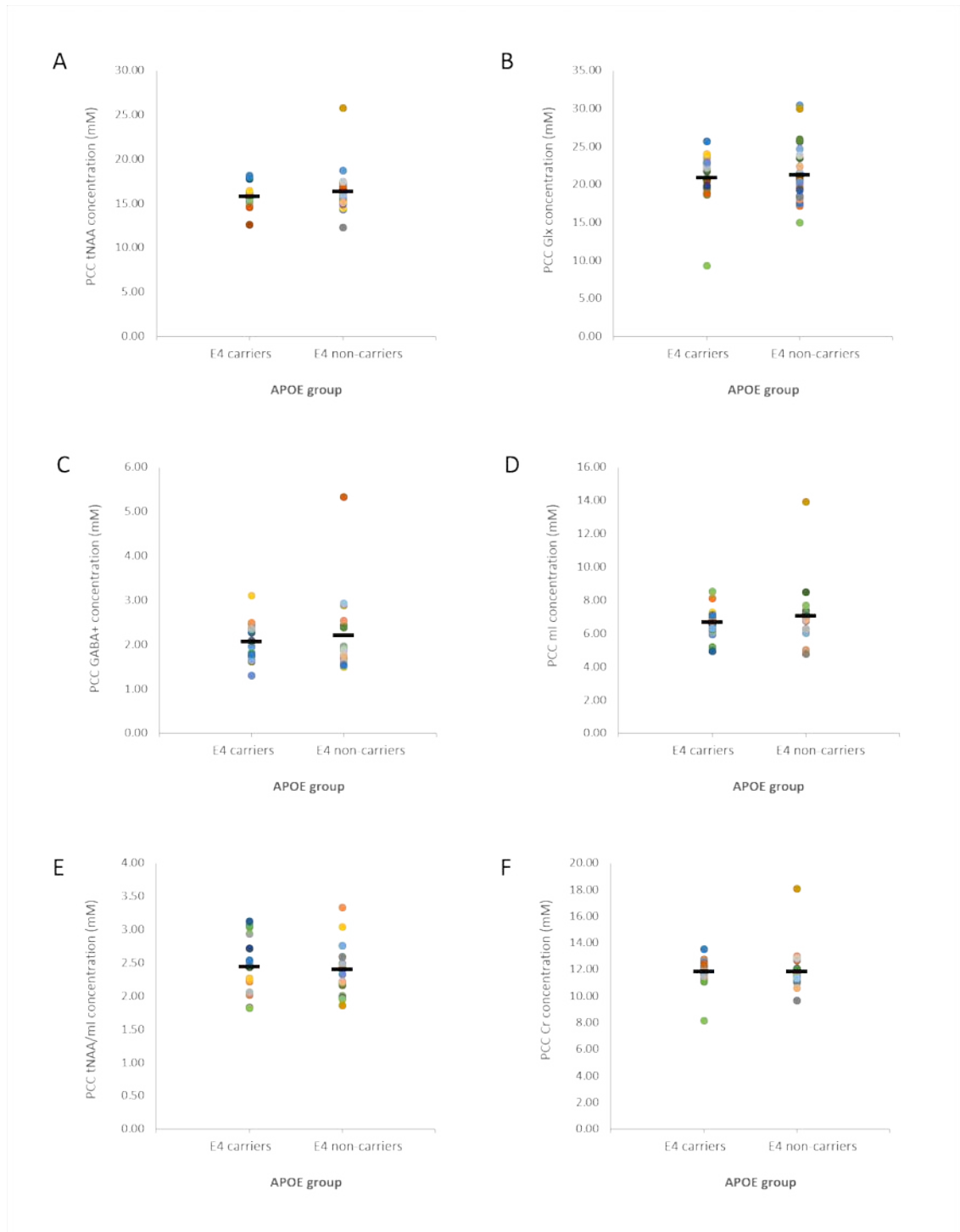


Figure 5.4: Comparison of PCC metabolites between *APOE*-E4 carriers and non-carriers. Values are in mM. The black horizontal bars are the mean concentration in each group, and each dot is an individual participant's metabolite concentration.

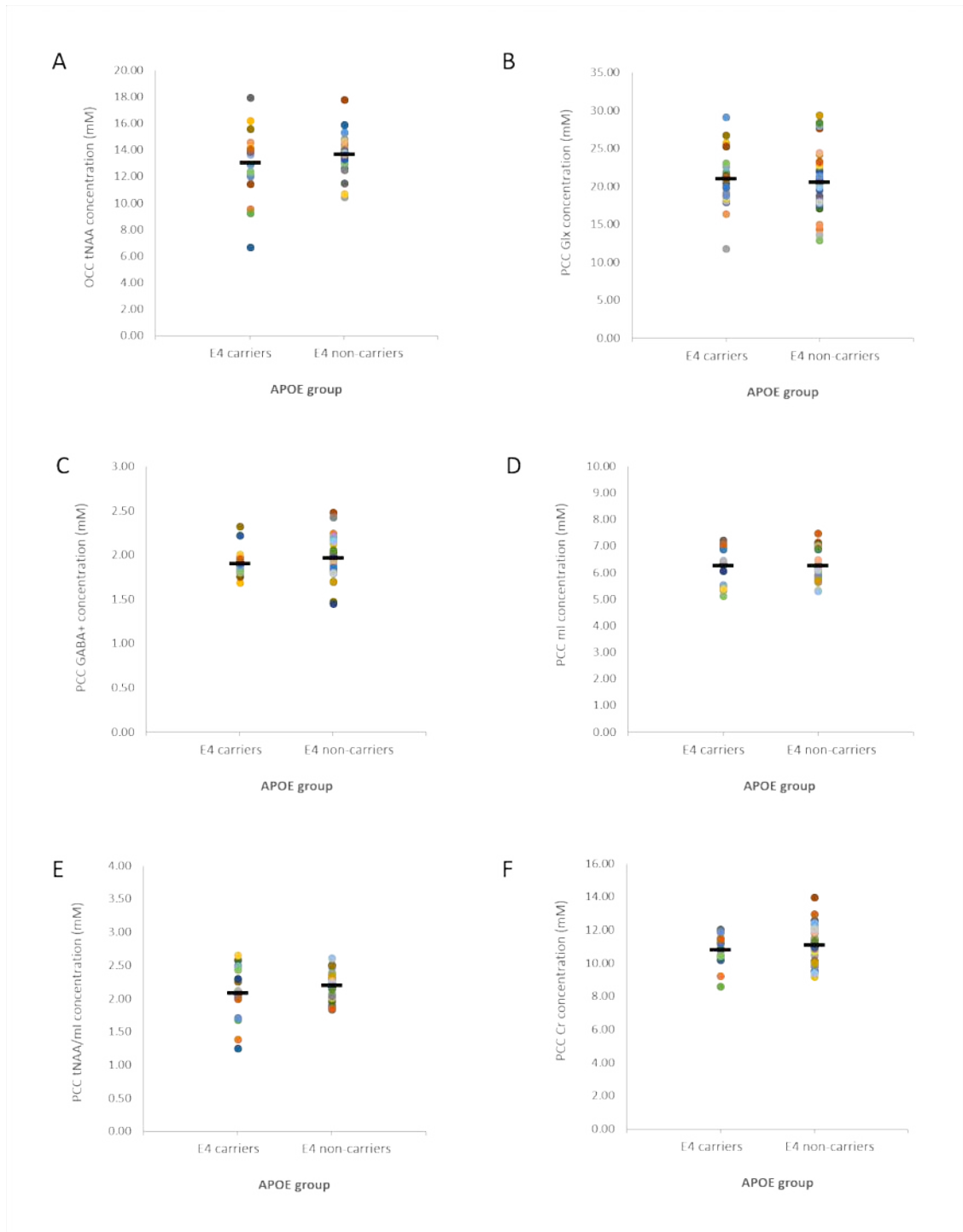


Figure 5.5: Comparison of metabolites in the OCC control voxel between APOE-E4 carriers and non-carriers. Values are in mM. The black horizontal bars are the mean concentration in each group, and each dot is an individual participant's metabolite concentration.

MRS voxel	MRS metabolite or ratio	Independent samples t-test		Effect size (Cohen's d)	Bayes (BF ₀₁)
		t	p		
PCC (voxel of interest)	tNAA	-0.85	0.40	-0.23	2.49
	Glx	-0.32	0.75	-0.10	3.22
	GABA+	-0.53	0.60	-0.19	2.68
	mI	-0.70	0.49	-0.24	2.49
	tNAA/mI	0.31	0.76	0.11	2.90
	Cr	-0.03	0.97	-0.01	3.36
OCC (control voxel)	tNAA	-0.99 (L)	0.33 (L)	-0.33	2.09
	Glx	0.32	0.75	0.10	3.24
	GABA+	-0.88	0.38	-0.26	2.47
	mI	0.00 (L)	1.00 (L)	0.001	3.24
	tNAA/mI	-0.96 (L)	0.35 (L)	-0.35	1.98
	Cr	-0.93	0.36	-0.28	2.39

Table 5.4: Comparison of MRS metabolites between APOE groups. A positive t-statistic and effect size indicate that APOE-E4 carriers have higher concentration of metabolite than non-carriers, and a negative t-statistic and effect size indicates E4 carriers have a lower level of that metabolite. Where samples did not show homogeneity of variance, as determined via Levene's test for equality of variance, this is indicated by (L), and the values that have been corrected for this have been used. Values are family-wise corrected, where a family is each metabolite in the two MRS voxels (i.e. PCC tNAA and OCC tNAA would be a family of 2, so p is significant at less than $0.05/2 = 0.025$). Bayes factors represent the strength of the evidence that there are no differences between groups.

5.4 Discussion

This Chapter investigated whether there were any differences in PCC biochemistry between young APOE-E4 carriers and non-carriers measured using MRS, which could underlie the BOLD alterations detected in the PCC of young APOE-E4 carriers in Shine et al. (2015). Building on the findings of Chapters 3 and 4, the main metabolite of interest was PCC tNAA. Additional metabolites tested were mI, Cr, GABA+ and Glx, and the ratio

tNAA/ml. This study found no differences in any of the PCC MRS metabolites, nor in the OCC control voxel, between *APOE*-E4 carriers and non-carriers aged 18-25 years old.

The finding of no PCC metabolite differences, indeed the strikingly similar distribution of all metabolites across the two groups, suggests that age 18-25 years may be too early to find any differences in MRS metabolites in individuals at increased risk of AD, as measured by *APOE*-E4 possession. For PCC tNAA, this is consistent with the finding of Calderon-Garciduenas et al. (2015) who detected no significant difference in tNAA/Cr or tNAA/ml in left or right parietal white matter between *APOE*-E4 carriers and non-carriers who had a mean age 9 years younger than those tested in this Chapter. The lack of difference in tNAA between groups, however, does not follow the pattern predicted from the work in Chapters 3 and 4. Based on these Chapters, which identified that a higher concentration of PCC tNAA was associated with reduced PCC deactivation during two paradigms to which the *APOE*-E4 carriers showed less strong PCC deactivation than the non-carriers (Shine et al., 2015), I had predicted that the young *APOE*-E4 carriers would have higher concentration of PCC tNAA than the non-carriers.

Linking to the various hypotheses regarding what the biological function of NAA may be, a lack of difference in tNAA between the young *APOE*-E4 carriers and non-carriers could suggest there are no differences in neuronal density, synapse density or mitochondrial function between groups at this young age (Murray et al., 2014; T. B. Patel & Clark, 1979; Rae, 2014; Stagg & Rothman, 2014). The introduction to this Chapter focused on the hypothesis that NAA is associated with mitochondrial metabolism, given the potential association between *APOE*-E4 and mitochondrial function. As outlined in the introduction, mitochondrial metabolism alterations have been detected in the PCC of young *APOE*-E4 carriers (Perkins et al., 2016; Valla et al., 2010) and a mechanism linking the *APOE*-E4 protein with mitochondrial dysfunction has been proposed (Huang, 2011; Mahley & Huang, 2012; Nakamura et al., 2009). The finding of no difference in tNAA concentration between *APOE* groups in this study could suggest that at age 18-25 years the *APOE*-E4 protein is not yet detrimental to mitochondria. This could be attributed to the proposal that the *APOE* protein is only synthesised by neurons following an insult or injury, for example, hypoxia (lack of oxygen), reactive oxygen species, or traumatic brain injury (Mahley & Huang, 2012). Under normal circumstances, the *APOE* protein is instead synthesised by astrocytes (Xu, 2006). Thus the MRS finding in this Chapter could imply that perhaps at ages 18-25 years there has not yet been a sufficient level of injury or insult, so the *APOE* protein is not being synthesised in neurons. Therefore, the toxic

fragments of *APOE*-E4 are not being produced in the neurons of the *APOE*-E4 carriers, so the mitochondria are not being damaged at this age, which may be why there is no differences in tNAA between groups. Studying tNAA in the PCC in an older cohort may reveal differences, as at a later age injury may have occurred, leading to neurons synthesising *APOE*. This temporal order of an immune response leading to neuronal alterations would be consistent with the findings in MCI and old *APOE*-E4 carriers that an mI change appears to precede a tNAA change in the PCC (Kantarci et al., 2000; Voevodskaya & Sundgren, 2016).

Consistent with the hypothesis that NAA is associated with mitochondrial function, one inference from this Chapter could be that tNAA may not be a very sensitive marker of mitochondrial energy metabolism. This is because the post-mortem studies by Valla et al. (2010) and Perkins et al. (2016) did find evidence of altered mitochondrial function, and an FDG-PET study found a lower level of glucose metabolism in this region in young *APOE*-E4 carriers (Reiman et al., 2004), whereas this MRS study did not find any difference in PCC tNAA between *APOE* groups. Having said this, although the minimum age of participants in these three studies was the same as that of the participants scanned for this Chapter, the mean age of participants in these three other studies was approximately 10 years older than the sample tested in this study (Reiman et al. (2004): age range 18-39, mean age 31 years; Valla et al. (2010) and Perkins et al. (2016): age range 18-40, mean age 34 years). Thus perhaps there were mitochondrial energy metabolism differences in participants aged 25-40 years in these other studies, but not in the participants aged 18-25 years, which would be consistent with the finding of no difference in tNAA concentration between the *APOE* groups in this Chapter. Thus, again, by repeating this MRS study in older *APOE*-E4 carriers and non-carriers, ideally around age 40, it would determine whether the mitochondrial alterations detected up to age 40 in Valla et al (2001), Perkins et al (2016) and Reiman et al (2004) can indeed be detected using MRS.

Turning to the additional metabolites compared between *APOE* groups in this Chapter, the lack of difference in mI between the *APOE* groups could support the proposal above that young *APOE*-E4 carriers do not have an immune response leading to inflammation at this age. Voevodskaya et al. (2016) detected that *APOE*-E4 carriers who are cognitively healthy with normal CSF amyloid aged between 60 and 80 years have higher PCC mI than *APOE*-E4 non-carriers. The finding of this Chapter that young *APOE*-E4 carriers do not have a different PCC mI concentration to the non-carriers at ages 18-

25, suggests that higher mI in *APOE*-E4 carriers is not present at all ages, but instead appears to develop later in life. Consistent with the proposal that mI is a marker of inflammation (Rae, 2014; Stagg et al., 2011), this suggests that an inflammatory immune response could occur before age 60 in *APOE* E4 carriers. Again, studying PCC MRS in *APOE*-E4 carriers around ages 40-50 years could inform us as to when the earliest possible immune change may occur. The finding of no difference in PCC Cr between the young *APOE* groups has methodological implications for future MRS studies in *APOE*-E4 carriers. This findings suggests that Cr could be used as the denominator of metabolite ratios at this age, since a difference in a metabolite ratio with Cr would therefore be unlikely to be related to a change in the Cr concentration. This would need replicating at older ages however, as this study does not rule out that PCC Cr may be correlated with age in the *APOE*-E4 carriers. Finally, the finding of no PCC Glx or GABA+ alteration between *APOE* groups again suggests that these concentrations are not different between young *APOE*-E4 carriers, and thus alterations in these metabolites are unlikely to contribute to alterations in activity between *APOE* groups at this age. Instead, as for Cr and mI, changes in GABA+ and Glx could relate to pathological changes later in life given that changes exist in AD and MCI.

The main implication of the lack of differences in MRS metabolites between the young *APOE* E4 carriers and non-carriers is that they cannot be driving the BOLD differences seen in young *APOE* E4 carriers. What then, if not biochemistry assessed via MRS, could be related to these activity alterations? This is a theme that will be returned to in the general discussion Chapter (Chapter 6).

5.4.1 Limitations

One limitation of our study could be that our MRS voxels are large, and therefore do not have high sensitivity to any subtle metabolite changes that may exist. This voxel size limitation, however, is an issue with all MRS studies, since large voxel sizes are required in order to achieve a sufficient signal-to-noise for metabolites present at low concentrations. An improvement to the PRESS acquisition used here would be to reduce the voxel size, ideally to 1.5cm³ if feasible, and place this as close as possible to the PCC ROI region identified in the Shine et al. (2015) and the clusters identified in Chapters 3

and 4 of this thesis where tNAA correlated with BOLD for scene tasks. This would improve the spatial specificity of the MRS measurement. This would be technically challenging though as individual differences in brain anatomy make precise voxel placement difficult, as discovered during data collection for this thesis. If, however, it was possible to place a smaller MRS voxel on the exact location of the fMRI ROI and clusters from Chapters 3 and 4, this could enhance sensitivity to detect any difference in this region, which may have been diluted by my use of a larger MRS voxel.

An additional limitation of this study is that the PCC and OCC voxels overlapped in several individuals. Thus the PCC metabolites measured from what should have been the control region affected late in AD, may actually contain regions of the cortex around the PCC that are proposed to be affected early in AD. Reducing the voxel size, as suggested above to improve the spatial specificity of the MRS measure, would also address the problem of overlap of voxels between the key and control ROI.

The sample size was smaller than I initially aimed for in this study. A larger sample size would have reduced the impact of loss of data, hopefully generating a sample size of 30 in each group, thereby matching larger sample sizes in previous MRS studies (e.g. n=28 per group in Reid et al., 2010). That said, the sample size for the PCC tNAA comparison between of 19 *APOE*-E4 carriers and 25 non-carriers was comparable to several other MRS studies comparing patient groups with controls (e.g. n=15 per group in Bai et al., 2014; n=17 per group in Falkenberg et al., 2014), and also with the most similar MRS studies by Tandon et al. (2013) and Yoo et al. (2009) who compared MRS in participants at risk of schizophrenia with non-risk participants. The sample size in Tandon et al. (2013) was 22 vs 22 and in Yoo et al. (2009) was 23 vs 24. These MRS studies suggest that our sample sizes was probably adequate, however, if replicated in a larger sample size greater confidence could be placed in the robustness of the findings.

5.4.2 Future directions

Relating this result to the findings from the MRS and fMRI studies in schizophrenia discussed in the introduction to this Chapter, the finding of a metabolite-BOLD relationship in healthy controls but no metabolite difference between groups also occurred in these studies. Interestingly, however, when the MRS-BOLD relationship was

tested in the patient and control groups, there was a difference in this relationship between the groups. This was demonstrated in Reid et al. (2014), who found no difference in ACC NAA/Cr or Glx/Cr between schizophrenia patients and controls, but did find a significant positive correlation between the ACC BOLD percent signal change in a Stroop task and both ACC NAA/Cr and ACC Glx/Cr in schizophrenia patients. This was not present in the control group. Similarly, in Falkenberg et al. (2014), there was no difference in right ACC Glx/Cr between schizophrenia patients and healthy controls, but there was a significant relationship between right ACC Glx/Cr and the BOLD percentage signal change during a cognitive control task in the intra-parietal lobule (IPL), where controls showed a negative relationship while patients showed a positive relationship. This pattern also extended to another disorder, Kleine Levin Syndrome (KLS), a hypersomnia disorder with behavioural disturbances including hyperphagia. There were no metabolite differences in the thalamus between patients and controls, yet there was a significant negative correlation between thalamic tNAA and BOLD during a working memory task in patients that was not present in controls (Vigren et al., 2013). In each of these studies the conclusion was that, although the metabolite concentration did not differ between groups, the biological mechanism of *how* this was related to BOLD may differ.

Thus a potential next step in MRS research in young *APOE-E4* carriers would be to investigate the relationship between PCC tNAA and PCC BOLD during the two tasks used in Chapters 3 and 4. If, following this MRS-BOLD study, there is no difference in tNAA-BOLD relationship between groups, this would support the assertion that there are no metabolite differences between *APOE* groups at this age, and confirm that it is unlikely that an MRS metabolite change underlies the BOLD change seen in this cohort.

5.4.3 Summary of Chapter

In summary, this Chapter found that no metabolite differences were evident in the PCC between young *APOE-E4* carriers and non-carriers. This implies that PCC MRS metabolite alterations do not exist at ages 18-25, but develop later in life, given reports noting alterations in older *APOE-E4* carriers, and in MCI and AD patients. This finding implies that the activity alteration identified in the PCC in Shine et al. (2015) is not

driven by an underlying MRS metabolite change, contrary to the overall hypothesis behind this thesis. To further examine this, an extension of this study would be to repeat in the young *APOE*-E4 carriers and non-carriers the correlations performed in Chapters 3 and 4 in order to assess the functional-biochemical relationship between PCC tNAA and PCC BOLD during scene perception and scene working memory tasks. If there is no alteration in this functional-biochemical relationship, this would additionally support the suggestion that the PCC BOLD alteration identified in Shine et al. (2015) is not related to an underlying alteration in PCC MRS. If this is the case, subsequent work should explore what other factors may be driving the PCC activity alteration in the young *APOE*-E4 carriers to better understand the mechanism. An additional future research avenue would be to compare PCC MRS later in life in *APOE*-E4 carriers and non-carriers, and fill the gap in research between age 18-25 years (tested here) and age 50 years, which is the lowest age tested in previous *APOE* MRS studies.

6 Chapter 6: General Discussion

The main aim of this thesis was to investigate whether the alteration seen in PCC BOLD in response to scene, but not object or face, conditions in young *APOE-E4* carriers (in Shine et al. (2015)) may be related to an alteration in the biochemistry of this region, as assessed using MRS. The purpose of this was to try to gain insight into the biochemical mechanism behind activity alterations in the PCC, which is an AD-vulnerable brain region, in young people at increased genetic risk of AD. To achieve this goal, Chapters 3 and 4 first focused on application of combined fMRI-MRS to test whether individual differences in PCC MRS metabolites correlated with individual differences in the PCC BOLD response during the scene conditions of a perception and a working memory task. Chapter 5 then applied MRS in the PCC of young *APOE-E4* carriers and non-carriers to test whether there were any differences in metabolite concentrations between these groups at ages 18-25 years.

While the main purpose of collecting fMRI data was to correlate this with MRS metabolites, this also allowed me to investigate activity in the PCC ROI and its relationship with performance on the two key experimental paradigms. The aim of this was to contribute to the understanding of PCC function, since there is no clear consensus as to the role of this region in the brain, nor the circumstances under which it deactivates, or how patterns of activation relate to cognition. Since the PCC is an important brain region affected early in AD and in *APOE-E4* carriers (see Introduction, Section 1.4 and 1.5), better understanding of its role in tasks that AD patients show behavioural impairments on could help understand the early changes that occur in this disease.

In this General Discussion, I summarise the main findings of this thesis, propose ideas for potential mechanisms that might underpin some of the findings, discuss some methodological considerations and limitations to this work, and suggest some future directions to extend the work of this thesis.

6.1 Summary of the three main findings

There were three main findings from this thesis:

(1) The fMRI-MRS analyses in Chapters 3 and 4 revealed that the concentration of PCC tNAA was positively correlated with the PCC BOLD response for the scene condition of the task applied in each Chapter. In Chapter 3, this was evident when comparing the scene odd-one-out condition relative to the size oddity baseline (contrast of scenes>size), and in Chapter 4 this was evident in the complex scene processing working memory condition (contrast of rooms 2back > rooms 1back). The correlations between PCC tNAA and PCC BOLD were detected using the voxelwise regressor approach in both Chapters; but additionally via the Pearson correlation approach (focused on the PCC ROI identified in Shine et al., 2015) in Chapter 3 (this point will be expanded on in Section 6.2.1). The direction of these correlations suggested that individuals who have a higher concentration of PCC tNAA show less PCC deactivation in the scene condition of each task. These correlations were found to be category sensitive, as they existed for scene, but not for face or object perception (Chapter 3), and for scene, but not shape working memory (Chapter 4). Category sensitivity, however, was not completely clear cut via the Pearson correlations, as the correlation between PCC tNAA and BOLD for scenes was not significantly different to the control correlations for faces or objects. When the variance shared between the BOLD response for faces and objects was removed from that for scenes, however, this confirmed the positive correlation between PCC tNAA and PCC BOLD for scenes. The tNAA-BOLD correlations were also regionally sensitive to the PCC, as no relationships between PCC BOLD and OCC metabolites were found. Again, however, although there was no significant correlation between OCC metabolites and PCC BOLD for scenes, there was no significant difference between the correlations of PCC BOLD for scenes and OCC or PCC metabolites. A possible explanation for this could be the overlap of PCC and OCC voxels in some individuals. Finally, these scene sensitive BOLD-MRS correlations appear to apply for tNAA only, as PCC GABA+ or Glx were not related to PCC BOLD for any condition in Chapter 3, and there was no scene-sensitive significant correlations for PCC GABA+ or Glx and PCC BOLD in the regressor approach in Chapter 4.

(2) The fMRI data from Chapters 3 and 4 found that the PCC ROI showed reduced deactivation when presenting complex scenes than for the other categories of stimuli. More specifically, in Chapter 3 there was reduced PCC deactivation to scenes compared to faces or objects, when all conditions were contrasted to the baseline condition of size,

and in Chapter 4 there was less deactivation to in the 2 back working memory conditions for scenes compared to shapes. These findings suggest that there is category sensitive response of the PCC ROI.

(3) The findings of Chapters 3 and 4 that reduced deactivation of the PCC is associated with a higher concentration of PCC tNAA led to the prediction that young *APOE-E4* carriers may have higher PCC tNAA than non-carriers, given that they showed reduced deactivation to scenes in Shine et al., (2015). Despite this, the analysis in Chapter 5 suggested that young healthy *APOE-E4* carriers and non-carriers do not have significant differences in PCC tNAA, nor in any other metabolite measured in the analysis, at ages 18-25.

6.1.1 Potential mechanisms behind the positive tNAA-BOLD relationships

Considering the literature outlined in Chapter 2 about the function of NAA, and examining other tNAA and BOLD studies in humans, animals and *in vitro*, there may be two potential mechanisms that could underlie the positive correlation between tNAA and BOLD detected in Chapters 3 and 4.

The first possible mechanism, as suggested in the discussion of Chapter 3, is based on the hypothesised association of NAA with the functional capacity of neuronal mitochondria. This hypothesis emerges from findings that NAA is synthesised in neuronal mitochondria (the site of aerobic respiration to produce ATP) (T. B. Patel & Clark, 1979); supporting this pharmacological inhibition of mitochondrial respiratory chain enzymes required for ATP production are associated with a decrease in NAA in a preparation of neuronal mitochondria (Bates et al., 1996), and the decrease and subsequent increase in ATP following traumatic brain injury is coupled with corresponding alterations in the level of NAA (Signoretti et al., 2001). These findings suggest that the greater the amount of NAA in a brain region, the greater the amount of aerobic respiration that could occur in order to produce ATP in mitochondria. ATP production is required following neuronal activity to replenish energy stores expended during this energy-demanding process (Logothetis, 2002). The BOLD response is an

indirect measure of the increase in nutrients (e.g. oxygen and glucose) delivered to the site of neuronal activity. The possible mechanism linking tNAA with BOLD, therefore, is that a higher BOLD response could represent greater functional capacity of the neuronal mitochondria to produce ATP, associated with the level of NAA.

The second potential mechanism is based on NAA being a precursor molecule for NAAG (Moffett, 2007; Rae, 2014). In most MRS studies, NAA and NAAG are combined as the tNAA measure, given that these metabolites have such similar resonant frequencies on the MRS spectrum. A recent functional MRS (fMRS) study, however, assessed NAA and NAAG separately and measured their concentrations in the occipital lobe before, during and after visual stimulation (Landim et al., 2016). They found that the level of NAAG increased during the visual stimulation period, while the level of NAA decreased, as NAA is the only known source of NAAG (Rae, 2014). Linking this with the BOLD response, NAAG has been associated with an increase in blood flow to a brain region following neuronal activity: upon neuronal stimulation NAAG is exported to astrocytes where it binds to the mGluR3 glutamate receptor, which results in the release of vasoactive agents that induce an increase in blood flow to that site, which would be measured as an increase in BOLD (Baslow, Dyakin, Nowak, Hungund, & Guilfoyle, 2005). In further support of this, Baslow et al. (2005) used a drug that blocks the breakdown of NAAG and found this caused an increased BOLD response for a few minutes. Since NAA is the only known source of NAAG, a higher concentration of NAA could mean a higher level of NAAG, which in turn could result in a higher BOLD response.

The relationship between tNAA and BOLD, and the second proposed mechanism outlined above, is likely to be a research topic of significant interest in future MRS-BOLD studies, enabled via a new MRS scan protocol able to separate NAA and NAAG, termed Hadamard Encoding and Reconstruction of MEGA-Edited Spectroscopy (HERMES) (Chan, Puts, Schar, Barker, & Edden, 2016). A potential future study, enabling more detailed investigation of the PCC tNAA-BOLD relationships identified in this thesis, would be to perform a similar fMRS study as in Landim et al., (2016), but instead of placing the MRS voxel in the occipital lobe and using visual gratings as stimuli, my experiment would place the voxel in the PCC and use different stimuli categories as stimuli, similar to the oddity task applied in Chapter 3. By using fMRS and the new HERMES protocol to quantify NAA and NAAG separately, it would be possible to assess whether the NAAG increase observed in the occipital lobe would also be present in PCC, and whether the NAAG concentration would correlate with the BOLD response. This study could further

our understanding of a potential mechanism that may link BOLD and tNAA concentrations in the PCC, and the relationship of MRS metabolites associated with behaviour.

6.1.2 Implications of the category sensitive BOLD response in the PCC ROI

The BOLD findings of Chapters 3 and 4 suggest that there is a category sensitive response of the PCC ROI, where there is less deactivation for scenes than other stimuli categories, and this holds across different cognitive domains (perception and working memory). One implication of this for future work could be to test whether this category sensitivity response also holds across the episodic memory domain. This is because the PCC has been implicated in episodic memory in several studies (demonstrated in the meta-analysis of Spreng et al, 2009), and notably PCC deactivation during encoding has been suggested to be linked with PCC activity during memory retrieval and successful memory performance via the encoding-retrieval (ER) flip account (Daselaar et al., 2009; Vannini et al., 2011). A future direction, therefore, could be to assess what impact (if any) the pattern of less deactivation to scene (compared to face or object) stimuli may have on activity at retrieval, and importantly what impact this may have on memory performance across different stimuli categories. Only one study has compared the ER flip across different stimuli categories in the healthy brain (during passive viewing of scenes and faces), but this study focused on a very posterior regions of the PCC (Daselaar et al., 2009) (see Figure 6.1). In comparison, the ROI from Shine et al. (2015) is quite a dorsal PCC region. Since the ROI from Shine et al. (2015) could be of relevance to AD pathogenesis – given that it was identified in *APOE-E4* carriers during the performance of task conditions known to be sensitive to behaviour impairments in AD patients (Bird et al., 2010; A. C. H. Lee et al., 2006, 2007; Pengas, Hodges, et al., 2010) – a development of the work in this thesis would be to study the impact of the category sensitive deactivation in the PCC ROI on activity during retrieval and memory performance across these different categories. This could help us gain insight into how the PCC ROI is associated with successful episodic memory performance, which could then benefit our understanding of the impact of PCC dysfunction in early AD on cognition.

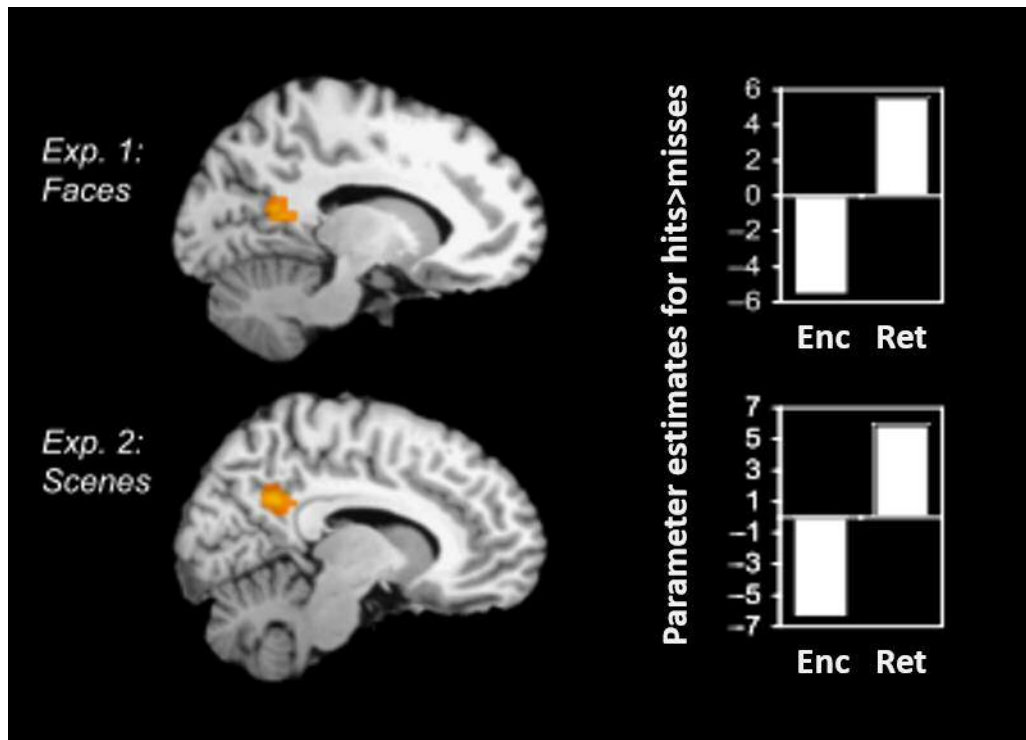


Figure 6.1: Study of encoding-retrieval flip for different categories of visual stimuli (faces and scenes). Bar graphs represent the parameter estimates for the contrast of hits>misses during encoding (“Enc”) and retrieval (“Ret”), i.e. the difference in activity for items that were subsequently remembered vs forgotten during Enc and Ret respectively. The parameter estimates suggest that there is deactivation during encoding and activation during retrieval for both faces and scenes, and clusters show the location of this activation differs depending on the stimuli category (image taken from Daselaar et al., 2009).

6.1.3 Potential reasons for no PCC MRS alterations in young *APOE-E4* carriers

The finding of no differences in tNAA, mI, Cho, Cr, GABA+ or Glx between *APOE-E4* carriers and non-carriers at age 18-25 years suggests that there are no biochemical alterations detectable via MRS at this young age. The discussion section of Chapter 5 offered suggestions for why this may be the case. These are split into more methodological reasons and more *APOE*-biology related reasons. The potential methodological reasons were that the use of a large PCC MRS voxel may have impacted on the ability to detect a subtle biochemical change that might only exist in a small region of the PCC. Additionally, the PCC MRS voxel may not have been sufficiently sensitive to

detect relative metabolic change, since it did not, in all subjects, overlap with the PCC ROI region where the activity alteration was detected in Shine et al. (2015), due to inter-individual variability in brain anatomy. The more *APOE*-biology related reasons include that ages 18-25 years may be too early for any metabolite alterations. Although alterations in biochemistry in the PCC of young *APOE*-E4 carriers have been suggested in FDG-PET studies of PCC glucose metabolism (e.g. Reiman et al., 2004), and post mortem studies of energy metabolism enzymes (Perkins et al., 2016; Valla et al., 2010), the mean age in these studies was approximately 10 years older than the participants tested in Chapter 5. Therefore, MRS changes may become evident at a later age than that tested in this thesis. To address this possibility, it would be useful to look at genotype/MRS associations across the lifespan, or even more convincingly, in a longitudinal study of participants as they move from early adulthood towards middle-age.

A further potential reason for the lack of metabolite differences evident between *APOE* groups could be an influence of other AD genetic risk variants on MRS metabolites. As noted in Chapter 1, mutations in the *APP*, *PSEN1* and *PSEN2* genes are associated with early onset AD, and GWAS studies have detected 19 additional risk gene variants that are associated with increased genetic risk of AD (Harold et al., 2009; Lambert et al., 2013). These findings have given rise to polygenic risk scores approaches, where an individual's cumulative risk score of the SNPs associated with AD can be calculated and used to look at brain alterations linked to a broader assessment of AD risk (Escott-Price et al., 2015). Without measuring these in this study, it is possible that the *APOE*-E4 carrier and non-carrier groups differ with respect to the possession of other risk genes implicated in AD, and that these may also affect PCC metabolites. A further extension of the work undertaken here would be to obtain polygenic risk scores for the participants included in the study in Chapter 5, to enable me to ask how polygenic risk score may be associated with inter-individual variation in MRS metabolites in the PCC.

A drawback of such a polygenic approach, however, is that very large sample sizes are often required, unless a very sensitive cognitive marker of AD risk was applied. For example, a recent study examining the relationship between polygenic risk and the volume of brain regions implicated in AD (hippocampus, entorhinal cortex, PCC, parahippocampal gyrus) used a sample size of 272 participants (Foley et al., 2016). An optimal experimental design would be to create a polygenic risk for a similar sized group to Foley et al. (2016), including possession of *APOE*-E4, and select participants at the highest and lowest risk scores to compare PCC MRS metabolites. This approach would

not have been feasible for this thesis, given time and the large cost of genotyping and scanning such a large number of participants, thus the best strategy for this thesis was identified as a focus on a single candidate gene, given the significant link between *APOE*-E4 and AD. This single gene accounts for more variance in AD risk than the combination of the other 19 genes (Escott-Price et al., 2015). That said, refining our understanding of AD risk via consideration of polygenic methods is likely to be an exciting future development in genetic neuroimaging for AD.

6.2 Methodological considerations and limitations

6.2.1 Choice of strategy to correlate BOLD with metabolites

Turning now to the consistency of the MRS-BOLD relationships between Chapters 3 and 4, there were consistent findings across both analysis methods applied in Chapter 3, specifically, the Pearson correlation and the regressor approach. This was not, however, the case in Chapter 4. As suggested in the discussion of Chapter 4, a potential reason for this could be that the PCC ROI taken from Shine et al. (2015) had some degree of overlap with the cluster identified in the regressor analysis in Chapter 3, but not in Chapter 4. Figure 6.2 demonstrates this point, as it shows the overlap of PCC ROI and the cluster in Chapter 3 and the spatially distinct cluster identified in Chapter 4.

This discrepancy suggests that the most sensitive strategy for detecting MRS-BOLD relationships could be the regressor approach. This involves examining which fMRI voxels within the larger MRS voxel area show a correlation with the MRS metabolites measured within that region. The ROI approach may be more sensitive to the BOLD activity of interest, but displacement of the MRS voxel from this functional ROI could risk that a correlation between MRS and BOLD may not be detected, if the BOLD response is quantified outside the cluster detected in the regressor analysis. This is a point that requires resolving in future studies, as there are currently no consistent recommendations for how to quantify the BOLD response to correlate with MRS, as many studies opt for different strategies, as demonstrated in Figure 2.6 in Chapter 2.

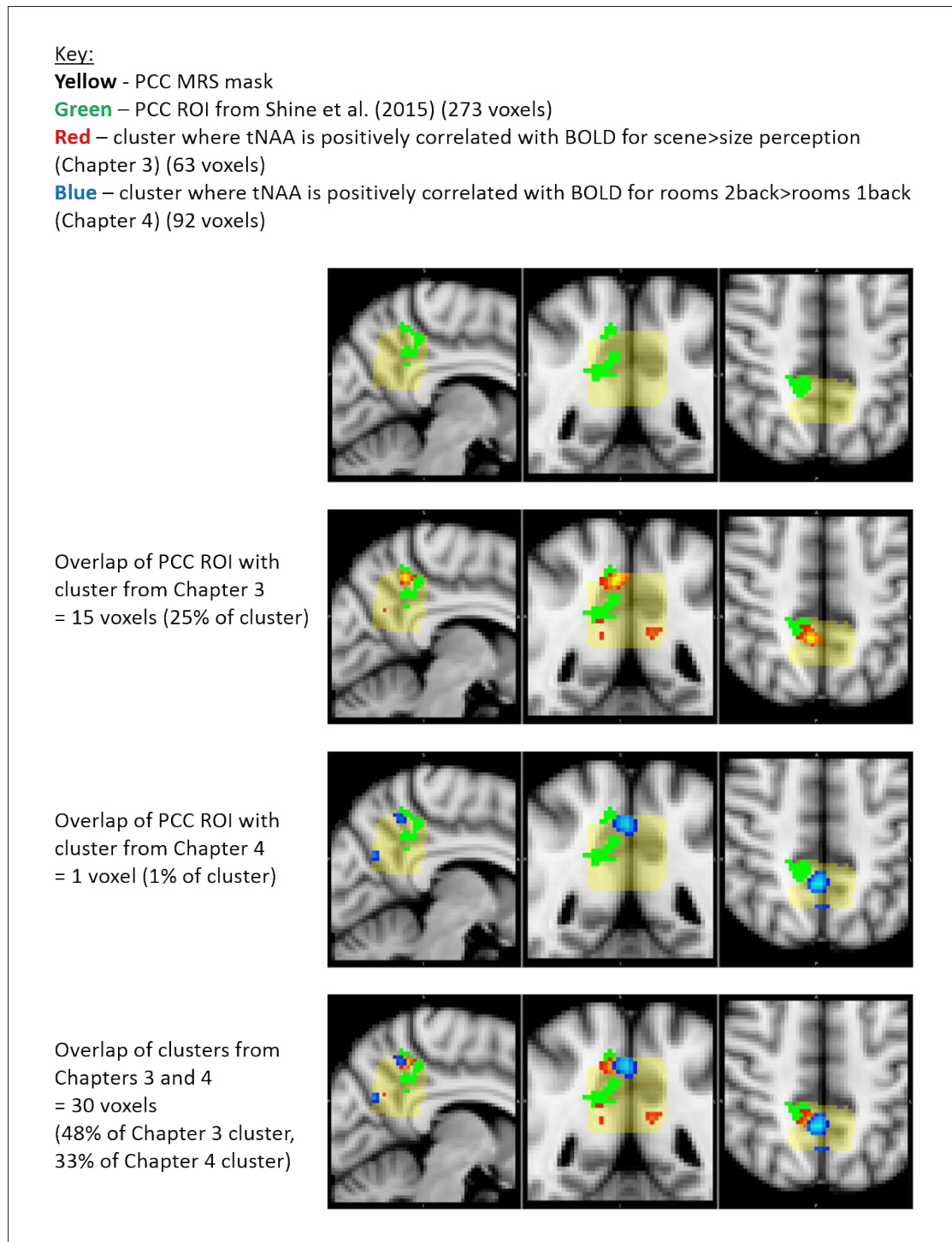


Figure 6.2: Location of PCC ROI from Shine et al. (2015) that was used to extract the BOLD percentage signal change in Chapters 3 and 4, and comparison of this location with the clusters determined via the regressor approach in both Chapters. Shows that there is some overlap of PCC ROI with cluster from Chapter 3, but no overlap with cluster in Chapter 4. Also the Clusters from Chapter 3 and 4 show some degree of overlap.

6.2.2 Statistics and corrections for multiple comparisons

Correction for multiple comparisons is an important issue in fMRI research. There are thousands of fMRI voxels in the brain, and therefore there are a very large number of statistical tests to be performed in an fMRI analysis. This is an issue because with an increasing number of statistical tests, there is an increase in the type I error rate, or the number of false positive results, i.e. detecting an incorrectly “active” fMRI voxel (Huettel et al., 2009). It is a challenge in fMRI to determine an appropriate level of correction to tackle this multiple comparisons problem. It is necessary to have a balance between a too lenient correction which would risk finding false positive results (type I error) and too stringent correction which would risk finding false negative results (type II error).

The importance of the choice of strategy for this balance has been highlighted in a recent high profile and much debated study, which investigated the type I and II error rates of different fMRI software packages. The main finding of the study was that most packages inflate the type II error rate (i.e. too many false positives), although in one situation they found correction was too conservative (for FSL’s FLAME1 package at a cluster defined threshold of $p < 0.001$) (Eklund, Nichols, & Knutsson, 2016). This study attracted much attention, as it made the claim that 40,000 fMRI studies could be based on false positive, although this has since been corrected, and authors now estimate this to be closer to 3,500 studies. Counter to this study however is the suggestion that by focusing on preventing false positives, perhaps we are being overly cautious and promoting false negatives (Lieberman & Cunningham, 2009). The topic of correction is a much debated one; there appear to be several different strategies of addressing this issue, although no clear recommendation.

The strategies applied in this thesis to address the multiple comparisons issue were based on previous literature that had performed similar analyses. These were to (a) apply a voxelwise threshold of $p < 0.001$ and clusterwise correction to $p < 0.05$ to the whole brain data for the BOLD percent signal change analysis within the fMRI ROI, and (b) for the follow up regressor analysis, apply a small-volume correction to test for fMRI voxels solely within this MRS voxel mask region (rather than across the whole brain, thus reducing the number of fMRI voxels tested), apply the voxelwise threshold of $p < 0.001$ then use AFNI’s 3dClustSim tool to calculate the cluster-size threshold of $p < 0.01$, based

on previous literature that also aimed to identify clusters within a pre-defined ROI (Hodgetts et al., 2015).

Such approaches may have had limitations however, based on the findings of Eklund et al., (2016). It is important to note in the context of the Eklund et al., (2016) paper that the AFNI 3dClustSim tool used in this thesis was the 2016 version, rather than the 2015 version in which a bug was detected that increased the type I error rate. Moving forwards, to improve correction for multiple comparisons, a tool that is beginning to become more common in fMRI includes permutation testing. This method performed the best in the tests of the Eklund et al., (2016) paper, as the number of false positives was the most similar to that expected across several fMRI analyses. An alternative recommendation from authors who are more concerned about false negative findings is for replication, since they propose that false positive results will not replicate (Lieberman & Cunningham, 2009). A combination of these approaches will be beneficial in future fMRI research to generate greater confidence in findings.

6.2.3 Interpretation of BOLD and BOLD-MRS relationships

A challenge in interpreting the BOLD response and the relationship between BOLD and MRS metabolites is that BOLD is an indirect measure of neuronal activity, as outlined in Section 2.2.1. Although the BOLD response has been shown to be coupled to neuronal activity, the exact physiological mechanisms behind it is not completely understood (Logothetis et al., 2001; Logothetis & Pfeuffer, 2004; Logothetis, 2002). Rather than simply reflecting the spiking activity of single neurons, BOLD is a complex measure that represents a culmination of many factors, including neurovascular coupling, local field potentials which represent the summation of local excitation and inhibition, cerebral blood flow, cerebral blood volume, and the metabolic consumption of oxygen and glucose (Singh, 2012).

In interpreting the MRS-BOLD results, therefore, it should be acknowledged that we are not directly assessing the direct relationship between neuronal activity and neurotransmitters or tNAA. Instead such metabolites may be having an indirect effect on BOLD via the vasculature of the brain. For example, in an MRS-BOLD study by Muthukumaraswamy et al. (2012), they identified that occipital GABA+ had a negative

correlation with occipital BOLD in response to viewing a visual grating, but also that occipital GABA+ was related to the latency and amplitude of the haemodynamic response function (Muthukumaraswamy et al., 2012). Related to this, as discussed in Section 6.1.1 above, one of the possible mechanisms that could link BOLD with tNAA in Chapters 3 and 4 of this thesis could be via the vasculature, as NAAG may have a vasodilatory effect, so could be associated with BOLD via an effect on cerebral blood flow. However, since the BOLD measure is so complex, and there are several hypotheses as to the role of tNAA in the brain, further studies will be necessary to tease the mechanisms behind this relationship apart.

The rationale behind the experiments in this thesis was to study whether alterations in the PCC BOLD response in young *APOE-E4* carriers could be related to alterations in PCC MRS metabolites. However, in considering the many factors that influence the BOLD response described above, there could be many further hypotheses as to why the PCC BOLD response in young *APOE-E4* carriers may be altered. For example, it could be the case that the *APOE-E4* carriers have altered neurovascular coupling in the PCC which contributes to their different PCC BOLD response, instead of there being a difference in the underlying neural signals. A strategy that could be used to address this is to combine fMRI with either electroencephalography (EEG) or magnetoencephalography (MEG), which can measure electrophysiological signals in the brain (for example oscillatory activity) (Singh, 2012). Such a multi-modal neuroimaging approach would provide complementary information on neurovascular coupling and neuronal activity, which could help us determine whether the altered BOLD signal is driven by alterations in the vasculature or in neuronal activity (this point will be returned to in the Future Directions Section (Section 6.3) below).

6.2.4 Limitations

6.2.4.1 Limitations of MRS

Although the MRS-BOLD approach applied in this thesis has advantages and it is promising in that it can contribute to knowledge of the biochemical underpinnings of the BOLD response in humans *in vivo*, there are some methodological limitations to this approach. The main limiting factor of MRS is that it requires large voxel sizes in order to

detect sufficient quantities of metabolites, given that they are at such low concentrations (Stagg & Rothman, 2014). This is particularly challenging for GABA+, as the concentration of GABA+ referenced to water tends to be below 3mM (Mullins et al., 2014; Rae, 2014). The large voxel size is a limitation because it reduces the spatial specificity of the metabolite measurement. This measurement represents the concentration over a volume of 8cm³ if the voxel size is 2x2x2cm, which is a relatively small voxel size in MRS. This is considerably larger than an fMRI voxel which is, instead, in the order of millimetres. This is a limitation of all MRS studies, however, rather than specific to the methods I applied in this thesis. A reduction in MRS voxel size may be possible at higher magnetic field strengths, e.g. a 7T MRI scanner, since this enables a higher SNR, and improved resolution of peaks on the MRS spectrum. Therefore, it is possible that voxel sizes may decrease in the future as more high-field MRS studies are performed, which will be beneficial in improving spatial specificity of MRS measures.

A further limitation was that the PCC and OCC MRS voxels overlapped in some individuals in all three experimental Chapters. This problem is in part related to the large size of the MRS voxels. The voxel placement method was developed in a pilot study of 3 male and 3 female participants to produce no or minimal overlap of the MRS voxels, which as stated above needed to be large in order to accurately quantify the metabolites. Due to the large between-subject variability of brain size, however, this method was not effective in all participants tested in the experiments in this thesis. In particular, occipital lobe dimensions varied greatly between participants, with some participants having a large enough occipital lobe to place the 3x3x3cm MRS voxel so that it did not overlap with the scalp, whereas in some individuals it was necessary to place this OCC voxel more anterior, which meant overlapping with the region occupied by the PCC MRS voxel. Similarly, the position of the lateral ventricles sometimes meant PCC voxel placement had to be more posterior to avoid these, which then meant the PCC voxel overlapped with the OCC voxel. To address this in future studies, smaller OCC voxel dimensions could be used (e.g. instead of 3x3x3cm, potentially 2x3x3cm), and the PCC voxel could be placed on the same rotate localiser as the OCC voxel, so that they are aligned side-by-side, rather than at an angle to each other.

6.2.4.2 Limitations of fMRI

A possible limitation of the fMRI analyses performed in Chapters 3 and 4 is the baseline condition used in the BOLD contrasts. In fMRI studies it is usually advantageous not to use rest as a baseline and instead use a task condition that is similar in basic requirements to the condition of interest. This is because the subtraction of such a baseline from the task condition of interest helps isolate the BOLD activity related to the cognitive task of interest (Henson, 2006; Price et al., 1997). For example, in the oddity task, the size baseline condition involved presentation of three images (similar to the other task conditions), and asked participants to make a low level perceptual decision about those three images. The design of this was to isolate BOLD differences due only to the stimuli category presented.

It would, however, be useful to have a rest baseline condition when studying PCC activity, as this would allow the contrast of the task condition relative to the resting state/DN activity of this region. Such an approach would have helped me draw conclusions about how the task-related PCC BOLD activity relates to its activity during the resting state.

For the fMRI analysis of Chapter 4, a rest baseline would have been an improvement on the analysis strategy implemented in Lee and Rudebeck (2010), which calculated the BOLD percent signal change for each condition relative to the unmodelled baseline. There is no control over what ‘cognitive function’ this unmodelled baseline may include, therefore it is difficult to interpret the meaning of the BOLD percentage signal change relative to this baseline. By adding rest blocks to this task I would have been able to interpret the BOLD percentage signal change as a change from the DN resting state activity. An alternative useful baseline condition would have been a 0back condition for each of the shape and scene stimuli categories, in order to replicate the 1back>0back and 2back>0back analyses that are commonly performed in n-back fMRI analyses (Ceko et al., 2015; Esposito et al., 2009; Hu et al., 2013; Mckiernan et al., 2003).

6.2.4.3 Sample sizes and participants

Although the sample size recruited for the studies in Chapters 3 and 4 were sufficient to match power calculations based on previous papers (e.g. Bai et al., 2014;

Falkenberg et al., 2014; Yoo et al., 2009), and considered of sufficient strength to detect MRS-BOLD correlations based on previous studies, the loss of data due to poor quality MRS spectra was greater than expected. This was especially the case for the PCC GABA+ measurements, in which over a third of the original 40 participants did not have sufficiently robust GABA+ data to correlate with BOLD and behaviour. The explanation for this large loss of data for PCC GABA+ is most likely related to the voxel size used here being smaller than that typically applied for GABA+ measurements (typically 3x3x3cm, as was applied in the OCC). The length of the scan for the PCC voxel was lengthened to take this into account, but this change did not seem to address this problem. The implication of this loss of data is that future studies measuring PCC GABA+ should use larger voxel sizes to improve data quality, and larger sample sizes to allow for loss of poor quality data.

Similarly, a larger sample size to compare MRS metabolites between *APOE-E4* carriers and non-carriers would improve the power to detect any subtle differences between groups. The sample size tested in Chapter 5 was comparable to several MRS studies that detected differences between groups (see Section 5.2.1), yet was smaller than in other MRS studies, as detailed in the discussion of Chapter 5. Increasing the sample size applied in Chapter 5, therefore, would be an improvement on the methods in this Chapter.

A further methodological consideration relates to the participants in Chapters 3 and 4. Based on the estimate that one in five people carry the *APOE-E4* allele (Farrer et al., 1997), it is likely that my sample of 33 participants in Chapters 3 and 4 could include 6 or 7 *APOE-E4* carriers. Given the findings of Shine et al. (2015) that *APOE-E4* carriers show less deactivation in the PCC ROI for scene oddity than non-carriers, but not for face or object oddity, it is possible that the inclusion of *APOE-E4* carriers in my sample may influence the failure to deactivate scenes compared to other visual categories. As a very rough attempt to simulate the removal of the effect of the *APOE-E4* allele on the BOLD data for the oddity task, the seven participants with the least deactivation of the PCC ROI compared to the scene oddity condition were removed from the comparison of BOLD across conditions. When the repeated-measures ANOVA was performed with this smaller sample size, the significant category sensitive response of the PCC remained: $F(2,54)=22.13$, $p<0.001$. This approach is just a very rough simulation of the data without the possible impact of *APOE-E4* carriers (assuming they show reduced deactivation for scene perception and oddity conditions, based on Shine et al. (2015)). To

confirm these ideas, a similar sized study to that performed in Chapter 3 could be performed consisting of only *APOE*-E4 non-carriers, determined via genotyping, to detect whether there are indeed differences in PCC ROI activity for scenes, faces and objects when the influence of *APOE*-E4 would be removed accurately.

6.2.4.4 Correlation not causality

A final issue to acknowledge that is that many of the analyses performed in Chapters 3 and 4 are correlational. As is well-acknowledged in neuroimaging, correlation does not mean causality. The findings in this thesis suggest there may be relationships between MRS and BOLD, and possibly between behaviour and MRS, yet this does not provide evidence that the concentration of PCC tNAA drives BOLD or behaviour. To strengthen support for the tNAA-BOLD relationships identified in Chapters 3 and 4, these findings should be replicated, ideally using larger sample sizes to increase power to detect such relationships, and as implemented here, using a complementary Bayes analysis to assess the strength of the evidence for such a relationships.

6.3 Future directions

As highlighted in previous Chapters of this thesis, the combined fMRI-BOLD approach applied in Chapters 3 and 4 is an attractive strategy to investigate functional-biochemical relationships in the brain *in vivo*, as MRS is a non-invasive technique (Duncan et al., 2013; Stagg & Rothman, 2014). Several recent studies have applied this approach to investigate GABA+ and Glx relationships with BOLD (Duncan et al., 2011; Enzi et al., 2012; Falkenberg et al., 2012; Harris et al., 2015; Hu et al., 2013; Kapogiannis et al., 2013; Lipp et al., 2015; Muthukumaraswamy et al., 2009, 2012), with fewer studies looking into tNAA and BOLD relationships (Hao et al., 2013; Reid et al., 2010; Vigren et al., 2013). One implication of the positive correlations between tNAA and BOLD in this thesis is that future MRS-BOLD studies should test for relationships of BOLD with tNAA, as well as the existing interest in GABA+ and Glx. Based on the scene category sensitive finding of the tNAA-BOLD relationships implied by the experiments included in this thesis, it might be interesting to further apply this approach in regions involved in high level perception, such as the parahippocampal place area (PPA), which is specialised for

scene perception (Epstein & Higgins, 2007; Epstein & Kanwisher, 1998), or the fusiform face area (FFA), which is specialised for face perception (Kanwisher & Yovel, 2006). My hypotheses for such an experiment would be that there would be a positive correlation between tNAA in the FFA and the FFA BOLD response to faces, but no relationship in the FFA between tNAA and BOLD for scenes. Whereas in the PPA, there would be a correlation of tNAA with PPA BOLD for scenes, but not for faces.

The main implication of the lack of differences in MRS metabolites between the young *APOE-E4* carriers and non-carriers is that metabolite alterations do not appear to be associated with the BOLD differences seen in young *APOE-E4* carriers. What then could be related to these activity alterations? One idea emerging from recent neuroimaging studies is the possibility that BOLD differences in *APOE-E4* carriers (compared to non-carriers) is potentially related to alteration in cerebral blood flow and cerebrovascular reactivity. This is because fMRI is an indirect measure of neuronal activity inferred from the increase in oxygenated blood arriving at the site of neuronal activity. This increase in oxygenated blood represents the increase in nutrients (e.g. oxygen and glucose) being delivered in order to replenish ATP stores that have been expended during the depolarisation of the neurons, rather than the neuronal activity directly (Logothetis & Pfeuffer, 2004; Logothetis, 2002). In support of this idea, a recent study has suggested that a large proportion (~70%) of the higher hippocampal fMRI activity detected in young *APOE-E4* carriers compared to non-carriers may be attributable to altered cerebrovascular reactivity in *APOE-E4* carriers (Suri et al., 2015). This technique has not been applied to the PCC, but would be an interesting future avenue of research helping inform the alteration in BOLD in PCC in the young *APOE-E4* carriers. Alongside such a perfusion study, it would be interesting to perform a study of neuronal activity, which could be achieved using magnetoencephalography (MEG). Application of a multimodal imaging strategy, involving collection of fMRI, perfusion and MEG data, on the same participants could help us tease apart whether the alterations in the PCC detected in Shine et al. (2015) arise from alterations in blood flow or whether they have a neuronal origin, thus contributing to knowledge of the impact of the *APOE-E4* allele on the brain at a young age.

6.4 Concluding Remarks

At the outset of this thesis I proposed that the combination of fMRI with MRS could be a beneficial approach in informing understanding of BOLD changes seen in young *APOE-E4* carriers (Shine et al., 2015). I hypothesised that the alteration in PCC ROI BOLD in the young *APOE-E4* carriers could be related to alterations in the biochemistry of this region, assessed via MRS. The work in Chapters 3 and 4 provided novel information that the PCC ROI BOLD response showed a category selective functional-biochemical response for scene perception and scene working memory conditions, which were the tasks in which the young *APOE-E4* carriers showed the altered BOLD response in Shine et al. (2015). This achieved my first aim of determining whether functional-biochemical relationships in the PCC can exist specifically for scenes. Despite these findings providing support for my overarching hypothesis of a biochemical alteration underpinning the functional alteration in the young *APOE-E4* carriers, there were no MRS differences between young *APOE-E4* carriers and non-carriers.

Although this result did not confirm my hypothesis, it does contribute to the literature in two important ways. First, since MRS metabolite differences exist in *APOE-E4* carriers over the age of 50, this narrows down the time window to study when MRS changes may arise. Regarding MRS work, future studies should explore PCC MRS changes between the ages of 25 and 50 to identify the earliest metabolic changes that can be assessed *in vivo* and non-invasively. Second, regarding *APOE-E4* carriers at age 18-25, the finding of no MRS metabolite differences between *APOE* groups indicates that the mechanism behind the altered BOLD response may not be related to MRS biochemistry. More research should be done combining fMRI with other neuroimaging techniques, such as MEG and perfusion imaging, in young *APOE-E4* carriers to further investigate why they show an altered BOLD response in the PCC to tasks sensitive to behavioural impairments in AD. If we can better understand the mechanisms related to activity alterations in this AD-vulnerable brain region, we may be able to improve our understanding of why the debilitating disorder of AD may develop, with the ultimate goal being to develop effective strategies and treatments for disease prevention.

References

- Aggleton, J. P., Pralus, A., Nelson, A. J. D., & Hornberger, M. (2016). Thalamic pathology and memory loss in early Alzheimer's disease: moving the focus from the medial temporal lobe to Papez circuit. *Brain*, *139*, 1877–1890. <http://doi.org/http://www.brain.oxfordjournals.org/lookup/doi/10.1093/brain/aww083>
- Alzheimer's Association. (2016). 2016 Alzheimer's Disease Facts and Figures. Retrieved from http://www.alz.org/documents_custom/2016-facts-and-figures.pdf
- Alzheimer, A. (1906). Über einen eigenartigen schweren Erkrankungsprozeß der Hirnrinde. *Neurol Central*, *25*, 1134.
- Amaro, E., & Barker, G. J. (2006). Study design in fMRI: Basic principles. *Brain and Cognition*, *60*(3), 220–232. <http://doi.org/10.1016/j.bandc.2005.11.009>
- Andrews-Hanna, J. R. (2012). The brain's default network and its adaptive role in internal mentation. *The Neuroscientist: A Review Journal Bringing Neurobiology, Neurology and Psychiatry*, *18*(3), 251–70. <http://doi.org/10.1177/1073858411403316>
- Andrews-Hanna, J. R., Reidler, J. S., Sepulcre, J., Poulin, R., & Buckner, R. L. (2010). Functional-Anatomic Fractionation of the Brain's Default Network. *Neuron*, *65*(4), 550–562. <http://doi.org/10.1016/j.neuron.2010.02.005>. Functional-Anatomic
- Anticevic, A., Repovs, G., Shulman, G. L., & Barch, D. M. (2010). When less is more: TPJ and default network deactivation during encoding predicts working memory performance. *NeuroImage*, *49*(3), 2638–2648.
- Bai, X., Edden, R. A. ., Gao, F., Wang, G., Wu, L., Zhao, B., ... Barker, P. B. (2014). Decreased γ -aminobutyric acid levels in the parietal region of patients with Alzheimer's disease. *Journal of Magnetic Resonance Imaging: JMRI*, *00*, 1–6. <http://doi.org/10.1002/jmri.24665>
- Barens, M. D., Henson, R. N. A. a, Lee, A. C. H. H., & Graham, K. S. (2010). Medial temporal lobe activity during complex discrimination of faces, objects, and scenes: Effects of viewpoint. *Hippocampus*, *20*(3), 389–401. <http://doi.org/10.1002/hipo.20641>
- Baslow, M. H., Dyakin, V. V., Nowak, K. L., Hungund, B. L., & Guilfoyle, D. N. (2005). 2-PMPA , a NAAG Peptidase Inhibitor , Attenuates Magnetic Resonance BOLD Signals in Brain of Anesthetized Mice. *Journal of Molecular Medicine*, *26*, 1–16. <http://doi.org/10.1385/JMN>
- Bateman, R. J., Xiong, C., Benzinger, T. L. S., Fagan, A. M., Goate, A., Fox, N. C., ... Morris, J. C. (2012). Clinical and biomarker changes in dominantly inherited Alzheimer's disease. *The New England Journal of Medicine*, *367*(9), 795–804. <http://doi.org/10.1056/NEJMoa1202753>

References

- Bates, T. E., Strangward, M., Keelan, J., Davey, G. P., Munro, P. M., & Clark, J. B. (1996). Inhibition of N-acetylaspartate production: implications for 1H MRS studies in vivo. *Neuroreport*, 7(8), 1397–1400.
- Batra, N. A., Seres-Mailo, J., Hanstock, C., Seres, P., Khudabux, J., Bellavance, F., ... Le Melledo, J. M. (2008). Proton Magnetic Resonance Spectroscopy Measurement of Brain Glutamate Levels in Premenstrual Dysphoric Disorder. *Biological Psychiatry*, 63(12), 1178–1184. <http://doi.org/10.1016/j.biopsych.2007.10.007>
- Bero, A. W., Yan, P., Roh, J. H., Cirrito, J. R., Stewart, F. R., Raichle, M. E., ... Holtzman, D. M. (2011). Neuronal activity regulates the regional vulnerability to amyloid- β deposition. *Nature Neuroscience*, 14(6), 750–6. <http://doi.org/10.1038/nn.2801>
- Binnewijzend, M., Schoonheim, M., Sanz-Arigita, E., Wink, A., van der Flier, W., Tolboom, N., ... Barkhof, F. (2012). Resting-state fMRI changes in Alzheimer's disease and mild cognitive impairment. *Neurobiology of Aging*, 33(9), 2018–28.
- Bird, C. M., Chan, D., Hartley, T., Pijnenburg, Y. a, Rossor, M. N., & Burgess, N. (2010). Topographical short-term memory differentiates Alzheimer's disease from frontotemporal lobar degeneration. *Hippocampus*, 20(10), 1154–69. <http://doi.org/10.1002/hipo.20715>
- Born, R., & Bradley, D. (2005). Structure and Function of Visual Area Mt. *Annual Review of Neuroscience*, 28(1), 157–189. <http://doi.org/10.1146/annurev.neuro.26.041002.131052>
- Boy, F., Evans, C. J., Edden, R. A. E., Lawrence, A. D., & Singh, K. D. (2011). Dorso-lateral prefrontal γ -amino butyric acid in men predicts individual differences in rash impulsivity. *Biological Psychiatry*, 70(9), 866–872. <http://doi.org/10.1016/j.biopsych.2011.05.030>.
- Braak, H., & Braak, E. (1991). Neuropathological stageing of Alzheimer-related changes. *Acta Neuropathologica*, 82, 239–259.
- Braak, H., & Braak, E. (1995). Staging of Alzheimer's Disease-Related Neurofibrillary Changes. *Neurobiology of Aging*, 16(3), 271–278.
- Braak, H., & Del Tredici, K. (2012). Where, when, and in what form does sporadic Alzheimer's disease begin? *Current Opinion in Neurology*, 25(6), 708–714. <http://doi.org/10.1097/WCO.0b013e32835a3432>
- Braak, H., Thal, D. R., Ghebremedhin, E., & Tredici, K. Del. (2011). Stages of the Pathologic Process in Alzheimer Disease: Age Categories From 1 to 100 Years, 70(11), 960–969.
- Buchhave, P., Minthon, L., Zetterberg, H., Wallin, A. K., Blennow, K., & Hansson, O. (2012). Cerebrospinal fluid levels of β -amyloid 1-42, but not of tau, are fully changed already 5 to 10 years before the onset of Alzheimer dementia. *Archives of General Psychiatry*, 69(1), 98–106. <http://doi.org/10.1001/archgenpsychiatry.2011.155>

References

- Buckner, R. L., Andrews-Hanna, J. R., & Schacter, D. L. (2008). The brain's default network: Anatomy, function, and relevance to disease. *Annals of the New York Academy of Sciences*, *1124*, 1–38. <http://doi.org/10.1196/annals.1440.011>
- Buckner, R. L., Snyder, A. Z., Shannon, B. J., LaRossa, G., Sachs, R., Fotenos, A. F., ... Mintun, M. A. (2005). Molecular, Structural, and Functional Characterization of Alzheimer's Disease: Evidence for a Relationship between Default Activity, Amyloid, and Memory. *Journal of Neuroscience*, *25*(34), 7709–7717. <http://doi.org/10.1523/JNEUROSCI.2177-05.2005>
- Calderon-Garciduenas, L., Kavanaugh, M., Block, M., D'Angiulli, A., Delgado-Chávez, R., Torres-Jardón, R., ... Diaz, P. (2012). Neuroinflammation, hyperphosphorylated tau, diffuse amyloid plaques, and down-regulation of the cellular prion protein in air pollution exposed children and young adults. *J Alzheimers Dis*, *28*(1), 93–107.
- Calderon-Garciduenas, L., Mora-Tiscareno, A., Franco-Lira, M., Zhu, H., Lu, Z., Solorio, E., ... D'Angiulli, A. (2015). Decreases in Short Term Memory, IQ, and Altered Brain Metabolic Ratios in Urban Apolipoprotein E4 Children Exposed to Air Pollution. *Journal of Alzheimer's Disease*, *45*, 757–770. <http://doi.org/10.3233/JAD-142685>
- Cao, J., & Zhang, S. (2014). Multiple Comparison Procedures. *JAMA*, *312*(5), 543. <http://doi.org/10.1001/jama.2014.9440>
- Cavassila, S., Deval, S., Huegen, C., Van Ormondt, D., & Graveron-Demilly, D. (2001). Cramér-Rao bounds: An evaluation tool for quantitation. *NMR in Biomedicine*, *14*(4), 278–283. <http://doi.org/10.1002/nbm.701>
- Ceko, M., Gracely, J. L., Fitzcharles, M. -a., Seminowicz, D. a., Schweinhardt, P., & Bushnell, M. C. (2015). Is a Responsive Default Mode Network Required for Successful Working Memory Task Performance? *Journal of Neuroscience*, *35*(33), 11595–11605. <http://doi.org/10.1523/JNEUROSCI.0264-15.2015>
- Chan, K. L., Puts, N. A. J., Schar, M., Barker, P. B., & Edden, R. A. E. (2016). HERMES : Hadamard Encoding and Reconstruction of MEGA-Edited Spectroscopy. *Magnetic Resonance in Medicine*, *76*, 11–19. <http://doi.org/10.1002/mrm.26233>
- Cirrito, J. R., Yamada, K. A., Finn, M. B., Sloviter, R. S., Bales, K. R., May, P. C., ... Holtzman, D. M. (2005). Synaptic activity regulates interstitial fluid amyloid-beta levels in vivo. *Neuron*, *48*(6), 913–922. <http://doi.org/10.1016/j.neuron.2005.10.028>
- Corder, E. H., Saunders, A. M., Strittmatter, W. J., Schmechel, D. E., Gaskell, P. C., Small, G. W., ... Haines, J. L. (1993). Gene Dose of Apolipoprotein E Type 4 Allele and the Risk of Alzheimer ' s Disease in Late Onset Families, *8*(14), 41–43.
- Cushman, L. A., Stein, K., & Duffy, C. J. (2008). Detecting navigational deficits in cognitive aging and Alzheimer disease using virtual reality. *Neurology*, *71*, 888–895.
- Das, U., Scott, D. a, Ganguly, A., Koo, E. H., Tang, Y., & Roy, S. (2013). Activity-induced convergence of APP and BACE-1 in acidic microdomains via an endocytosis-

References

- dependent pathway. *Neuron*, 79(3), 447–60.
<http://doi.org/10.1016/j.neuron.2013.05.035>
- Daselaar, S. M., Prince, S. E., Dennis, N. a, Hayes, S. M., Kim, H., & Cabeza, R. (2009). Posterior midline and ventral parietal activity is associated with retrieval success and encoding failure. *Frontiers in Human Neuroscience*, 3(July), 13.
<http://doi.org/10.3389/neuro.09.013.2009>
- De Bondt, T., De Belder, F., Vanhevel, F., Jacquemyn, Y., & Parizel, P. M. (2014). Prefrontal GABA concentration changes in women-Influence of menstrual cycle phase, hormonal contraceptive use, and correlation with premenstrual symptoms. *Brain Research*, 1597, 129–138. <http://doi.org/10.1016/j.brainres.2014.11.051>
- Den Heijer, T., Van Der Lijn, F., Koudstaal, P. J., Hofman, A., Van Der Lugt, A., Krestin, G. P., ... Breteler, M. M. B. (2010). A 10-year follow-up of hippocampal volume on magnetic resonance imaging in early dementia and cognitive decline. *Brain*, 133(4), 1163–1172. <http://doi.org/10.1093/brain/awq048>
- Dennis, N. a, Browndyke, J. N., Stokes, J., Need, A., Burke, J. R., Welsh-Bohmer, K. a, & Cabeza, R. (2010). Temporal lobe functional activity and connectivity in young adult APOE varepsilon4 carriers. *Alzheimer's & Dementia : The Journal of the Alzheimer's Association*, 6(4), 303–11. <http://doi.org/10.1016/j.jalz.2009.07.003>
- Donahue, M. J., Near, J., Blicher, J. U., & Jezard, P. (2010). Baseline GABA concentration and fMRI response. *NeuroImage*, 53(2), 392–8.
<http://doi.org/10.1016/j.neuroimage.2010.07.017>
- Dreisbach, G. (2012). Mechanisms of Cognitive Control: The Functional Role of Task Rules. *Current Directions in Psychological Science*, 21(4), 227–231.
<http://doi.org/10.1177/0963721412449830>
- Dubois, B., Hampel, H., Feldman, H. H., Scheltens, P., Aisen, P., Andrieu, S., ... Jack, C. R. (2016). Preclinical Alzheimer's disease: Definition, natural history, and diagnostic criteria. *Alzheimer's & Dementia*, 12, 292–323.
<http://doi.org/10.1016/j.jalz.2016.02.002>
- Duncan, N. W., Enzi, B., Wiebking, C., & Northoff, G. (2011). Involvement of glutamate in rest-stimulus interaction between perigenual and supragenual anterior cingulate cortex: a combined fMRI-MRS study. *Human Brain Mapping*, 32(12), 2172–82.
<http://doi.org/10.1002/hbm.21179>
- Duncan, N. W., Wiebking, C., Munoz-Torres, Z., & Northoff, G. (2013). How to investigate neuro-biochemical relationships on a regional level in humans? Methodological considerations for combining functional with biochemical imaging. *Journal of Neuroscience Methods*, 221, 183–188.
<http://doi.org/10.1016/j.jneumeth.2013.10.011>
- Duncan, N. W., Wiebking, C., & Northoff, G. (2014). Associations of regional GABA and glutamate with intrinsic and extrinsic neural activity in humans-A review of

References

- multimodal imaging studies. *Neuroscience and Biobehavioral Reviews*, 47C, 36–52. <http://doi.org/10.1016/j.neubiorev.2014.07.016>
- Edden, R. A. E., Puts, N. A. J., Harris, A. D., Barker, P. B., & Evans, C. J. (2014). Gannet: A batch-processing tool for the quantitative analysis of gamma-aminobutyric acid-edited MR spectroscopy spectra. *Journal of Magnetic Resonance Imaging*, 40(6), 1445–1452. <http://doi.org/10.1002/jmri.24478>
- Eklund, A., Nichols, T. E., & Knutsson, H. (2016). Cluster failure : Why fMRI inferences for spatial extent have inflated false-positive rates. *PNAS*, 113(33), 7900–7905. <http://doi.org/10.1073/pnas.1612033113>
- Emir, U. E., Tuite, P. J., & Öz, G. (2012). Elevated pontine and putamenal GABA levels in mild-moderate Parkinson disease detected by 7 tesla proton MRS. *PloS One*, 7(1), e30918. <http://doi.org/10.1371/journal.pone.0030918>
- Ende, G. (2015). Proton Magnetic Resonance Spectroscopy: Relevance of Glutamate and GABA to Neuropsychology. *Neuropsychology Review*, 25, 315–325. <http://doi.org/10.1007/s11065-015-9295-8>
- Enzi, B., Duncan, N. W., Kaufmann, J., Tempelmann, C., Wiebking, C., & Northoff, G. (2012). Glutamate modulates resting state activity in the perigenual anterior cingulate cortex - a combined fMRI-MRS study. *Neuroscience*, 227, 102–9. <http://doi.org/10.1016/j.neuroscience.2012.09.039>
- Epperson, C. N., Haga, K., Mason, G. F., Sellers, E., & Gueorguieva, R. (2002). Cortical gamma-Aminobutyric Acid Levels Across the Menstrual Cycle in Healthy Women and Those With Premenstrual Dysphoric Disorder. *Arch Gen Psychiatry*, 59, 851–858.
- Epperson, C. N., O'Malley, S., Czarkowski, K. a, Gueorguieva, R., Jatlow, P., Sanacora, G., ... Mason, G. F. (2005). Sex, GABA, and nicotine: the impact of smoking on cortical GABA levels across the menstrual cycle as measured with proton magnetic resonance spectroscopy. *Biological Psychiatry*, 57(1), 44–8. <http://doi.org/10.1016/j.biopsych.2004.09.021>
- Epstein, R. a, & Higgins, J. S. (2007). Differential parahippocampal and retrosplenial involvement in three types of visual scene recognition. *Cerebral Cortex*, 17, 1680–93. <http://doi.org/10.1093/cercor/bhl079>
- Epstein, R., & Kanwisher, N. (1998). A cortical representation of the local visual environment. *Nature*, 392(6676), 598–601.
- Erlander, M. G., Tillakaratne, N. J. K., Feldblum, S., Patel, N., & Tobin, A. J. (1991). Two Genes Encode Distinct Glutamate Decarboxylases. *Neuron*, 7, 91–100.
- Escott-Price, V., Sims, R., Bannister, C., Harold, D., Vronskaya, M., Majounie, E., ... Williams, J. (2015). Common polygenic variation enhances risk prediction for Alzheimer's disease. *Brain*, 138(12), 3673–3684. <http://doi.org/10.1093/brain/awv268>

References

- Esposito, F., Aragri, A., Latorre, V., Popolizio, T., Scarabino, T., Cirillo, S., ... Di Salle, F. (2009). Does the default-mode functional connectivity of the brain correlate with working-memory performances? *Archives Italiennes de Biologie*, *147*, 11–20.
- Falkenberg, L. E., Specht, K., & Westerhausen, R. (2011). Attention and cognitive control networks assessed in a dichotic listening fMRI study. *Brain and Cognition*, *76*, 276–285. <http://doi.org/10.1016/j.bandc.2011.02.006>
- Falkenberg, L. E., Westerhausen, R., Craven, A. R., Johnsen, E., Kroken, R. a, L Berg, E.-M., ... Hugdahl, K. (2014). Impact of glutamate levels on neuronal response and cognitive abilities in schizophrenia. *NeuroImage: Clinical*, *4*, 576–84. <http://doi.org/10.1016/j.nicl.2014.03.014>
- Falkenberg, L. E., Westerhausen, R., Specht, K., & Hugdahl, K. (2012). Resting-state glutamate level in the anterior cingulate predicts blood-oxygen level-dependent response to cognitive control. *Proceedings of the National Academy of Sciences of the United States of America*, *109*(13), 5069–73. <http://doi.org/10.1073/pnas.1115628109>
- Farrant, M., & Nusser, Z. (2005). Variations on an inhibitory theme: phasic and tonic activation of GABA(A) receptors. *Nature Reviews. Neuroscience*, *6*(3), 215–229. <http://doi.org/10.1038/nrn1625>
- Farrer, L. A. L. A., Cupples, A., Haines, J. L., Hyman, B., Kukull, W. A. W. A., Mayeux, R., ... the APOE and Alzheimer Disease Meta Analysis Consortium. (1997). Effects of Age, Sex, and Ethnicity on the Association Between Apolipoprotein E Genotype and Alzheimer Disease. *Journal of the American Medical Association*, *278*, 1349–1356.
- Faul, F., Erdfelder, E., Buchner, A., & Lang, A.-G. (2009). Statistical power analyses using G*Power 3.1: tests for correlation and regression analyses. *Behavior Research Methods*, *41*(4), 1149–60. <http://doi.org/10.3758/BRM.41.4.1149>
- Fayed, N., Modrego, P. J., Rojas-Salinas, G., & Aguilar, K. (2011). Brain glutamate levels are decreased in Alzheimer's disease: a magnetic resonance spectroscopy study. *American Journal of Alzheimer's Disease and Other Dementias*, *26*(6), 450–6. <http://doi.org/10.1177/1533317511421780>
- Filippini, N., Ebmeier, K. P., MacIntosh, B. J., Trachtenberg, A. J., Frisoni, G. B., Wilcock, G. K., ... Mackay, C. E. (2011). Differential effects of the APOE genotype on brain function across the lifespan. *NeuroImage*, *54*(1), 602–10. <http://doi.org/10.1016/j.neuroimage.2010.08.009>
- Filippini, N., MacIntosh, B. J., Hough, M. G., Goodwin, G. M., Frisoni, G. B., Smith, S. M., ... Mackay, C. E. (2009). Distinct patterns of brain activity in young carriers of the APOE-epsilon4 allele. *Proceedings of the National Academy of Sciences of the United States of America*, *106*(17), 7209–7214. <http://doi.org/10.1073/pnas.0811879106>
- Fleisher, A. S., Chen, K., Quiroz, Y. T., Jakimovich, L. J., Gomez, M. G., Langois, C. M., ... Reiman, E. M. (2012). Florbetapir PET analysis of amyloid- β deposition in the

- presenilin 1 E280A autosomal dominant Alzheimer's disease kindred: A cross-sectional study. *The Lancet Neurology*, 11(12), 1057–1065. [http://doi.org/10.1016/S1474-4422\(12\)70227-2](http://doi.org/10.1016/S1474-4422(12)70227-2)
- Foley, S. F., Tansey, K. E., Caseras, X., Lancaster, T., Bracht, T., Parker, G., ... Linden, D. (2016). Multimodal brain imaging reveals structural differences in Alzheimer's disease polygenic risk carriers: A study in healthy young adults. *Biological Psychiatry*, 1(22), 1–8. <http://doi.org/10.1016/j.biopsych.2016.02.033>
- Ford, T. C., & Crewther, D. P. (2016). A Comprehensive Review of the 1H-MRS Metabolite Spectrum in Autism Spectrum Disorder. *Frontiers in Molecular Neuroscience*, 9(March), 1–14. <http://doi.org/10.3389/fnmol.2016.00014>
- Fox, N. C., Warrington, E. K., Stevens, J. M., & Rossor, M. N. (1996). Atrophy of the hippocampal formation in early familial Alzheimer's disease. A longitudinal MRI study of at-risk members of a family with an amyloid precursor protein 717Val-Gly mutation. *Ann N Y Acad Sci*, 777, 226–232. http://doi.org/Thesis_references-Converted#106
- Fransson, P., & Marrelec, G. (2008). The precuneus/posterior cingulate cortex plays a pivotal role in the default mode network: Evidence from a partial correlation network analysis. *NeuroImage*, 42(3), 1178–84. <http://doi.org/10.1016/j.neuroimage.2008.05.059>
- Gasparovic, C., Arfai, N., Smid, N., & Feeney, D. M. (2001). Decrease and Recovery of N-Acetylaspartate/Creatine in Rat Brain Remote from Focal Injury. *Journal of Neurotrauma*, 18(3), 241–246. <http://doi.org/10.1089/08977150151070856>
- Gatz, M., Reynolds, C., Fratiglioni, L., Johansson, B., Martimer, J., Berg, S., ... Pedersen, N. (2006). Role of Genes and Environments for Explaining Alzheimer Disease. *Arch Gen Psychiatry*, 63, 168–174.
- Gimenez, M., Junque, C., Narberhaus, C. A. A., Caldu, X., Segarra, D., Vendrell, P., ... Mercader, J. (2004). Medial temporal MR spectroscopy is related to memory performance in normal adolescent subjects, 15(4), 18–22. <http://doi.org/10.1097/01.wnr.00001>
- Godbolt, A. K., Waldman, A. D., Macmanus, D. G., Schott, J. M., Frost, C., Cipolotti, L., ... Rossor, M. N. (2006). MRS shows abnormalities before symptoms in familial Alzheimer disease. *Neurology*, 66, 718–722.
- Gomar, J. J., Gordon, M. L., Dickinson, D., Kingsley, P. B., Uluğ, A. M., Keehlisen, L., ... Goldberg, T. E. (2014). APOE Genotype Modulates Proton Magnetic Resonance Spectroscopy Metabolites in the Aging Brain. *Biological Psychiatry*, 75(9), 686–692. <http://doi.org/10.1016/j.biopsych.2013.05.022>
- Govindaraju, V., Young, K., & Maudsley, A. A. (2000). Proton NMR chemical shifts and coupling constants for brain metabolites. *NMR in Biomedicine*, 13(3), 129–153. [http://doi.org/10.1002/1099-1492\(200005\)13:3<129::AID-NBM619>3.0.CO;2-V](http://doi.org/10.1002/1099-1492(200005)13:3<129::AID-NBM619>3.0.CO;2-V)

References

- Graham, K. S., Barense, M. D., & Lee, A. C. H. (2010). Going beyond LTM in the MTL: a synthesis of neuropsychological and neuroimaging findings on the role of the medial temporal lobe in memory and perception. *Neuropsychologia*, *48*(4), 831–53. <http://doi.org/10.1016/j.neuropsychologia.2010.01.001>
- Greicius, M. D., Srivastava, G., Reiss, A. L., & Menon, V. (2004). Default-mode network activity distinguishes Alzheimer's disease from healthy aging: evidence from functional MRI. *Proceedings of the National Academy of Sciences of the United States of America*, *101*(13), 4637–42. <http://doi.org/10.1073/pnas.0308627101>
- Greicius, M. D., Supekar, K., Menon, V., & Dougherty, R. F. (2009). Resting-state functional connectivity reflects structural connectivity in the default mode network. *Cerebral Cortex*, *19*(1), 72–78. <http://doi.org/10.1093/cercor/bhn059>
- Guterstam, A., Björnsdotter, M., Gentile, G., & Ehrsson, H. H. (2015). Posterior Cingulate Cortex Integrates the Senses of Self-Location and Body Ownership. *Current Biology*, *25*(12), 1416–1425. <http://doi.org/10.1016/j.cub.2015.03.059>
- Haase, A. (1986). Localization of Unaffected Spins in NMR Imaging and Spectroscopy (LOCUS Spectroscopy). *Magnetic Resonance in Medicine*, *9*(6), 963–969.
- Hadjikhani, N., Liu, a K., Dale, a M., Cavanagh, P., & Tootell, R. B. (1998). Retinotopy and color sensitivity in human visual cortical area V8. *Nature Neuroscience*, *1*(3), 235–41. <http://doi.org/10.1038/681>
- Hafkemeijer, A., van der Grond, J., & Rombouts, S. a R. B. (2012). Imaging the default mode network in aging and dementia. *Biochimica et Biophysica Acta*, *1822*(3), 431–41. <http://doi.org/10.1016/j.bbadis.2011.07.008>
- Hagmann, P., Cammoun, L., Gigandet, X., Meuli, R., Honey, C. J., Van Wedeen, J., & Sporns, O. (2008). Mapping the structural core of human cerebral cortex. *PLoS Biology*, *6*(7), 1479–1493. <http://doi.org/10.1371/journal.pbio.0060159>
- Han, S. D., & Bondi, M. W. (2008). Revision of the apolipoprotein E compensatory mechanism recruitment hypothesis. *Alzheimer's & Dementia: The Journal of the Alzheimer's Association*, *4*(4), 251–4. <http://doi.org/10.1016/j.jalz.2008.02.006>
- Hao, X., Xu, D., Bansal, R., Dong, Z., Liu, J., Wang, Z., ... Peterson, B. S. (2013). Multimodal magnetic resonance imaging: The coordinated use of multiple, mutually informative probes to understand brain structure and function. *Human Brain Mapping*, *34*(2), 253–71. <http://doi.org/10.1002/hbm.21440>
- Harada, M., Kubo, H., Nose, A., Nishitani, H., & Matsuda, T. (2011). Measurement of variation in the human cerebral GABA level by in vivo MEGA-editing proton MR spectroscopy using a clinical 3 T instrument and its dependence on brain region and the female menstrual cycle. *Human Brain Mapping*, *32*(5), 828–33. <http://doi.org/10.1002/hbm.21086>
- Harold, D., Abraham, R., Hollingworth, P., Sims, R., Gerrish, A., Hamshere, M. L., ...

- Williams, J. (2009). Genome-wide association study identifies variants at CLU and PICALM associated with Alzheimer's disease. *Nature Genetics*, *41*(10), 1088–93. <http://doi.org/10.1038/ng.440>
- Harris, A. D., Puts, N. a J., Anderson, B. a, Yantis, S., Pekar, J. J., Barker, P. B., & Edden, R. a E. (2015). Multi-Regional Investigation of the Relationship between Functional MRI Blood Oxygenation Level Dependent (BOLD) Activation and GABA Concentration. *PloS One*, *10*(2), e0117531. <http://doi.org/10.1371/journal.pone.0117531>
- Hartley, T., Bird, C. M., Chan, D., Cipolotti, L., Husain, M., Vargha-khadem, F., & Burgess, N. (2007). The Hippocampus Is Required for Short-Term Topographical Memory in Humans, *48*, 34–48. <http://doi.org/10.1002/hipo>
- Hassabis, D., & Maguire, E. A. (2007). Deconstructing episodic memory with construction. *Trends in Cognitive Sciences*, *11*(7), 299–306. <http://doi.org/10.1016/j.tics.2007.05.001>
- Henson, R. (2006). Efficient Experimental Design for fMRI, 193–210.
- Hepp, H. H., Maier, S., Hermle, L., & Spitzer, M. (1996). The Stroop effect in schizophrenic patients. *Schizophrenia Research*, *22*(3), 187–195.
- Hodgetts, C. J., Postans, M., Shine, J. P., Jones, D. K., Lawrence, A. D., & Graham, K. S. (2015). Dissociable roles of the inferior longitudinal fasciculus and fornix in face and place perception. *eLife*, *4*, 1–25. <http://doi.org/10.7554/eLife.07902>
- Hodgetts, C. J., Shine, J. P., Lawrence, A. D., Downing, P. E., & Graham, K. S. (2016). Evidencing a Place for the Hippocampus Within the Core Scene Processing Network. *Human Brain Mapping*, *37*(11), 3779–3974. <http://doi.org/10.1002/hbm.23275>
- Hoerst, M., Weber-Fahr, W., Tunc-Skarka, N., Ruf, M., Bohus, M., Schmahl, C., & Ende, G. (2010). Correlation of glutamate levels in the anterior cingulate cortex with self-reported impulsivity in patients with borderline personality disorder and healthy controls. *Archives of General Psychiatry*, *67*(9), 946–954. <http://doi.org/10.1001/archgenpsychiatry.2010.93>
- Hollingworth, P., Harold, D., Jones, L., Owen, M. J., & Williams, J. (2011). Alzheimer's disease genetics: Current knowledge and future challenges. *International Journal of Geriatric Psychiatry*, *26*(8), 793–802. <http://doi.org/10.1002/gps.2628>
- Hu, Y., Chen, X., Gu, H., & Yang, Y. (2013). Resting-state glutamate and GABA concentrations predict task-induced deactivation in the default mode network. *The Journal of Neuroscience: The Official Journal of the Society for Neuroscience*, *33*(47), 18566–73. <http://doi.org/10.1523/JNEUROSCI.1973-13.2013>
- Huang, Y. (2011). Roles of apolipoprotein E4 (ApoE4) in the pathogenesis of Alzheimer's disease: lessons from ApoE mouse models. *Biochemical Society Transactions*, *39*(4), 924–32. <http://doi.org/10.1042/BST0390924>

References

- Huang, Y., & Mahley, R. W. (2014). Apolipoprotein E: structure and function in lipid metabolism, neurobiology, and Alzheimer's diseases. *Neurobiology of Disease, 72 Pt A*, 3–12. <http://doi.org/10.1016/j.nbd.2014.08.025>
- Hubel, D. ., & Wiesel, T. . (1959). Receptive fields of single neuronse in the cat's striate cortex. *Journal of Physiology, 148*, 574–591.
- Huettel, S. A., Song, A. W., & McCarthy, G. (2009). *Functional Magnetic Resonance Imaging*.
- Huijbers, W., Vannini, P., Sperling, R. a, C M, P., Cabeza, R., & Daselaar, S. M. (2012). Explaining the encoding/retrieval flip: memory-related deactivations and activations in the posteromedial cortex. *Neuropsychologia, 50*(14), 3764–74. <http://doi.org/10.1016/j.neuropsychologia.2012.08.021>
- Hutcheson, N. L., Reid, M. a, White, D. M., Kraguljac, N. V, Avsar, K. B., Bolding, M. S., ... Lahti, A. C. (2012). Multimodal analysis of the hippocampus in schizophrenia using proton magnetic resonance spectroscopy and functional magnetic resonance imaging. *Schizophrenia Research, 140*(1-3), 136–42. <http://doi.org/10.1016/j.schres.2012.06.039>
- Irish, M., Halena, S., Kamminga, J., Tu, S., Hornberger, M., & Hodges, J. R. (2015). Scene construction impairments in Alzheimer's disease – a unique role for the posterior cingulate cortex. *Cortex, 73*, 10–23. <http://doi.org/10.1016/j.cortex.2015.08.004>
- Jack, C. R., Knopman, D. S., Jagust, W. J., Petersen, R. C., Weiner, M. W., Aisen, P. S., ... Trojanowski, J. Q. (2013). Tracking pathophysiological processes in Alzheimer's disease: an updated hypothetical model of dynamic biomarkers. *Lancet Neurology, 12*(2), 207–16. [http://doi.org/10.1016/S1474-4422\(12\)70291-0](http://doi.org/10.1016/S1474-4422(12)70291-0)
- Jack, C. R., Knopman, D. S., Jagust, W. J., Shaw, L. M., Aisen, P. S., Weiner, M. W., ... Trojanowski, J. Q. (2010). Hypothetical model of dynamic biomarkers of the Alzheimer's pathological cascade. *Lancet Neurology, 9*(1), 119–28. [http://doi.org/10.1016/S1474-4422\(09\)70299-6](http://doi.org/10.1016/S1474-4422(09)70299-6)
- Jarosz, A. F., & Wiley, J. (2014). Journal of Problem Solving What Are the Odds? A Practical Guide to Computing and Reporting Bayes Factors, 7, 2–9.
- Jenkinson, M. (2003). Fast, automated, N-dimensional phase-unwrapping algorithm. *Magnetic Resonance in Medicine, 49*(1), 193–197. <http://doi.org/10.1002/mrm.10354>
- Jenkinson, M., Bannister, P., Brady, M., & Smith, S. (2002). Improved Optimization for the Robust and Accurate Linear Registration and Motion Correction of Brain Images, 841, 825–841. <http://doi.org/10.1006/nimg.2002.1132>
- Jessen, F., Gur, O., Block, W., Ende, G., Frolich, L., Hammen, T., ... Traber, F. (2009). A multicenter H-MRS study of the medial temporal lobe in AD and MCI. *Neurology, 72*(20), 1735–1740. <http://doi.org/10.1212/WNL.0b013e3181a60a20>

References

- Johnson, K. a, Fox, N. C., Sperling, R. a, & Klunk, W. E. (2012). Brain imaging in Alzheimer disease. *Cold Spring Harbor Perspectives in Medicine*, 2(4), a006213. <http://doi.org/10.1101/cshperspect.a006213>
- Jones, D. K., Christiansen, K. F., Chapman, R. J., & Aggleton, J. P. (2013). Distinct subdivisions of the cingulum bundle revealed by diffusion MRI fibre tracking: implications for neuropsychological investigations. *Neuropsychologia*, 51(1), 67–78. <http://doi.org/10.1016/j.neuropsychologia.2012.11.018>
- Jung, R. E., Haier, R. J., Yeo, R. a, Rowland, L. M., Petropoulos, H., Levine, A. S., ... Brooks, W. M. (2005). Sex differences in N-acetylaspartate correlates of general intelligence: an 1H-MRS study of normal human brain. *NeuroImage*, 26(3), 965–72. <http://doi.org/10.1016/j.neuroimage.2005.02.039>
- Jung, R. E., Yeo, R. A., Chiulli, S. J., Sibbitt, W. L., Weers, D. C., Hart, B. L., & Brooks, W. M. (1999). Biochemical markers of cognition: a proton MR spectroscopy study of normal human brain. *Neuroreport*, 10(16), 3327–31. Retrieved from <http://www.ncbi.nlm.nih.gov/pubmed/10599840>
- Kantarci, K., Jack Jr, C. R., Xu, T. C., Campeau, N. G., O'Brien, P. C., Smith, G. E., ... Petersen, R. C. (2000). Regional metabolic patterns in mild cognitive impairment and Alzheimer's disease: A 1H-MRS Study. *Neurology*, 55(2), 210–217.
- Kantarci, K., Smith, G. E., Ivnik, R. J., Petersen, R. C., Bradley, F., Knopman, D. S., ... Jr, C. R. J. (2002). 1H Magnetic Resonance Spectroscopy, Cognitive Function, and Apolipoprotein E Genotype in Normal Aging, Mild Cognitive Impairment and Alzheimer's Disease. *J Int Neuropsychol Soc*, 8(7), 934–942.
- Kantarci, K., Weigand, S. D., Petersen, R. C., Boeve, B. F., Knopman, D. S., Gunter, J., ... Jack, C. R. (2007). Longitudinal 1H MRS changes in mild cognitive impairment and Alzheimer's disease. *Neurobiology of Aging*, 28(9), 1330–9. <http://doi.org/10.1016/j.neurobiolaging.2006.06.018>
- Kantarci, K., Weigand, S. D., Przybelski, S. A., Preboske, G. M., Pankratz, V. S., Murphy, M. C., ... Petersen, R. C. (2013). MRI and MRS predictors of mild cognitive impairment in a population-based sample.
- Kanwisher, N., & Yovel, G. (2006). The fusiform face area: a cortical region specialized for the perception of faces. *Philosophical Transactions of the Royal Society of London. Series B, Biological Sciences*, 361(1476), 2109–28. <http://doi.org/10.1098/rstb.2006.1934>
- Kapogiannis, D., Reiter, D. a, Willette, A. a, & Mattson, M. P. (2013). Posteromedial cortex glutamate and GABA predict intrinsic functional connectivity of the default mode network. *NeuroImage*, 64, 112–9. <http://doi.org/10.1016/j.neuroimage.2012.09.029>
- Klunk, W. E., Engler, H., Nordberg, A., Wang, Y., Blomqvist, G., Holt, D. P., ... Långstro, B. (2004). Imaging Brain Amyloid in Alzheimer ' s Disease with Pittsburgh Compound-

References

B, 306–319.

- Kunz, L., Schroder, T. N., Lee, H., Montag, C., Lachmann, B., Sariyska, R., ... Axmacher, N. (2015). Reduced grid-cell-like representations in adults at genetic risk for Alzheimer's disease. *Science*, *350*(6259), 430–433. <http://doi.org/10.1126/science.aac8128>
- Laakso, M. P., Hiltunen, Y., Könönen, M., Kivipelto, M., Koivisto, A., Hallikainen, M., & Soininen, H. (2003). Decreased brain creatine levels in elderly apolipoprotein E epsilon 4 carriers. *Journal of Neural Transmission (Vienna, Austria : 1996)*, *110*(3), 267–275. <http://doi.org/10.1007/s00702-002-0783-7>
- Lambert, J. C., Ibrahim-Verbaas, C. a, Harold, D., Naj, a C., Sims, R., Bellenguez, C., ... Amouyel, P. (2013). Meta-analysis of 74,046 individuals identifies 11 new susceptibility loci for Alzheimer's disease. *Nature Genetics*, *45*(12), 1452–8. <http://doi.org/10.1038/ng.2802>
- Landim, R., Edden, R., Foerster, B., Li, L., Covolan, R., & Castellano, G. (2016). Investigation of NAA and NAAG dynamics underlying visual stimulation using MEGA-PRESS in a functional MRS experiment. *Magnetic Resonance Imaging*, *34*(3), 239–45.
- Lee, A. C. H., Buckley, M. J., Gaffan, D., Emery, T., Hodges, J. R., & Graham, K. S. (2006). Differentiating the roles of the hippocampus and perirhinal cortex in processes beyond long-term declarative memory: a double dissociation in dementia. *The Journal of Neuroscience : The Official Journal of the Society for Neuroscience*, *26*(19), 5198–203. <http://doi.org/10.1523/JNEUROSCI.3157-05.2006>
- Lee, A. C. H., Buckley, M. J., Pegman, S. J., Spiers, H., Scahill, V. L., Gaffan, D., ... Graham, K. S. (2005). Specialization in the medial temporal lobe for processing of objects and scenes. *Hippocampus*, *15*(6), 782–97. <http://doi.org/10.1002/hipo.20101>
- Lee, A. C. H., Levi, N., Davies, R. R., Hodges, J. R., & Graham, K. S. (2007). Differing profiles of face and scene discrimination deficits in semantic dementia and Alzheimer's disease. *Neuropsychologia*, *45*(9), 2135–46. <http://doi.org/10.1016/j.neuropsychologia.2007.01.010>
- Lee, A. C. H., & Rudebeck, S. R. (2010). Investigating the Interaction between Spatial Perception and Working Memory in the Human Medial Temporal Lobe, 2823–2835.
- Lee, A. C. H., Scahill, V. L., & Graham, K. S. (2008). Activating the medial temporal lobe during oddity judgment for faces and scenes. *Cerebral Cortex (New York, N.Y. : 1991)*, *18*(3), 683–96. <http://doi.org/10.1093/cercor/bhm104>
- Lee, I. A., & Preacher, K. J. (2013). Calculation for the test of the difference between two dependent correlations with one variable in common. Retrieved from Available from <http://quantpsy.org>.
- Leech, R., Braga, R., & Sharp, D. J. (2012). Echoes of the Brain within the Posterior Cingulate Cortex, *32*(1), 215–222. <http://doi.org/10.1523/JNEUROSCI.3689-1198>

11.2012

- Leech, R., & Sharp, D. J. (2013). The role of the posterior cingulate cortex in cognition and disease. *Brain : A Journal of Neurology*. <http://doi.org/10.1093/brain/awt162>
- Li, B. S. Y., Wang, H., & Gonen, O. (2003). Metabolite ratios to assumed stable creatine level may confound the quantification of proton brain MR spectroscopy. *Magnetic Resonance Imaging*, 21(8), 923–928. [http://doi.org/10.1016/S0730-725X\(03\)00181-4](http://doi.org/10.1016/S0730-725X(03)00181-4)
- Lieberman, M. D., & Cunningham, W. A. (2009). Type I and Type II error concerns in fMRI research: Re-balancing the scale. *Social Cognitive and Affective Neuroscience*, 4(4), 423–428. <http://doi.org/10.1093/scan/nsp052>
- Lipp, I., Evans, C. J., Lewis, C., Murphy, K., Wise, R. G., & Caseras, X. (2015). The Relationship between Fearfulness, GABA+, and Fear-Related BOLD Responses in the Insula. *PLoS One*, 10(3), e0120101. <http://doi.org/10.1371/journal.pone.0120101>
- Lithfous, S., Dufour, A., & Després, O. (2013). Spatial navigation in normal aging and the prodromal stage of Alzheimer's disease: insights from imaging and behavioral studies. *Ageing Research Reviews*, 12(1), 201–13. <http://doi.org/10.1016/j.arr.2012.04.007>
- Liu, C.-C., Kanekiyo, T., Xu, H., & Bu, G. (2013). Apolipoprotein E and Alzheimer disease: risk, mechanisms and therapy. *Nature Reviews. Neurology*, 9(2), 106–18. <http://doi.org/10.1038/nrneurol.2012.263>
- Logothetis, N. K. (2002). The neural basis of the blood-oxygen-level-dependent functional magnetic resonance imaging signal. *Philosophical Transactions of the Royal Society B: Biological Sciences*, 357(1424), 1003–1037. <http://doi.org/10.1098/rstb.2002.1114>
- Logothetis, N. K., Pauls, J., Augath, M., Trinath, T., & Oeltermann, A. (2001). Neurophysiological investigation of the basis of the fMRI signal. *Nature*, 412(6843), 150–7. <http://doi.org/10.1038/35084005>
- Logothetis, N. K., & Pfeuffer, J. (2004). On the nature of the BOLD fMRI contrast mechanism. *Magnetic Resonance Imaging*, 22(10 SPEC. ISS.), 1517–1531. <http://doi.org/10.1016/j.mri.2004.10.018>
- Londono, A. C., Castellanos, F. X., Arbelaez, A., Ruiz, A., Aguirre-Acevedo, D. C., Richardson, A. M., ... Lopera, F. (2013). An (1)H-MRS framework predicts the onset of Alzheimer's disease symptoms in PSEN1 mutation carriers. *Alzheimer's & Dementia : The Journal of the Alzheimer's Association*, 10(5), 552–561. <http://doi.org/10.1016/j.jalz.2013.08.282>
- Lustig, C., Snyder, A. Z., Bhakta, M., O'Brien, K. C., McAvoy, M., Raichle, M. E., ... Buckner, R. L. (2003). Functional deactivations: change with age and dementia of the Alzheimer type. *Proc Natl Acad Sci U S A*, 100(24), 14504–14509.

References

<http://doi.org/10.1073/pnas.2235925100>\r2235925100 [pii]

Lynn, S. K., & Barrett, L. F. (2014). "Utilizing" Signal Detection Theory. *Psychological Science*, 25(9), 1663–1673. <http://doi.org/10.1177/0956797614541991>

Maddock, R. J., & Buonocore, M. H. (2012). MR Spectroscopic Studies of the Brain in Psychiatric Disorders. In *Brain Imaging in Behavioural Neuroscience* (pp. 199–249). Springer-Verlag Berlin Heidelberg. <http://doi.org/10.1007/7854>

Mahley, R. W., & Huang, Y. (2012). Apolipoprotein e sets the stage: response to injury triggers neuropathology. *Neuron*, 76(5), 871–85. <http://doi.org/10.1016/j.neuron.2012.11.020>

Mansouri, F. A., Buckley, M. J., Mahboubi, M., & Tanaka, K. (2015). Behavioral consequences of selective damage to frontal pole and posterior cingulate cortices. *Proceedings of the National Academy of Sciences of the United States of America*, 112(29), E3940–3949. <http://doi.org/10.1073/pnas.1422629112>

Markram, H., Toledo-Rodriguez, M., Wang, Y., Gupta, A., Silberberg, G., & Wu, C. (2004). Interneurons of the neocortical inhibitory system. *Nature Reviews. Neuroscience*, 5(10), 793–807. <http://doi.org/10.1038/nrn1519>

Martin, D., & Barke, K. (1998). Are GAD65 and GAD67 associated with specific pools of GABA in brain? *Perspectives on Developmental Neurobiology*, 5(2-3), 119–129.

McKhann, G. M., Knopman, D. S., Chertkow, H., Hyman, B. T., Jack, C. R., Kawas, C. H., ... Phelps, C. H. (2011). The diagnosis of dementia due to Alzheimer's disease: recommendations from the National Institute on Aging-Alzheimer's Association workgroups on diagnostic guidelines for Alzheimer's disease. *Alzheimer's & Dementia: The Journal of the Alzheimer's Association*, 7(3), 263–9. <http://doi.org/10.1016/j.jalz.2011.03.005>

Mckiernan, K. A., Kaufman, J. N., Kucera-Thompson, J., & Binder, J. R. (2003). A Parametric Manipulation of Factors Affecting Task-induced Deactivation in Functional Neuroimaging. *Journal of Cognitive Neuroscience*, 15(3), 394–408.

Mescher, M., Merkle, H., Kirsch, J., Garwood, M., & Gruetter, R. (1998). Simultaneous in vivo spectral editing and water suppression. *NMR in Biomedicine*, 11(6), 266–72. Retrieved from <http://www.ncbi.nlm.nih.gov/pubmed/9802468>

Mikkelsen, M., Singh, K. D., Sumner, P., & Evans, C. J. (2015). Comparison of the Repeatability of GABA-Edited Magnetic Resonance Spectroscopy with and without Macromolecule Suppression, 00, 1–8. <http://doi.org/10.1002/mrm.25699>

Minoshima, S., Giordani, B., Berent, S., Frey, K. a, Foster, N. L., & Kuhl, D. E. (1997). Metabolic reduction in the posterior cingulate cortex in very early Alzheimer's disease. *Annals of Neurology*, 42(1), 85–94. <http://doi.org/10.1002/ana.410420114>

References

- Modi, S., Rana, P., Kaur, P., Rani, N., & Khushu, S. (2014). Glutamate level in anterior cingulate predicts anxiety in healthy humans: A magnetic resonance spectroscopy study. *Psychiatry Res*, *224*(1), 34–41.
- Moffett, J. R. (2007). N-Acetylaspartate in the CNS: From Neurodiagnostics to Neurobiology, *81*(2), 89–131.
- Moghaddam, B., & Javitt, D. (2012). From revolution to evolution: the glutamate hypothesis of schizophrenia and its implication for treatment. *Neuropsychopharmacology: Official Publication of the American College of Neuropsychopharmacology*, *37*(1), 4–15. <http://doi.org/10.1038/npp.2011.181>
- Monacelli, A. M., Cushman, L. A., Kavcic, V., & Duffy, C. J. (2003). Spatial Disorientation in Alzheimer's Disease. *JAMA Neurology*, *61*, 1491–1497. <http://doi.org/10.1001/archneur.1989.00520400045018>
- Mosconi, L., Sorbi, S., de Leon, M. J., Li, Y., Nacmias, B., Myoung, P. S., ... Pupi, A. (2006). Hypometabolism exceeds atrophy in presymptomatic early-onset familial Alzheimer's disease. *Journal of Nuclear Medicine: Official Publication, Society of Nuclear Medicine*, *47*(11), 1778–1786. <http://doi.org/47/11/1778> [pii]
- Mullins, P. G., McGonigle, D. J., O'Gorman, R. L., Puts, N. a J., Vidyasagar, R., Evans, C. J., & Edden, R. a E. (2014). Current practice in the use of MEGA-PRESS spectroscopy for the detection of GABA. *NeuroImage*, *86*, 43–52. <http://doi.org/10.1016/j.neuroimage.2012.12.004>
- Murray, M. E., Przybelski, S. a., Lesnick, T. G., Liesinger, a. M., Spsychalla, a., Zhang, B., ... Kantarci, K. (2014). Early Alzheimer's Disease Neuropathology Detected by Proton MR Spectroscopy. *Journal of Neuroscience*, *34*(49), 16247–16255. <http://doi.org/10.1523/JNEUROSCI.2027-14.2014>
- Muthukumaraswamy, S. D., Edden, R. A. E., Jones, D. K., Swettenham, J. B., & Singh, K. D. (2009). Resting GABA concentration predicts peak gamma frequency and fMRI amplitude in response to visual stimulation in humans, *106*(20), 2–7.
- Muthukumaraswamy, S. D., Evans, C. J., Edden, R. a E., Wise, R. G., & Singh, K. D. (2012). Individual variability in the shape and amplitude of the BOLD-HRF correlates with endogenous GABAergic inhibition. *Human Brain Mapping*, *33*(2), 455–65. <http://doi.org/10.1002/hbm.21223>
- Nakagawa, S. (2004). A farewell to Bonferroni: The problems of low statistical power and publication bias. *Behavioral Ecology*, *15*(6), 1044–1045. <http://doi.org/10.1093/beheco/arh107>
- Nakamura, T., Watanabe, A., Fujino, T., Hosono, T., & Michikawa, M. (2009). Apolipoprotein E4 (1-272) fragment is associated with mitochondrial proteins and affects mitochondrial function in neuronal cells. *Molecular Neurodegeneration*, *4*, 35. <http://doi.org/10.1186/1750-1326-4-35>

References

- Nikolaidis, A., Baniqued, P. L., Kranz, M. B., Scavuzzo, C. J., Barbey, A. K., Kramer, A. F., & Larsen, R. J. (2016). Multivariate Associations of Fluid Intelligence and NAA. *Cerebral Cortex*, *bhw070*. <http://doi.org/10.1093/cercor/bhw070>
- Northoff, G., Walter, M., Schulte, R. F., Beck, J., & Dydak, U. (n.d.). GABA concentration in the human anterior cingulate cortex predicts negative BOLD response in fMRI Supporting online material: Supplementary Figure 1 Supplementary Table 1 Supplementary Table 2 Supplementary Methods.
- Northoff, G., Walter, M., Schulte, R. F., Beck, J., Dydak, U., Henning, A., ... Boesiger, P. (2007). GABA concentrations in the human anterior cingulate cortex predict negative BOLD responses in fMRI. *Nature Neuroscience*, *10*(12), 1515–7. <http://doi.org/10.1038/nn2001>
- Olman, C. A., Davachi, L., & Inati, S. (2009). Distortion and Signal Loss in Medial Temporal Lobe, *4*(12). <http://doi.org/10.1371/journal.pone.0008160>
- Osborne, J. W., & Overbay, A. (2004). The power of outliers (and why researchers should always check for them). *Practical Assessment, Research & Evaluation*, *9*(6).
- Oz, G., Alger, J. R., Barker, P. B., Bartha, R., Bolan, P. J., Brindle, K. M., ... Hurd, R. E. (2014). Clinical Proton MR Spectroscopy in Central Nervous System. *Radiology*, *270*(3).
- Oz, G., Nelson, C. D., Koski, D. M., Henry, P.-G., Marjanska, M., Deelchand, D. K., ... Clark, H. B. (2010). Noninvasive detection of presymptomatic and progressive neurodegeneration in a mouse model of spinocerebellar ataxia type 1. *The Journal of Neuroscience: The Official Journal of the Society for Neuroscience*, *30*(10), 3831–8. <http://doi.org/10.1523/JNEUROSCI.5612-09.2010>
- Pai, M., & Jacobs, W. J. (2004). Topographical disorientation in community-residing patients with Alzheimer ' s disease, (July 2003), 250–255.
- Parker, A., & Gaffan, D. (1997). The effect of anterior thalamic and cingulate cortex lesions on object-in-place memory in monkeys. *Neuropsychologia*, *35*(8), 1093–1102. [http://doi.org/10.1016/S0028-3932\(97\)00042-0](http://doi.org/10.1016/S0028-3932(97)00042-0)
- Parvizi, J., Hoesen, G. W. Van, Buckwalter, J., & Damasio, A. (2006). Neural connections of the posteromedial cortex in the macaque, *103*(5), 1563–1568.
- Patel, T. B., & Clark, J. B. (1979). Synthesis of N-acetyl-l-aspartate by rat brain mitochondria and its involvement in mitochondrial/cytosolic carbon transport. *Biochemical Journal*, *184*(3), 539–546. <http://doi.org/10.1042/bj1840539>
- Patel, T., Blyth, J. C., Griffiths, G., Kelly, D., & Talcott, J. B. (2014). Moderate relationships between NAA and cognitive ability in healthy adults: implications for cognitive spectroscopy. *Frontiers in Human Neuroscience*, *8*(February), 39. <http://doi.org/10.3389/fnhum.2014.00039>

References

- Paul, E. J., Larsen, R. J., Nikolaidis, A., Ward, N., Hillman, C. H., Cohen, N. J., ... Barbey, A. K. (2016). Dissociable Brain Biomarkers of Fluid Intelligence. *NeuroImage*, *137*, 201–211. <http://doi.org/10.1016/j.neuroimage.2016.05.037>
- Pengas, G., Hodges, J. R., Watson, P., & Nestor, P. J. (2010). Focal posterior cingulate atrophy in incipient Alzheimer's disease. *Neurobiology of Aging*, *31*(1), 25–33. <http://doi.org/10.1016/j.neurobiolaging.2008.03.014>
- Pengas, G., Patterson, K., Arnold, R. J., Bird, C. M., Burgess, N., & Nestor, P. J. (2010). Lost and Found: Bespoke Memory Testing for Alzheimer's Disease and Semantic Dementia, *21*, 1347–1365. <http://doi.org/10.3233/JAD-2010-100654>
- Perkins, M., Wolf, A. B., Chavira, B., Shonebarger, D., Meckel, J. P., Leung, L., ... Valla, J. (2016). Altered energy metabolism pathways in the posterior cingulate in young adult apolipoprotein E4 carriers. *Journal of Alzheimer's Disease*, *53*, 95–106. <http://doi.org/10.3233/JAD-151205>
- Petersen, R. C. (2004). Mild cognitive impairment as a clinical entity and treatment target. *Archives of Neurology*, *62*(7), 1160–1163; discussion 1167. <http://doi.org/10.1001/archneur.62.7.1160>
- Petrella, J. R., Prince, S. E., Wang, L., Hellegers, C., & Doraiswamy, P. M. (2007). Prognostic value of posteromedial cortex deactivation in mild cognitive impairment. *PLoS ONE*, *2*(10), 1–7. <http://doi.org/10.1371/journal.pone.0001104>
- Pflugshaupt, T., Nösberger, M., Gutbrod, K., Weber, K. P., Linnebank, M., & Brugger, P. (2014). Bottom-up Visual Integration in the Medial Parietal Lobe. *Cerebral Cortex (New York, N.Y. : 1991)*, (August). <http://doi.org/10.1093/cercor/bhu256>
- Piekema, C., Kessels, R. P. C., Mars, R. B., Petersson, K. M., & Fernández, G. (2006). The right hippocampus participates in short-term memory maintenance of object-location associations. *NeuroImage*, *33*(1), 374–382. <http://doi.org/10.1016/j.neuroimage.2006.06.035>
- Pihlajamäki, M., & Sperling, R. A. (2009). Functional MRI assessment of task-induced deactivation of the default mode network in Alzheimer's disease and at-risk older individuals. *Behavioural Neurology*, *21*(1-2), 77–91. <http://doi.org/10.3233/BEN-2009-0231>
- Pilatus, U., Lais, C., Rochmont, A. du M. de, Kratzsch, T., Frolich, L., Maurer, K., ... Pantel, J. (2009). Conversion to dementia in mild cognitive impairment is associated with decline of N-acetylaspartate and creatine as revealed by magnetic resonance spectroscopy. *Psychiatry Research - Neuroimaging*, *173*(1), 1–7. <http://doi.org/10.1016/j.pscychresns.2008.07.015>
- Pizzi, S. D., Padulo, C., Brancucci, A., Bubbico, G., Edden, R., Ferretti, A., ... Bonanni, L. (2016). GABA content within the ventromedial prefrontal cortex is related to trait anxiety. *Soc Cogn Affect Neurosci*, *11*(5), 758–766.

References

- Poldrack, R. A., Mumford, J. A., & Nichols, T. E. (2011). *Handbook of Functional MRI Data Analysis*. Cambridge University Press.
- Price, C. J., Moore, C. J., & Friston, K. J. (1997). Subtractions, conjunctions, and interactions in experimental design of activation studies. *Human Brain Mapping, 5*(4), 264–272. [http://doi.org/10.1002/\(SICI\)1097-0193\(1997\)5:4<264::AID-HBM11>3.0.CO;2-E](http://doi.org/10.1002/(SICI)1097-0193(1997)5:4<264::AID-HBM11>3.0.CO;2-E)
- Prince, M., Knapp, M., Guerchet, M., McCrone, P., Prina, M., Comas-Herrera, A Wittenberg, R., ... Salimkumar, A. (2014). *Dementia UK: Update*. *Alzheimer's Society*.
- Protas, H. D., Chen, K., Langbaum, J. B., Fleisher, a S., Alexander, G. E., Lee, W., ... Reiman, E. M. (2013). Posterior cingulate glucose metabolism, hippocampal glucose metabolism, and hippocampal volume in cognitively normal, late-middle-aged persons at 3 levels of genetic risk for Alzheimer disease. *JAMA Neurol, 70*(3), 320–325. <http://doi.org/10.1001/2013.jamaneurol.286>
- Rae, C. D. (2014). A guide to the metabolic pathways and function of metabolites observed in human brain 1H magnetic resonance spectra. *Neurochemical Research, 39*(1), 1–36. <http://doi.org/10.1007/s11064-013-1199-5>
- Raichle, M. E., MacLeod, a M., Snyder, a Z., Powers, W. J., Gusnard, D. a, & Shulman, G. L. (2001). A default mode of brain function. *Proceedings of the National Academy of Sciences of the United States of America, 98*(2), 676–82. <http://doi.org/10.1073/pnas.98.2.676>
- Rasgon, N. L., Thomas, M. a, Guze, B. H., Fairbanks, L. a, Yue, K., Curran, J. G., & Rapkin, a J. (2001). Menstrual cycle-related brain metabolite changes using 1H magnetic resonance spectroscopy in premenopausal women: a pilot study. *Psychiatry Research, 106*(1), 47–57. Retrieved from <http://www.ncbi.nlm.nih.gov/pubmed/11231099>
- Reid, M. a, Stoeckel, L. E., White, D. M., Avsar, K. B., Bolding, M. S., Akella, N. S., ... Lahti, A. C. (2010). Assessments of function and biochemistry of the anterior cingulate cortex in schizophrenia. *Biological Psychiatry, 68*(7), 625–33. <http://doi.org/10.1016/j.biopsych.2010.04.013>
- Reiman, E. M., Chen, K., Alexander, G. E., Caselli, R. J., Bandy, D., Osborne, D., ... Hardy, J. (2004). Functional brain abnormalities in young adults at genetic risk for late-onset Alzheimer's dementia. *Proceedings of the National Academy of Sciences of the United States of America, 101*(1), 284–9. <http://doi.org/10.1073/pnas.2635903100>
- Reiman, E. M., & Jagust, W. J. (2012). Brain imaging in the study of Alzheimer's disease. *NeuroImage, 61*(2), 505–16. <http://doi.org/10.1016/j.neuroimage.2011.11.075>
- Reiman, E. M., Langbaum, J. B. S., & Tariot, P. N. (2010). Alzheimer's prevention initiative: a proposal to evaluate presymptomatic treatments as quickly as possible. *Biomarkers in Medicine, 4*(1), 3–14. <http://doi.org/10.2217/bmm.09.91>
- Ries, M. L., Schmitz, T. W., Kawahara, T. N., Torgerson, B. M., Trivedi, M. a, & Johnson, S. C.

- (2006). Task-dependent posterior cingulate activation in mild cognitive impairment. *NeuroImage*, 29(2), 485–92. <http://doi.org/10.1016/j.neuroimage.2005.07.030>
- Riese, F., Gietl, A., Zölch, N., Henning, A., O’Gorman, R., Kälin, A. M., ... Michels, L. (2015). Posterior cingulate γ -aminobutyric acid and glutamate/glutamine are reduced in amnesic mild cognitive impairment and are unrelated to amyloid deposition and apolipoprotein E genotype. *Neurobiology of Aging*, 36(1), 53–9. <http://doi.org/10.1016/j.neurobiolaging.2014.07.030>
- Rocchi, A., Pellegrini, S., Siciliano, G., & Murri, L. (2003). Causative and susceptibility genes for Alzheimer’s disease: A review. *Brain Research Bulletin*, 61(1), 1–24. [http://doi.org/10.1016/S0361-9230\(03\)00067-4](http://doi.org/10.1016/S0361-9230(03)00067-4)
- Ross, A. J., & Sachdev, P. S. (2004). Magnetic resonance spectroscopy in cognitive research. *Brain Research. Brain Research Reviews*, 44(2-3), 83–102. <http://doi.org/10.1016/j.brainresrev.2003.11.001>
- Rouder, J. N., Speckman, P. L., Sun, D., Morey, R. D., & Iverson, G. (2009). Bayesian t tests for accepting and rejecting the null hypothesis. *Psychonomic Bulletin & Review*, 16(2), 225–237. <http://doi.org/10.3758/PBR.16.2.225>
- Rusted, J. M., Evans, S. L., King, S. L., Dowell, N., Tabet, N., & Tofts, P. S. (2013). APOE e4 polymorphism in young adults is associated with improved attention and indexed by distinct neural signatures. *NeuroImage*, 65, 364–73. <http://doi.org/10.1016/j.neuroimage.2012.10.010>
- Scoville, W. B., & Milner, B. (1957). Loss of recent memory after bilateral hippocampal lesions. *The Journal of Neuropsychiatry and Clinical Neurosciences*, 20, 11–21. <http://doi.org/10.1136/jnnp.20.1.11>
- Seeley, W. W., Crawford, R. K., Zhou, J., Miller, B. L., & Greicius, M. D. (2009). Neurodegenerative diseases target large-scale human brain networks. *Neuron*, 62(1), 42–52. <http://doi.org/10.1016/j.neuron.2009.03.024>
- Seo, S. W., Lee, J. H., Jang, S. M., Kim, S. T., Chin, J., Kim, G. H., ... Na, D. L. (2012). Neurochemical alterations of the entorhinal cortex in amnesic mild cognitive impairment (aMCI): a three-year follow-up study. *Archives of Gerontology and Geriatrics*, 54(1), 192–6. <http://doi.org/10.1016/j.archger.2011.04.002>
- Serrano-Pozo, A., Frosch, M. P., Masliah, E., & Hyman, B. T. (2011). Neuropathological alterations in Alzheimer disease. *Cold Spring Harbor Perspectives in Medicine*, 1(1), 1–23. <http://doi.org/10.1101/cshperspect.a006189>
- Shine, J. P., Hodgetts, C. J., Postans, M., Lawrence, A. D., & Graham, K. S. (2015). APOE- ϵ 4 selectively modulates posteromedial cortex activity during spatial perception and memory in young healthy adults. *Nature Publishing Group*, 5(16322), 1–12. <http://doi.org/10.1038/srep16322>

References

- Signoretti, S., Marmarou, A., Tavazzi, B., Lazzarino, G., Beaumont, A., & Vagnozzi, R. (2001). N-Acetylaspartate (NAA) is considered a neuron-specific metabolite and its reduction a marker of neuronal loss. The objective of this study was to evaluate the time course of NAA changes in varying grades of traumatic brain injury (TBI), in concert with t. *J Neurotrauma*, *18*(10), 977–991.
- Singh, K. D. (2012). Which “neural activity” do you mean? fMRI, MEG, oscillations and neurotransmitters. *NeuroImage*, *62*(2), 1121–1130. <http://doi.org/10.1016/j.neuroimage.2012.01.028>
- Smith, S. M. (2002). Fast robust automated brain extraction. *Human Brain Mapping*, *17*(3), 143–55. <http://doi.org/10.1002/hbm.10062>
- Soghomonian, J., & Martin, D. L. (1998). Two isoforms of glutamate decarboxylase : why ?, *19*(December).
- Sperling, R. a, Aisen, P. S., Beckett, L. a, Bennett, D. a, Craft, S., Fagan, A. M., ... Phelps, C. H. (2011). Toward defining the preclinical stages of Alzheimer’s disease: recommendations from the National Institute on Aging-Alzheimer’s Association workgroups on diagnostic guidelines for Alzheimer’s disease. *Alzheimer’s & Dementia: The Journal of the Alzheimer’s Association*, *7*(3), 280–92. <http://doi.org/10.1016/j.jalz.2011.03.003>
- Spreng, R. N., Mar, R. A., & Kim, A. S. N. (2008). The Common Neural Basis of Autobiographical Memory , Prospection , Navigation , Theory of Mind , and the Default Mode : A Quantitative Meta-analysis, 489–510.
- Stagg, C. J., Bachtiar, V., & Johansen-Berg, H. (2011). What are we measuring with GABA magnetic resonance spectroscopy? *Communicative & Integrative Biology*, *4*(5), 573–5. <http://doi.org/10.4161/cib.4.5.16213>
- Stagg, C. J., & Rothman, D. L. (Eds.). (2014). *Magnetic Resonance Spectroscopy: Tools for Neuroscience Research and Emerging Clinical Applications*. Elsevier.
- Stan, A. D., Schirda, C. V, Bertocci, M. a, Bebko, G. M., Kronhaus, D. M., Aslam, H. a, ... Phillips, M. L. (2014). Glutamate and GABA contributions to medial prefrontal cortical activity to emotion: implications for mood disorders. *Psychiatry Research*, *223*(3), 253–60. <http://doi.org/10.1016/j.psychresns.2014.05.016>
- Streiner, D. L. (2015). Best (but oft-forgotten) practices: The multiple problems of multiplicity-whether and how to correct for many statistical tests. *American Journal of Clinical Nutrition*, *102*(4), 721–728. <http://doi.org/10.3945/ajcn.115.113548>
- Suri, S., Heise, V., Trachtenberg, A. J., & Mackay, C. E. (2013). The forgotten APOE allele: a review of the evidence and suggested mechanisms for the protective effect of APOE ε2. *Neuroscience and Biobehavioral Reviews*, *37*(10 Pt 2), 2878–86. <http://doi.org/10.1016/j.neubiorev.2013.10.010>
- Suri, S., Mackay, C. E., Kelly, M. E., Germuska, M., Tunbridge, E. M., Frisoni, G. V. B., ...

References

- Filippini, N. (2015). Reduced cerebrovascular reactivity in young adults carrying the APOE ϵ 4 allele. *Alzheimer's and Dementia*, 11(6), 648–657. <http://doi.org/10.1016/j.jalz.2014.05.1755>
- Suzuki, K., Yamadori, A., Hayakawa, Y., & Fujii, T. (1998). Pure topographical disorientation related to dysfunction of the viewpoint dependent visual system. *Cortex*, 34, 589–599.
- Takahashi, N., & Kawamura, M. (2002). Pure topographical disorientation - the anatomical basis of landmark agnosia. *Cortex*, 38, 717–725.
- Takahashi, N., Kawamura, M., Shiota, J., Kasahata, N., & Hirayama, K. (1997). Pure topographic disorientation due to right retrosplenial lesion. *Neurology*, 49(2), 464–469.
- Tandon, N., Bolo, N. R., Sanghavi, K., Mathew, I. T., Francis, A. N., Stanley, J. a, & Keshavan, M. S. (2013). Brain metabolite alterations in young adults at familial high risk for schizophrenia using proton magnetic resonance spectroscopy. *Schizophrenia Research*, 148(1-3), 59–66. <http://doi.org/10.1016/j.schres.2013.05.024>
- Tanzi, R. E., & Bertram, L. (2001). New frontiers in Alzheimer's disease genetics. *Neuron*, 32(2), 181–184. [http://doi.org/info:doi/10.1016/S0896-6273\(01\)00476-7](http://doi.org/info:doi/10.1016/S0896-6273(01)00476-7)
- Trachtenberg, A. J., Filippini, N., Cheeseman, J., Duff, E. P., Neville, M. J., Ebmeier, K. P., ... Mackay, C. E. (2012). The effects of APOE on brain activity do not simply reflect the risk of Alzheimer's disease. *Neurobiology of Aging*, 33(3), 618.e1–618.e13. <http://doi.org/10.1016/j.neurobiolaging.2010.11.011>
- Tulving, E. (1972). Episodic and Semantic Memory. In *Organisation of Memory* (pp. 382–403).
- Tuminello, E. R., & Han, S. D. (2011). The Apolipoprotein E Antagonistic Pleiotropy Hypothesis: Review and Recommendations. *International Journal of Alzheimer's Disease*, 2011, 1–12. <http://doi.org/10.4061/2011/726197>
- Urenjak, J., Williams, S. R., Gadian, D. G., & Noble, M. (1992). Specific expression of N-acetylaspartate in neurons, oligodendrocyte-type-2 astrocyte progenitors, and immature oligodendrocytes in vitro. *Journal of Neurochemistry*, 59(1), 55–61. <http://doi.org/10.1111/j.1471-4159.1992.tb08875.x>
- Urrila, A. S., Hakkarainen, A., Heikkinen, S., Vuori, K., Stenberg, D., Häkkinen, A.-M., ... Porkka-Heiskanen, T. (2003). Metabolic imaging of human cognition: an fMRI/1H-MRS study of brain lactate response to silent word generation. *Journal of Cerebral Blood Flow and Metabolism : Official Journal of the International Society of Cerebral Blood Flow and Metabolism*, 23(8), 942–8. <http://doi.org/10.1097/01.WCB.0000080652.64357.1D>
- Utevsky, A. V, Smith, D. V, & Huettel, S. a. (2014). Precuneus is a functional core of the default-mode network. *The Journal of Neuroscience: The Official Journal of the*

- Society for Neuroscience*, 34(3), 932–40. <http://doi.org/10.1523/JNEUROSCI.4227-13.2014>
- Valla, J., Yaari, R., Wolf, A., Kusne, Y., Beach, T., Roher, A., ... Reiman, E. M. (2010). Reduced Posterior Cingulate Mitochondrial Activity in Expired Young Adult Carriers of the APOE ε4 Allele, the Major Late-Onset Alzheimer's Susceptibility Gene. *J Alzheimers Dis*, 22(1), 307–313. <http://doi.org/10.3233/JAD-2010-100129>. Reduced
- Van Cauwenberghe, C., Van Broeckhoven, C., & Sleegers, K. (2016). The genetic landscape of Alzheimer disease: clinical implications and perspectives. *Genetics in Medicine : Official Journal of the American College of Medical Genetics*, 18(5), 421–430. <http://doi.org/10.1038/gim.2015.117>
- van den Heuvel, M. P., & Sporns, O. (2013). Network hubs in the human brain. *Trends in Cognitive Sciences*, 17(12), 683–696. <http://doi.org/10.1016/j.tics.2013.09.012>
- Vann, S. D., Aggleton, J. P., & Maguire, E. a. (2009). What does the retrosplenial cortex do? *Nature Reviews. Neuroscience*, 10(11), 792–802. <http://doi.org/10.1038/nrn2733>
- Vannini, P., O'Brien, J., O'Keefe, K., Pihlajamäki, M., Laviolette, P., & Sperling, R. a. (2011). What goes down must come up: role of the posteromedial cortices in encoding and retrieval. *Cerebral Cortex (New York, N.Y.: 1991)*, 21(1), 22–34. <http://doi.org/10.1093/cercor/bhq051>
- Vigren, P., Tisell, A., Engström, M., Karlsson, T., Leinhard Dahlqvist, O., Lundberg, P., & Landtblom, A.-M. (2013). Low thalamic NAA-concentration corresponds to strong neural activation in working memory in Kleine-Levin syndrome. *PloS One*, 8(2), e56279. <http://doi.org/10.1371/journal.pone.0056279>
- Violante, I. R., Ribeiro, M. J., Edden, R. A. E., Guimaraes, P., Bernardino, I., Rebola, J., ... Castelo-Branco, M. (2013). GABA deficit in the visual cortex of patients with neurofibromatosis type 1: Genotype-phenotype correlations and functional impact. *Brain*, 136(3), 918–925. <http://doi.org/10.1093/brain/aws368>
- Voevodskaya, O., & Sundgren, P. C. (2016). Myo-inositol changes precede amyloid pathology and relate to APOE genotype in Alzheimer disease, 0.
- von Bonin, G., & Bailey, P. (1947). *The Neocortex of Macaca mulatta*. Urbana: University of Illinois Press.
- Waite, L. M. (2015). Treatment for Alzheimer's disease: Has anything changed? *Australian Prescriber*, 38(2), 60–63.
- Walecki, J., Barcikowska, M., Ćwikła, J. B., & Gabryelewicz, T. (2011). N-acetylaspartate, choline, myoinositol, glutamine and glutamate (glx) concentration changes in proton MR spectroscopy (¹H MRS) in patients with mild cognitive impairment (MCI). *Med Sci Monit*, 17(12), 105–111.

References

- Wang, H., Tan, L., Wang, H.-F., Liu, Y., Yin, R.-H., Wang, W.-Y., ... Yu, J.-T. (2015). Magnetic Resonance Spectroscopy in Alzheimer's Disease: Systematic Review and Meta-Analysis. *Journal of Alzheimer's Disease*, 46(4), 1049–1070. <http://doi.org/10.3233/JAD-143225>
- Wang, T., Xiao, S., Li, X., Ding, B., Ling, H., Chen, K., & Fang, Y. (2012). Using proton magnetic resonance spectroscopy to identify mild cognitive impairment. *International Psychogeriatrics / IPA*, 24(1), 19–27. <http://doi.org/10.1017/S1041610211000962>
- Watanabe, T., Shiino, A., & Akiguchi, I. (2010). Absolute quantification in proton magnetic resonance spectroscopy is useful to differentiate amnesic mild cognitive impairment from Alzheimer's disease and healthy aging. *Dementia and Geriatric Cognitive Disorders*, 30(1), 71–77. <http://doi.org/10.1159/000318750>
- Wechsler, D. (1974). Wechsler intelligence scale for children- revised. *The Psychological Corporation, New York*.
- Wiame, E., Tyteca, D., Pierrot, N., Desmedt, J., Vikkula, M., Courtoy, P. J., ... Schaftingen, E. V. A. N. (2010). Molecular identification of aspartate N-acetyltransferase and its mutation in hypoacetylaspartia, 136, 127–136. <http://doi.org/10.1042/BJ20091024>
- Wilson, M., Reynolds, G., Kauppinen, R. a, Arvanitis, T. N., & Peet, A. C. (2011). A constrained least-squares approach to the automated quantitation of in vivo ¹H magnetic resonance spectroscopy data. *Magnetic Resonance in Medicine: Official Journal of the Society of Magnetic Resonance in Medicine / Society of Magnetic Resonance in Medicine*, 65(1), 1–12. <http://doi.org/10.1002/mrm.22579>
- World Health Organization. (2012). Dementia: a public health priority. *Dementia*, 112. http://doi.org/978_92_4_156445_8
- Xu, Q. (2006). Profile and Regulation of Apolipoprotein E (ApoE) Expression in the CNS in Mice with Targeting of Green Fluorescent Protein Gene to the ApoE Locus. *Journal of Neuroscience*, 26(19), 4985–4994. <http://doi.org/10.1523/JNEUROSCI.5476-05.2006>
- Yoo, S. Y., Yeon, S., Choi, C.-H., Kang, D.-H., Lee, J.-M., Shin, N. Y., ... Kwon, J. S. (2009). Proton magnetic resonance spectroscopy in subjects with high genetic risk of schizophrenia: investigation of anterior cingulate, dorsolateral prefrontal cortex and thalamus. *Schizophrenia Research*, 111(1-3), 86–93. <http://doi.org/10.1016/j.schres.2009.03.036>
- Zhang, Y., Brady, M., & Smith, S. (2001). Segmentation of brain MR images through a hidden Markov random field model and the expectation-maximization algorithm. *IEEE Transactions on Medical Imaging*, 20(1), 45–57. <http://doi.org/10.1109/42.906424>
- Zhou, Y., Dougherty, J. H., Hubner, K. F., Bai, B., Cannon, R. L., & Hutson, R. K. (2008).

References

Abnormal connectivity in the posterior cingulate and hippocampus in early Alzheimer's disease and mild cognitive impairment. *Alzheimer's & Dementia: The Journal of the Alzheimer's Association*, 4(4), 265-70. <http://doi.org/10.1016/j.jalz.2008.04.006>